



**National Library
of Canada**

**Bibliothèque nationale
du Canada**

Canadian Theses Service

Service des thèses canadiennes

Ottawa, Canada
K1A 0N4

NOTICE

The quality of this microform is heavily dependent upon the quality of the original thesis submitted for microfilming. Every effort has been made to ensure the highest quality of reproduction possible.

If pages are missing, contact the university which granted the degree.

Some pages may have indistinct print especially if the original pages were typed with a poor typewriter ribbon or if the university sent us an inferior photocopy.

Reproduction in full or in part of this microform is governed by the Canadian Copyright Act, R.S.C. 1970, c. C-30, and subsequent amendments.

AVIS

La qualité de cette microforme dépend grandement de la qualité de la thèse soumise au microfilmage. Nous avons tout fait pour assurer une qualité supérieure de reproduction.

S'il manque des pages, veuillez communiquer avec l'université qui a conféré le grade.

La qualité d'impression de certaines pages peut laisser à désirer, surtout si les pages originales ont été dactylographiées à l'aide d'un ruban usé ou si l'université nous a fait parvenir une photocopie de qualité inférieure.

La reproduction, même partielle, de cette microforme est soumise à la Loi canadienne sur le droit d'auteur, SRC 1970, c. C-30, et ses amendements subséquents.

THREE PHASE RUNOFF MODEL FOR SMALL PRAIRIE RIVERS

BY

JAMES MICHAEL BYRNE

A THESIS

**SUBMITTED TO THE FACULTY OF GRADUATE STUDIES AND RESEARCH
IN PARTIAL FULFILLMENT OF THE REQUIREMENTS FOR THE DEGREE OF
DOCTOR OF PHILOSOPHY**

IN

**WATER RESOURCES,
DEPARTMENT OF CIVIL ENGINEERING.**

EDMONTON, ALBERTA

FALL, 1990



**National Library
of Canada**

**Bibliothèque nationale
du Canada**

Canadian Theses Service Service des thèses canadiennes

**Ottawa, Canada
K1A 0N4**

The author has granted an irrevocable non-exclusive licence allowing the National Library of Canada to reproduce, loan, distribute or sell copies of his/her thesis by any means and in any form or format, making this thesis available to interested persons.

The author retains ownership of the copyright in his/her thesis. Neither the thesis nor substantial extracts from it may be printed or otherwise reproduced without his/her permission.

L'auteur a accordé une licence irrévocable et non exclusive permettant à la Bibliothèque nationale du Canada de reproduire, prêter, distribuer ou vendre des copies de sa thèse de quelque manière et sous quelque forme que ce soit pour mettre des exemplaires de cette thèse à la disposition des personnes intéressées.

L'auteur conserve la propriété du droit d'auteur qui protège sa thèse. Ni la thèse ni des extraits substantiels de celle-ci ne doivent être imprimés ou autrement reproduits sans son autorisation.

ISBN 0-315-64799-X

THE UNIVERSITY OF ALBERTA

RELEASE FORM

NAME OF AUTHOR: James Michael Byrne

TITLE OF THESIS: Three Phase Runoff Model for Small Prairie Rivers

DEGREE: Doctor of Philosophy

YEAR THIS DEGREE GRANTED: 1990

Permission is hereby granted to THE UNIVERSITY OF ALBERTA LIBRARY to reproduce single copies of this thesis and to lend or sell such copies for private, scholarly or scientific research purposes only.

The author reserves other publication rights, and neither the thesis nor extensive extracts from it may be printed or otherwise reproduced without the author's written permission.



James Michael Byrne

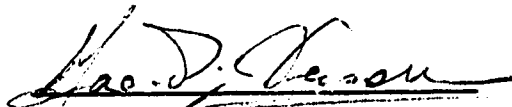
54 Carleton Road West
Lethbridge, Alberta
CANADA T1K 3X5

Fall, 1990

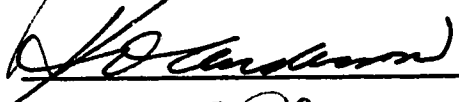
THE UNIVERSITY OF ALBERTA
FACULTY OF GRADUATE STUDIES AND RESEARCH

THE UNDERSIGNED CERTIFY THEY HAVE READ, AND RECOMMEND TO
THE FACULTY OF GRADUATE STUDIES AND RESERACH FOR
ACCEPTANCE, A THESIS ENTITLED THREE PHASE RUNOFF MODEL FOR
SMALL PRAIRIE RIVERS SUBMITTED BY JAMES MICHAEL BYRNE IN
PARTIAL FULFILLMENT FOR THE DEGREE OF DOCTOR OF PHILOSOPHY
IN WATER RESOURCES, DEPARTMENT OF CIVIL ENGINEERING.

J.P. Verschuren, Supervisor



K. Anderson



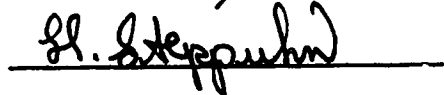
D.S. Chanasyk



P. Steffler



H. Steppuhn



Date: 1990 10 09

ABSTRACT

The hydrologic processes of small, low-relief watersheds on the plains in southeastern Alberta are analyzed to determine the precipitation-runoff relationships under different soil fluid states; and to test the hypothesis that the state of the soil fluid has a dominant control on runoff generation. A conceptual runoff model based on the dominant state of the soil fluid(s) is developed. The conceptual runoff model is referred to as a three phase runoff model. The three states (phases) are frozen, saturated (liquid) and unsaturated (liquid-gaseous). The state of the dominant fluid at any time governs the water depth from snowmelt or rainfall that is available for runoff. A soil in a frozen condition has a limited infiltration capacity. The saturated (often inundated) condition has a runoff coefficient that would approach 1.0 in most cases. The unsaturated condition has the greatest potential to reduce surface runoff, both through replenishment of the available soil water and percolation of water to the groundwater system.

Runoff processes are modelled for a number of years at 35 climate stations over a study area containing a number of small watersheds. The analysis includes interpolation of modelled estimates of fall soil moisture, spring snow water equivalent and snowmelt infiltration to frozen soils on a one kilometre square grid system over a watershed. These data are combined to estimate the basin spring runoff depth for the hydrologic period of record for the basin. Regression models demonstrate there is a linear relationship between the spring runoff depth and spring snowmelt runoff volume, and that the snowmelt (frozen soil) runoff contributing area and depression storage losses are constant from year to year.

Analyses of the unsaturated soil system for a period of 22 years indicate there is no runoff from rainfall when the soil water is not frozen; excepting precipitation on the saturated areas of the watershed directly connected to the drainage channel system.

DEDICATION

For Cheryl, Brendan, Kalyn, Davyn and Jayme.

Finally, the spring runoff depth - spring runoff volume analysis is applied to a number of basins in southeastern Alberta, with the results showing that both the snowmelt runoff contributing area and depression storage losses remain constant from year to year. A geomorphological method for estimating snowmelt runoff contributing area and depression storage losses is developed from the multi-basin analysis.

ACKNOWLEDGEMENTS

The author extends a sincere thank you to Dr. Jac Verschuren for his guidance and personal support throughout this work.

The patience and support of the Department of Geography and the Faculty of Arts and Science, University of Lethbridge, was most appreciated.

The study was supported by funds from Alberta Environment, Research Management Division, and the Water Resources Institute at the University of Lethbridge.

This study could not have been completed without the understanding and support of my wife Cheryl, and my children Brendan, Kalyn, Davyn and Jayme.

Table of Contents

1. INTRODUCTION	1
1.1. Background	1
1.2. Study Objective and Components	3
1.3. Description of the Study Area	3
1.4. Study Chapters	5
1.5. References	8
2. LITERATURE REVIEW	14
2.1. Introduction	14
2.2. Soil Water Retention	14
2.2.1. Classical soil water definitions	15
2.2.2. Properties controlling unsaturated water storage	16
2.2.2.1. Soil texture	16
2.2.2.2. Soil structure	17
2.2.2.3. Soil organic matter	17
2.2.3. Soil water budgeting	18
2.2.4. Snow-soil interactions	19
2.2.4.1. Guymon (1978)	20
2.2.4.2. Santeford (1978)	20
2.2.4.3. Gray et al. (1983)	21

2.2.4.4. Granger et al. (1984) and Gray et al. (1985)	22
2.3. Evapotranspiration	23
2.3.1. Potential and Actual Evapotranspiration	23
2.3.2. Formulas for Estimating ETP and ET	24
2.3.2.1. Empirical formulas for ETP/ET estimation	24
2.3.2.2. Mass transfer techniques for estimating ETP/ET	26
2.3.3. Morton's ET	28
2.4. Depression Storage Studies in Prairie Soils	32
2.4.1. Macro depression storage studies	32
2.4.1.1. Meyboom (1966)	33
2.4.1.2. US Geological Survey (1968)	35
2.4.1.3. Card (1979)	36
2.4.2. Micro depression storage studies	38
2.4.2.1. Mitchell and Jones (1976), (1978)	38
2.4.2.2. Gayle and Skaggs (1978)	39
2.4.2.3. Summary - Depression Storage Literature	40
2.5. Contributing Area	40
2.5.1. Contributing Area Studies	40
2.5.1.1. Card (1979)	41
2.5.1.2. Taylor (1982)	41
2.5.1.3. Gray, Landine and McKay (1985)	43
2.5.1.4. PFRA (1978), (1983), (1985)	44
2.5.1.5. Holocek (1988)	45
2.6. References	48
3. CONCEPTUAL MODEL OF PRAIRIE HYDROLOGY	60

3.1. Introduction	60
3.2. Conceptual Model of Prairie Runoff Functions	60
3.2.1. Frozen Soil Phase	61
3.2.1.1. Freeze-up Moisture Levels and Winter Moisture Migration	61
3.2.1.2. Net Vapour Transfer to the Snowpack	62
3.2.1.3. Depth of Fresh Snowfall	63
3.2.1.4. Snowmelt Infiltration to Frozen Soils	63
3.2.2. Active Soil Runoff Phase	64
3.2.3. Saturated Soil Phase	65
3.3. Summary	66
3.4. References	67
4. BLOCK KRIGING ANALYSIS	68
4.1. Kriging Theory	70
4.1.1. The semi-variogram and nugget variance	70
4.1.2. Equations for block kriging	72
4.2. Applications	73
4.3. Summary	73
4.4. References	75
5. FROZEN SOIL PHASE ASSESSMENT RIBSTONE CREEK NEAR CZAR	78
5.1. Introduction	78
5.2. Climatic Model for Determining Point Runoff Depth	79

5.3. Spatial Analysis of Modelled Climatic Data	82
5.4. Determining Basin Values for WP, SWE and INF	82
5.5. Determining AREA1 and DS for Ribstone Creek	84
5.6. Summary	86
5.7. References	87
6. ACTIVE SOIL PHASE ASSESSMENT - RIBSTONE CREEK	97
6.1. Introduction	97
6.2. Methodology	97
6.3. Conclusions	102
7. SATURATED SOIL PHASE ASSESSMENT RIBSTONE CREEK	128
7.1. Conceptual Model of Prairie Runoff Functions	128
7.2. Theory of Saturated Soil Phase Operation	129
7.3. Developing a Representative Basin Climate File	131
7.4. Basin Storage - Outflow Relationship	132
7.5. Assessing Saturated Area Variability	134
7.6. Discussion	135
7.7. Modelling Three Phase Runoff Response	137
7.8. Conclusions	140
7.9. References	141
8. FROZEN SOIL PHASE ASSESSMENT FOR SEVERAL BASINS	153

8.1. Introduction	153
8.2. Spring runoff depth - spatial patterns	154
8.3. Simplified hydrograph separation	156
8.4. Multi-basin analysis of frozen soil contributing area	157
8.5. Relating AREA1 to basin geomorphology	161
8.5.1. Determining drainage density	162
8.5.2. Drainage density and runoff depth relationship	164
8.5.3. Determining micro-depression storage for any study area basin	165
8.6. Summation	168
8.7. References	170
9. SYNTHESIS	203
9.1. Introduction	203
9.2. Conclusions	204
Appendix A. WP, SWE and θ_p Spatial Fields for Ribstone Creek, 1968-80	207
Appendix B. STUDY AREA WP AND SWE SPATIAL FIELDS, 1960-81	247
Appendix C. SNOWMELT ALGORITHM	290
C.1. References	292

List of Tables

Table 1-1:	Drainage Basins in the Study Area	10
Table 2-1:	Soil texture and related moisture storage capability.	52
Table 2-2:	Water budget for a prairie pothole, North Dakota (Eisenlohr, 1972)	53
Table 2-3:	Results of Mitchell and Jones (1976) for micro depression storage depths on test plots of variable relief.	54
Table 2-4:	Unit runoff potential URP, observed runoff and apparent contributing area (Gray et al., 1985)	55
Table 2-5:	Fourteen selected flood events, Spring Creek, Alberta.	56
Table 4-1:	Selected application of kriging in earth/atmospheric sciences.	76
Table 5-1:	Semi-variograms for WP, SWE and θ_p for 1968 - 80	89
Table 5-2:	Runoff depths and volumes for Ribstone Creek	90
Table 6-1:	Active soil phase runoff depths (mm) for the individual stations.	104
Table 7-1:	SWE (mm) values for stations near Ribstone Creek	142
Table 7-2:	Assessment of the extent of the saturated area for Ribstone Creek	143

Table 8-1:	Spring runoff depth (SRD) in mm for eight watersheds.	171
Table 8-2:	Spring runoff volumes (m³) for eight watersheds.	172
Table 8-3:	Regression data for nine Alberta basins.	173
Table 8-4:	AREA1 and depression storage deficit estimates.	174
Table 8-5:	Drainage density and runoff depth relationships.	175
Table 8-6:	Depression storage, area and channel slope data.	176
Table 8-7:	AREA1 and depression storage deficit estimates.	177

List of Figures

Figure 1-1:	Runoff volume vs. annual precipitation for three basins in east central Alberta.	11
Figure 1-2:	General location of the study region in Alberta.	12
Figure 1-3:	Southeastern Alberta watersheds and climate stations. Several stations outside these boundaries were used where necessary. Study watersheds are: 1 - Alkali, 2 - Berry, 3 - Blood Indian, 4 - Buffalo, 5 - Bullpound, 6 - Iron, 7 - Monitor, 8 - Ribstone, 9 - Sounding Creeks. Circles are climate station locations.	13
Figure 2-1:	Depression storage - variable contributing area interaction in a prairie environment (Card, 1979)	57
Figure 2-2:	Unit runoff potential and volume relationship for Wascana Creek, Saskatchewan (after Gray et al., 1985). The best fit line equation is $RUNOFF = 3.3E8 URP - 3157534$, $r^2=0.947$.	58
Figure 2-3:	Storage - runoff relationships for Spring Creek, Alberta, developed by Holocek (1988). The Y(est) and X(est) values are the normalized basin storage and normalized contributing area.	59

Figure 4-1:	Theoretical linear and spherical semivariograms.	77
Figure 5-1:	Spatial distribution of WP for the 1973-74 winter. The relative area is defined by an x in the active elements.	91
Figure 5-2:	Spatial distribution of SWE for the 1973-74 winter. The relative area is defined by an x in the active elements.	92
Figure 5-3:	Spatial distribution of the frozen soilwater level WP for the 1973-74 winter. Relative area is defined by a dot in active elements.	93
Figure 5-4:	Relationship of WP and spring runoff, 1968-80.	94
Figure 5-5:	Relationship of SWE and spring runoff, 1968-80.	95
Figure 5-6:	Relationship of (SWE-INF) and spring runoff, 1968-80.	96
Figure 6-1:	Climate stations near the Ribstone Creek watershed.	106
Figure 6-2:	Active soil phase plots for Coronation.	107
Figure 6-3:	Active soil phase plots for Brownfield.	111
Figure 6-4:	Active soil phase plots for Hughendon.	115
Figure 6-5:	Active soil phase plots for Hemaruka.	119
Figure 6-6:	Active soil phase plots for Metisko.	123
Figure 6-7:	Annual runoff hydrographs, Ribstone Creek near Edgerton	127
Figure 7-1:	Ribstone Creek hydrograph, Water Survey Data.	144
Figure 7-2:	Saturated area estimates versus basin storage.	145

Figure 7-3:	In saturated area versus basin storage.	146
Figure 7-4:	Exponential SAREA function.	147
Figure 7-5:	Recorded and simulated (broken) hydrographs. The SAREA curve has been turned off, thus the smooth recession limb.	148
Figure 7-6:	Simulation with exponential SAREA function 1.	149
Figure 7-7:	Simulation with exponential SAREA function 2.	150
Figure 7-8:	SAREA curve 1, 1969 runoff.	151
Figure 7-9:	SAREA curve 1, 1971 runoff.	152
Figure 8-1:	Spring runoff depth over the study area, water equivalent	178
Figure 8-2:	Monitor creek regression plot, AREA1 analysis.	199
Figure 8-3:	1964-65 snowfall over the study area.	200
Figure 8-4:	1964-65 SWE depth for the study area.	201
Figure 8-5:	Scatter plot of SRD-DS and drainage density.	202
Figure A-1:	1968 WP spatial field in mm H ₂ O equivalent.	208
Figure A-2:	1969 WP spatial field in mm H ₂ O equivalent.	209
Figure A-3:	1970 WP spatial field in mm H ₂ O equivalent.	210
Figure A-4:	1971 WP spatial field in mm H ₂ O equivalent.	211
Figure A-5:	1972 WP spatial field in mm H ₂ O equivalent.	212
Figure A-6:	1973 WP spatial field in mm H ₂ O equivalent.	213
Figure A-7:	1974 WP spatial field in mm H ₂ O equivalent.	214

Figure A-8:	1975 WP spatial field in mm H₂O equivalent.	215
Figure A-9:	1976 WP spatial field in mm H₂O equivalent.	216
Figure A-10:	1977 WP spatial field in mm H₂O equivalent.	217
Figure A-11:	1978 WP spatial field in mm H₂O equivalent.	218
Figure A-12:	1979 WP spatial field in mm H₂O equivalent.	219
Figure A-13:	1980 WP spatial field in mm H₂O equivalent.	220
Figure A-14:	1968 SWE spatial field in mm H₂O equivalent.	221
Figure A-15:	1969 SWE spatial field in mm H₂O equivalent.	222
Figure A-16:	1970 SWE spatial field in mm H₂O equivalent.	223
Figure A-17:	1971 SWE spatial field in mm H₂O equivalent.	224
Figure A-18:	1972 SWE spatial field in mm H₂O equivalent.	225
Figure A-19:	1973 SWE spatial field in mm H₂O equivalent.	226
Figure A-20:	1974 SWE spatial field in mm H₂O equivalent.	227
Figure A-21:	1975 SWE spatial field in mm H₂O equivalent.	228
Figure A-22:	1976 SWE spatial field in mm H₂O equivalent.	229
Figure A-23:	1977 SWE spatial field in mm H₂O equivalent.	230
Figure A-24:	1978 SWE spatial field in mm H₂O equivalent.	231
Figure A-25:	1979 SWE spatial field in mm H₂O equivalent.	232
Figure A-26:	1980 SWE spatial field in mm H₂O equivalent.	233
Figure A-27:	1968 θ_p spatial field in mm H₂O equivalent.	234
Figure A-28:	1969 θ_p spatial field in mm H₂O equivalent.	235
Figure A-29:	1970 θ_p spatial field in mm H₂O equivalent.	236

Figure A-30:	1971 θ_p spatial field in mm H ₂ O equivalent.	237
Figure A-31:	1972 θ_p spatial field in mm H ₂ O equivalent.	238
Figure A-32:	1973 θ_p spatial field in mm H ₂ O equivalent.	239
Figure A-33:	1974 θ_p spatial field in mm H ₂ O equivalent.	240
Figure A-34:	1975 θ_p spatial field in mm H ₂ O equivalent.	241
Figure A-35:	1976 θ_p spatial field in mm H ₂ O equivalent.	242
Figure A-36:	1977 θ_p spatial field in mm H ₂ O equivalent.	243
Figure A-37:	1978 θ_p spatial field in mm H ₂ O equivalent.	244
Figure A-38:	1979 θ_p spatial field in mm H ₂ O equivalent.	245
Figure A-39:	1980 θ_p spatial field in mm H ₂ O equivalent.	246
Figure B-1:	1960 - Study area winter precip., mm H ₂ O.	248
Figure B-2:	1961 - Study area winter precip., mm H ₂ O.	249
Figure B-3:	1962 - Study area winter precip., mm H ₂ O.	250
Figure B-4:	1963 - Study area winter precip., mm H ₂ O.	251
Figure B-5:	1964 - Study area winter precip., mm H ₂ O.	252
Figure B-6:	1965 - Study area winter precip., mm H ₂ O.	253
Figure B-7:	1966 - Study area winter precip., mm H ₂ O.	254
Figure B-8:	1967 - Study area winter precip., mm H ₂ O.	255
Figure B-9:	1968 - Study area winter precip., mm H ₂ O.	256
Figure B-10:	1969 - Study area winter precip., mm H ₂ O.	257
Figure B-11:	1970 - Study area winter precip., mm H ₂ O.	258
Figure B-12:	1971 - Study area winter precip., mm H ₂ O.	259

Figure B-13:	1972 - Study area winter precip., mm H ₂ O.	260
Figure B-14:	1973 - Study area winter precip., mm H ₂ O.	261
Figure B-15:	1974 - Study area winter precip., mm H ₂ O.	262
Figure B-16:	1975 - Study area winter precip., mm H ₂ O.	263
Figure B-17:	1976 - Study area winter precip., mm H ₂ O.	264
Figure B-18:	1977 - Study area winter precip., mm H ₂ O.	265
Figure B-19:	1978 - Study area winter precip., mm H ₂ O.	266
Figure B-20:	1979 - Study area winter precip., mm H ₂ O.	267
Figure B-21:	1980 - Study area winter precip., mm H ₂ O.	268
Figure B-22:	1960 - Study area SWE, mm H ₂ O.	269
Figure B-23:	1961 - Study area SWE, mm H ₂ O.	270
Figure B-24:	1962 - Study area SWE, mm H ₂ O.	271
Figure B-25:	1963 - Study area SWE, mm H ₂ O.	272
Figure B-26:	1964 - Study area SWE, mm H ₂ O.	273
Figure B-27:	1965 - Study area SWE, mm H ₂ O.	274
Figure B-28:	1966 - Study area SWE, mm H ₂ O.	275
Figure B-29:	1967 - Study area SWE, mm H ₂ O.	276
Figure B-30:	1968 - Study area SWE, mm H ₂ O.	277
Figure B-31:	1969 - Study area SWE, mm H ₂ O.	278
Figure B-32:	1970 - Study area SWE, mm H ₂ O.	279
Figure B-33:	1971 - Study area SWE, mm H ₂ O.	280
Figure B-34:	1972 - Study area SWE, mm H ₂ O.	281

Figure B-35:	1973 - Study area SWE, mm H₂O.	282
Figure B-36:	1974 - Study area SWE, mm H₂O.	283
Figure B-37:	1975 - Study area SWE, mm H₂O.	284
Figure B-38:	1976 - Study area SWE, mm H₂O.	285
Figure B-39:	1977 - Study area SWE, mm H₂O.	286
Figure B-40:	1978 - Study area SWE, mm H₂O.	287
Figure B-41:	1979 - Study area SWE, mm H₂O.	288
Figure B-42:	1980 - Study area SWE, mm H₂O.	289

Chapter 1

INTRODUCTION

1.1. Background

The quantity of runoff available for natural and human utilization on the prairies of eastern Alberta is highly variable from year to year. There is no apparent direct link between the annual precipitation and runoff volume. For example, the apparent lack of any relationship is demonstrated in Figure 1-1,¹ a scatter plot of annual precipitation versus annual runoff for three drainage basins located in the southeastern quartile of Alberta. However, streamflow is a function of precipitation inputs and the physical, vegetative and climatic characteristics of a watershed (Viessman et al., 1977). The difficulty in assessing the precipitation-runoff relationship must be related to the relative ability of the watershed characteristics to modify and/or retain precipitation inputs.

The interactions of the physical, vegetative and climatic conditions that prevent precipitation from becoming runoff are often termed hydrologic abstractions or losses from runoff. These include interception storage, available water holding capacity (AWHC) of the soil, evapotranspiration (ET), and depression storage (Viessman et al., 1977). Implicit within these are related abstractions such as infiltration and deep percolation.

¹Figures and tables are grouped at the end of each chapter.

Interception is a minor consideration on grasslands, with values ranging from 0.1 to 1.0 mm for 25 cm high canopies of bluegrass and rough fescue (Branson et al., 1981). The AWHC of soils is typically 100 to 250 times greater than the upper value for interception storage reported by Branson et al. (Hansen et al., 1980). Depression storage is an important abstraction on the plains (Card, 1979; Eisenlohr et al., 1972).

The above discussion suggests that the principal hydrologic abstractions affecting runoff in the study area are the soil/vegetation systems, ET and depression storage. A fourth variable, the basin contributing area must be considered as well. A number of studies have addressed the concept of variable contributing area (Card, 1979; Chanasyk, 1980; Gray et al., 1985; Holocek, 1988; PFRA 1978; 1983; 1985; Stichling and Blackwell, 1957; Taylor, 1982 and many others). These studies generally argue the spatial variation in soil properties, precipitation and topography result in the contributing area of a watershed fluctuating in areal extent between and during storms.

This treatise will focus on identifying the relative impacts of the soil/vegetation, ET and depression storage abstractions on the hydrology of the plains in eastern Alberta. A central component of the study will be to define the effect of precipitation phase on these abstractions. Thirty five percent of the annual precipitation at Coronation occurs as snowfall (Alberta Environment, undated). Runoff due to snowmelt comprises most of the annual streamflow for the study area basins. This is not unexpected given that the effects of ET, the AWHC of the soil and deep percolation will be minimized in late fall, winter and early spring due to cold temperatures and frozen soil.

1.2. Study Objective and Components

The following are the objectives of this study.

1. To determine the impact of precipitation phase (rain or snow) on the annual runoff volume for basins in the study area.
2. To determine the relative impacts of evapotranspiration and depression storage on the annual runoff volume.
3. To assess the applicability of the concept of variable contributing area(s) models to plains watersheds, under both snowmelt and rainfall conditions.

1.3. Description of the Study Area

The study area encompasses the southeastern section of the province of Alberta bordered in the east by the Alberta-Saskatchewan border; in the south by the Red Deer River; on the west Highway 2; and in the north by the North Saskatchewan River. The region's rivers and climate stations are presented in Figure 1-2.

Within this general area, there are a number of small basins. These include Alkali, Berry, Blood Indian, Buffalo, Bullpound, Iron, Monitor, Ribstone and Sounding Creeks. Some of the basic statistics of these creeks are listed in Table 1-1.

Regulated reaches should not be utilized in the analysis since the recorded flow hydrograph does not reflect direct responses to snowmelt and rainfall inputs.

Gross and effective contributing areas for the basins is provided in the table. These two parameters are defined conceptually (PFRA, 1983):

The gross drainage area of a stream at a specific location is that plane area,

enclosed by its drainage divide, which might be expected to entirely contribute runoff to that specific location under extremely wet conditions. The gross drainage boundary is the drainage divide (i.e. the height of land between adjoining watersheds).

and

The effective ... drainage area is that portion of the drainage basin which might be expected to entirely contribute runoff to the main stream during a flood with a return period of two years. This area excludes marsh and slough areas and other natural storage areas which would prevent runoff from reaching the main stream in a year of average runoff.

PFRA (1983) has delineated these areas for most prairie rivers and streams from 1:50,000 topographic map sheets. These estimates are somewhat subjective because the map scale does not provide sufficient contour detail to determine the basin area accurately. However, the PFRA figures still indicate the tremendous variability that may be encountered, even when analyzing only the macro-scale environment.

The physiography of the eastern Alberta is relatively consistent. Macro-scale features are demonstrated by the gross changes in elevation. The southwest corner of the study area has an elevation of approximately 915 m above sea level. Proceeding north, northeast or east to the far extreme of the area results in an elevation drop to values in the range of 600 m. This is over distances of 200 to 360 km. Therefore, the macro-slope of the land ranges from 0.0016 to 0.0009. This lack of a regional slope, combined with a generally dry climate has resulted in a very poorly formed drainage network. Macro-topography dominates the hydrology of the entire area by failing to provide the energy slope sufficient to create a reasonable drainage network.

Within the region, the meso-scale topography is dominated by the effects of glaciation. Ground moraine and hummocky moraine deposits dominate. Most of the

area is covered with large till plains with irregular surfaces, resulting in the formation of many closed drainage basins with characteristic prairie sloughs and potholes.

1.4. Study Chapters

The following paragraphs provide a brief summary of the chapters that follow in this thesis.

Chapter 2 provides a literature review of the hydrologic variables identified by the opening discussion and study objectives. Section 2.1 provides an introduction to the chapter. The discussion in section 2.2 focuses on the role of the soil system in hydrology, particularly as applied to semi-arid plains. The topics include soil properties controlling water storage in a classical active soil system; and a discussion of snow-soil interactions. This is followed, in section 2.3, by a review of methods available to model ET for large areas. Section 2.4 reviews a number of studies of depression storage systems, on both the micro- and macro- scale, with particular emphasis on the net runoff loss that has been observed or estimated for a number of different locales and conditions. Finally, a number of studies of contributing area for flatland basins are discussed in section 2.5. These include several studies that were oriented to areas with similar physiography and climate to eastern Alberta.

The literature review addresses the hydrologic abstractions theorized in the study objectives as being important to the study area.

Chapter 3 introduces a Three Phase contributing area conceptual model based on the state of the soil system. The conceptual model hypothesizes that in the study area, the soil phase controls runoff as follows. The frozen soil phase yields high runoff volumes since losses are restricted to frozen soil infiltration, which is a relatively minor loss. The active soil phase generally yields no runoff since the soil moisture

deficit in the study area is generally very high, hence any rainfall infiltrates. The saturated soil phase is that area of the basin inundated and connected to the drainage network - the runoff coefficient for these areas is assumed to be 1.

Interpolation of climatic data proved to be a critical issue for this treatise. A numerical spatial analysis methodology for detailed interpolation of climatic data is discussed in chapter 4. The method is kriging, a technique for making optimal, unbiased estimates of regionalized variables at specified grid intervals using structured statistical relationships derived from a set of data values. This application is theoretically correct if the point data values are accepted as regionalized variables; i.e. $z(x,y)$ is a regionalized variable if z takes its value according to location x,y . Spatial analysis is utilized in later chapters to estimate snowmelt runoff depths for all elements of a one square kilometre grid over a drainage area.

Chapter 5 provides an assessment the annual snowmelt runoff volume. A drainage basin is assessed on an element by element basis to determine the snowmelt runoff volume for a number of years. The basin snowmelt runoff depth is statistically related to the recorded runoff. This relationship provides estimates of the snowmelt runoff contributing area and the depression storage deficit for the basin.

Chapter 6 assesses runoff from rainfall during the open water season. The output from a soil water budget model for all stations indicates there is no rainfall runoff from the active soil phase at any time. Therefore, any summer runoff that occurs would have to be from the saturated areas of the basin.

An assessment of the dynamics of the saturated area of a basin is provided in Chapter 7. The saturated area in the watershed is studied by analyzing the hydrograph response to rainfall inputs from spring and summer storms. A saturated area function

based on detention storage is developed and used to simulate the response of the outflow to summer rains on the saturated zone. The summer runoff from the saturated area is demonstrated to be minimal.

Chapter 8 provides an assessment of the frozen soil area for a number of basins. The role of the frozen soil phase as the major generator of runoff volume for prairie watersheds is supported by the analysis and discussion. The difficulties in the analysis are related primarily to the degree of regulation on the watersheds included. River basins with significant runoff regulation and withdrawal for consumptive uses such as livestock watering were difficult to include because the recorded runoff values do not relate directly to the climatic input. There were very few basins with natural runoff regimes, therefore the relationships developed were subject to statistical significance problems due to the low n value. Nevertheless, the results support the hypothesis that frozen soil runoff area is a constant for years in which there is sufficient spring snow water equivalent to overcome the combined losses to frozen soil infiltration and micro depression storage. Further, the results are applied with independently measured values of channel lengths, basin slopes and depression storage areas to derive relationships for basin depression storage and frozen soil phase area.

Chapter 9 provides a synthesis of the study, and a review and restatement of the conclusions from the individual chapters.

1.5. References

Alberta Environment, undated. Climate of Alberta, tables of temperature, precipitation and sunshine, report for 1980. Published by Alberta Environment from data compiled by the Atmospheric Environment Service, Environment Canada.

Branson, F.A., G.F. Gifford, K.G. Renard and R.F. Hadley, 1981. Rangeland Hydrology. Toronto: Kendal/Hunt Publishing Company

Card, J.R., 1979. *Synthesis of streamflow in a prairie environment*. In: 'The Hydrology of Areas of Low Precipitation,' Proceedings of the Canberra Symposium, December.

Chanasyk, D.S., 1980. A land use hydrologic response model. Unpubl. Ph.D. thesis, University of Alberta, Department of Civil Engineering, Edmonton, Alberta.

Eisenlohr, W.S. Jr., and others, 1972. *Hydrology of prairie potholes in North Dakota*. USGS professional paper 585-a.

Gray, D.M., P.G. Landine and R.J. Granger, 1985. *Simulating infiltration into frozen prairie soils in streamflow models*. Can. J. Earth Sci. 22, 464-472.

Hansen, V.E., O.W. Israelson and G.E. Stringham, 1980. Irrigation Principles and Practices. Toronto: John Wiley and Sons, INC.

Holocene, G., 1988. *Storage-effective drainage (SED) runoff model*. J. Hydrol., 98:295-314.

PFRA, 1985, 'The determination of gross and effective drainage areas for the prairie provinces.' Regina, Sask., Hydrology Report #104, Addendum #1.

PFRA, 1983, 'The determination of gross and effective drainage areas for the prairie provinces.' Regina, Sask., Hydrology Report #104.

PFRA, 1978, 'Report on calculations of gross and effective areas for the prairie provinces.' Regina, Sask., Hydrology Memorandum #25.

Stichling, W. and S.R. Blackwell, 1957. *Drainage area as a hydrologic factor on the Canadian prairies*. IUGG Proceedings, Vol. III, Toronto, Ontario.

Taylor, Colin H., 1982. *The effect on storm runoff response of seasonal variations in contributing zones in small watersheds*. Nordic Hydrology, 13: 165-182.

Viessman, W.J., John W. Knapp, G.L. Lewis and T.E. Harbaugh, 1977. Introduction to hydrology, San Francisco: Harper and Row, Publishers.

Table 1-1: Drainage Basins in the Study Area

Basin Name	WSC St.	PFRA Areas (km ²)		WSC Record	Mean Annual Q 1000s m ³	
		Gross	Effect			
Alkali Ck.	05ck005	590.0	377.4	1962-	2,140.	N
Berry Ck.	05ch007	3721.3	2377.1	1964-	11,400.	R
	05ch008	1546.2	1022.5	1967-	11,500.	R
Blood Indian	05ck001	694.6	604.2	1964-	2,710.	R
Buffalo Ck.	05fe002	709.1	247.6	1972-	5,650.	N
Bullpound Ck.	05cg003	1473.7	1066.3	1964-	3,650.	R
	05cg002	209.3	200.5	1962-80	1,840.	R
Iron Ck.	05fb002	3488.7	976.4	1965-	18,500.	N
	05cj005	2261.5	*****	1954-	76,800.	R
Monitor Ck.	05ga003	1438.0	326.3	1954-	3,310.	R
Ribstone Ck.	05fd005	1830.1	697.0	1968-	4,520.	N
Sounding Ck.	05ga008	2995.6	868.4	1970-	2,570.	R

In the far right column, R and N indicate the watershed is either regulated or natural flow, respectively.

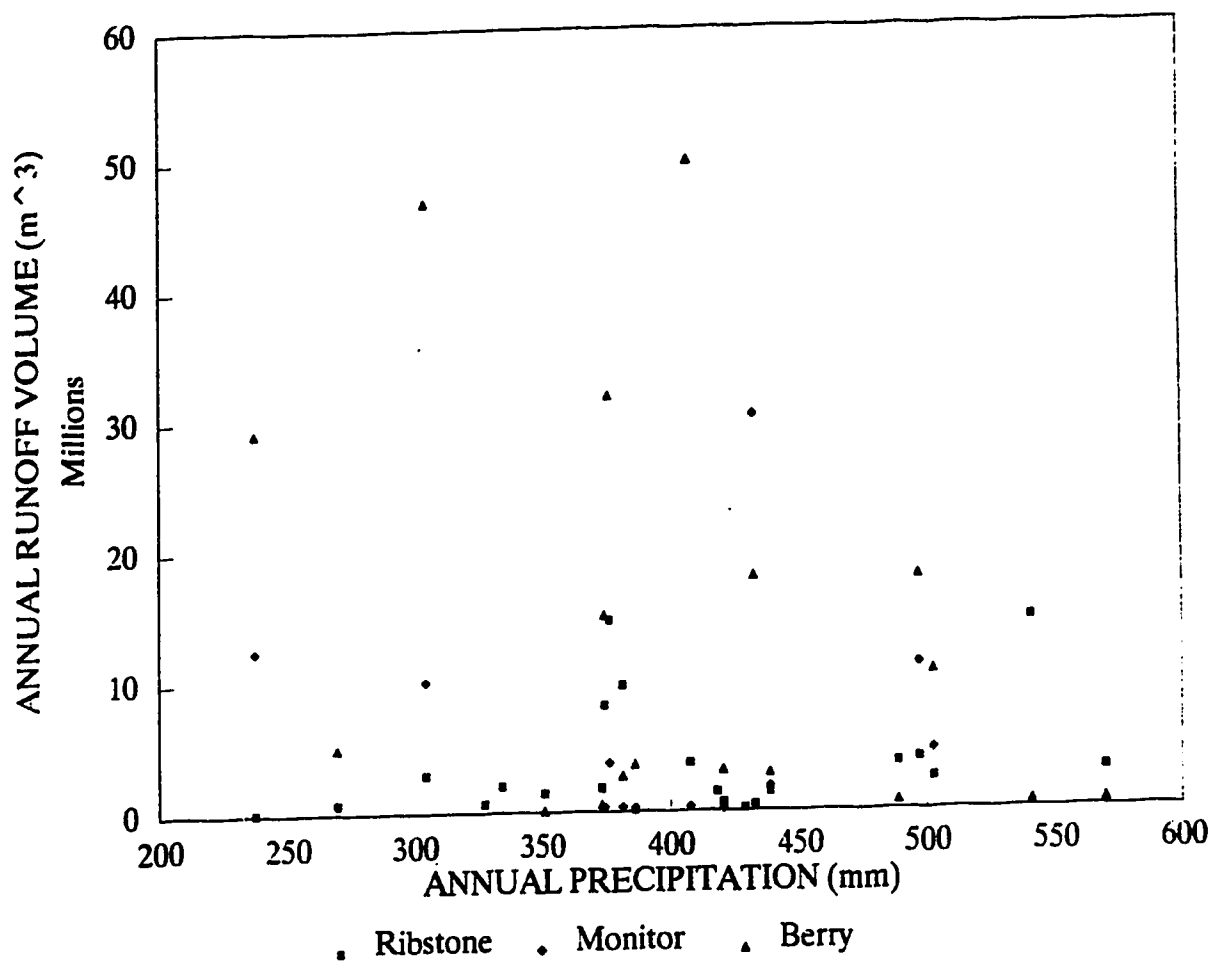


Figure 1-1: Runoff volume vs. annual precipitation for three basins in east central Alberta.



Figure 1-2: General location of the study region in Alberta.

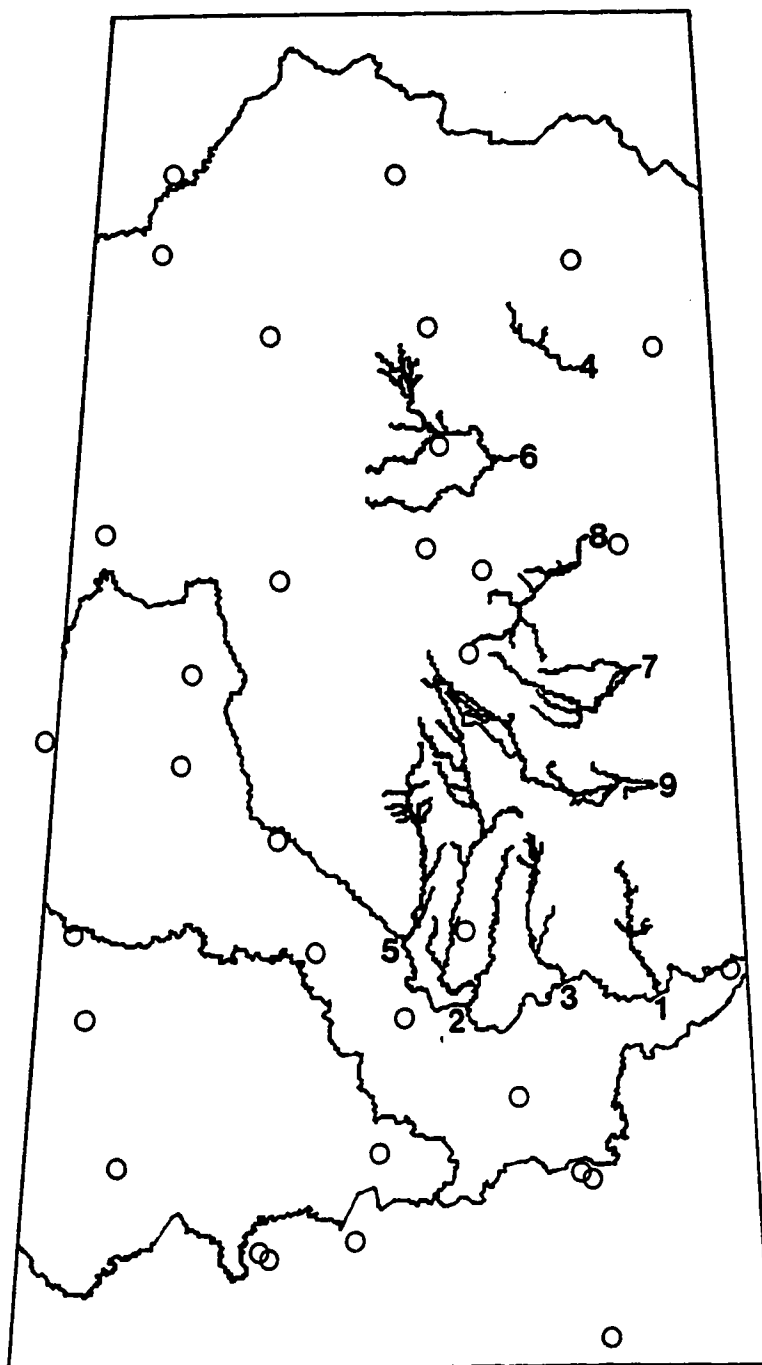


Figure 1-3: Southeastern Alberta watersheds and climate stations. Several stations outside these boundaries were used where necessary. Study watersheds are: 1 - Alkali, 2 - Berry, 3 - Blood Indian, 4 - Buffalo, 5 - Bullpound, 6 - Iron, 7 - Monitor, 8 - Ribstone, 9 - Sounding Creeks. Circles are climate station locations.

Chapter 2

LITERATURE REVIEW

2.1. Introduction

The discussion in this chapter reviews the individual and interactive roles of the soil, evapotranspiration, depression storage and drainage basin contributing area(s) in the hydrologic cycle. This thesis contends these are the variables that control the basin runoff. During periods when the soil water is frozen, soil related abstractions from precipitation/snowmelt are varied but minimal. Depression storage and contributing area are the major controls on the runoff yield. During periods when the soil water is unfrozen, a high evapotranspiration rate results in rapid depletion of any available soil water, so that runoff generally does not occur. Rainfall in excess of the soil infiltration capacity collects in localized small depressions, and either evaporates or subsequently infiltrates.

2.2. Soil Water Retention

Soil may be characterised as a combination of three different matter phases: solids, liquids and gases. The solid materials are either mineral or organic in origin. The soil mineral components are characterised principally by solids (grains), although some amount of mineral material is contained in a dissolved state in the soil water. This is a miniscule amount on a relative scale. Soil water occupies some portion of the porosity,² and soil gases, principally air, fill that portion of the voids not occupied by

²Soil porosity is generally defined as the ratio of the total volume of the pore space to the total volume of soil.

soil water. The quantities of soil air and water vary inversely; largely dependent on precipitation, the evapotranspiration potential and the water storage capability of the soil.

2.2.1. Classical soil water definitions

Soil water has been classified as hygroscopic, capillary and gravitational (Hansen et al., 1980). Hygroscopic water is molecularly bound to the soil grains, and does not readily move into or out of the soil under the forces of capillary tension or gravitational drainage. Capillary water is water in excess of the hygroscopic water that does not readily drain out of the soil under the force of gravity. Gravitational water is the water in excess of both hygroscopic and capillary water that will drain from the soil under the force of gravity. The boundary between capillary and gravitational water has been termed the field capacity of the soil, and is defined as the volume of water in the soil after gravitational water has been drained. The lower limit of capillary water is the permanent wilting point of the soil, and is defined as the soil water level at which plants can no longer withdraw adequate water to maintain plant needs. Capillary water is usually defined as the available water between the limits of field capacity and wilting point. This water is 'available' for plant use. The available water is considered as a reservoir for soil moisture budgeting.

These definitions are recognized as being theoretically incorrect (Hillel, 1980). However, they are convenient for some aspects of hydrology and soil water management.

2.2.2. Properties controlling unsaturated water storage

The quantity of available water is affected by the intermolecular forces and tensions within the soil matrix. These forces and tensions are affected most by soil texture and structure, and the organic matter content of the soil.

The definition of available water as water in excess of the hygroscopic water that does not readily drain out of the soil under the force of gravity is a simplification. Water held against the force of gravity may be held by true capillary forces; it may be water adsorbed to soil particles; and in the case of some soils (typically coarse grained soils), water may be retained in micro pools on the upper grain surface (Ward, 1975).

2.2.2.1. Soil texture

Texture is a definition of the size of the mineral particles making up the soil. These may range in size from gravel particles (>1.0 mm in diameter) to sand (0.05 to 1.0 mm), silt (0.002 - 0.05 mm) and clay (<0.002 mm) (Hansen et al., 1980).

Soil texture is used to classify a soil: sands are coarse materials, and sandy soils are considered to be coarse textured. Silts and clays are medium and fine textured soils, respectively. Soils with no dominant particle size; i.e. with approximately equal percentages of sand, silt and clay, are generally referred to as loams.

The particle size that dominates the mineral matrix determines the size of the greatest number of the pore spaces. Further, total porosity generally increases with decreasing grain size, assuming the soil structure has not been destroyed (Brady, 1990). Therefore, a soil with a predominance of fine grains will have a greater porosity and a greater capillary attraction than one with larger grains.

Adsorbed water is generally electrostatically attracted to the surface of the soil grains. The quantity of adsorbed water is dependent on the surface area of the grains.

The specific surface of a soil is the total surface area of the particles in a given unit volume of soil (Hillel, 1971). The specific surface increases with decreasing grain size, and as particles tend from spherical to elongated shapes. Clay particles are generally platy (Hillel, 1971) and therefore contribute a much greater surface area to a given soil volume. The specific surface of a sand may be less than $1 \text{ m}^2/\text{g}$ while the specific surface for a clay such as montmorillonite may as high as $800 \text{ m}^2/\text{g}$ (Ward, 1975).

A number of authors have developed estimates of available water storage values for different soil textures. Some of these are presented in Table 2-1.

2.2.2.2. Soil structure

Soil structure is the interconnection of soil particles into composite granules or aggregates. Structural formation takes place primarily in fine and medium textured soils, whereas in coarse soils, grain sizes are typically too large to facilitate multiple grain clumping (Hillel, 1971). A fine grained, well structured soil has a secondary "pore volume" made up of the spaces between the soil granules. In this type of soil, moisture storage is more difficult to define because the secondary pore volume created by the structure has a 'random' nature.

Factors that influence soil structure include physical processes, organic matter decay, physico-chemical colloidal interactions and soil tillage (Brady, 1990).

2.2.2.3. Soil organic matter

Soil organic matter contributes to the water storage capability of the soil. A given mass of humus (organic material) has an colloidal ability to hold water that far exceeds that of clays (Brady, 1990). The charged surfaces of humus particles act to create and maintain the soil structural components as well.

2.2.3. Soil water budgeting

Soil water budgeting is the process of determining how much water is present in the soil profile, and accounting for the inputs to and outputs from the soil, as defined by

$$\frac{dS}{dt} = I - O \quad (2.1)$$

where $\frac{dS}{dt}$ is the change in storage with respect to time, and I and O are inputs and outputs, respectively.

Expanding equation (2.1) to a form for modeling soil water content at any time t provides:

$$S_t = S_{t-1} + P_t - ET_t - DP_t - R_t \quad (2.2)$$

where S_{t-1} and S_t are the soil water storage at times t-1 and t and P = precipitation, ET = evapotranspiration, DP = deep percolation to groundwater, and R = runoff; during time interval t-1 to t.

The value of S_t at t = 1 must be known or estimated. P is available from standard climatic data and ET may be estimated with any of the methods discussed below. DP is difficult to determine without detailed field data, but in an arid environment, it is usually small enough to be neglected, except in exceptional cases. Shjeflo (1968) supports the contention that there is virtually no classical deep percolation in arid and semi-arid areas (classical being spatially uniform deep percolation of infiltration in excess of the currently available capillary storage). This is also supported by Freeze and Banner (1970), who stated that "only very intense rainfall (i.e. 350 mm or more in

several days) will cause ... a water table rise, and this only under favorable conditions of water table depth, soil type and antecedent soil moisture content." Meyboom (1966) reported that about 3% of annual precipitation contributed to groundwater through deep percolations from a small slough.

The runoff depth R is the precipitation in excess of the infiltration capacity of the soil. For an environment with a very low slope, a reasonable assumption is that the soil infiltration capacity is equal to the available capillary storage, since very little gradient exists to cause excess precipitation to run off. Practically speaking, some infiltration continues after the soil has reached field capacity; therefore, the infiltration capacity may be assumed to be greater than the available capillary storage.

2.2.4. Snow-soil interactions

The complexities of the interactions between the snowpack and the soil are rarely addressed in hydrology. Some of the lumped hydrologic models that are currently under use, such as the UBC watershed and flow model, do not present any method for dealing with either vapour or liquid water transfer between these two entities (Quick and Pipes, 1976). One prominent paper (Lvovich, 1980), in a review entitled 'Soil trend in hydrology' does not make any reference to the interactive role of snow and soil, preferring instead to concentrate completely on the role of the active soil phase.

This section presents a review of several papers that have begun the task of defining the inter-relations of the snowpack and the soil profile.

2.2.4.1. Guymon (1978)

Guymon reviewed snow-soil interactions as addressed in 39 papers dating from as early as 1943. A number of these papers were from the 1950s, '60s and early '70s; and hence, may be considered as somewhat dated. In introducing the paper, Guymon observed that the "paucity of a significant literature concerning snow-soil interactions is surprising since it is presumed that in most cases one would have to deal with such interaction to adequately deal with snow hydrology."

Theoretically, snow-soil interactions comprise a number of processes; including multi-phase fluid movement in porous media under hydraulic and thermal gradients, where the porous media conditions are under constant change due to fluid movement and phase changes. Air temperature and boundary layer wind conditions create the temperature gradient between soil and the atmosphere, and hence influence the rate of phase change and removal of water vapour to the atmosphere.

There is no practical physical or algorithmic method for simulating this system on an extensive geographic scale. However, semi-empirical methods based on the principal variables may be applied. A discussion of several applications follows.

2.2.4.2. Santeford (1978)

The interaction between the snowpack and a moss/soil layer was investigated over three years for a site in the Alaskan interior. Snow pillow sites were monitored with thermocouples at elevations of -30, -15, 0, 15, 30 and 45 cm from the soil surface, both at the pillow and a control case nearby. The initial objective was to investigate the effect of a snow pillow on the snowpack, soil temperature and moisture movement regimes. Therefore, vapour barriers were placed on the soil surface near the pillow in an attempt to separate these two effects. Fall soil moisture conditions were sampled prior to these installations. These conditions were measured again in spring, prior to any appreciable snowmelt.

Spring snowmelt typically occurred over a moss layer that remained frozen throughout much of the snowmelt period. Melting that did occur in the moss was quite late in the snowmelt period, and was limited to the upper layer.

Differences in the soil and snowpack moisture conditions between the snow pillow and vapour barrier locations, and the natural site were quite remarkable. The natural site recorded losses of soil moisture of approximately 20 mm (50%) for the three years, while the two sites with vapour movement inhibited lost between 5 and 10 mm (10-25%). However, the natural snowpack in early spring averaged about 30 mm greater in water equivalent. Large ice buildups were found on the lower sides of the vapour barriers.

Santeford concluded that under the temperature regimes for that area, there is a transfer of moisture from the soil to snow overwinter. Snow pillow and vapour barrier snowpacks provided close measures of the precipitation, but not of the total natural spring snowpack. The discrepancy is about 25 - 30 percent of an average moisture contained in the spring snowpack.

2.2.4.3. Gray et al. (1983)

This study took place in west central Saskatchewan. Soil moisture measurements were taken to a depth of 1.6 metres at a number of sites using a two-probe gamma density meter. These measurements were taken from early fall, through winter and into spring beyond the end of the snowmelt period for a period of five years.

In assessing the soil moisture changes over winter, two depths zones were identified. Zone one was identified as the upper 30 cm of soil, and was characterized as a depth from which moisture losses over winter were common. Zone two is the greater soil depth immediately below zone one. Typically this zone tended to gain moisture over winter. Water loss from zone one was hypothesized to be principally in a vapour

mode, while the lower zone probably had greater liquid water movements in response to freezing and/or drainage related to frost penetration. The general result was that the surficial zone typically tended to have lower moisture conditions in spring than were typical of the fall.

A wide range of moisture changes were observed for both soil zones over the period from freeze-up to the end of snowmelt. In some years, the layers would gain water; in others water was lost. Both layers recorded losses in excess of 33 mm of water, and gains of up to 15 mm for the upper zone, and 43 mm for the lower. On average, the lower zone gained about 10 mm, while the upper zone lost about 3 mm. Spring snowmelt infiltration would replace the moisture loss in the upper layer, but did not tend to have any effect on the lower soil zone. The control mechanism was refreezing of liquid snowmelt water in the upper soil zone.

Further changes in the soil moisture regime were not notable until the entire profile had thawed.

2.2.4.4. Granger et al. (1984) and Gray et al. (1985)

These papers focused on the development and application of an empirical model to simulate snowmelt infiltration to frozen soil. The depth of infiltration was related to the depth of an impermeable ice-soil layer and the ice-water content of the soil above the impermeable layer. The snow water equivalent at the beginning of melting was also observed to affect infiltration to frozen soil (Gray et al., 1983; Gray et al., 1985). The reasoning for inclusion of snow water equivalent is that infiltration will be subject to some degree to the heat introduced to the upper soil profile by infiltrating meltwater. However, no explanation of this physical phenomenon is presented.

2.3. Evapotranspiration

Evapotranspiration (ET) is the sum of two processes: evaporation and transpiration. Evaporation is defined as the vapourization of liquid water. In order for this change of phase to occur, there must be a heat input, defined as the latent heat of vapourization (L_v). Transpiration, as a biological process, is much more complicated than evaporation. However, for the purposes here, transpiration is defined as the net transfer of soil water to the atmosphere by the vegetation system. Again, this is a vapourization process, and requires the same input of (L_v) per unit volume of water.

2.3.1. Potential and Actual Evapotranspiration

Actual evapotranspiration is controlled by the water supply. If there is little water, either on the surface (ponded or in the surficial soil layer) or within the soil root zone, then very little ET can take place. If there is an unlimited water supply available, then ET is governed by climate conditions, and by the vegetation type and stage of growth (Gray, 1970).

The concept of potential ET (ETP) has been developed as the upper limit on ET. ETP has typically been defined based on the assumption of a water supply adequate to meet all vegetative needs (Thornthwaite, 1944; Penman and others, 1956). Given an adequate water supply, meteorological variables, including radiation, temperature, humidity and wind, are generally considered to have the strongest affect on ETP (Ward, 1975).

2.3.2. Formulas for Estimating ETP and ET

ETP and ET may be estimated with a number of techniques, including mass balance, energy balance, mass transfer, or from empirical formula developed from field observations with lysimeters. Neither mass or energy balance techniques are appropriate for use in this thesis. The analytical basis of the thesis applies a mass balance to determine runoff. Therefore, the method cannot be used to determine ET. Energy balance techniques require detailed radiation data that is not widely recorded. For these reasons, the discussion here focuses on the empirical formulas and on mass transfer techniques.

2.3.2.1. Empirical formulas for ETP/ET estimation

Much work has been carried out in developing empirical methods for estimating ET relates to irrigation crop studies. These methods, including Blaney and Criddle (1962), Jensen and Haise (1963), and many others, generally utilized climatic parameters as indices to reflect the potential water use by a reference crop, given an unlimited water supply. A representative empirical formula is the Jensen-Haise equation:

$$ETP_{JH} = C_t (T - T_x) R_s \quad (2.3)$$

where

ETP_{JH} = Jensen-Haise potential ET, mm water

T = Mean temperature for the time period, ° C

R_s = solar radiation, mm water

$$C_t = 1 / ((38. - 3.6 E / 305.) + 7.3 C_h)$$

$$C_h = 37.5 / (e_2 - e_1) \text{ mm Hg}$$

$$T_x = 27.5 - 0.33 (e_2 - e_1) - E / 1000$$

e_2 and e_1 = are the saturation vapour pressures for the mean maximum and mean minimum temperatures for the warmest month of the year, and

E = station elevation in metres.

The potential evapotranspiration ETP predicted by a method like OJensen-Haise is usually adjusted to estimate actual water consumption ET_{co} by any crop with a regionally defined, empirical coefficient K_{co} (Krogman and Hobbs, 1976): that relates the crop stage of growth and/or the percent of ground cover to the ETP calculation:

$$ET_{co} = K_{co} \text{ ETP} \quad (2.4)$$

where ET_{co} = actual evapotranspiration for crop co, K_{co} = regional coefficient for the crop, and ETP = reference potential evapotranspiration.

The application of Jensen-Haise is based on the assumption that there is an adequate water supply in the soil for the vegetation to utilize. This is the case in an irrigation situation, but during most of the time on the prairies, there is typically a moisture stress situation so that water use and growth proceeds slowly. Even at a time when there is adequate moisture, vegetation may not be capable of transpiring at the rate predicted by Jensen-Haise because the biomass quantity is low, reflecting previous dry conditions.

2.3.2.2. Mass transfer techniques for estimating ETP/ET

Mass transfer techniques for estimating ETP/ET are typically based on the formula first attributed to Dalton (Viessman et al., 1977):

$$E = f(u) (e_w - e_a) \quad (2.5)$$

where E is the evaporation, $f(u)$ is a function of the wind speed, and e_w is the saturation vapour pressure at the water surface temperature, and e_a is the actual vapour pressure of the air.

Penman(1948) developed a method for estimating ETP based on mass transfer techniques and a partitioning of incoming radiant energy to both evaporation and to heating of the air. The mass transfer equation took the form of (Ward, 1975):

$$Ea = 0.35 (e_w - e_a) (1 + U/100) \quad (2.6)$$

where Ea is a measure of the evaporation power of the air in mm/day; e_w , e_a are as in equation (2.5) with units of mm/Hg; and U is the windspeed in miles/day at a height of 2 m above the ground. E will increase with increasing turbulent mixing (windspeed) or with an increase in the vapour pressure gradient between the water and the air. The net radiation (H) available for evaporation is estimated with:

$$H = A - B \quad (2.7)$$

where A is the incoming shortwave radiation and B is the outgoing longwave radiation. H , A and B have units of mm/day. A and B are estimated as:

$$A = (1-r) Ra (0.18 + 0.55 n/N) \quad (2.8)$$

and

$$B = \sigma Ta^4 (0.56 - 0.09 e_a^{0.5}) (0.10 + 0.90 n/N) \quad (2.9)$$

where r is the reflection coefficient of the evaporating surface; Ra is the theoretical radiation total received at the surface, assuming no atmosphere; n/N is the ratio of actual to possible sunshine hours; σTa^4 is the theoretical reflected radiation, assuming no atmosphere; Ta is the mean air temperature in ° K; σ is the Stefan-Boltzmann constant; and e_a is as in equation (2.5).

Penman's potential evaporation is determined by combining equations (2.6) and (2.7) (Ward, 1975):

$$E = (\Delta/\gamma H + Ea)/(\Delta/\gamma + 1) \quad (2.10)$$

where Δ/γ is a dimensionless ratio of Δ , the slope of the saturation vapour pressure curve at the mean air temperature, and γ , the constant of the wet and dry bulb psychrometer equation; and E is the Penman potential evaporation.

Penman provides a detailed method for estimating both potential evaporation and ETP. ETP is estimated by using estimates of the vegetative cover reflectivity for r in

equation (2.8). Hansen et al. (1980) utilized a reflectivity of 0.23 (for a green growing crop) to estimate the potential daily water use by alfalfa. Surface reflectivity varies from 0.05 for open water to around 0.25 for an extended short greencrop (Ward, 1975).

2.3.3. Morton's ET

Morton(1978) has developed a method for estimating regional evapotranspiration based on a complimentary relationship between potential evaporation as estimated with Penman's equation and actual areal ET. The complimentary relationship assumes that the regional climatic conditions are the result of the available water supply, rather than the ET being a function of the climatic conditions.

Morton defines the complimentary relationship as

$$ET + ETP = 2 ETW \quad (2.11)$$

where ET is the actual areal evapotranspiration, ETP is the Morton potential ET, and ETW is the ET rate that would occur if there was an unlimited supply of water.

In order for this relationship to hold true, then

$$\frac{d ETP}{dt} + \frac{d ET}{dt} = 0 \quad (2.12)$$

Equation (2.11) predicts that for a situation with no water available, $ET=0$, and the $ETP=2 ETW$. With an increasing water supply, ET rises and ETP declines, to a point where $ET=ETP=ETW$ in a fully wet environment.

ET is a function of the available water supply, and is not easily determined.

However, *ETP* and *ETW* may be estimated from routine climate data. The complimentary relationship allows an estimate to be made of *ET* by rearranging equation (2.11):

$$ET = 2 ETW - ETP \quad (2.13)$$

The Morton model is somewhat more complicated than *ETP* models discussed earlier, but most of the complexity is due to the methodology adopted to predict radiation components from sunshine durations, and to additional functions that allow the model to be applicable over the globe (Morton, 1978).

The potential evapotranspiration *ETP* is defined for the Morton model as:

$$ETP_M = D R_A + (1-L) f_A (v-v_D) \quad (2.14)$$

where

R_A = net radiation for the surface (W/m^2)

f_A = vapour transfer coefficient ($W m^{-2} mbar^{-1}$)

v and v_D = saturation vapour pressures for the air and dewpoint temperature (mbar)

$D = (1 + \lambda / \Delta)^{-1}$

Δ = rate of change of saturation vapour with respect to air temperature ($mbar ^\circ C^{-1}$)

$\lambda = \gamma p + 4 \varepsilon \sigma (T + 273)^3 / f_A$ ($mbar ^\circ C^{-1}$)

γ = psychrometric constant ($^\circ C^{-1}$)

p = atmospheric pressure at station altitude (mbar)

σ = Stefan-Boltzmann constant ($\text{W m}^{-2} \text{ } ^\circ \text{K}^{-4}$)

ϵ = surface emissivity (dimensionless)

T = air temperature ($^\circ \text{C}$)

Equation (2.14) is the Penman formula as modified by Kohler and Parmele in 1967 (Morton, 1978).

Equation (2.14) predicts that as the difference between the air and dewpoint temperatures rises, evaporation will increase.

Equation (2.14) may be used in combination with equation (2.13) used to predict regional evapotranspiration in two cases:

1. Areas sufficiently large that the effect of the regional water supply on the regional airmass temperature and humidity are fully developed;
2. Areas small enough that evaporation from the area would not have any significant effect on the overlying airmass.

The assumption in equation (2.13) that ETP in an arid environment is twice the potential in a fully wet (humid) environment (ETW) was evaluated by Morton (1978) for a number of areas where the total aridity and fully watered assumptions were met. For two evaporation pans in southern California, one in an irrigated area, and the second in a dry desert, the regression relationship between the two potentials for the months of January to June was:

$$ETW = 0.40 + 0.57 ETP$$

This relationship had a correlation coefficient $R = 0.995$, and a standard error $SE_e = 0.5 \text{ mm/day}$. For July through December, the SE_e and R values were the same but the equation became

$$ETW = 0.36 + 0.518 ETP.$$

Both of these are quite close to the theoretical equation of

$$ETW = 0.5 ETP$$

thus supporting the assumption of equation (2.13).

Morton's ET calculation offers a further advantage that other methods discussed previously do not. There is no need for explicit maintenance of the soil water reservoir because Morton's technique calculates the ET based on the humidity of the overlying air. A certain humidity level indicates that some quantity of water has been evapotranspired. This lack of dependence on explicit knowledge of the available water supply releases the modeller from the need to quantify the soil water reservoir. Given an initial condition where the assumption of full available water holding capacity is reasonable, the modeller may assume that prior to any runoff taking place, rainfall must first replace the water that has been evapotranspired.

Morton has verified the use of the model for estimating the areal ET for periods of five years for 115 river basins world wide. These analyses included a large number of basins on the Canadian plains. The model estimates of net monthly winter time vapour transfer between the snow and the atmosphere (winter ET) have been validated using the Spring Creek research watershed in Alberta, and with data from White River, Ontario (Morton, 1978).

The Morton model estimates of "winter ET" are a reflection of the regional humidity. No information is available regarding whether water transfer to the atmosphere reflects a net loss from the snowpack, or from the soil, or some combination of net watergain or loss by either. The Morton model may be used to estimate the net water

exchange between the soil and the atmosphere during periods with no snow cover; and to estimate the net water exchange between the snow and the atmosphere when there is a snow cover on the watershed. During periods when the snow cover is in place, the soil water content is assumed to be stagnant. Previous discussion in this chapter (Gray, Granger and Dyck, 1983) reported average losses of about 3 mm of water from the upper 30 cm. of the soil. The assumption made here is that treating the soil water in the upper layer as stagnant is not unreasonable.

2.4. Depression Storage Studies in Prairie Soils

The role of depression storage in hydrology is qualitatively understood, but is very difficult to determine quantitatively. Within the literature, there is no attempt to define any boundary between what might be characterised as micro or macro depression storage. The definition developed here is that micro depression storage is storage that is sufficiently shallow that the combined effects of evapotranspiration and percolation to the regional groundwater system effectively empty the storage within a time frame of hours or days. A pothole or slough that maintains standing water throughout the spring and summer would be a macro depression.

The role of depression storage in the runoff regime of low relief, prairie watersheds is in significant dispute within the literature. A number of studies have been reviewed that deal with two modes of depression storage: macro and micro depression storage.

2.4.1. Macro depression storage studies

2.4.1.1. Meyboom (1966)

Meyboom carried out a detailed field study of the control exerted by phreatophytic vegetation (willow rings) on the groundwater flow around a slough in the Allan Hills of south central Saskatchewan. The Allan Hills are poorly drained, hummocky terrain with a multitude of small, surficially closed drainage basins. The slough that was studied has a well defined vegetation sequence typical of the aspen parkland of Saskatchewan.

Piezometers were utilized to monitor the flow conditions along a north south radius of the slough for a period in excess of 400 days. The hydraulic head observations at depths ranging from 1.5 to 15 metres were utilized to construct groundwater flownets for the different seasons.

The investigation provides two positive results. First, the role of the willow rings in controlling the movement of water from the slough to the regional groundwater system during part of the year is well defined. During periods when the slough contains water, and for short periods thereafter, there is a groundwater mound centred on the slough that results in both vertical flow of water to the regional system, and lateral flow of water that raises the watertable in the vicinity of the slough. Early in this period, there is little transpiration of groundwater (or soil water) by the willows. Once the slough is empty, the mound subsides due to hydraulic outflow and increasing transpiration by the willows. A groundwater table cone of depression is established as the willows continue to actively transpiring water from the saturated zone. This results in a reversed groundwater flow during the summer and fall, with water flow towards the willow ring to replace transpiration losses. Water that flowed laterally from the slough in spring flows laterally back to the slough (willow ring) in summer and fall. This flow continues after transpiration ceases in the fall until the watertable

depression under the willow ring has been eliminated. Once this has occurred, the groundwater flow is inferred as normal by Meyboom, meaning the groundwater flow near the slough follows the same trend as the regional groundwater system.

The net result of these changes is a seasonal reversal of the groundwater flow pattern around the slough. The spring groundwater mound beneath the slough is gradually removed by vertical and lateral flow, and by transpiration from the willows. As the hydraulic gradients outward from the mound decline to zero, transpiration continues, so that into summer and fall, the watertable below the willows is depressed, and the lateral flow pattern is reversed.

A second result of Meyboom's work is the water balance analysis that estimates the net contribution of the slough to the regional groundwater system for the period May 31, 1964 to June 1, 1965. The contribution to the regional groundwater flow is assumed to be equal to the net, rather than gross, outflow from the willow ring. For the period, the net contribution to the regional groundwater system is estimated as 10.7 mm as a depth over the drainage area around the slough. This was about 3 percent of the precipitation during the period of study. Meyboom indicates that during wetter or drier periods, the net contribution would be significantly higher or lower, respectively.

The slough setting will always be critical to the above interactions. Meyboom's study focused on one slough near the edge of the aspen parkland. Grassland sloughs are surrounded by vegetation that may or may not be phreatophytic. Largely permanent sloughs would maintain outflow longer, assuming outflow is in fact the dominant condition. Sloughs in groundwater discharge areas have very different hydrologic and ecologic regimes.

2.4.1.2. US Geological Survey (1968)

The USGS conducted a number of related studies on the hydrology of prairie potholes in North Dakota, including Shjeflo (1968), Eisenlohr and others (1972), and Sloan (1972). This subsection is a summary of these three papers.

The North Dakota region is described as a glacial drift plain of low relief, with numerous local potholes or sloughs originating from the meltout of dead ice blocks. The area has poorly established surface drainage, characterised principally by small surficially closed drainages surrounding the sloughs. This description is typical of eastern Alberta.

The dominant type of pothole in the North Dakota region is an effluent pothole - i.e. the slough contributed positively to the regional groundwater system. Sloughs in North Dakota that were felt to be dominantly influent are characterised by being at a very low relative elevation.

Table 2-2 presents a budget for pothole 8 monitored by Eisenlohr (1972). The seepage losses given are 152 mm (as a depth from the pothole) over a six month period. This is about twenty percent of the total water loss that is recorded for the pothole. However, this pothole had one of the lowest seepage rates of any of the potholes under study. Seepage rates in several of the other potholes ranges up to 2.7 times greater than that of pothole 8. High seepage rates to the groundwater system were recorded for potholes with a significant phreatophyte population. Potholes that were clear of phreatophytes had very low outflow seepage. The greater seepage losses were hypothesized to be due to water outflow along channels created by old and current plant roots. Pothole 8 was relatively free of phreatophyte growth. This is evident from the low seepage losses, and from the low transpiration total reported in Table 2-2.

Runoff inflow to the potholes for the years 1960-64 was dominated by snowmelt runoff over frozen soil. Shjeflo (1968) reported snowmelt to rainfall runoff ratios of 35:1, 1.4:1, 10.8:1, 1.1:1, and 1.6:1 for pothole 3. The average ratio of snowmelt runoff to rainfall runoff for the five years is about 10:1. These ratios demonstrate the general dominance of winter snows in the runoff interaction of the region. During years in which the ratio is low, potholes were either going dry or had very low water levels. For a pothole to retain standing water, a net annual gain from snowmelt runoff is required. The sum of the losses from pothole 8 during the summer period was 686 mm, while the rainfall runoff and rainfall directly onto the pothole was only 521 mm. The net loss of 165 mm would have to be made up from storage. The summer precipitation total of 439 mm is 70 mm above the long term average. Evapotranspiration and seepage outflow are relatively constant from year to year. The only source of water to make up the deficit is snowmelt runoff.

Some of the sloughs in North Dakota either overflowed or had some evidence of having overflowed in the past. However, no drainage pattern has been established other than small closed basins. The lack of any channel network indicates these sloughs do not linkup with surface drainage at any time. The only possible contributions to streamflow from the potholes is through seepage to the regional groundwater table.

2.4.1.3. Card (1979)

Card's study focused on developing statistical relationships for runoff as a function of precipitation and temperature. Within this process, a theoretical description of the role of depression storage in prairie hydrology was developed from observations on topographic maps and airphotos.

Card described depression storage as a medium for controlling the contributing area.

Figure 2-1 presents a schematic representation of the theory. Successive depressions fill according to the local runoff rate, and eventually begin to contribute to the streamflow once the depression storage is full. The following points describe the process with respect to the figure:

1. Depressions within area A of the figure are defined as directly draining to the main channel network , and with insignificant depression storage capability;
2. Area B contains depressions with significant storage, but that do overflow and drain into area A and the channel network;
3. Area C depressions, when full, flow directly to the channels of area B;
4. A further number of depression storage defined areas may exist, contributing in a similar manner once the storage capability has been met;
5. Area N depressions show no evidence of ever having overflowed, consequently there is no surface runoff contribution to streamflow from area N.

Card assigned general levels of frequency of overflowing: area A contributes almost always; area B less frequently; and so on to area N that could potentially contribute, but there has never been an event of sufficient magnitude.

The weakness in Card's analysis is the use of 1:50,000 NTS sheets that do not have sufficient resolution on either the horizontal or vertical (7.62 m contour interval) to define the depression storage. Depending on the terrain, individual depressions may or may not be easily recognized, and the storage capability may be very difficult to define, even in relative terms.

2.4.2. Micro depression storage studies

2.4.2.1. Mitchell and Jones (1976), (1978)

The objectives of these studies was the quantification of surficial micro depression storage and development of a depth-storage model. Elevation data were collected for 258 surfaces on five soils and three artificial surfaces with a 2.54 cm grid. The soils and artificial surfaces were small laboratory bins. Surface areas dealt with ranges from 91 x 91 cm impervious styrofoams to 1 x 2 m soil plots. Soil textures included silt loam, silty clay and loamy sand.

The absolute relief on each surface was measured relative to the lowest point on the surface (the lowest point became the elevation datum). Absolute relief was related to the observed depression storage depth with a relationship

$$S_d = a D^b \quad (2.15)$$

where S_d = micro depression storage depth, D = absolute relief of the surface and a, b are regression coefficients.

The results of this study are presented in Table 2-3 (the regression were run by Mitchell and Jones on data values measured in inches, therefore, inches are the units presented here). The range of micro depression storage depths in Table 2-3 is quite large, and represents a significant portion of the total surface relief. For example, the loamy sand (L S), with an N value of 40, recorded a range of 2.8 to 7.9 inches of relief. The micro depression storage range for this soil type was from 0.792 to 4.37 inches. Other soils demonstrated higher ranges, and the peak value recorded was about 7.5 inches of storage. The R^2 values are all very high, reflecting a strong relationship between the micro relief and the micro depression storage.

2.4.2.2. Gayle and Skaggs (1978)

This study investigated the relative roles of macro and micro depression storage for a number of agricultural fields. All surfaces tested were disturbed with cultivators and disks.

Micro depression storage was measured using 40 cm diameter test plots treated with a soil sealant to prevent any infiltration. Careful attention was given to minimizing the disruption of the micro structure of the surface during sealing. Measured quantities of water were evenly applied to the surface, until runoff began. Micro depression storage was calculated as the total volume of water minus the runoff volume.

Micro depression storage depths for the soil surfaces ranged from less than 1.0 mm to 33 mm, depending on the soil type and surface operation (cultivated, planted, harvested, etc.). Organic and sandy loam soils had generally low micro storage values, ranging up to 4 mm. However, freshly cultivated organic soil consistently had storage depths of 14 to 23 mm. Fine textured soils had values less than 3 mm except in the case of fresh cultivation, where storage was consistently in the 7 to 8 mm range.

Macro depression storage was measured on flat cultivated fields with elevation surveys. Surface storage took place in undulations in the furrow bottoms. Organic and sandy soils demonstrated high macro storage capability in all cases, relative to micro storage. These ranged from 13 mm for stubble type land to 33 mm for recently worked soil. However, storage levels declined as rainfall and other elements compacted the soil.

These results indicate small scale depression storage is highly variable, depending on soil type and land use/tillage practices. A prediction was made that flatlands with in the North Carolina Tidewater Region have macro storage values of 15 mm or more.

2.4.2.3. Summary - Depression Storage Literature

Major or macro depressions in a prairie environment interact to some degree with the regional drainage (Card, 1979), but the very existence of macro depressions indicates that most do not overflow and contribute to surface runoff to a significant degree. If overflow does occur, major hydrologic events since the last glaciation would have downcut the depression outlet, thereby destroying the depression (Eisenlohr, 1972).

Micro depressions may account for significant regional water retention, with values reported to be in the range of 10 mm up to 150 mm or more. This storage is very difficult to assess for any area since the micro relief is the principal control variable, and there is no practical explicit method for estimating the spatial variation in micro relief over a basin of the area of interest to this study. The only approach that is possible at this time for dealing with the micro depression storage capability of a basin are implicit methods that estimate the micro storage over the basin.

2.5. Contributing Area

Contributing area is the most important parameter in prairie hydrology in many situations, and yet it is the parameter for which there appears to be the least understanding. A number of studies have been carried out dealing with contributing area as either a static and dynamic factor in the watershed. Discussion of these studies follows.

2.5.1. Contributing Area Studies

2.5.1.1. Card (1979)

The investigation carried out by Card was outlined in the review of depression storage literature. In making a case for the interaction of depression storage and contributing area, Card presents the following supporting quotation (Stichling and Blackwell, 1957):

Drainage area is usually regarded as the most obvious and readily available factor in a hydrologic study of a basin. Accordingly, formulas and graphs have been developed to determine the runoff characteristics of an area using drainage area as the common denominator. However, the drainage area of streams in regions subjected to glacial transformation and deposition is often difficult to determine. On the Canadian prairies, for instance, great fluctuations in the drainage basin boundaries have been observed in dry and wet years and in different seasons of the year.

However, Card offers no evidence from Stichling and Blackwell, or any other source that supports that quantitative observations have been made.

2.5.1.2. Taylor (1982)

The variation in storm runoff due to expansion and contraction of a saturated zone(s) in two watersheds in south-central Ontario was investigated by Taylor (1982). The study watersheds were located in an area with a thick glacial till cover, and with numerous drumlinoid features composed of sandy till. The low lying swales between the drumlins were typically wetlands that fluctuated in size, depending on the available water and the season. Spring snowmelt typically provided the highest runoff quantities. Both watersheds had very low general slopes (< 3 percent), with localized slopes of around 8 percent on the drumlins. Significant portions of both watersheds were reported to be very flat, and one of the watershed was undergoing a significant urbanization.

The saturated areas were mapped in the field on a regular basis. Outflows were

measured with several weir installations, and a network of rainfall and snow gauges were used to record inputs. Snow water equivalent surveys were carried out as well.

A baseline relationship was developed relating the surveyed saturated area A_s to the current streamflow volume and an antecedent precipitation index. The relationship for A_s as a function of streamflow provided a good statistical fit ($R = 0.967$); evidence that the saturated area was interacting with the runoff network. The relationship was

$$A_s = 0.155 + 0.0034 Q$$

This relationship was used to forecast the quick runoff expected from 27 runoff events. Initially, the predictions were not accurate, but this was found to be due to the assumption of a static saturated area extent proportional to the antecedent discharge. The actual area would expand quite quickly under conditions with a high moisture index; i.e. spring and early summer. A better estimate of the extent of the saturated area was achieved by using peak flow for an event, rather than the discharge at the beginning of the event. Using peak flow resulted in a better estimate of the saturated area, and a stronger relationship between predicted and observed quick flow runoff. This is not surprising since peak flow and the extent of the saturated area are strongly related. This method would not be functional for predicting runoff since the peak runoff is required to estimate the mean size of the saturated area. However, Taylor documents the rapid response of saturated areas to rainfall inputs in several low slope watersheds.

2.5.1.3. Gray, Landine and McKay (1985)

This paper focused on estimating the apparent contributing area for spring snowmelt for Wascana Creek at Sedley, a 1634 km² basin located 50 km southeast of Regina, Saskatchewan. The basin topography is characterised as flat to gentle rolling, with poor drainage development because of the low regional relief. Most of the basin is under cultivation, with dryland cereal crops being the predominant crop.

Standard climatic and Water Survey of Canada snowmelt data were used to develop estimates of the unit runoff potential (URP) and an "apparent" contributing area for snowmelt runoff for a number of years. The data are presented in Table 2-4 and are plotted in Figure 2-2. URP is defined as:

$$URP = SWE + PPT - INF \quad (2.16)$$

where SWE is the spring snow water equivalent, PPT is any precipitation occurring during snowmelt and INF is the infiltration to frozen soils. All values were in mm of water.

A strong linear relationship was found here between URP (a length) and the streamflow volume (length³) ($r^2=0.947$). The slope of the regression line must have the units of length² (an area), and the intercept units of length³. Therefore, the slope of the line represents the area over which URP is integrated to produce a runoff volume. The fact the relationship is linear indicates the slope is constant, thereby implying the spring snowmelt contributing area is a constant. This observation is unexpected given the general assumption that prairie rivers operate with a variable runoff area that increases with increasing runoff depth. The slope of the regression

line in Figure 2-2 is 0.332 - adjusting the units indicates the area would be 332 km².³

The regression contributing area was different from the average of the "apparent" contributing areas calculated by Gray et al., presented in Table 2-4. The apparent area was the area that gave the closest estimate of recorded runoff volume for each year. However, the URP values were not adjusted to reflect any losses to depression storage. The intercept on the Y axis (runoff volume) as -3157534 m³. This value represents the depression storage capability of the basin.

2.5.1.4. PFRA (1978), (1983), (1985)

PFRA (1978) assessed the gross and effective drainage areas for 1191 hydrometric stations on the Canadian prairies. Gross and effective drainage area definitions were adopted as follows:

The gross drainage area of a stream at a specified location is the plane area, enclosed by its drainage divide, which might be expected to entirely contribute runoff to that specific location under extremely wet conditions. The gross drainage boundary is the drainage divide (i.e. the height of land between adjoining watershed).

The effective drainage area is that portion of a drainage basin which might be expected to entirely contribute runoff to the main stream during a flood with a return period of two years. This area excludes marsh and slough areas and other natural storage areas which would prevent runoff from reaching the main stream in a year of "average" runoff.

Assessments of the gross and effective areas were carried out on 1:50,000 NTS map sheets, as was the work carried out by Card (1979). Both of these studies depended

³This value is slightly different than the value reported by Gray et al. They adjusted the 1978 URP to reflect snow survey data from the channel network - this adjustment was not applied to the other data points. The regression here uses the unadjusted 1978 URP value.

heavily on a conceptual, qualitative approach that began, particularly in the case of the PFRA, with an assumption that the variable area concept was the governing control in prairie hydrology. This assumption has not been proven, and may not be proven with qualitative assessments from 1:50,000 maps. The contour interval of these maps is likely far too great to allow for resolution of small topographic features that control depression and detention storage.

2.5.1.5. Holocek (1988)

This work presented a storage-effective drainage (SED) model that describes the contributing area function of Spring Creek, a low slope basin that is characterized by Holocek as both a prairie basin and a basin covered with pristine boreal forest. Spring Creek is in fact a forested basin, and the prairie reference is most likely an indication that the basin is relatively flat (John Taggart, Alberta Environment, Hydrology Division, pers. comm.). The Spring Creek Watershed is 112 km².

The SED model assumes the contributing area extent for any storm is dependent on the basin water storage. With greater basin storage, the contributing area will be greater. A runoff coefficient ϕ is defined as $\phi=R/P$ where R is the runoff depth (mm) spread over the maximum contributing area C , and P is the precipitation depth (mm). The relative contributing area $x_i=A_i/C$, where A_i is the actual area contributing for event i . x_i is therefore dimensionless, having limits of $0 < x < 1$. Holocek defines the relative basin storage y_i in the same manner. For event i , the relative basin storage $y_i=S_i/S_{\max}$, where S_i is the actual basin storage, and S_{\max} is the maximum basin water storage capability. Basin storage was simulated using mass balance techniques.

Fourteen selected flood events occurring between 1966 and 1983 were analyzed. The data are included here as Table 2-5. The data have been plotted in three formats in Figure 2-3. Figure 2-3A is a scatter plot of the actual runoff depth estimate against

the basin storage, as estimated by Holocek's water balance model. Holocek's principal thesis was that the basin storage at time t determined what the contributing area would be for a storm beginning at time t . However, storage and runoff depth did not relate that well (Figure 2-3A). This is not unexpected since there is no consideration given for the adjustment to basin storage that would occur from the rainfall depth prior to significant runoff beginning. Figure 2-3B is a plot of basin storage against the runoff coefficient $\phi = R/P$, as defined earlier. This relationship does allow for the initial losses to basin storage, and it is obvious from the figure that the two parameters have a strong linear relationship. The break in the relationship as the line nears the x axis is not unexpected. As the basin dries, the moisture conditions reach a threshold point at which virtually all the area in the basin is at a low moisture storage capacity, and hence, no runoff is generated because the soil is very dry, and all rain is absorbed. For Spring Creek, this point appears to be around a basin storage depth of approximately 110 to 120 mm. Below this threshold point, there is likely only a very small wet area in the basin, and the runoff coefficient ϕ changes very slowly with changes in storage.

Figure 2-3C presents the SED curve as defined by Holocek for the Spring Creek watershed. The curve is a plot of normalized basin storage and normalized contributing area. The curve shape imposed upon the points by Holocek is presented in the figure as well. This curve is defined by

$$X_{est} = \alpha / (1 + \beta \exp(\gamma Y_{est})) \quad (2.17)$$

where α , β and γ have been defined with regression iterations as 0.780, 1021.317 and -13.534, respectively. This equation was utilized to generate the curve in Figure 2-3C.

The SED model describes a basin response to rainfall events as a function of the

basin water storage. The runoff depth from a given basin input varies linearly with the basin storage for values in excess of about 100 mm (Figure 2-3B). Below that threshold value, the runoff coefficient, and therefore, the runoff, is minimal.

There has been some unpublished success with applying the SED model to several other basins in Alberta (John Taggart, Alberta Environment, Hydrology Division, pers. comm.).

2.6. References

Blaney, H.F. and W.D. Criddle, 1950. *Determining water requirements in irrigated areas from climatological and irrigation data*. USDA Soil Conservation Service, Tech. paper 96.

Brady, N.C., 1990. *The Nature and Properties of Soils*, 10th ed. New York: MacMillan Publishing Company.

Card, J.R., 1979. *Synthesis of streamflow in a prairie environment*. In: 'The Hydrology of Areas of Low Precipitation,' Proceedings of the Canberra Symposium, December.

Eisenlohr, W.S. Jr., and others, 1972. *Hydrology of prairie potholes in North Dakota*. USGS professional paper 585-a.

England, C.B., 1970. *Land capability: a hydrologic response unit in agricultural watersheds*. USDA, ARS 41-172.

Freeze, R. A. and J. Banner, 1970. *The mechanism of natural groundwater recharge and discharge 2. Laboratory column experiments and field measurements*. WRR 6,1.

Gayle, G.A. and R.W. Skaggs, 1978. *Surface storage on bedded cultivated lands*. Transactions of the ASAE. 21:101-109.

Granger, R.J., D.M. Gray and G.E. Dyck, 1984. *Snowmelt infiltration to frozen prairie soils*. Can. J. Earth Sci. 21:669-677.

Gray, D.M., ed., 1970. *Handbook on the Principles of Hydrology*. National Research Council of Canada, Ottawa.

Gray, D.M., R.J. Granger and G.E. Dyck, 1983. *Overwinter soil moisture changes*.

Meeting of American Society of Agricultural Engineers, Session: Infiltration and Porous Media Flow, Chicago, IL., Dec. 14, Paper 83-2513.

Gray, D.M., P.G. Landine and R.J. Granger, 1985. *Simulating infiltration into frozen prairie soils in streamflow models*. Can. J. Earth Sci. 22:464-472.

Gray, D.M., P.G. Landine and G.A. McKay, 1985. *Forecasting streamflow from snowmelt in a prairie environment*. CSCE Annual Conference, Saskatoon, Sask., May 27-31.

Guymon, G.L., 1978. *A review of snow-soil interaction*. in Proceedings: Modeling of snow cover runoff. U.S Army Cold Regions Research and Engineering Laboratory, Hanover, N.H., Sept. 26-28.

Hansen, V.E., O.W. Israelson and G.E. Stringham, 1980. *Irrigation Principles and Practices*. Toronto: John Wiley and Sons, INC.

Hillel, D., 1980. *Applications of Soil Physics*. Toronto: Academic Press.

Hillel, D., 1971. *Soil and Water: Physical Principles and Processes*. New York: Academic Press, Inc.

Holocek, G., 1988. *Storage-effective drainage (SED) runoff model*. J. Hydrol., 98:295-314.

Jensen, M.E. and H.R. Haise, 1963. *Estimating evapotranspiration from solar radiation*. ASCE, Journal of the Irrigation and Drainage Division, 103, IR2, 15-41.

Kohler, M.A. and L.H. Parmele, 1967. *Generalized estimates of free-water evaporation*. WRR, 3:996-1005.

Krogman, K.K. and E.H. Hobbs, 1976. *Scheduling irrigation to meet crop demands*. Canada Department of Agriculture Pub. No. 1590.

Lvovich, M.I., 1980. *Soil trend in hydrology*. Hydrological Sciences Bulletin, 25, 1.

Mitchell, J. K. and B. A. Jones, 1976. *Micro relief surface depression storage: analysis of models to describe the depth storage function*. AWRA Water Resources Bulletin, 12, 6.

Mitchell, J. K. and B. A. Jones, 1978. *Micro relief surface depression storage: changes during rainfall events and their application to rainfall-runoff models*. AWRA Water Resources Bulletin, 14, 4.

Morton, F.I. 1978. *Estimating evapotranspiration from potential evaporation: practicality of an iconoclastic approach*. J. Hydrol., 38:1-32.

Oosterveld, M. and C. Chang, 1980. *Empirical relationships between laboratory determinations of soil texture and moisture retention*. Can. Ag. Eng., 22:149-151.

Penman, H.L., 1948. *Natural evaporation from open water, bare soil and grass*. Proc. R. Soc. London, Ser. A., 193:120-145.

Penman, H.L. and others, 1956. *Discussions of evaporation etc.*, Neth. J. Agric. Sci., 4:87-97.

PFRA, 1985, *The determination of gross and effective drainage areas for the prairie provinces*. Regina, Sask., Hydrology Report #104, Addendum #1.

PFRA, 1983, *The determination of gross and effective drainage areas for the prairie provinces*. Regina, Sask., Hydrology Report #104.

PFRA, 1978, Report on calculations of gross and effective areas for the prairie provinces. Regina, Sask., Hydrology Memorandum #25.

Quick, M. C. and A. Pipes, 1976. *A combined snowmelt and rainfall runoff model*. CJCE 3, 449-460.

Santeford, H.S., 1978. *Snow soil interactions in interior Alaska*. In: S.C. Colbeck and M. Ray, eds. *Proceedings of Modeling Snowcover Runoff*. U.S Army Corps of Eng., Cold Regions Research Lab., Hanover, N.H.

Shjeflo, J. B., 1968. *Evapotranspiration and the water budget of prairie potholes in North Dakota*. USGS professional paper 585-b.

Sloan, C. E., 1972. *Groundwater hydrology of prairie potholes in North Dakota*. USGS professional paper 585-c.

Stichling, W. and S.R. Blackwell, 1957. *Drainage area as a hydrologic factor on the Canadian prairies*. IUGG Proceedings, Vol. III, Toronto, Ontario.

Taylor, C. H., 1982. *The effect on storm runoff response of seasonal variations in contributing zones in small watersheds*. Nordic Hydrology, 13: 165-182.

Thornthwaite, C.W., 1944. A contribution to the report of the Committee on Transpiration and Evaporation, Trans. AGU, 25:686-693.

Ward, R.C. 1975. *Principles of Hydrology*, 2nd. ed. London: McGraw Hill Book Company (UK) Limited.

Table 2-1: Soil texture and related moisture storage capability.

Soil Texture	Approx. Water Storage cm/m		
	1	2	3
sandy	13.3	8.	-
sandy loam	12.3	12.	11.3
loam	15.6	17.	13.9
silt loam	19.9	-	16.0
clay loam	12.7	19.	14.6
silty clay	12.3	21.	12.3
clay	11.5	23.	13.9

1 = England (1970)
 2 = Hansen et al. (1980)
 3 = Osterveld and Chang (1980)

Table 2-2: Water budget for a prairie pothole, North Dakota (Eisenlohr, 1972)

Component	May to Oct. depth mm
evaporation	332.
transpiration	201.
net seepage outflow	153.

Total Decrease	686.
	=====
precipitation	439.
runoff	82.

Total Increase	521.
	=====
computed decrease in storage	165.
measured decrease in storage	165.

Residual Error	0

All values are depths on the pothole surface.

Table 2-3: Results of Mitchell and Jones (1976) for micro depression storage depths on test plots of variable relief.

Soil	N	Relief		Measured		Regression		Coefficients		R ²	
		max.	min.	max.	min.	max.	min.	a	b	max.	min.
Si L	40	10.1	3.7	5.04	0.68	.486	.0028	3.59	1.41	.998	.992
Si L	56	11.8	4.9	4.99	1.77	.127	.0029	3.33	2.05	.999	.990
L S	40	7.9	2.8	4.37	0.79	.321	.0005	4.51	1.83	.999	.989
Si C	62	12.9	9.0	7.49	4.45	.039	.0013	3.37	2.23	.999	.996
All	214	12.9	3.7	7.49	0.68	.486	.0005	4.51	1.41	.999	.989

Storage was related to relief with $S_d = aD^b$.

Table 2-4: Unit runoff potential URP, observed runoff and apparent contributing area (Gray et al., 1985)

	Unit Runoff Potential mm	Observed Streamflow Volume 10⁻⁶ m³	"Apparent" Contributing Area km²
1972	25.1	3.63	144
1974	90.0	24.00	267
1976	63.0	21.50	341
1978	16.8	3.00	188
1979	47.0	12.75	271
1980	26.0	4.25	163
1982	64.6	19.13	296

URP = SWE + PPT - INF

SWE = spring snow water equivalent

PPT = precipitation during snowmelt

INF = snowmelt infiltration to frozen soil

Table 2-5: Fourteen selected flood events, Spring Creek, Alberta.

Flood No.	date	P mm	D mm	R/P	S mm	Y _{est}	X _{est}
1	05/15/79	38.0	32.3	0.850	256.	1.000	.850
2	04/24/69	25.3	15.4	0.609	200.7	.784	.777
3	06/11/79	88.9	50.0	0.562	184.3	.720	.781
4	07/25/83	99.6	53.0	0.532	186.9	.730	.729
5	06/24/76	105.7	52.1	0.493	176.6	.690	.714
6	08/16/76	114.3	55.8	0.488	186.6	.729	.669
7	07/10/71	46.7	26.4	0.565	198.4	.775	.729
8	06/25/71	48.3	19.9	0.412	171.5	.670	.615
9	06/13/71	66.5	22.2	0.334	151.0	.590	.566
10	06/12/68	69.4	15.2	0.219	145.9	.570	.384
11	08/03/76	56.7	8.4	0.148	128.0	.500	.296
12	08/27/66	70.4	5.2	0.074	99.8	.390	.196
13	06/27/75	78.7	5.2	0.066	112.6	.440	.150
14	08/21/67	12.7	0.01	0.001	3.8	.015	.067

P = precipitation D = runoff S = basin storage at storm start
Y_{est} = normalized storage X_{est} = normalized contributing area
data from Holocene (1988).

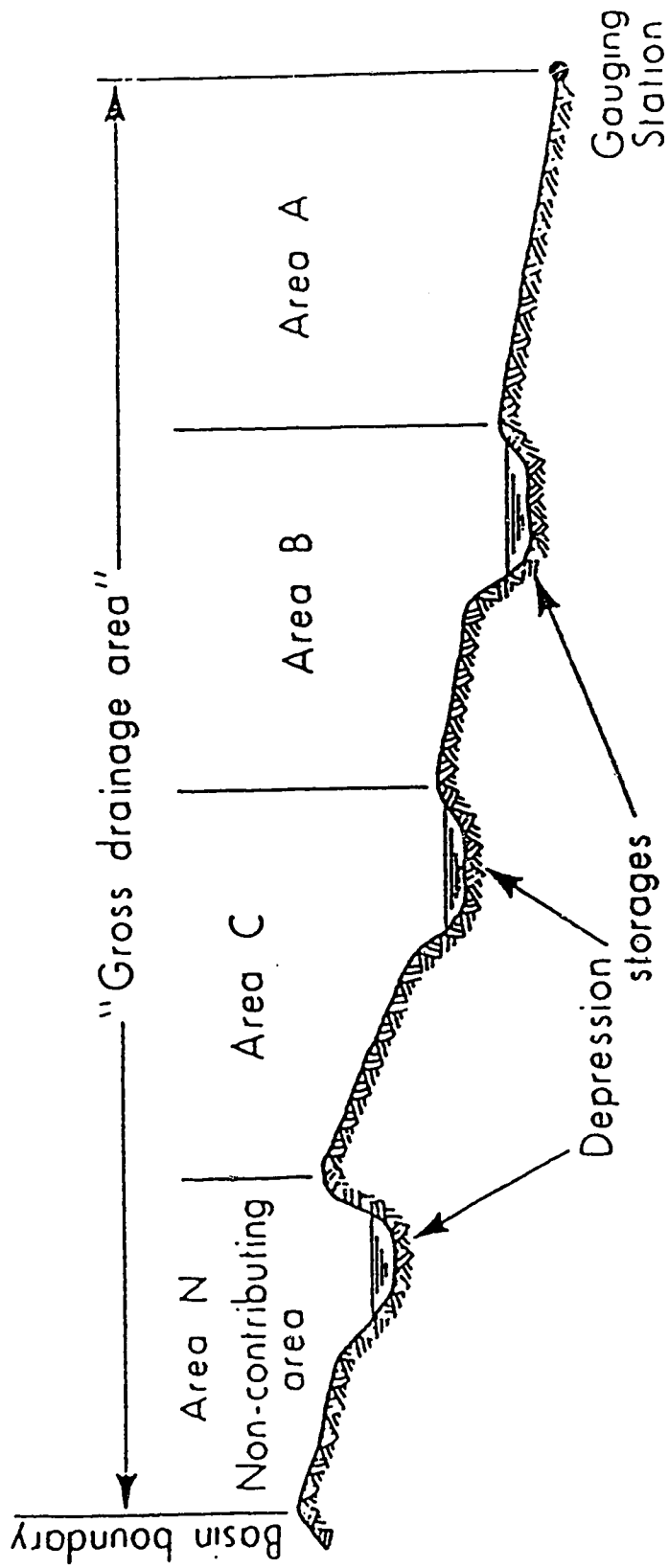


Figure 2-1: Depression storage - variable contributing area interaction in a prairie environment (Card, 1979)

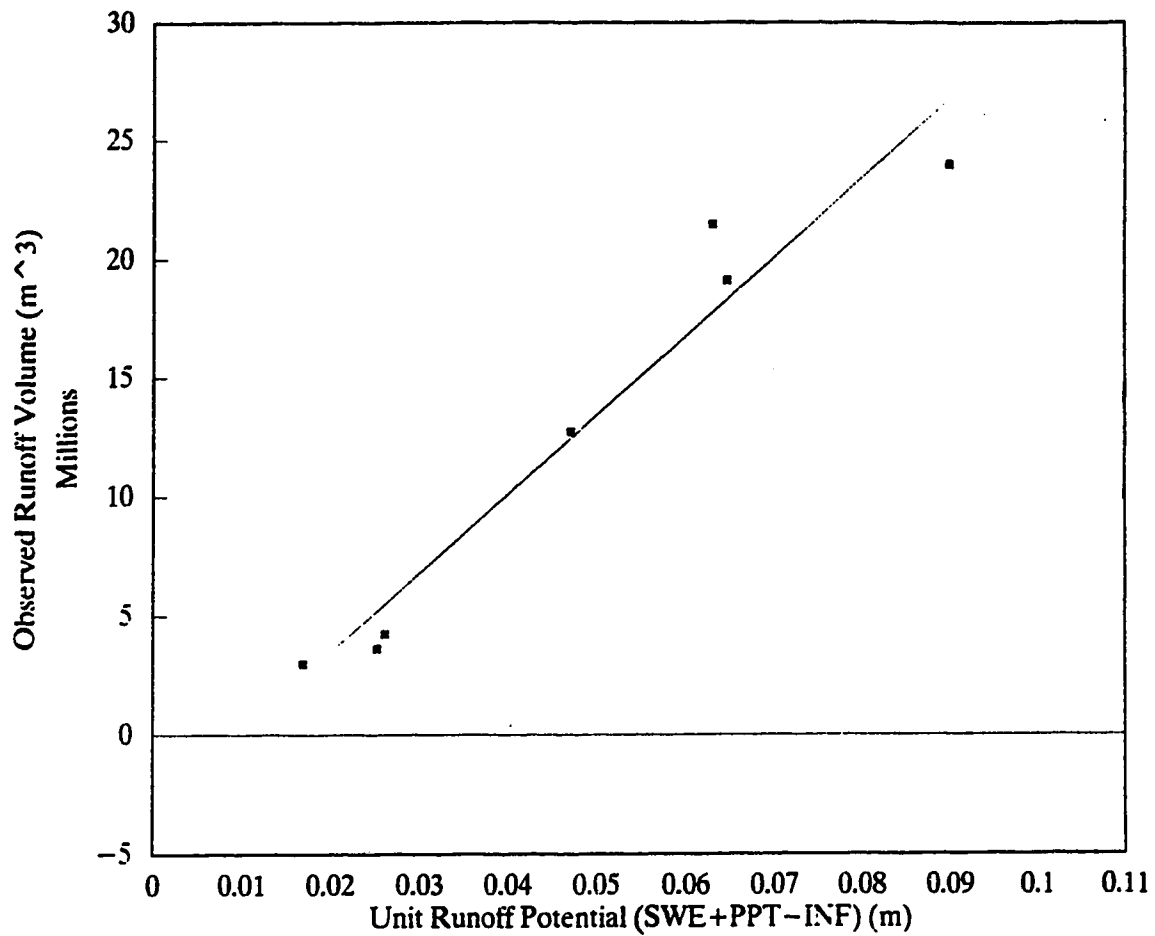


Figure 2-2: Unit runoff potential and volume relationship for Wascana Creek, Saskatchewan (after Gray et al., 1985). The best fit line equation is $\text{RUNOFF} = 3.3\text{E}8 \text{ URP} - 3157534$, $r^2=0.947$.

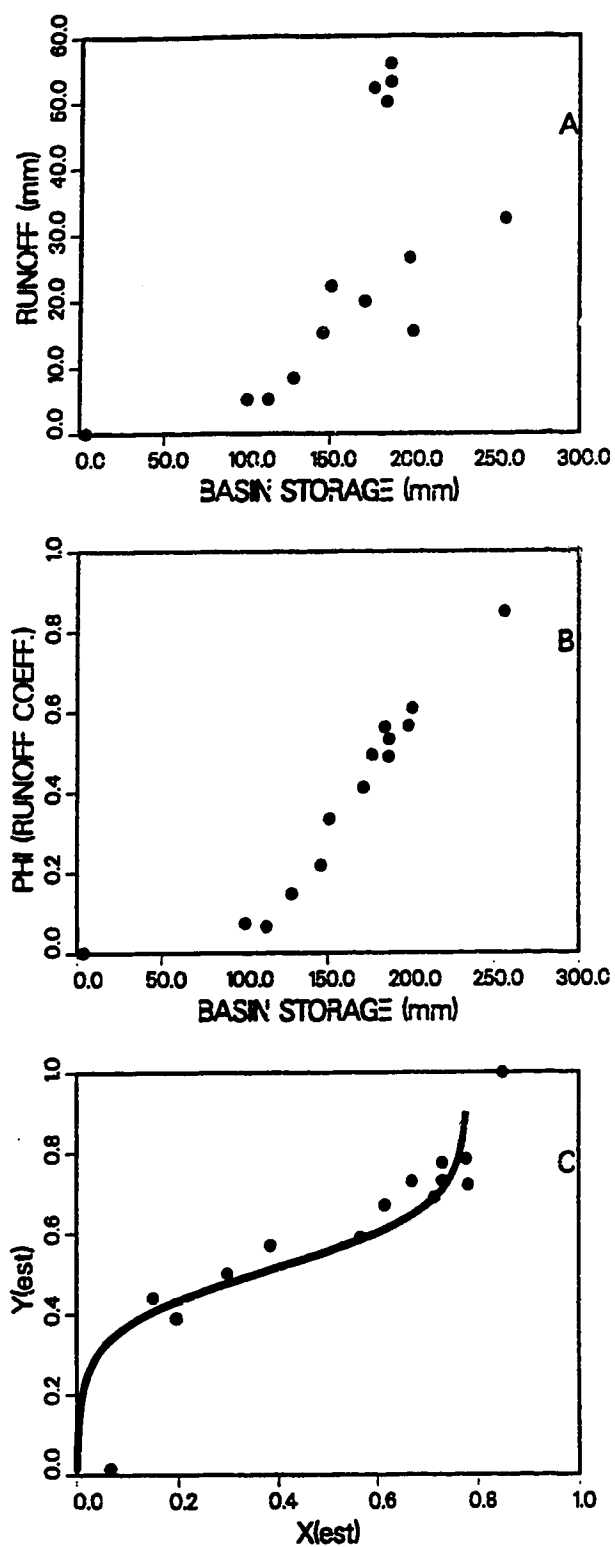


Figure 2-3: Storage - runoff relationships for Spring Creek, Alberta, developed by Holocek (1988). The Y(est) and X(est) values are the normalized basin storage and normalized contributing area.

Chapter 3

CONCEPTUAL MODEL OF PRAIRIE HYDROLOGY

3.1. Introduction

This chapter introduces the concept of a three phase runoff control model. The model responds to the dominant soil phase at the time of rainfall or snowmelt. The concept of a three phase soil model in hydrology was developed over a period of time spent studying hydrograph response to climatic inputs. Several observations have led to the current theory. These include:

1. Peak runoff events for most small prairie rivers are obviously snowmelt based.
2. Summertime runoff responses to high intensity rainfall events are never more than a small fraction of the average spring snowmelt runoff.
3. Rainfall events in summer provide an immediate runoff response while snowmelt and rain on snow events have a significant delay in runoff. The discussion below hypothesizes this immediate response could only occur from rainfall on a saturated area.

3.2. Conceptual Model of Prairie Runoff Functions

The conceptual model of prairie runoff functions hypothesized here represents a river basin hydrologic response in terms of the temporal soil conditions. The three soil conditions or phases are:

1. The frozen soil phase - deals with snowmelt and rainfall when the soil water is frozen and, except for initial infiltration losses, essentially impermeable.

2. The active soil phase - deals with snowmelt and rainfall as inputs to the active soil moisture system. Inputs are allocated to the soil moisture deficit first, then depression storage and finally, to streamflow runoff.
3. The saturated soil phase - deals with those areas within the watershed directly connected to the channel network and fully saturated during the runoff season. These areas are assumed to have a runoff coefficient of 1.0; virtually all of the rainfall contributes to streamflow.

3.2.1. Frozen Soil Phase

The short period of snowmelt over frozen soils generates most of the runoff on the prairies. Factors influencing the actual runoff depth include:

- soil moisture levels at freeze-up
- over winter soil moisture migration
- snow water equivalent
- net vapour transfer to the snowpack
- snowmelt infiltration to frozen soil

As is commonly expected in nature, these factors and their net effects are strongly related.

3.2.1.1. Freeze-up Moisture Levels and Winter Moisture Migration

The proportion of liquid water in the soil mantle when freeze-up begins determines the initial condition for a complex thermal-mass transfer process. This process, in response to gradients determined by soil and air temperature and humidity regimes, continually transfers energy and water between soil layers, the snow pack and the atmosphere. The moisture within the system is subject to gradients that draw it to the freezing front (Hoekstra, 1966; Kinoshita, 1975; Guymon, 1978). Liquid flow in frozen soils is so closely coupled with heat flow that any dynamic modelling must address the two processes simultaneously (Cary et al., 1978). Freezing of water at the frost front inhibits effective soil porosity and permeability. If soil water content at freeze-up were high, sufficient water will be available to create an impermeable frozen soil-ice layer at a shallow depth. With low fall moisture conditions, the ice layer will likely

form at a greater depth and may not block the soil to the same degree (Gray et al., 1983). The degree of soil permeability blockage would also depend on soil properties such as texture and structure.

Some moisture redistribution will take place prior to freezing. If the fall soil moisture level was very high in the surface layer (i.e. the top 20-50 cm), and very low in subsequent layers, then soil pressure (tension) and gravitational gradients will cause for some redistribution of soil water from the top layer to the deeper ones. The effect of the soil cooling as frost penetration begins will slow this process. As the freezing front migrates downward, the gradients will overcome the unfrozen redistribution forces (Guymon, 1978).

The net result of the above process is an ice-soil layer at shallow depths (15-50 cm) that restricts snowmelt infiltration to the profile depth between the surface and the ice layer. The depth of formation of the ice layer is theorized to relate to availability of soil water. High water content would result in formation of a thicker ice layer at a shallower depth.

3.2.1.2. Net Vapour Transfer to the Snowpack

The moisture redistribution described above is a result of the winter soil "climate". The snowpack overlying the soil is an integral and highly variable part of this "climate". The principal factor determining the magnitude of the temperature-moisture gradients in the soil is the air mass temperature. Snow, at the soil-air interface, affects the heat transfer, and therefore the vapour transfer, between the soil and the air. Heat flowing from the soil carries quantities of water vapour from the upper soil layer and base of the snowpack to the upper snow depths, where the vapour condenses and freezes due to the colder temperatures. This process results in a gradual lowering of the ice-water content of the upper soil layer (the depth above the

impermeable frost layer) over winter, with most of this moisture serving to enhance the snowpack water equivalent. Santeford (1978) in a study comparing late winter snow water equivalents of natural snowpacks and snowpacks cut off from the soil with a vapour barrier, recorded 25 to 50 percent higher snow water equivalents in the natural snowpack. As well, the underside of the vapour barriers were characterized by large ice accumulations. He concluded that the moisture transfer for most winters represents approximately 25-30 percent of the natural snowpack.

3.2.1.3. Depth of Fresh Snowfall

Snow acts as an insulator or resistor to the heat/vapour flow from soil to air. It directly follows that a greater depth of snow will serve to slow the moisture transfer out of the soil. Further, one would expect that a deep snowpack will condense and retain greater quantities of soil vapour. It appears likely that in most years the snowpack retains most or all of the soil vapour loss. However, in low snow years, significant portions of the soil vapour may escape to the airmass. Defining this quantity would be very difficult. However, in a year of low snowfall, runoff levels will be minimal. Consequently the relative error i.e. the error in the combined simulative analysis as a percentage of the total, will be large.

3.2.1.4. Snowmelt Infiltration to Frozen Soils

The theoretical basis of snowmelt infiltration into frozen soils is dominated by the same heat and mass transfer variables as over winter soil moisture variation. However, on an empirical basis, the depth of infiltration may be related to the depth of the impermeable ice-soil layer and the ice-water content of the soil above. A second variable, the snow water equivalent at the beginning of melting, also affects infiltration to frozen soil (Gray et al., 1983; Gray et al., 1985). The reasoning for inclusion of snow water equivalent is that infiltration will be subject to some degree to the heat introduced to the upper soil profile. While the snowpack exists, the principal

heat source contacting the soil is melt-water. Therefore, greater quantities of meltwater result in a greater heat input to the soil. Subsequent expansion and melting in the surficial soils creates greater storage capability.

3.2.2. Active Soil Runoff Phase

The runoff generated by the active soil phase is assumed to be negligible except for very large rainfall events. In this case, runoff events are very rapid. The factors that control the possibility of runoff are:

- soil moisture deficit
- soil infiltration capability
- depression storage

Aspects of depression storage were discussed under the frozen soil phase. The only difference in the operation of depression storage between the two phases in the active soil phase maintains a minimal infiltration rate from depression storage. This rate would be nil during the frozen soil phase.

The Conceptual Model assumes soil infiltration capability is equal to the soil moisture deficit. Once sufficient rainfall has occurred to meet this deficit, the surplus begins to accumulate as micro depression storage. This approach to the soil infiltration function implies the rainfall rate never exceeds the infiltration rate. This assumption is theoretically incorrect, but is argued to be functional for the following reasons. Precipitation in excess of the infiltration capacity will pond in local micro depression storage. Infiltration will continue from these accumulations. Continued rainfall, if in excess of the soil infiltration rate, will partition between further supplementation of depression storage and subsequent infiltration. This process may continue for an extended period of time before depression storage is overcome. During this time period, the soil moisture deficiency will be, for all intents and purposes, satisfied.

The occurrence of high intensity convective storms will not alter the above approach. These storms are local in nature and therefore tend to cover only small portions of the watershed. Even if an individual storm track does align somewhat with the drainage network, the total rainfall necessary to overcome the combined effects of high initial soil infiltration capacity and micro depression storage would have to be extreme. The 25 year return period 24 hour storm for the study area is about 100 mm. The chance of such a storm aligning with any drainage basin is miniscule.

3.2.3. Saturated Soil Phase

The concept of the saturated soil phase in prairie runoff describes the hydrologic response of inundated or saturated areas directly connected to the surface drainage network. The most notable examples are river valley bottomlands that are inundated during spring snowmelt, and remain in that state for some portion of the runoff season. Obviously, the actual channel network forms part of the saturated phase. The discussion in Section 3.2.2 illustrated the minimal chance of rainfall runoff from the active soil phase. This, combined with the fact the saturated area has a runoff coefficient of 1.0, presents strong support for the concept of the saturated soil phase being virtually the only source of runoff from summer rainfall.

The saturated area is a dynamic factor in the watershed. In the spring, shortly after the snowmelt runoff peak, the saturated area is at its greatest extent. From that point onward, a general decline in the area over summer will occur; interrupted by short term expansion in response to rainfall inputs.

3.3. Summary

A conceptual model describing the hydrologic processes of arid prairie watersheds as a function of the dominant soil condition(s) was presented. The three phases refer to frozen, active and saturated soil conditions. The discussion outlined the major operational characteristics that are felt to dominate each soil phase. Discussion and analyses presented in the chapters to follow provide further assessments of the viability of the three phase model for describing prairie hydrologic processes.

3.4. References

Cary, J.W., R.I. Papendick and G.S. Campbell, 1978. *Water and salt movement in unsaturated frozen soil: Principles and field observations*. Abstract in: S.C. Colbeck and M. Ray, eds. *Proceedings of Modeling Snowcover Runoff*. U.S. Army Corps of Eng., Cold Regions Research Lab., Hanover, N.H.

Gray, D.M., R.J. Granger and G.E. Dyck, 1983. *Overwinter soil moisture changes*. Meeting of American Society of Agricultural Engineers, Session: Infiltration and Media Flow, Chicago, IL., Dec. 14, Paper 83-2513.

Gray, D.M., P.G. Landine and R.J. Granger, 1985. *Simulating infiltration into frozen Prairie soils in streamflow models*. Canadian Journal of Earth Sciences, 22:464-472.

Guymon, G.L., 1978. *A review of snow-soil interaction*. in *Proceedings: Modeling of snow cover runoff*. U.S Army Cold Regions Research and Engineering Laboratory, Hanover, N.H., Sept. 26-28, p. 297-303.

Hoekstra, P., 1966. *Moisture movement in soils under temperature gradients with the cold-side temperature below freezing*. WRR, 2(2):241-250.

Kinosita, S., 1975. *Soil-water movement and heat flux in freezing ground*. Proc. Conf. on soil-water problems in cold regions, Calgary, Alberta, pp.33-41.

Santeford, H.S., 1978. *Snow soil interactions in interior Alaska*. In: S.C. Colbeck and M. Ray, eds. *Proceedings of Modeling Snowcover Runoff*. U.S. Army Corps of Eng., Cold Regions Research Lab., Hanover, N.H.

Chapter 4

BLOCK KRIGING ANALYSIS

A standard problem in hydrology and many other fields is the accuracy of methods used to estimate the variability in space of data measured at discrete locations. A number of standard methods are available: including weighted averages; Thiessen polygons and isopleth mapping. However, each of these methods were deemed to be inadequate for this study for the following reasons. The climate stations in the study area were spaced quite far apart, relative to the distances and areas involved with the individual drainage basins. In a number of cases, there were no climate stations within a basin (for example, Sounding, Alkali, Blood Indian and Buffalo Creeks), and often the spacing of the stations near to the basins was found to be inadequate to provide a reasonable estimate of basin conditions with either weighted averages or Thiessen polygons. Standard interpolation methods used in the contouring packages that were available could not be depended upon to produce reliable results when using irregularly spaced data. Attempts to relate single station data to hydrologic data with the climatic/ hydrologic model met with limited success. This is not unexpected, and is verified by the spatial plots presented analyses presented later in this treatise for Ribstone Creek, and for the entire study area. These plots demonstrate there is a significant variation in climate inputs over small distances in the study area. Results were no better when several stations near a basin were used to develop a "representative climate station" with weighted averages. At first there was no way to determine if this was due to poor representation by the climate data; or the model.

However, the results of the exercise with data from the spatial analysis support the model as a reasonable representation of runoff events. Further, the spatial fields developed for the accumulated snow water equivalent runoff (SWE) demonstrate a great degree of spatial variation in the data, supporting the contention that neither a single station nor group of stations using simple interpolative approaches could provide reasonable representation of the basin snow/soil water conditions.

There are a number of advanced methods that may be utilized to develop spatial fields from irregularly spaced data. These include: (Waters, 1981).

1. Contouring.
2. Trend surface analysis.
3. Spline fitting/interpolation.
4. Spatial autocorrelation.
5. Nonlinear surface fitting.
6. Kriging.
7. Double fourier analysis.
8. Multivariate statistical analysis.

The method used here to estimate the spatial characteristics of the spring snow conditions is kriging, a spatial interpolation technique that uses the semi-variogram function describing the rate of change of the variable of interest in space. Kriging is a costly approach to spatial analysis in terms of CPU time requirements. But in return for this investment, kriging consistently returns higher surface correlations and lower

surface error measures than any of the other spatial analysis and interpolation techniques (Waters, 1981).

An additional reason for adopting kriging as the spatial analysis tool for this study is the capability to interpolate to any element size. For individual basins, the kriging program was used to predict the snow water equivalent for 1 km² elements over an area covering the basin. From the kriging end, this was somewhat of an overkill, since in many cases, the difference in values between adjoining elements was less than 1 mm of water. However, the stream channel digitizing was carried out on a 1 km² grid, so it was advantageous to use the kriging routine to interpolate to the same scale.

4.1. Kriging Theory

4.1.1. The semi-variogram and nugget variance

Kriging is based on the theory of regionalized variables. A regionalized variable is spread out in space (and/or in time) and demonstrates a certain structure that may be mathematically described (Matheron, 1965; 1967). This definition is applicable to most earth science and atmospheric variables.

The spatial dependence of the regionalized variable is characterized by the semivariogram function, a measure of the similarity, on average, between points a given distance h apart (Burgess and Webster, 1980). The semivariance is defined as (Yates, 1948; Burgess and Webster, 1980a):

$$\gamma(h) = 1/2 \text{ var } [z(i) - z(i+h)] \quad (4.1)$$

and is a measure of the average change between pairs of point a distance h apart. The semivariogram is a plot of the mean value of $\gamma(h)$ for all points a distance h apart

against h . Therefore, the semivariogram is a statistical definition of the structural trend in the variable z in space. The semivariogram is determined with regression analysis, and the correlation coefficient provides a measure of how well the function describes the spatial structure of z .

The shape of the semivariogram is expected to be either linear or spherical, as seen in Figure 4-1. One might expect that at some distance d , the relationship between data pairs would decline such that the semivariogram would approach a slope of zero. This is shown in Figure 4-1, as both semivariograms reach distances with $h=d$, and the function slopes approach zero abruptly (for the linear model) or asymptotically. Pairs of points separated by distance $h \geq d$ have no direct relationship with each other.

Theoretically speaking, the semivariogram should have $\gamma(h)=0$ when $h=0$. However, data errors always result in the function having a y intercept $\neq 0$. This value is termed the nugget variance and represents the data variation over distances much smaller than the sampling distance. These errors, if incorporated in the analysis, tend to give too much weight to the local variation, as characterized by the nugget variance, to the point where the regional trend in the variable may be seriously masked. Block kriging develops an estimate of the value of $z(i)$ by using the mean value for a number of points within a defined block size with point $z(i)$ at the centre. The size of the block is selected such that its dimensions are greater than the nugget variance distance. The distance is determined as the distance necessary to shift the semivariogram function so the x intercept $= 0$.

4.1.2. Equations for block kriging

The interpolation method used in kriging has been well defined by a number of authors. The value of a regionalized variable Z at any location x_0 is determined as the weighted average of the observed values in the region, ie. (Burgess and Webster, 1980b)

$$Z_0 = \lambda_1 Z(x_1) + \lambda_2 Z(x_2) + \dots + \lambda_n Z(x_n) \quad (4.2)$$

This is the equation for punctual (point) kriging, with the only difference being in determining the weighting coefficient λ . In block kriging, the semi-variances between input data points and the interpolation grid points are replaced by the average semi-variances between the input data points and all grid points within the region. The optimum combination of weights, ie the optimal values for λ , are chosen for block V such that the block estimation variance σ^2_V is minimized. This value is defined as (Trangmar et al., 1985):

$$\sigma^2_V = \sum_{i=1}^n \lambda_i \gamma_i(x_i, V) + \mu_V - \gamma(V, V) \quad (4.3)$$

where $\gamma(x_i, V)$ is the average semi-variance between the sample points x_i in the neighbourhood and those in the block V . $\gamma(V, V)$ is the average semi-variance between points within block V , and μ_V is a Lagrangian parameter associated with minimization (Lagrangian multipliers provide a methodology for determining maxima and minima of a function). The within block variance $\gamma(V, V)$ accounts for the nugget variance (local unexplained or random variation around a point) and any variance associated with samples occurring within the block. The equation for estimation variance for punctual kriging is

$$\sigma^2_V = \sum_{i=1}^n \lambda_i \gamma_i(x_i, V) + \mu \quad (4.4)$$

The third term of equation (4.3) is absent in equation (4.4). Hence, the estimation variance for block kriging will always be less than that of punctual kriging because of the removal of the unexplained error within the block (Trangmar et al., 1985; Burgess and Webster, 1980b). This results in a smoother data field - Trangmar et al. (1985) demonstrated improvements of up to 20% in average estimation precision of block kriging analysis over punctual kriging. This benefit is particularly advantageous when regional patterns of a parameter are of greater interest than localized point estimates.

The Lagrangian multipliers for any block are solved subject to the constraint that the given value at any input data point is returned.

4.2. Applications

Block kriging has been utilized in many different studies to estimate the spatial variation/pattern of regionalized variables. A summary of the diversity of studies that are in the literature is presented in Table 4-1.

4.3. Summary

The field of geostatistics, and specifically kriging, offers the best available quantitative tool for estimating regionalized variable values and spatial trends. Kriging allows the user to estimate the probable error associated with the estimate of the regionalized variable at any point (block).

The benefit of this tool to sciences dealing with regionalized variables is significant. Most modeling applications in hydrology and climatology are based on punctual data that are often poorly placed for interpolation and extrapolation to other locations or

over the region of concern. Kriging provides a viable method for carrying out the interpolative studies that are so necessary to these fields. This benefit is clearly demonstrated by the improvements in results of the analyses of spring snow water equivalent and runoff to be presented in the coming chapters.

4.4. References

AES Canada, 1985. Personal comm., Marvin Olson, Atmospheric Environment Service, Downsview, Ontario.

Burgess, T.M. and R. Webster, 1980a. *Optimal interpolation and isorithmic mapping of soil properties: I. The semi-variogram and punctual kriging.* J. Soil Sci. 31:315-331.

Burgess, T.M. and R. Webster, 1980b. *Optimal interpolation and isorithmic mapping of soil properties: I. Block Kriging.* J. Soil Sci. 31:333-341.

Delhomme, J.P., 1978. *Kriging in the hydrosciences.* Advances in water resources, 1:251-266.

Journel, A.G. and Ch.J. Huijbregts, 1978. Mining geostatistics. London: Academic Press.

Sykes, J., 1985. Personal comm., University of Waterloo, Waterloo, Ontario.

Trangmar, B.B., R.S. Yost and G. Uehara, 1985. *Application of geostatistics to spatial studies of soil properties.* Advances in Agronomy, 38:45-98.

Vieira, S.R., D.R. Nielson and J.W. Biggar, 1981. *Spatial variability of field measured infiltration rate.* Soil Sci. Soc. Am. J. 45:1040-1048.

Table 4-1: Selected application of kriging in earth/atmospheric sciences.

Discipline	Parameter(s)
Soil Science	
Vieira et al., 1981	- Field measured infiltration rate
Burgess and Webster, 1980a	- loam thickness, stone content
Kuilenburg et al., 1982	- soil moisture storage capacity
Climatology	
Delhomme, 1978	- optimizing rainfall networks
AES Canada, 1985	- acidic deposition
Earth Science	
Krige, 1951; 1960	- gold ore concentration
Delhomme, 1978	- piezometric surface
Journel & Huijbregts, 1978	- generalized mining applications
Sykes, J. 1985	- piezometric surface

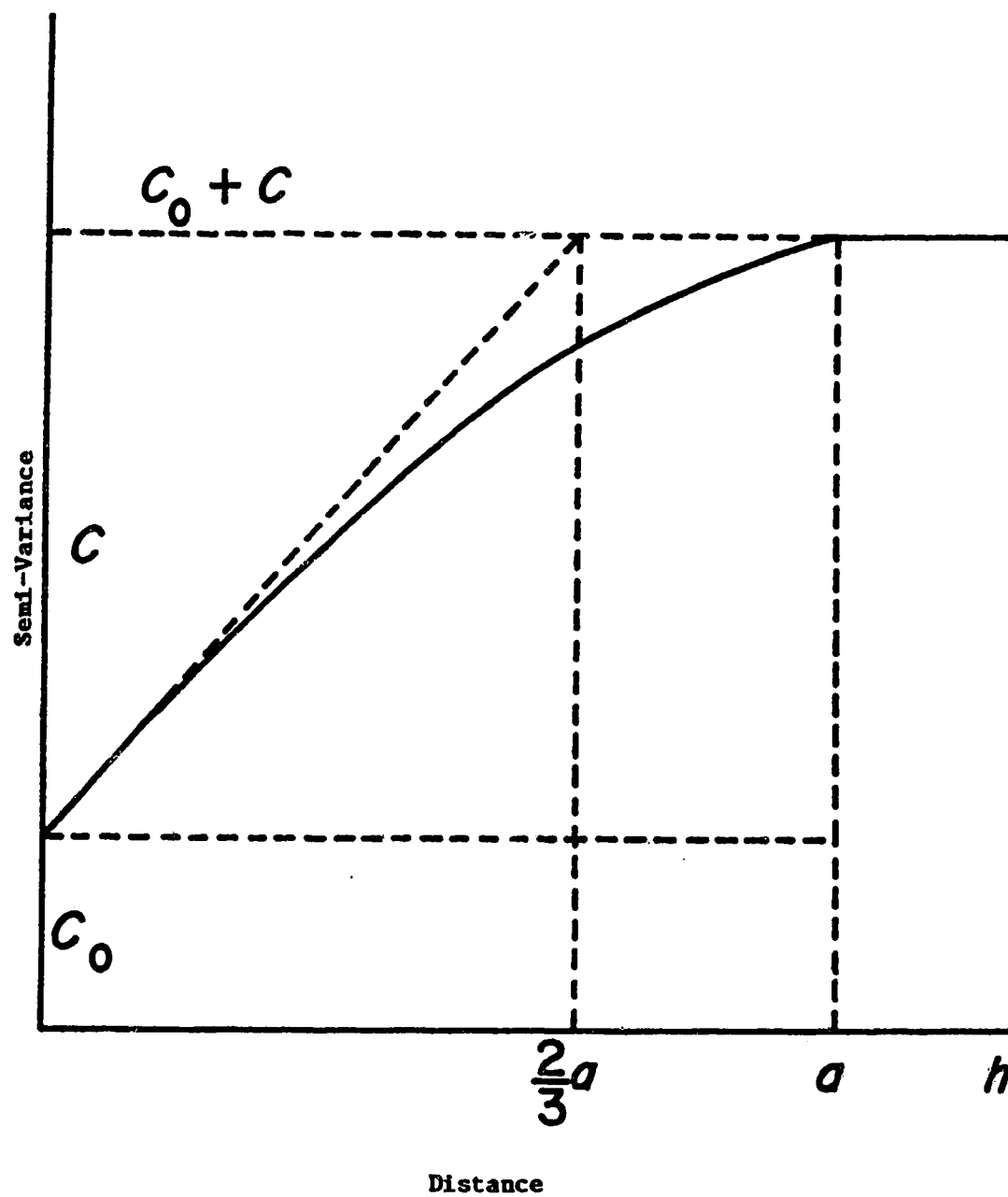


Figure 4-1: Theoretical linear and spherical semivariograms.

Chapter 5

FROZEN SOIL PHASE ASSESSMENT

RIBSTONE CREEK NEAR CZAR⁴

5.1. Introduction

A major research thrust of many hydrologists during the 1970s and '80s has focused on the theory of dynamic or variable contributing areas (Bevin and Wood, 1983; Taylor, 1982; Anderson and Kneale, 1980; Lee and Delleur, 1976; Engman and Rogowski, 1974). Dynamic area theory is based on the assumption that only part of a watershed contributes to the runoff, and that the contributing area varies depending on the basin moisture status. The interactions of soil water storage deficits (defined as the available storage at any time), infiltration rates and rain or snowmelt input determine the moisture status at any location. As infiltration capacity and/or available soil water storage are exceeded at any location, depressions begin to fill, and when this abstraction is met, runoff begins contributing to streamflow. However, these processes do not apply to the frozen runoff phase in prairie environments. In a frozen soil, the soil water storage capacity and infiltration rate are both limited (as discussed in Chapters 2). Local runoff occurs with relatively small inputs of snowmelt or rainfall, because of the limited storage capacity of the frozen soil. Once this storage

⁴A version of this chapter has been published. Byrne, 1989. Canadian Water Resources Journal, 14:2,17-28.

capacity is met, the local depression storage is the only parameter preventing streamflow runoff.

The discussion following presents a series of analyses designed to assess the frozen soil/snowmelt phase for a prairie watershed. A climatic model is utilized to estimate the winter precipitation WP, the spring snow water equivalent SWE and the spring soilwater levels θ_p at the beginning of snowmelt for a number of climate stations for the years 1968 through 1980. Kriging, an optimal spatial interpolation technique, is applied to estimate each of these variables for a one kilometre square grid over a drainage basin. A third modeling step utilizes SWE and θ_p for each grid square, determining the local snowmelt infiltration to frozen soils and the actual depth of runoff. These values are integrated over the basin to develop a single runoff depth. The final step involves regression analysis of the annual spring runoff depths and volumes, to develop estimates of the depression storage losses and the frozen soil phase contributing area.

5.2. Climatic Model for Determining Point Runoff Depth

The relationship of runoff volume due to snowmelt may be characterized mathematically as:

$$RVOL_s = \left(\sum_{i=1}^m AREA1 [S_i + P_i - INFS_i] \right) - DS \quad (5.1)$$

where:

$RVOL_s$ = snowmelt runoff volume

i = day counters for the winter/snowmelt period

m = last day of snowmelt

***AREA1* = frozen soil phase contributing area**

***S* = snowmelt on day *i* as equivalent water depth**

***P* = rainfall on day *i* (depth)**

***INFS* = snowmelt infiltration to frozen soil on day *i* (depth)**

***DS* = the depression storage deficit (volume).**

The intent here is to solve equation (5.1) to find values or functions describing *AREA1* and *DS*. The solution to this equation is directly attainable under the following basic assumptions. *RVOL_s* may be estimated from Water Survey data by using hydrograph separation techniques. *P* is a standard climate parameter for all stations used in this study. Snowmelt *S*, for the purposes here, may be treated as a lumped sum, the spring snow-water equivalent *SWE*. The climatic model calculates *SWE* at a climate station as

$$SWE = \sum_{i=Nov.1}^{ETDAY} [SNO_i + P_i - V_{si}] \quad (5.2)$$

where

***SNO_i* and *P_i* = daily snowfall and rainfall**

***V_{si}* = daily vapour transfer to/from snowpack to/from atmosphere**

= Morton evapotranspiration

***V_{si}* could be either negative or positive, depending on the prevailing conditions.**

***ETDAY* is defined as the date upon which the frozen soil phase of the conceptual**

model ceases to function. On *ETDAY*, the active soil phase begins, and precipitation will be allocated to soil water and other losses ahead of runoff. For this analysis, *ETDAY* was defined in an arbitrary manner as twenty days beyond the end of snowmelt, as determined by the snowmelt algorithm (Pipes and Quick, 1977 - see Appendix C). It is of interest to note that *ETDAY* is a "hydrologic" date and will occur on different dates for different stations, depending generally on the local station climate each spring. In general, *ETDAY* occurs later with increasing latitude.

The snowmelt infiltration is determined with (Gray et al.,1985)

$$INF = 5 (1 - \theta_p) SWE^{0.584} \quad (5.3)$$

θ_p = the degree of pore saturation in the top 30 cm of soil. INF is calculated using the SWE on the first day of snowmelt.

The climate model was utilized to estimate, for the 1968 through 1980 runoff years, the depth of winter precipitation WP, the spring snow water equivalent SWE and the spring soil water level θ_p at thirty-four climate stations within the study area. SWE was estimated with equation (5.2). For WP, equation (5.2) was utilized with V_s set to 0. θ_p was assumed to be the fall soil water content, as calculated with the climate model. Equation (5.2) was used to estimate the fall soil water content by setting the counter in the equation from i = May 1 to October 31 of the previous year. The only difference for the model is that the storage medium is the soil profile instead of the snowpack.

Morton's evaporation/evapotranspiration model (Morton, 1978) was utilized to estimate the net vapor transfer to/from the snowpack. Morton's model is based on the

principle that regional temperature and humidity data reflect the availability of water for evaporation/sublimation. Earlier discussion of the complexities of the soil-snow-atmosphere interaction does not preclude the use of Morton's model to estimate the net result in terms of the SWE. In fact, the results support the use of Morton's model, and suggest that adding greater complexity to the analysis may not provide sufficient benefit to justify the efforts. No other functional sublimation/condensation model for winter conditions has been found in the literature.

The relationship of WP, SWE and θ_p at any one station or group of stations to the runoff for a particular basin is poorly defined, given the variability between the stations, and the lack of knowledge on the relative response of a basin to inputs defined for a climate station. Attempts to develop relationships using the climate data from single stations, including stations located within a basin, did not provide consistent results. Therefore, an analytical tool was required to estimate the spatial variability of WP, SWE and θ_p .

5.3. Spatial Analysis of Modelled Climatic Data

In order to minimize the error involved in estimating the net basin input from climate station data, kriging, a spatial analysis technique from the field of geostatistics, was employed. Kriging theory and methodology is described in Chapter 4.

5.4. Determining Basin Values for WP, SWE and INF

The watershed selected for analysis is Ribstone Creek near Czar, Water Survey of Canada (WSC) station 05FD005. Ribstone Creek was chosen because it lies very near the centre of the study area, and is reported by the WSC to have natural flow conditions.

Block kriging analysis has been applied to the climatic model output for thirty-four

stations in order to estimate WP, SWE and INF for the years 1968-80. Each variable was estimated for one km² elements over the basin. The semivariograms utilized for each year are presented in Table 5-1. Figures 5-1, 5-2, and 5-3 present spatial fields of these parameters for 1974, the year of greatest runoff.⁵ The spatial patterns of WP and SWE are generally equivalent. Both demonstrate a trend from a minimal value near the basin outlet (WSC Station 05FD005) to a maximum in the southwestern corner of the basin. The variation in WP and SWE over the basin is about 70 and 60 mm, respectively. The extent of the variability illustrates why the results from a single station did not accurately reflect the basin situation. The spatial distribution of θ_p (Figure 5-3) for 1974 demonstrates a range of about 15% from the southeast to the northwest for the figure, but the range is only 6-7% for the basin (area marked with dots). This level of variability is typical of most years, as can be seen from the spatial diagrams in Appendix A.

Estimates of WP, SWE AND θ_p , integrated for the basin, were developed with the following methodology. The extent of the watershed is estimated from 1:50,000 NTS map sheets by assigning each square kilometre as in or out depending on channel contact i.e. if a channel was shown within the block on the map, then the block was included; if no channel was shown, the block was excluded. There is undoubtedly some error in this approach with regard to both the theoretical basis and possible errors and omissions on the map sheets. However, the intent is not to define explicitly the area of the basin, but only to define 'relative areas' that would be expected to have the greatest impact on runoff. The relative area defined by the above process are marked in Figures 5-1 and 5-2 with crosses, and in Figure 5-3 with dots. The integrated value of WP and SWE for the basin for each spring was determined as the

⁵The spatial diagrams for all years for Ribstone Creek are included in Appendix A.

mean of the kriged values for the one square kilometre blocks within the relative area. SWE-INF was calculated for each grid square using equation (5.2) and the values of SWE and θ_p estimated by the kriging analysis. The values of WP, SWE and SWE-INF, integrated over the basin, are presented in Table 5-2. Figures 5-4, 5-5 and 5-6 present the relationships of WP, SWE and SWE-INF to the recorded spring runoff volume.

5.5. Determining AREA1 and DS for Ribstone Creek

The r^2 value for the analysis in Figure 5-4 is 0.72. Significant scatter of the data points is notable and not unexpected, given the approximate nature of the comparison. The amount of scatter declines in Figure 5-5 ($r^2=0.79$), due to the introduction of a winter evapotranspiration, simulated in the modeling exercise with Morton's evapotranspiration. This is a very approximate approach to take to modeling the complexities of soil-snow-atmospheric interaction. However, even this approximation results in a significant improvement in the quality of the relationship. The principle of diminishing returns may be used to argue that developing a complex soil-snow-atmospheric model may not be justified, particularly with the further improvement gained in Figure 5-6, with the inclusion of infiltration parameters.

The decline in SWE (Figure 5-2) as opposed to the WP values (Figure 5-1) is quite notable. However, a decline in snow-water equivalent over-winter is not unexpected in east central Alberta. In some winters, warm, dry (chinook) winds result in significant snow sublimation. Beaty (1975) reported sublimation/evaporation losses in the range of 59 to 80 percent of the snowpack in the White Mountains of California, an area with a cold, dry winter climate.

The regression equation in Figure 5-6 further improves the significance of the relationship ($r^2=0.87$), and provides the best basis for estimates of depression storage

DS and frozen soil contributing area AREA1. DS is the only abstraction not directly dealt with prior to the regression analysis. The regression equation dictates the y-intercept has the dimensions of volume. Since the intercept is less than zero, it represents an abstraction; in this case, the depression storage losses integrated over the basin. The slope of the regression line has the dimensions of area; and as such, is an estimate of AREA1. Therefore, for Ribstone Creek, $AREA1 = 320 \text{ km}^2$, and the depression storage capability of the basin = $5,900,000 \text{ m}^3$, or 18 mm as a depth over the contributing portion of the basin.

The AREA1 value is virtually constant; this dictates the frozen soil (or snowmelt) contributing area is a constant, once the basin frozen soil infiltration and depression storage values have been met. This is contrary to the variable area theory generally felt to be applicable to prairie watersheds by Card (1979) and PFRA (1985). However, neither of these studies present supporting data. They simply subscribe to the theory on the basis of qualitative assessment. PFRA (1985) estimated the gross and effective drainage areas for Ribstone Creek as 1830.1 and 697 km^2 , respectively. They indicate the contributing area for a two-year event would approximate the effective area; and would approach the gross area in an extreme flood. These are geomorphological assessments: the areas are delineated on 1:50,000 NTS map sheets. These values are both much higher than the estimate of AREA1. However, the AREA1 value developed here is felt to have a greater validity because it is found from a detailed hydrologic analysis.

The magnitude of the DS abstraction implies there were essentially no contributions to runoff from the frozen soil phase in 1968, 1973, 1977 and 1980. The SWE-INF values in these years were very close to the DS deficit (Table 5-2). Runoff in these years would have been due almost entirely to the melting of snow and ice within the

channel network. Estimating the volume of runoff that might be due to snow and ice in the channel system from the analysis here is not feasible. Even a cursory examination of the SWE vs runoff data for the low flow years reveals there is no apparent relationship. This is not unexpected when one considers the relative error in the analysis is very large for low flow years. For example, an error of 10 mm in SWE is acceptable for 1974; but for 1968 and 1977, this error level is most of the predicted runoff. Further, in low flow years, abstractions for local water use (such as livestock watering systems) could add significantly to the error.

5.6. Summary

A detailed method has been developed for estimating two parameters; the areal extent of the frozen soil contributing area, and the related depression storage losses. A series of models are utilized: a climatic model with a daily time step provides estimates of snowpack water equivalent over winter fall and spring soilwater contents; snowmelt infiltration to frozen soils; and the spring runoff potential at a climate station. The climate model runs have been carried out for the years 1968 to 1980 for thirty-four climate stations in the study area. A spatial analysis (block kriging) model provides optimized interpolation of climate station data to one kilometre square elements over a watershed. A final program integrates the optimized spatial patterns for the climate parameters into an estimate of the spring runoff depth over the basin.

An assessment for Ribstone Creek near Czar, a small basin on the eastern Alberta prairies provides an estimate of a snowmelt contributing area of 320 km²; and a depression storage abstraction of 18 mm over this area. The principal source of runoff is from snowmelt over this area, but if the spring snow-water equivalent is not sufficient to meet frozen soil infiltration capacity and the depression storage deficit, then the only source of streamflow is the snow quantity that has drifted into the channel network.

5.7. References

- Anderson, M.G. and P.G. Kneale, 1980. *Topography and hillslope soil water relationships in a catchment of low relief*. J. Hydrol., 47:115-128.
- Beaty, C. B., 1975, *Sublimation or melting: observations from the White Mountains, California and Nevada, USA* Journal of Glaciology, 14:275-286.
- Bevin, K. and E. F. Wood, 1983. *Catchment geomorphology and the dynamics of runoff contributing areas*. J. Hydrol., 65: 139-158.
- Card, J.R., 1979. *Synthesis of streamflow in a prairie environment*. In: 'The Hydrology of Areas of Low Precipitation', Proceedings of the Canberra Symposium, December.
- Engman, E. T. and A.S. Rogowski, 1974. *A partial area model for storm flow synthesis*. WRR, 10: 464-472.
- Gray, D.M., P.G. Landine and R.J. Granger, 1985. *Simulating infiltration into frozen prairie soils in streamflow models*. Can. J. Earth Sci. 22:464-472.
- Lee, M.T. and J.W. Delleur, 1976. *A variable source area model of the rainfall-runoff process based on the watershed stream network*. WRR 12:1029-1036.
- Morton, F.I. 1978. *Estimating evapotranspiration from potential evaporation: practicality of an iconoclastic approach*. J. Hydrol. 38:1-32.
- PFRA, 1985. *The determination of gross and effective drainage areas for the prairie provinces*. Regina, Sask., Hydrology Report #104, Addendum #1.
- Pipes, Anthony and Michael C. Quick, 1977. *UBC watershed model users guide*. Dept. of Civil Engineering, University of British Columbia.

Taylor, Colin H., 1982. *The effect on storm runoff response of seasonal variations in contributing zones in small watersheds*. Nordic Hydrology, 13:165-182.

Table 5-1: Semi-variograms for WP, SWE and θ_p for 1968 - 80

DIR	WP			SWE			θ_p		
	a	b	r^2	a	b	r^2	a	b	r^2
1968 0	23	4.65	.99	57	2.59	.98	3	0.35	.98
90	108	3.32	.91	181	2.83	.97			
1969 0	215	0.86	.88	144	2.69	.91	68	0.3	.90
90	230	2.56	.95	223	3.32	.91			
1970 0	382	1.83	.72	91	2.36	.72	3	0.62	.96
90	223	5.08	.97	44	4.21	.98	5	0.52	.88
1971 0	191	3.5	.78	105	4.13	.87	8	0.71	.71
90	208	5.65	.96	9	7.06	.99	51	0.16	.78
1972 0	404	3.41	.72	21	7.6	.99	2	0.37	.83
90	55	8.3	.95	-125	7.78	.86	16	0.19	.99
1973 0	131	1.35	.99	142	0.61	.94	-40	0.94	.98
90	141	2.06	.99	157	0.56	.87	-17	0.76	.90
1974 0	175	17.7	.92	70	15.6	.91	4	0.86	.95
90	177	24.	.90	149	19.8	.90	23	0.86	.98
1975 0	177	16.2	.85	-408	13.7	.98	-25	0.71	.99
90	34	26.3	.78	65	17.	.73	11	0.24	.93
1976 0	551	0.66	.79	366	1.19	.75	6	0.31	.93
90	-70	7.21	.98	-88	6.18	.99	13	0.32	.99
1977 0	82	2.37	.93	-35	2.73	.99	-2	0.5	.99
90	278	0.99	.71	185	0.6	.80	22	0.3	.99
1978 0	170	5.7	.99	77	6.4	.99	23	0.21	.96
90	203	3.42	.93	148	3.91	.90	7	0.31	.78
1979 0	445	1.86	.99	232	3.16	.93	43	0.7	.96
90							-3	1.04	.96
1980 0	740	1.98	.86	771	0.77	.96	-7	0.65	.89
90									

Note - Most cases were anisotropic, with angle of view = 90°
 In cases with no values under DIR = 90° , the angle of view was 180° (essentially isotropic).

Table 5-2: Runoff depths and volumes for Ribstone Creek

year	WP mm	SWE mm	SWE-INF mm	SNOWMELT RUNOFF m ³
1968	77	29	13	260,192
1969	122	71	45	11,390,503
1970	119	63	30	4,221,000
1971	134	74	40	10,803,175
1972	127	80	36	252,000
1973	78	41	13	9,331
1974	228	163	102	29,203,773
1975	205	114	61	9,732,506
1976	110	67	27	1,079,338
1977	63	32	9	138,771
1978	95	59	30	266,982
1979	87	54	25	336,552
1980	100	53	21	93,475

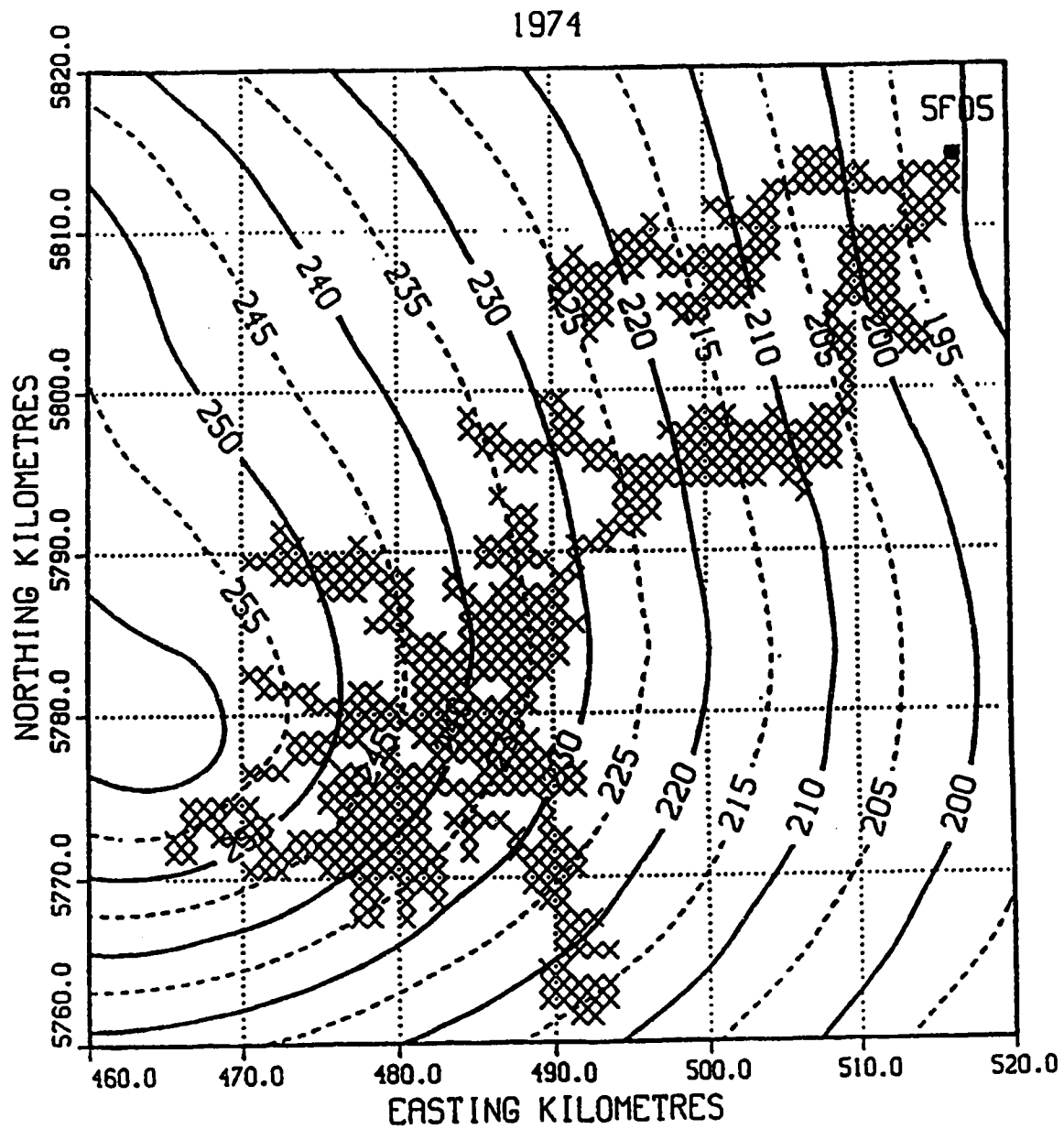


Figure 5-1: Spatial distribution of WP for the 1973-74 winter.
 The relative area is defined by an x in the active elements.

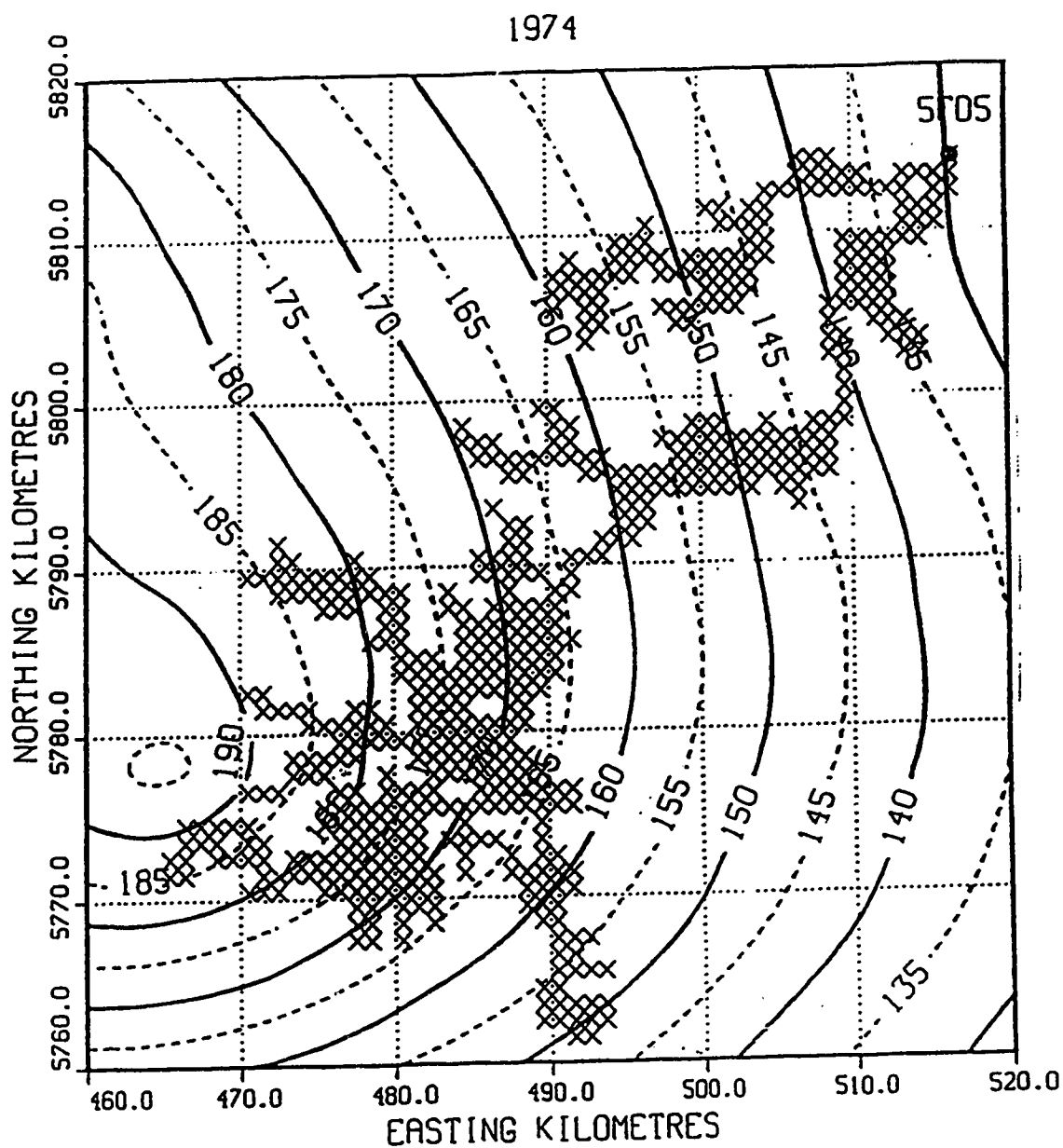


Figure 5-2: Spatial distribution of SWE for the 1973-74 winter.
The relative area is defined by an x in the active elements.

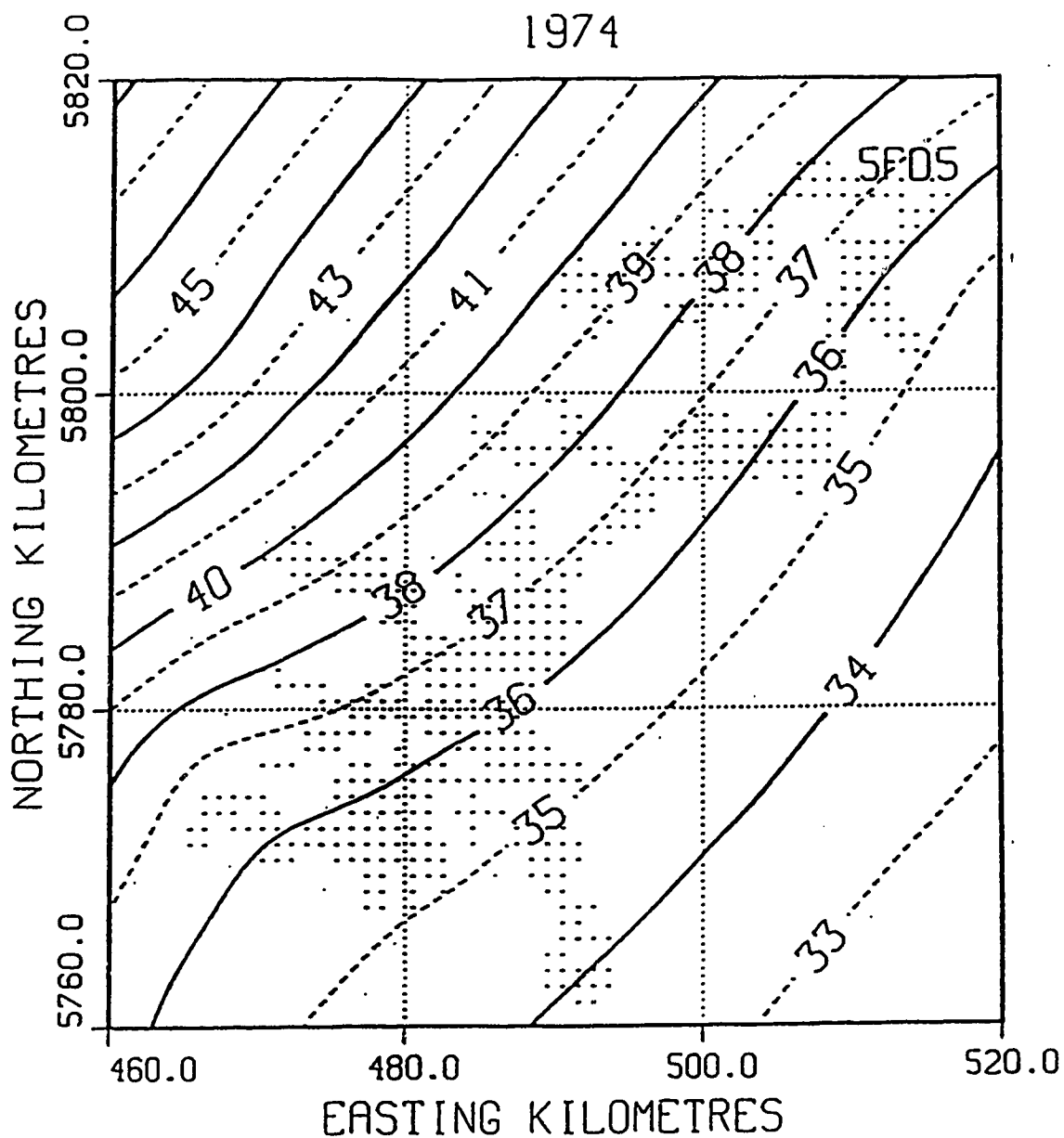


Figure 5-3: Spatial distribution of the frozen soilwater level WP for the 1973-74 winter. Relative area is defined by a dot in active elements.

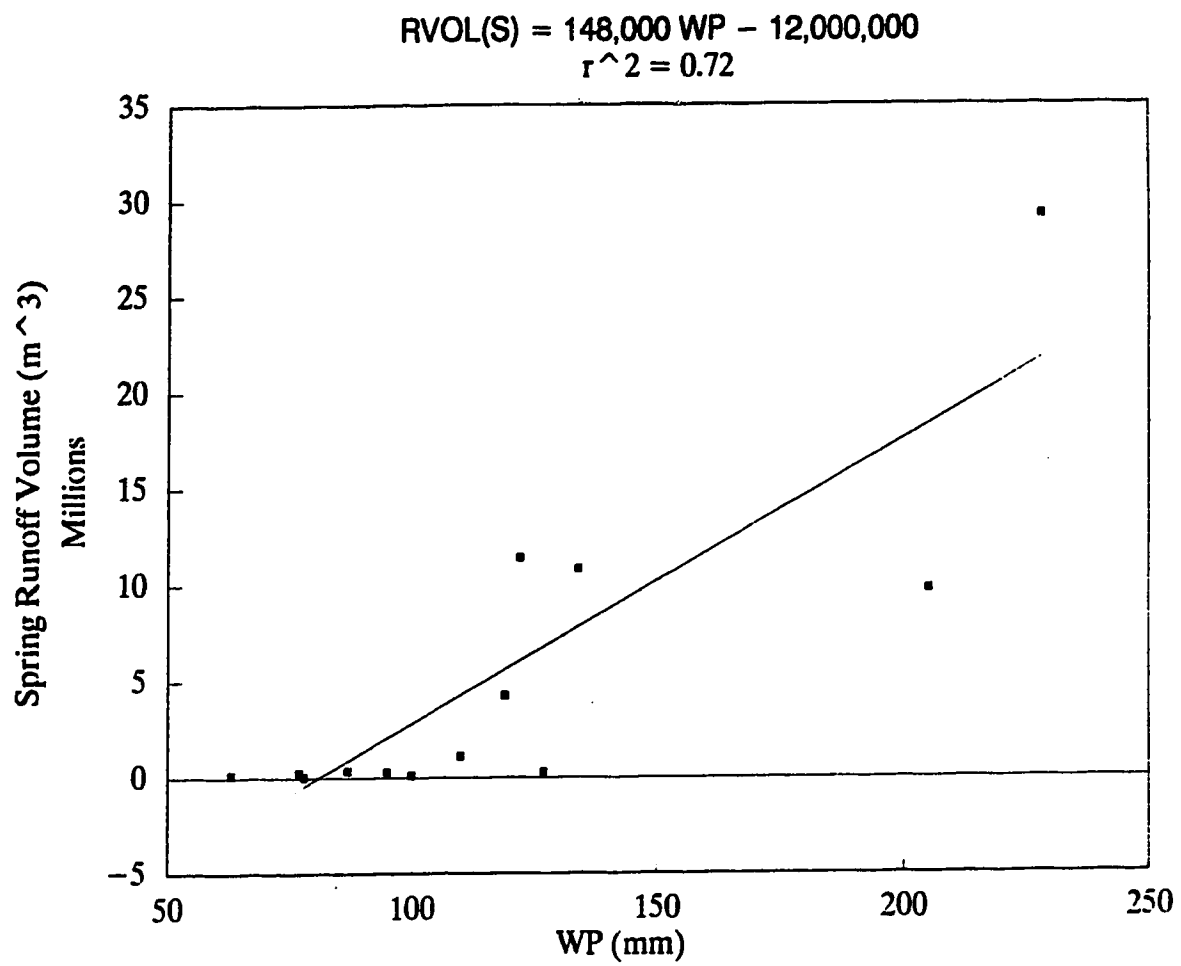


Figure 5-4: Relationship of WP and spring runoff, 1968-80.

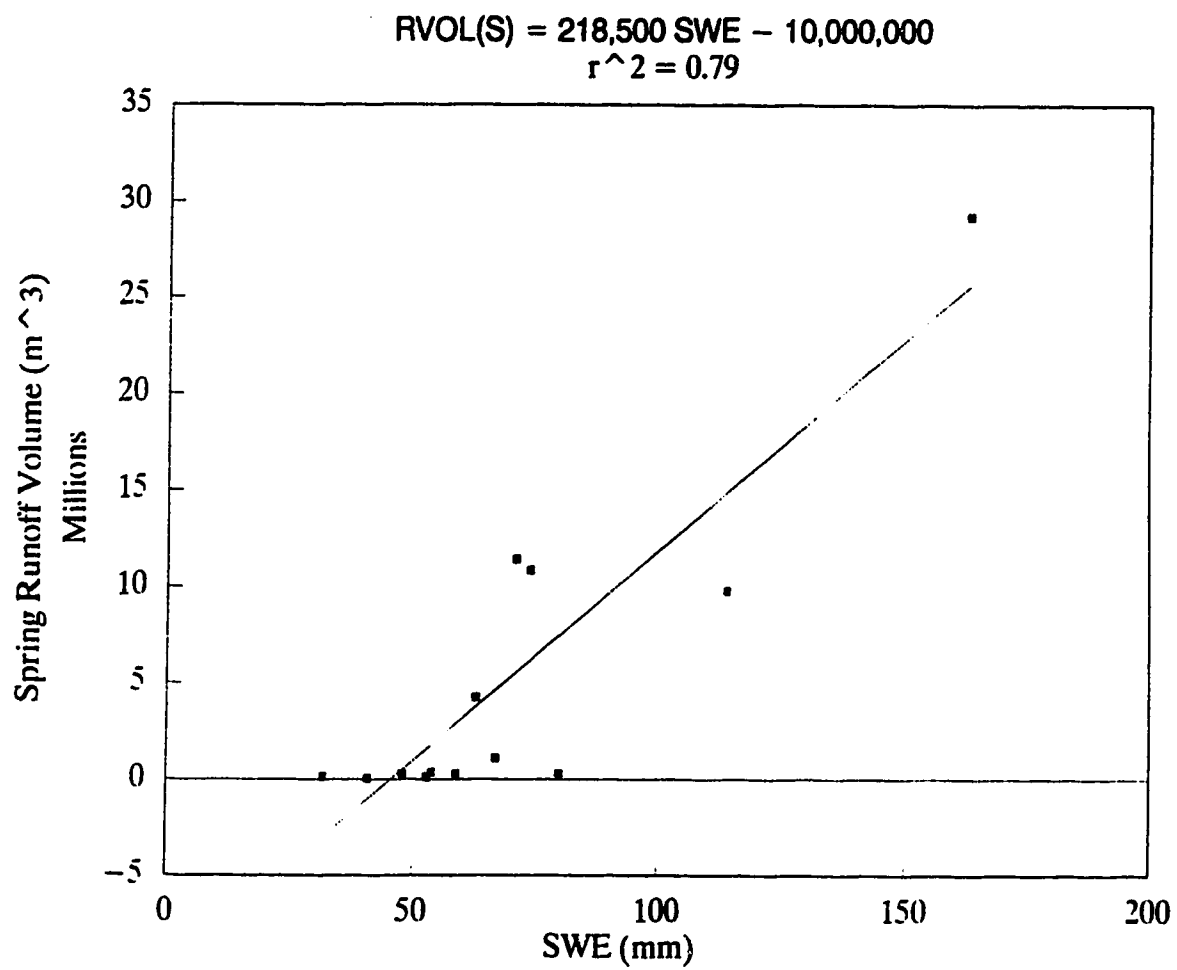


Figure 5-5: Relationship of SWE and spring runoff, 1968-80.

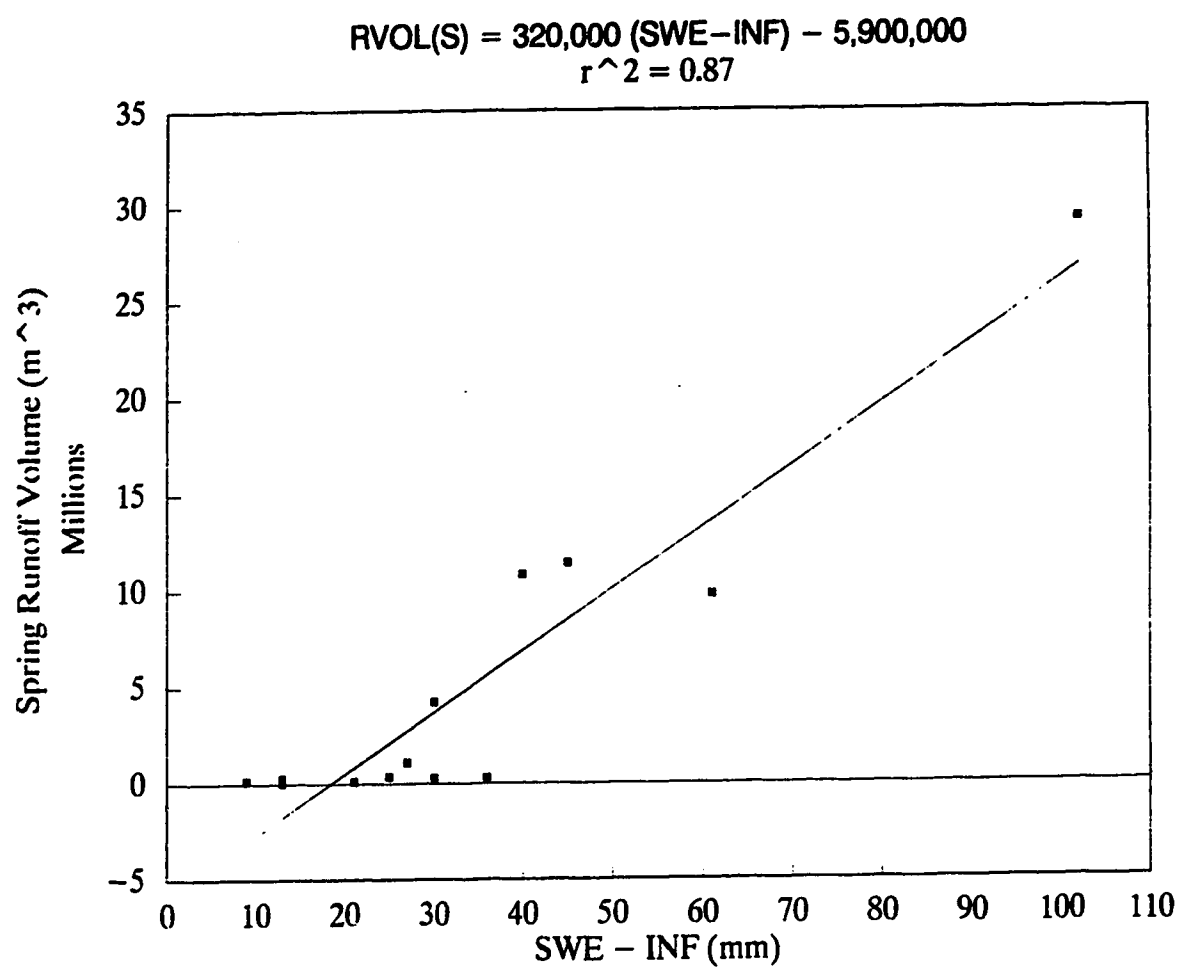


Figure 5-6: Relationship of (SWE-INF) and spring runoff, 1968-80.

Chapter 6

ACTIVE SOIL PHASE ASSESSMENT - RIBSTONE CREEK

6.1. Introduction

A conceptual operational model for the active soil phase of prairie river basins was discussed earlier. A central assumption of that discussion stated that very little, if any, of the runoff for any basin within the study area results from runoff from the active (vegetation growth) soil phase. This section presents an analysis of the active season runoff potential for the climate stations near Ribstone Creek. The results of the analysis support the contention of the conceptual model regarding little or no active soil phase runoff. The operation mode of the active soil phase, as theorized in the conceptual model, was discussed in Section 3.2.2. The reader is referred to that section for background information.

6.2. Methodology

Attempts to verify the active phase theory must deal with a number of problems, the greatest of which is the sheer physical volume of data that must be examined. Assessing Ribstone Creek near Czar required a daily analysis of soil and climate conditions for the period 1960 through 1981. This is a greater time span than was possible for the frozen and saturated soil phases because the analysis did not require runoff data, which was only available for Ribstone Creek for 1968 on. If the climate model had predicted a number of significant active phase runoff events, the Water

Survey data would have been very helpful in verifying the impact of the storm. However, the lack of streamflow data was not a major problem since the model presents evidence that there is minimal runoff from the active soil phase.

The climate model operated for the open season with

$$SOIL_i = SOIL_{i-1} + P_i - ET_i \quad (6.1)$$

where SOIL, P and ET are the soil moisture deficit, precipitation and Morton evapotranspiration for day i, i-1 etc. The equation was subject to several conditions. A boundary condition at day 1 of the active soil season is required. The soil moisture deficit on day 1 of each active season was initially assumed to be equal to the deficit on October 31 of the previous year, plus any estimated snowmelt infiltration to frozen soil. The validity of the assumption of no change in soil moisture deficit over winter is admittedly questionable for several reasons, including:

1. There is no information available to verify the fall soil moisture deficit as simulated;
2. Potential changes that could occur in the soil moisture level over winter are ignored.

In spite of these reservations, the analysis is felt to provide a reasonable set of results.

The model run for five climate stations under the above scenario results in there being no runoff at any time from the active soil phase. However, recognizing the weakness of the assumption (of no change in soil water over winter) led to a repeat of the analysis with an assumption that the soil moisture deficit was 0 each spring; i.e. the soil was set to field capacity at the start of each annual simulation. This assumption is definitely incorrect, and is very conservative with respect to the

analysis. There were probably very few years in which the spring soil water in the area of Ribstone Creek approximated field capacity. By starting the season with the soil assumed to be at field capacity, the chance for runoff generation by the simulation model is artificially increased in most years. The test hypothesis is that no runoff occurs from the active soil phase. The chance of proving the null hypothesis is greater if the initial soil water conditions are assumed to be at maximum each year. Therefore, the assumption is conservative with respect to the test hypothesis. The data presented here is for the case of the most conservative analysis with spring soil water conditions assumed to be at the wettest.

Plots of the soil moisture conditions for five stations near to the Ribstone Creek watershed are presented in Figures 6-2 to 6-6. The locations of the stations relative to the stream channel network are shown in Figure 6-1.

The analysis utilized equation (6.1) with a condition that soil moisture conditions at field capacity are at a datum of 0. This is obvious in each plot- the soil moisture for the beginning of the year always runs at 0 for the initial months. The active soil phase begins simulating once ETDAY has been past.⁶ Possible runoff events from the active soil phase are displayed on the annual plots as one day peaks that extend above $y = 0$. For example, in Figure 6-2 (1962) there is an apparent runoff peak in mid-July that exceeds 60 mm and in September a small blip representing approximately 5 mm. The July, 1962 storm is notable on Figures 6-3 to 6-6 as well.

The runoff occurrences at any station of a magnitude approaching 50 mm or more were compiled by year and month of occurrence. The runoff depth at the other five stations for each of the events was compiled as well. The data is presented in Table

⁶ETDAY was defined in earlier as the date twenty days beyond the end of snowmelt.

6-1. The storm of July, 1962 is characterized by the values in row 1 of the table: the estimates runoff depths for Coronation, Brownfield, Hughendon, Hemaruka and Metsiko are 65, 110, 30, 70 and 35 mm, respectively. Eight storms that appear to have had some potential to yield runoff from the active soil zone are notable over the twenty-two year period 1960-81.

The net effect of each station on the Ribstone drainage was estimated using the regression equation developed in Chapter 5 (see Table 5-1 and related discussion). The estimated depth of potential runoff over the basin is presented in column 7 of Table 6-1. Column 8 is column 7 minus the depression storage deficit for Ribstone Creek as determined in Chapter 5. Values less than 0 were set to 0.

The data in column 8 indicates there were three events: July, 1962; June, 1973 and May, 1977 (September, 1969 is ignored as inconsequential) that may have resulted in basin wide runoff from the active soil phase at Ribstone Creek. This point in itself supports the hypothesis to the degree that no appreciable quantity of runoff originates from the active soil phase. Assuming these events did generate runoff, three days out of twenty-two years is scientifically notable, but insignificant in terms of water supply or management. However, several points argue the magnitude of these events is not sufficient to have created runoff.

1. The storms were likely of a low intensity type, given that all of the stations received a significant amount of rainfall. Therefore, the rain would have continued to infiltrate while building up in the micro-depression storage. This continuing infiltration would have absorbed significant amounts of water.

2. As discussed previously, the analysis is conservative in terms of

allowing runoff from the active soil phase. Inspection of the Coronation plots for 1961 and 1962 (Figure 6-2) indicates the relative level of the conservatism. In 1961, the soil moisture level at the end of the year is less than -200 mm of water. This represents a 200 mm soil moisture deficit from field capacity. This amount is neglected for spring 1962, since the analysis sets the soil level back to field capacity. This argument applies to the June 1973 and May 1977 storms as well. The previous year deficits that were ignored in those cases were greater than -100 and -75 mm, respectively.

3. The frozen soil phase analysis in Chapter 5 provided an estimate for the snowmelt contributing area of about 320 km² for Ribstone Creek. Assuming the runoff depths for the active soil phase did occur, then the runoff volumes would have been approximately 15, 7 and 13.4 million m³. Reference to Table 7-2 indicates the two bigger values would be ranked second and third in magnitude for the period of record. In fact, these three events are almost indistinguishable on plots of the annual hydrographs for Ribstone Creek near Edgerton, a water survey station downstream from Czar. The hydrographs are plotted in Figure 6-7. The Edgerton station is used here because there was data for 1962 as well.

The discussion above is subject to one small caveat. The use of Morton evapotranspiration is felt to be the most practical and accurate in a study such as this. However, the results of the analysis lead to an observation that the Morton model may overestimate areal evapotranspiration slightly, so that over a long period of time, the cumulative error may amount to a significant amount. For the individual stations, the deficits over 22 years ranged from 300 to almost 900 mm if the spring soil condition was not reset (three stations just less than 300, and the other two with errors of 600

and 900 mm). An error of 300 mm over twenty-two years is probably quite acceptable - this is about 13.6 mm per year. However, the upper error for one station approaches 40 mm per year. One explanation for this may be the method with which Morton's model may have been derived. Morton ET is based on a closed basin analysis i.e.

$$ET = P - R \quad (6.2)$$

where P is precipitation and R is runoff. However, in the case of many basins, including Ribstone Creek near Czar, the micro-depression storage very likely does not ever contribute to local streamflow, but instead infiltrates to the regional groundwater system, and only becomes runoff outside the basin of interest. The estimate of micro depression storage for Ribstone Creek was 18 mm. The average error in Morton's ET for the basin on an annual basis is 22 mm. Admittedly, this may be a coincidence, and is subject to other conditions such as changes in long term basin storage. Nevertheless, the feeling here is that Morton's model would be improved by an attempt to incorporate an open (as opposed to closed) basin analysis.

6.3. Conclusions

The analysis presented in this chapter strongly supports the contention that there is virtually no runoff from the active soil phase for the geographic area characterized by the climate stations in and around the watershed Ribstone Creek near Czar in east central Alberta. The Ribstone area is representative of a much larger area in eastern Alberta and western Saskatchewan, to which the same hypothesis may be extended with a reasonable confidence since Ribstone is near the northwestern border of the area. Climate conditions become drier and hotter as one proceeds south. Therefore, there would be even less chance of active phase runoff in the more southerly regions.

The conclusions here dispute the classical hydrologic theory of variable contributing

area. It would appear that under most conditions, the theory of an expanding contributing area with increasing rainfall depth does not apply in the study region for this project. If there is a variable area that does function under these climate conditions, it is likely the saturated area created by the spring snowmelt runoff. The next chapter addresses this soil phase.

The author acknowledges that localized exceptions to the above discussion may occur. In other words, it may be possible to measure runoff from some isolated subsection of a drainage during the active soil season. However, the consequence of this runoff in terms of watershed management and/or water supply is trivial in comparison to the annual runoff.

Table 6-1: Active soil phase runoff depths (mm) for the individual stations.

	Coronation	Brownfield	Hughendon	Hemaruka	Metisko	Basin	- DP
62/07	65	110	30	70	35	65	47
63/07	0	20	20	0	40	13	0
64/09	0	0	40	55	12	9	0
68/09	0	50	15	0	30	19	1
70/06	0	15	60	0	25	14	0
73/06	40	80	10	35	5	40	22
73/08	0	45	48	0	0	18	0
77/05	40*	70*	160*	50*	50*	60	42

* combined several storms about 10 to 15 days apart.
 Basin = regression estimate for the basin from the five stations
 - DP = Basin minus depression storage deficit for Ribstone Creek.
 = 18 mm from chapter 7 analysis.

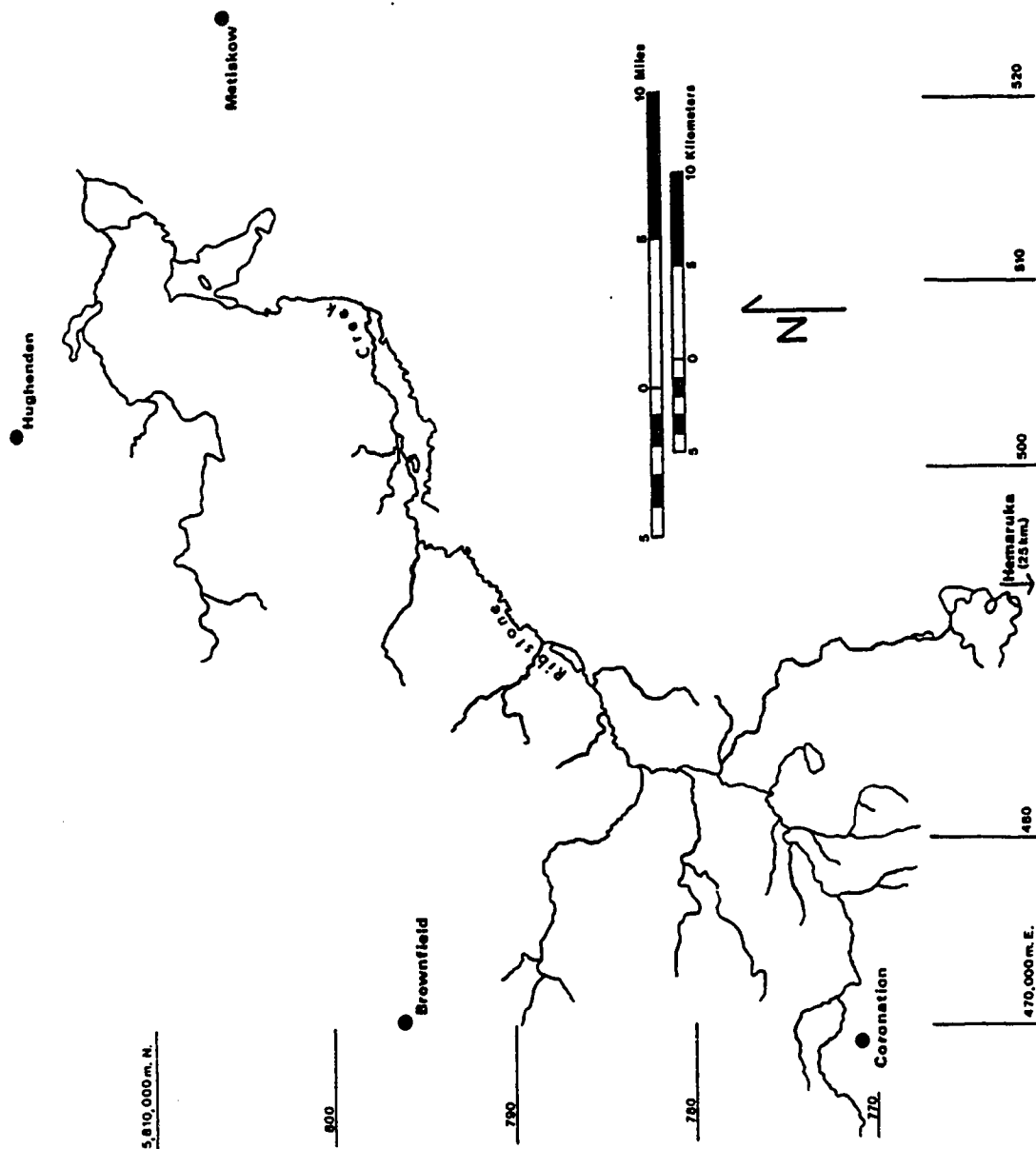


Figure 6-1: Climate stations near the Ribstone Creek watershed.

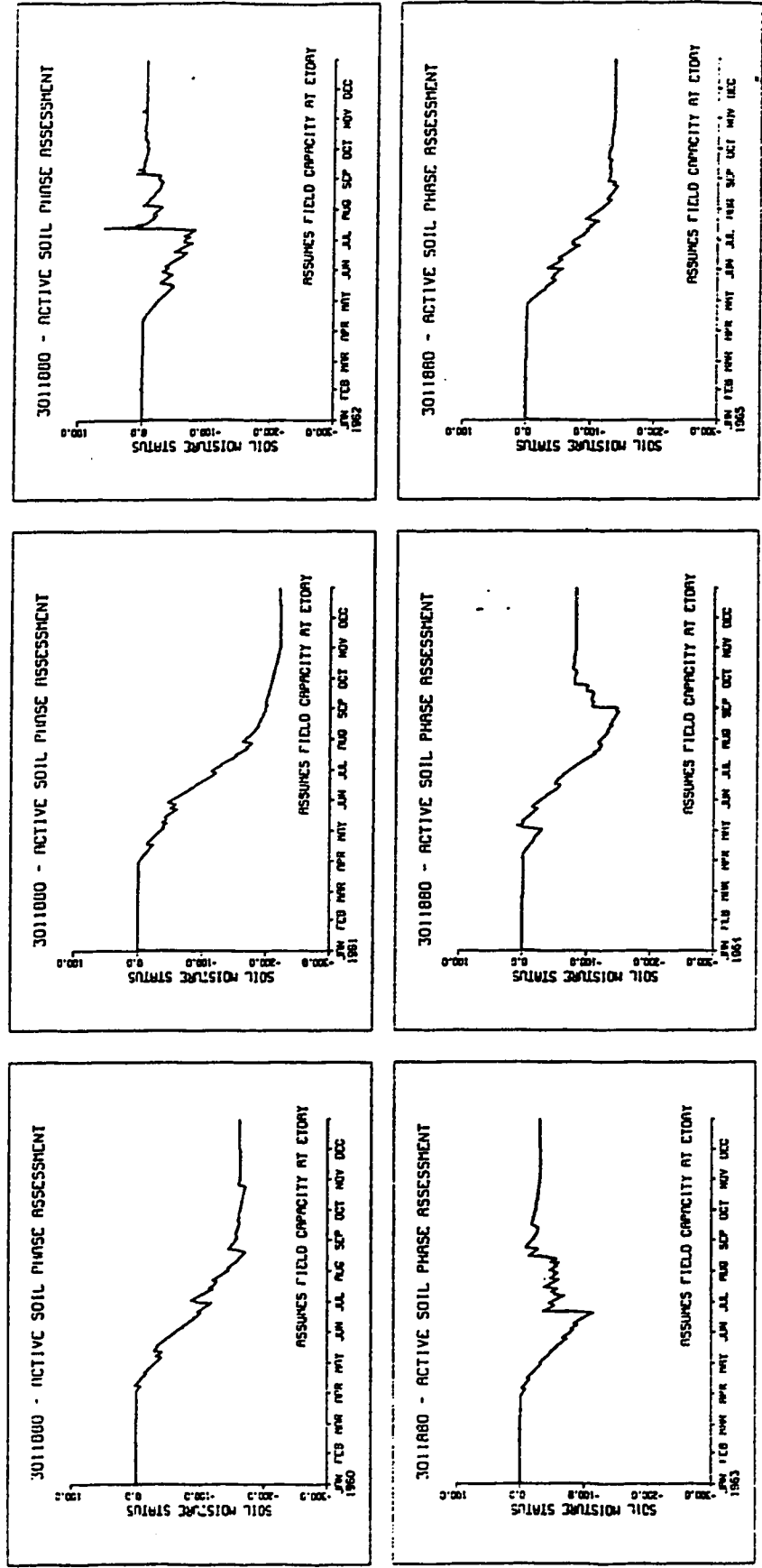


Figure 6-2: Active soil phase plots for Coronation.

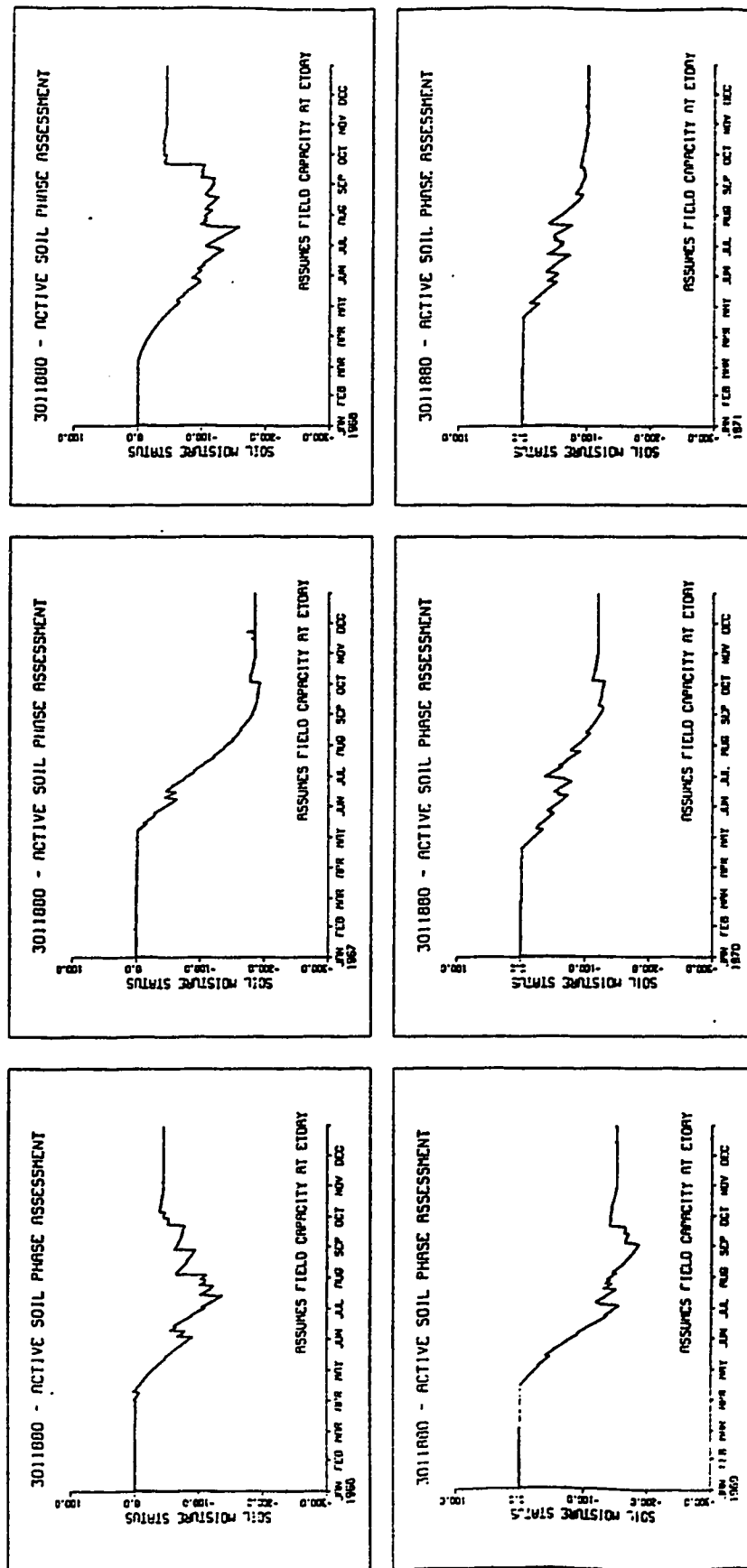


Figure 6-2, - continued.

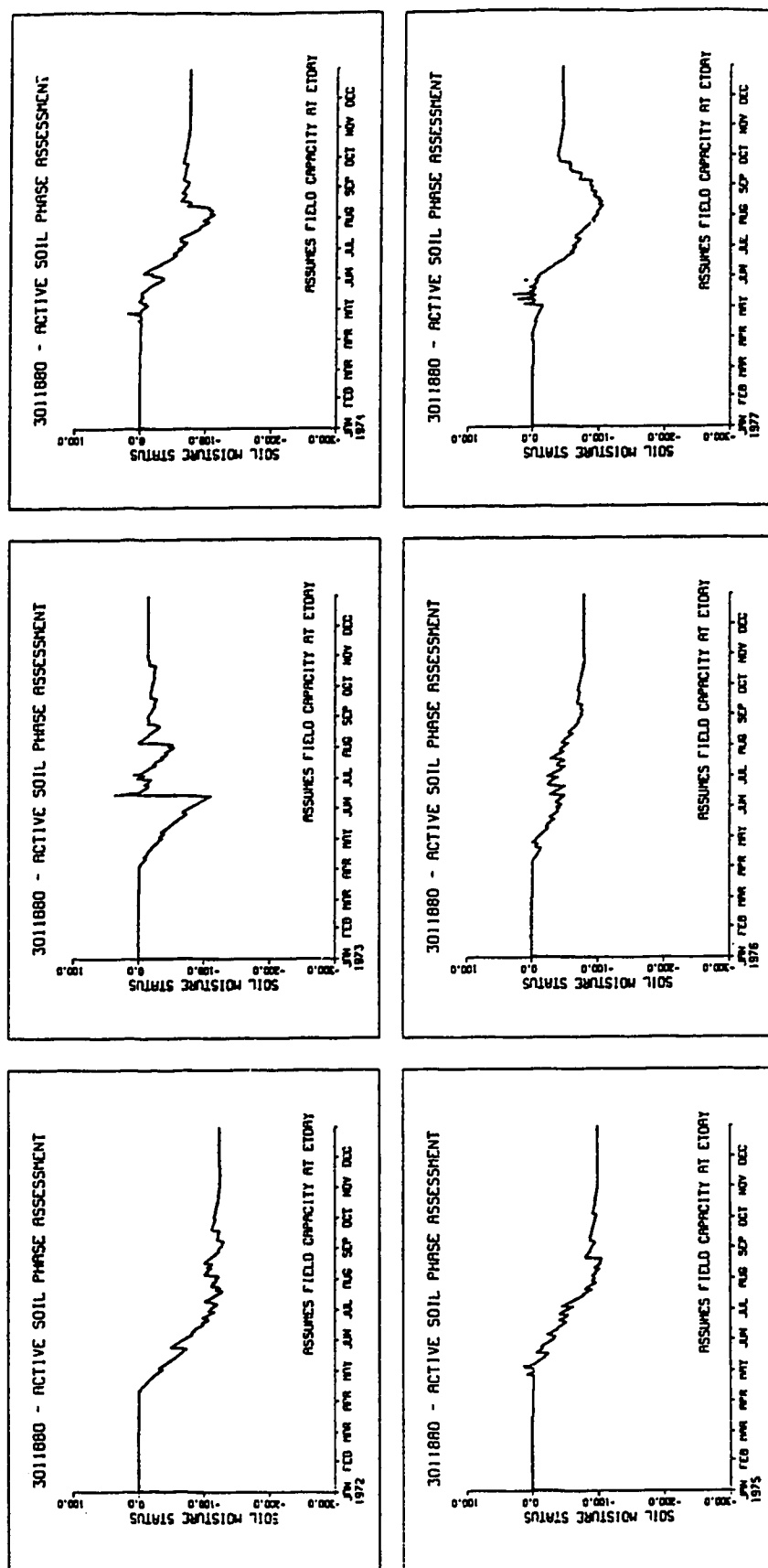


Figure 6-2, - continued.

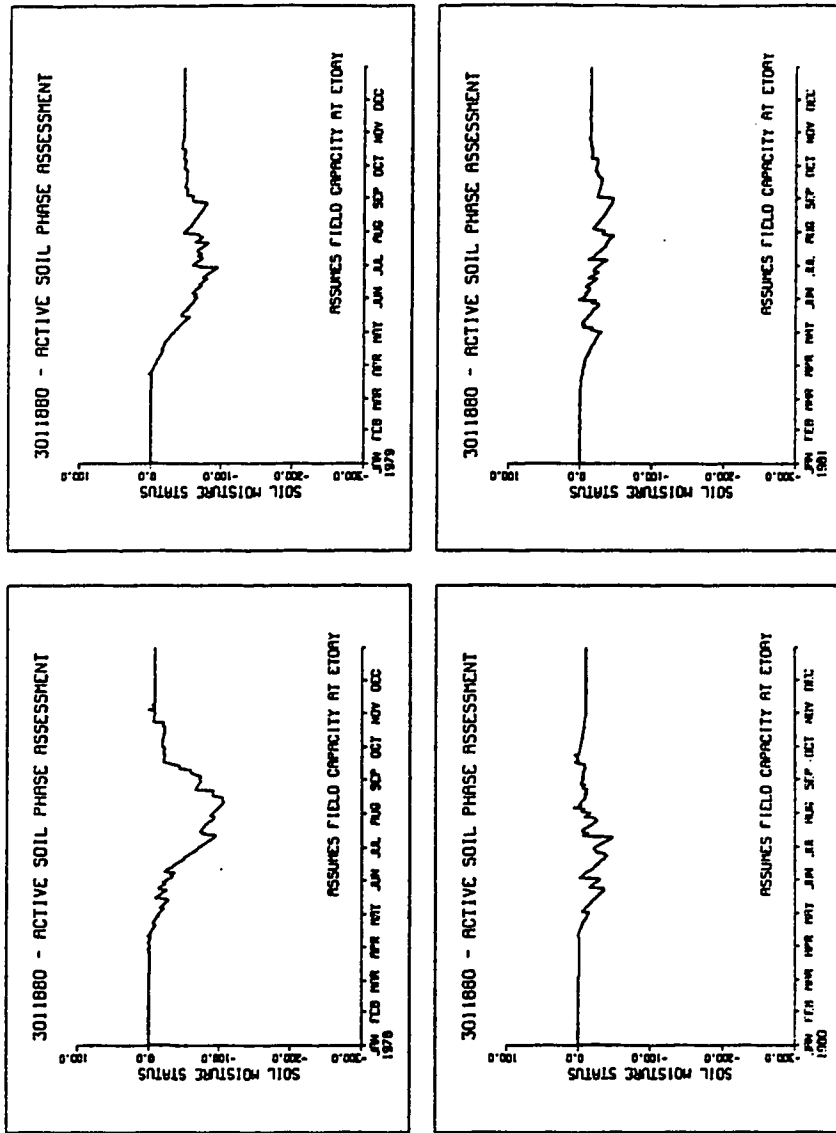


Figure 6-2, - concluded.

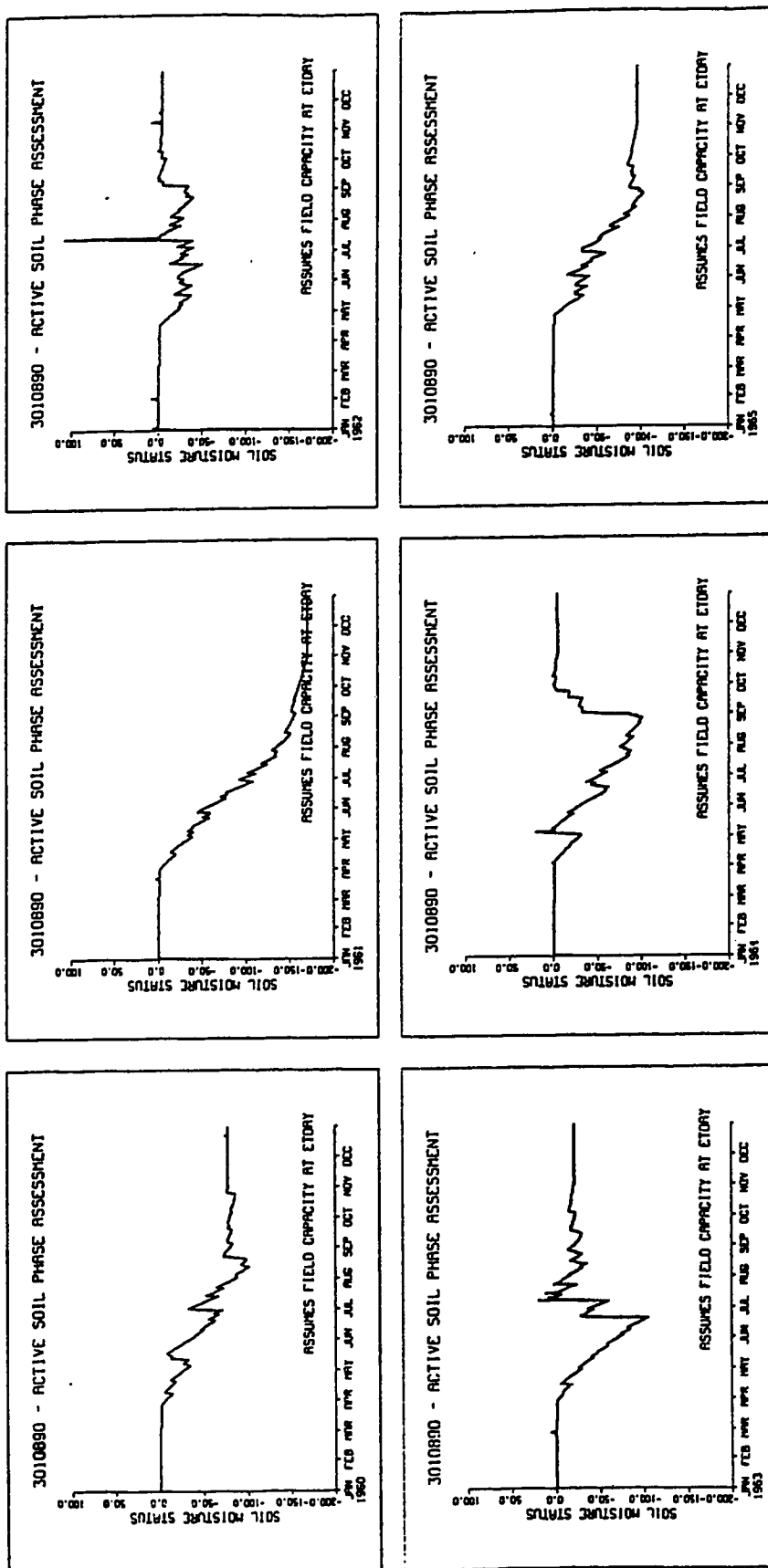


Figure 6-3: Active soil phase plots for Brownfield.

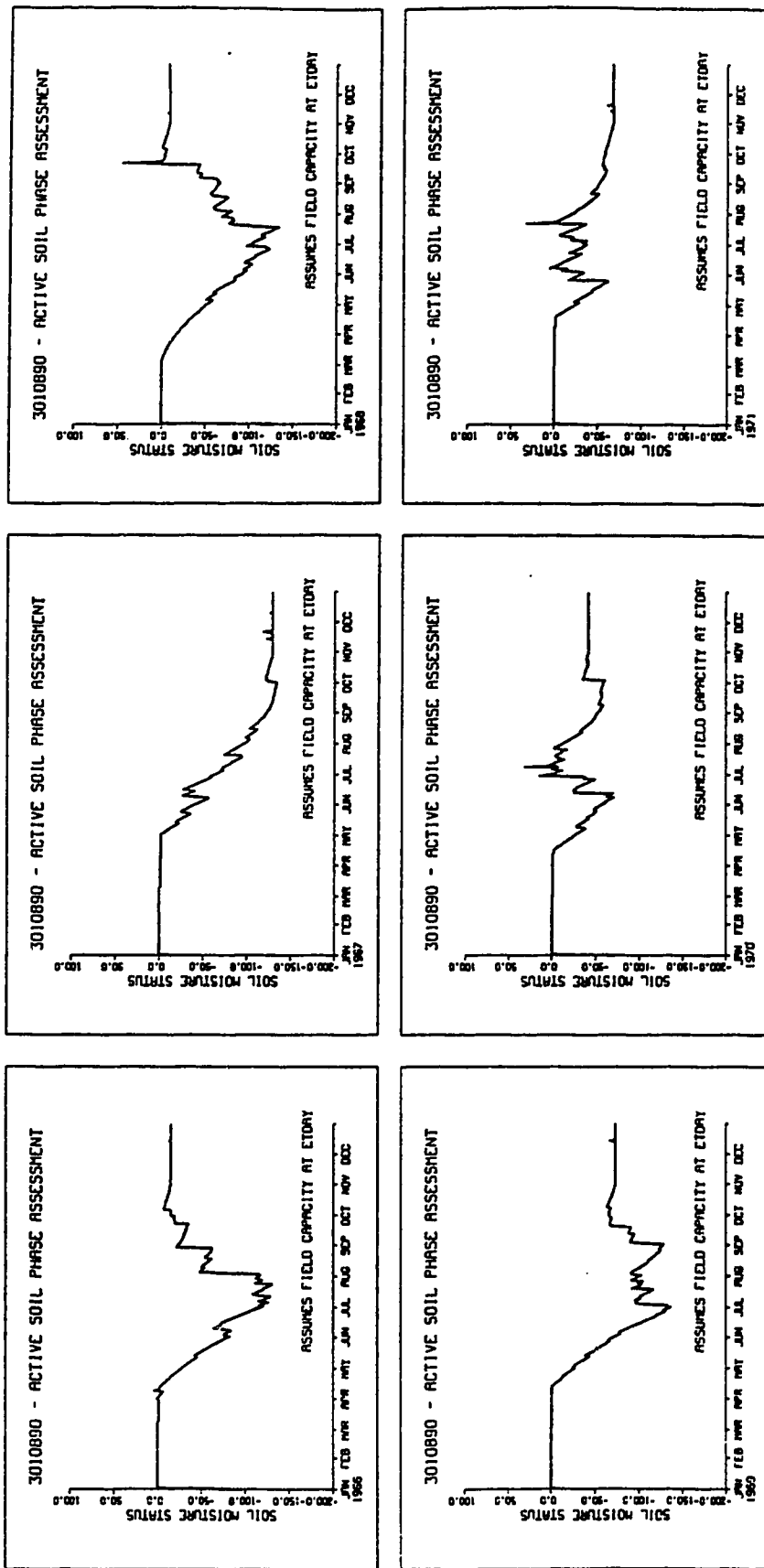


Figure 6-3, - continued.

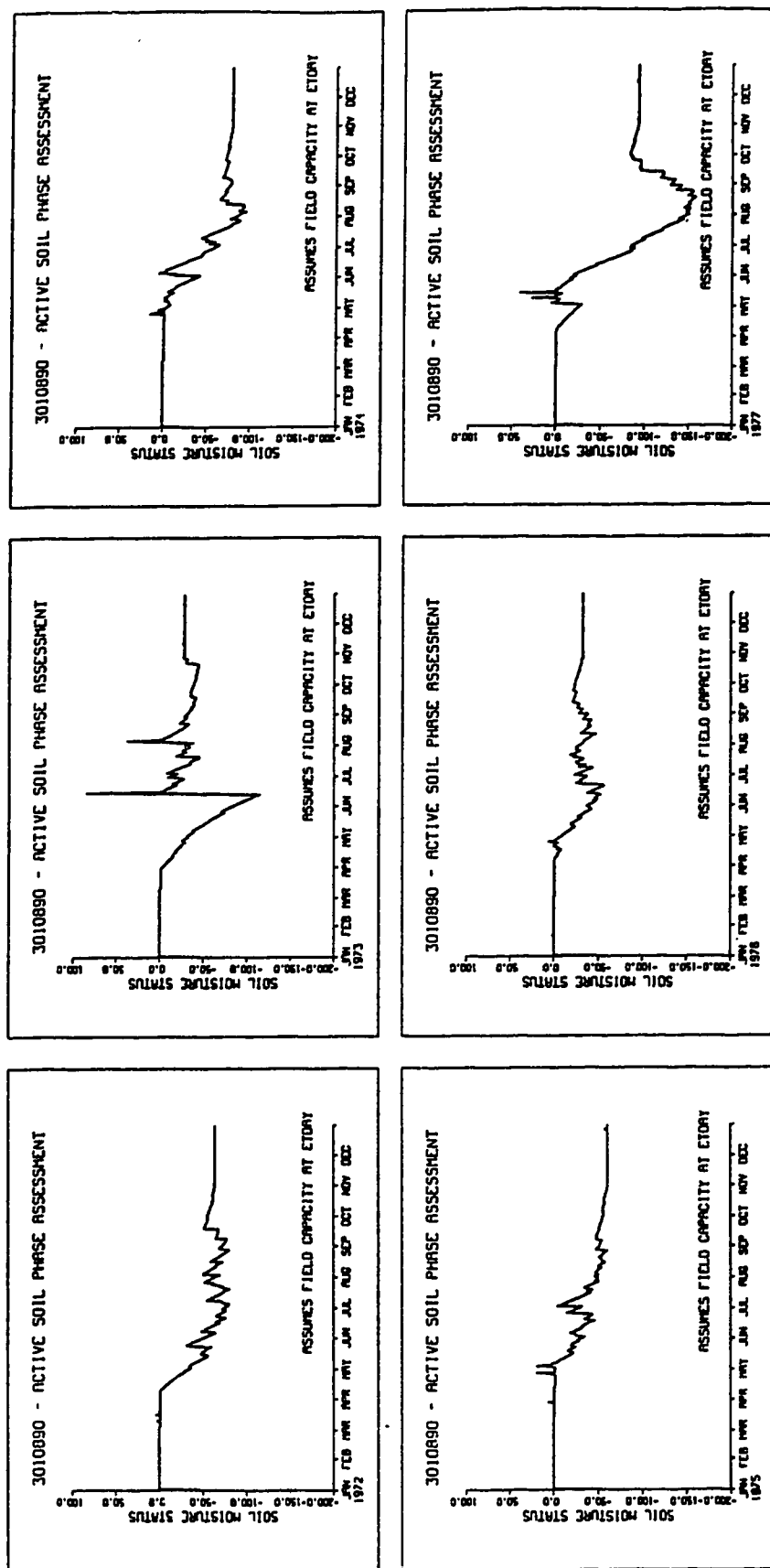


Figure 6-3, - continued.

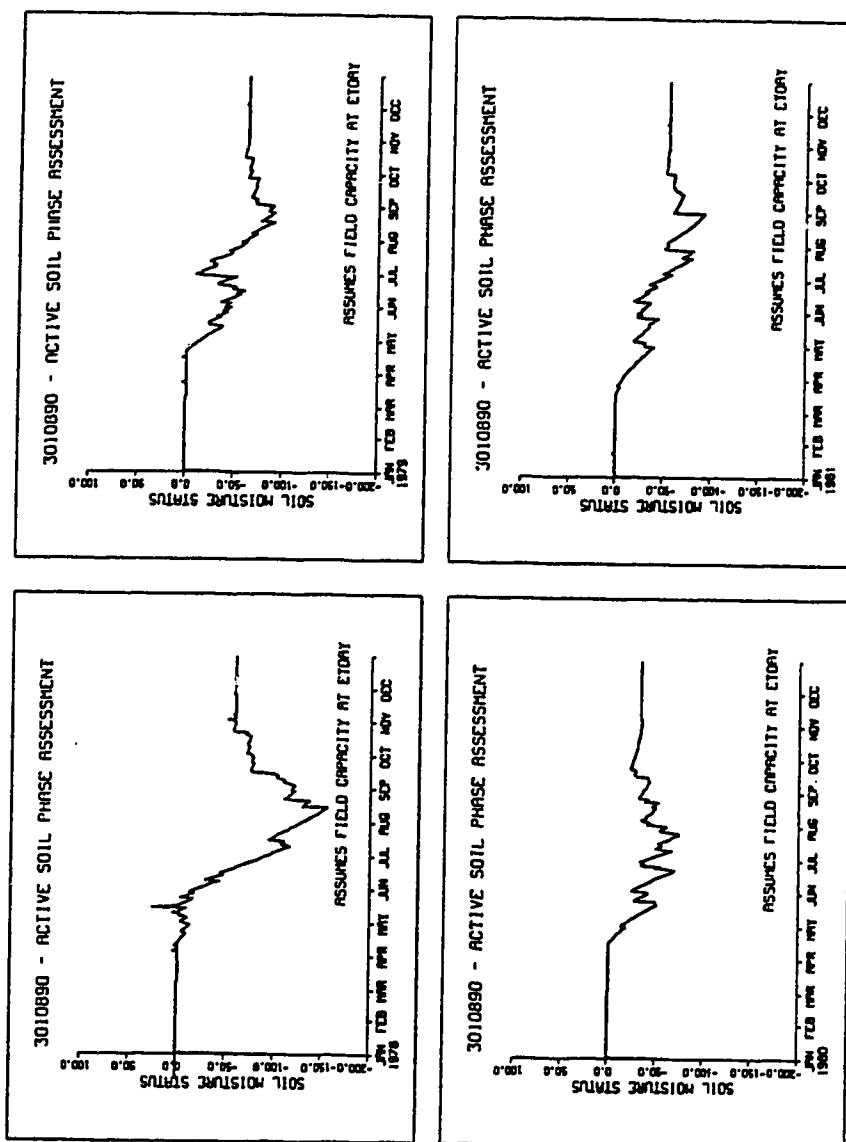


Figure 6-3, - concluded.

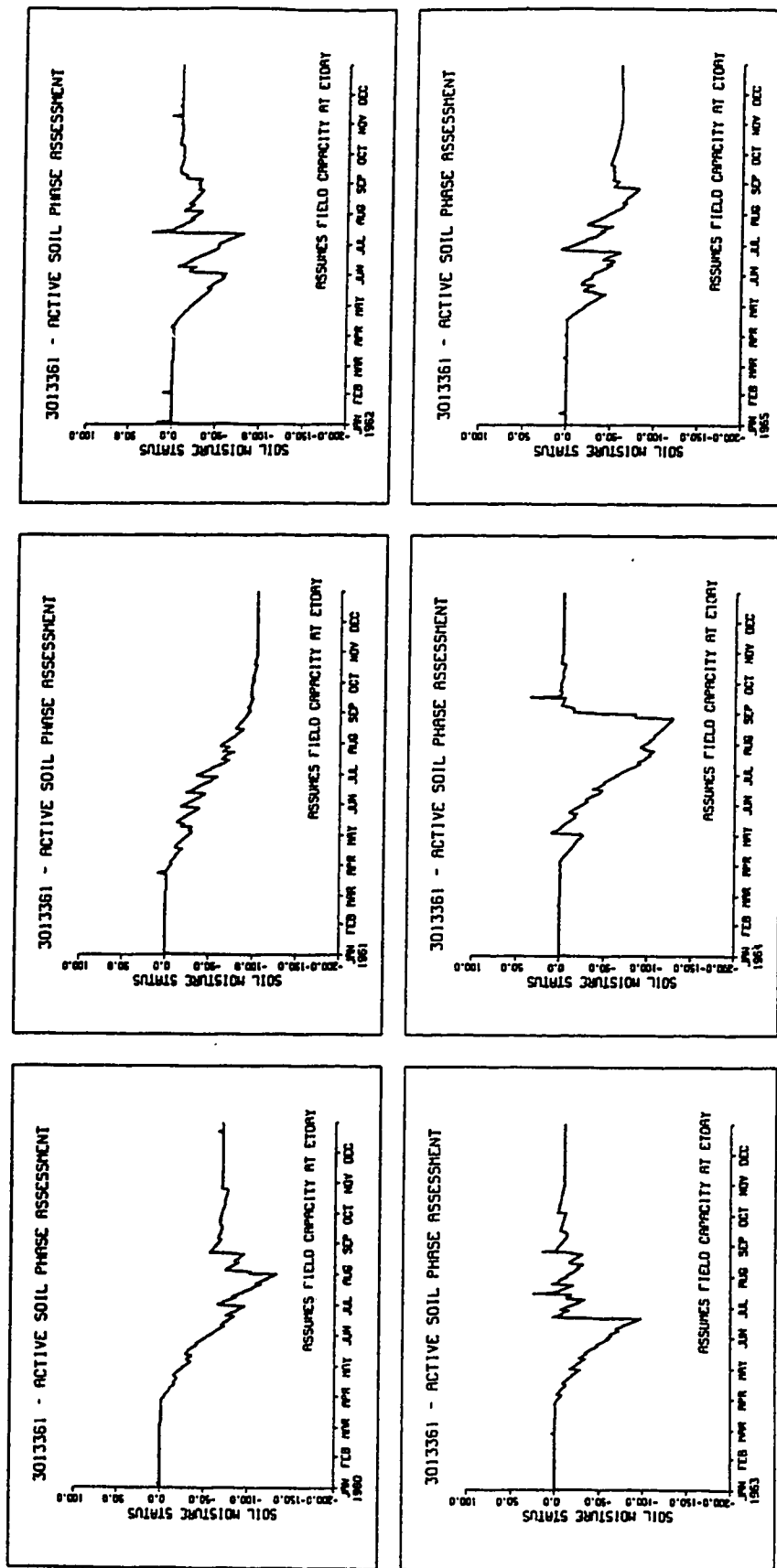


Figure 6-4: Active soil phase plots for Hughendon.

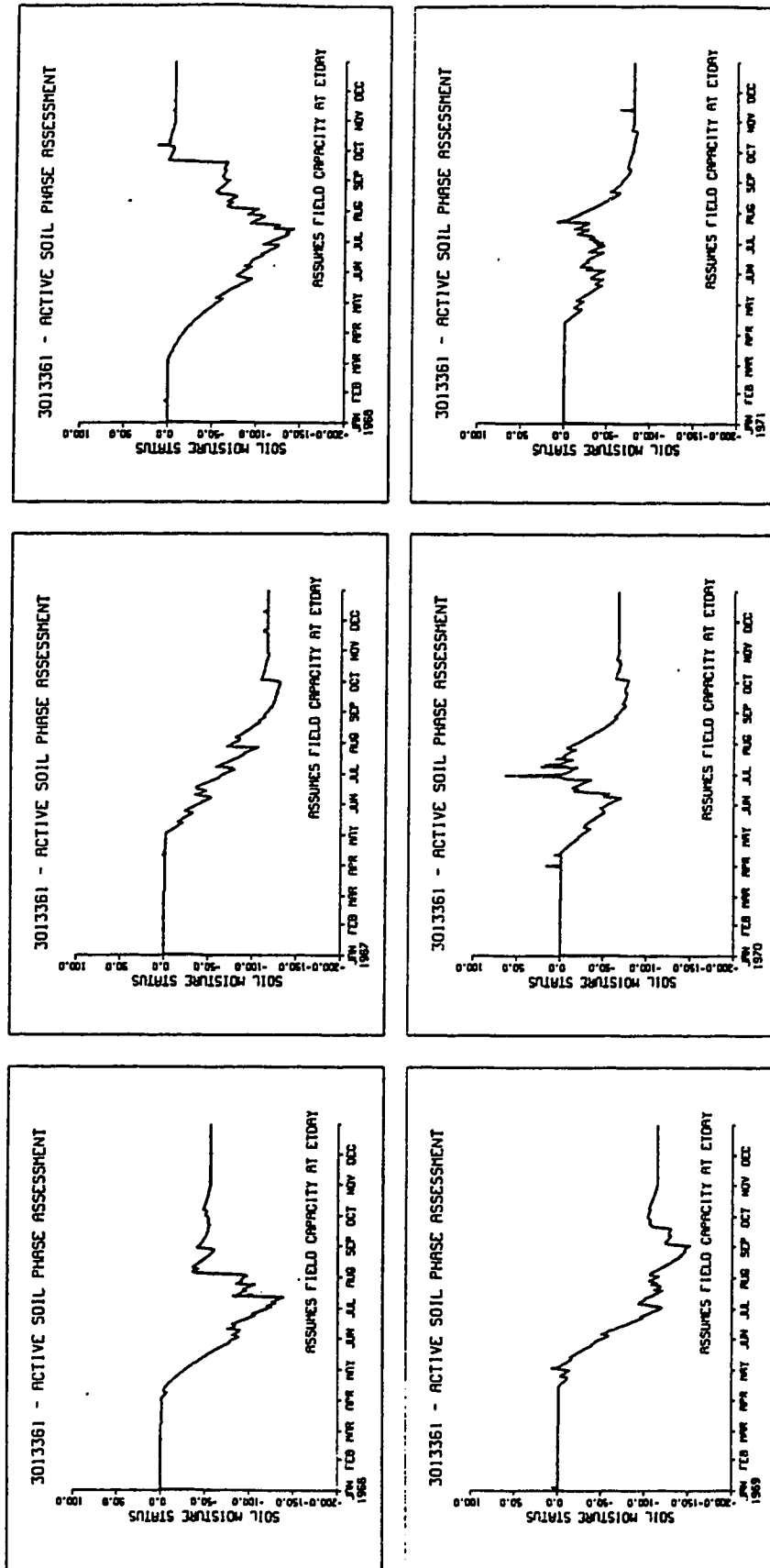


Figure 6-4, - continued.

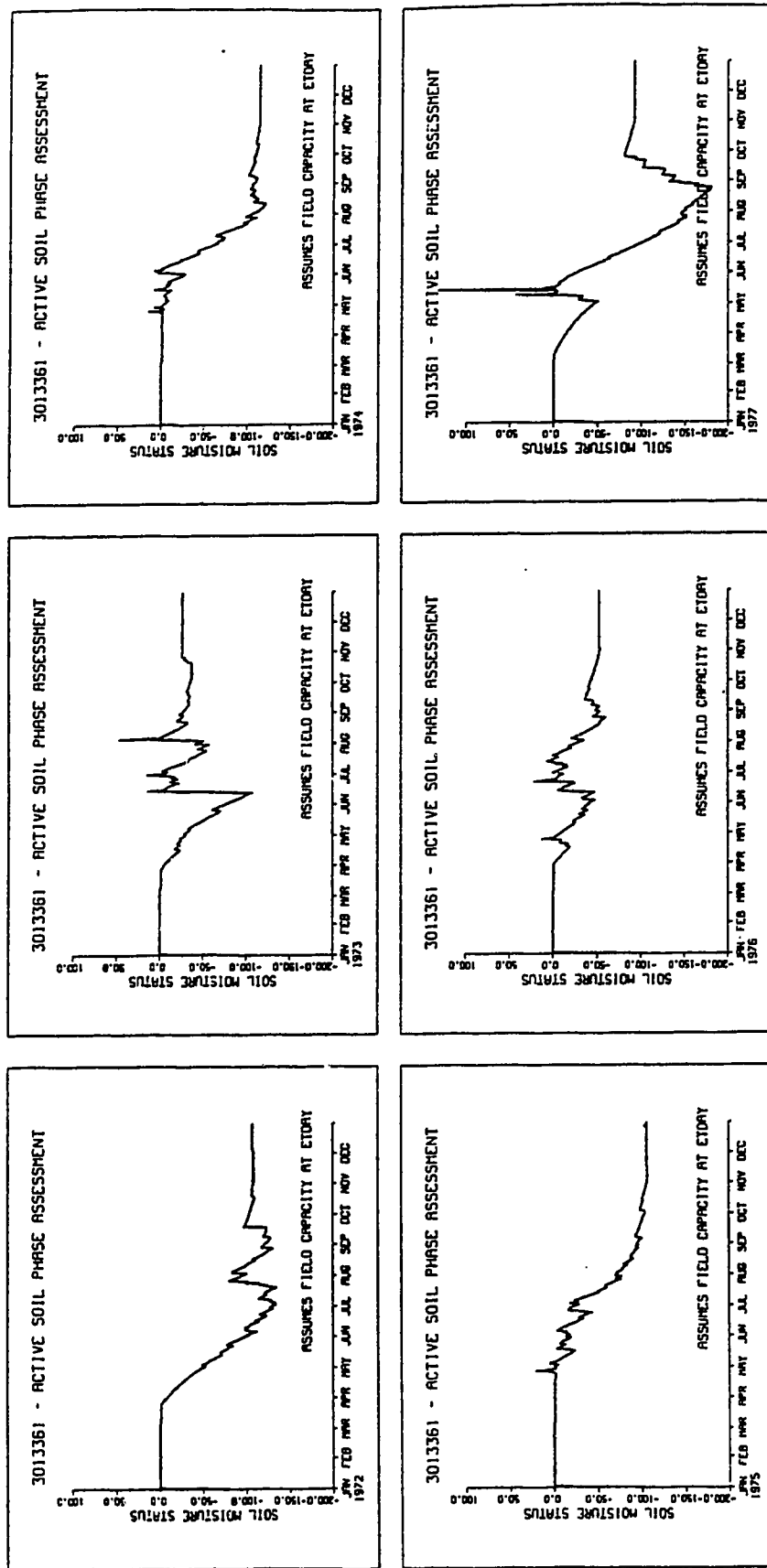


Figure 6-4, - continued.

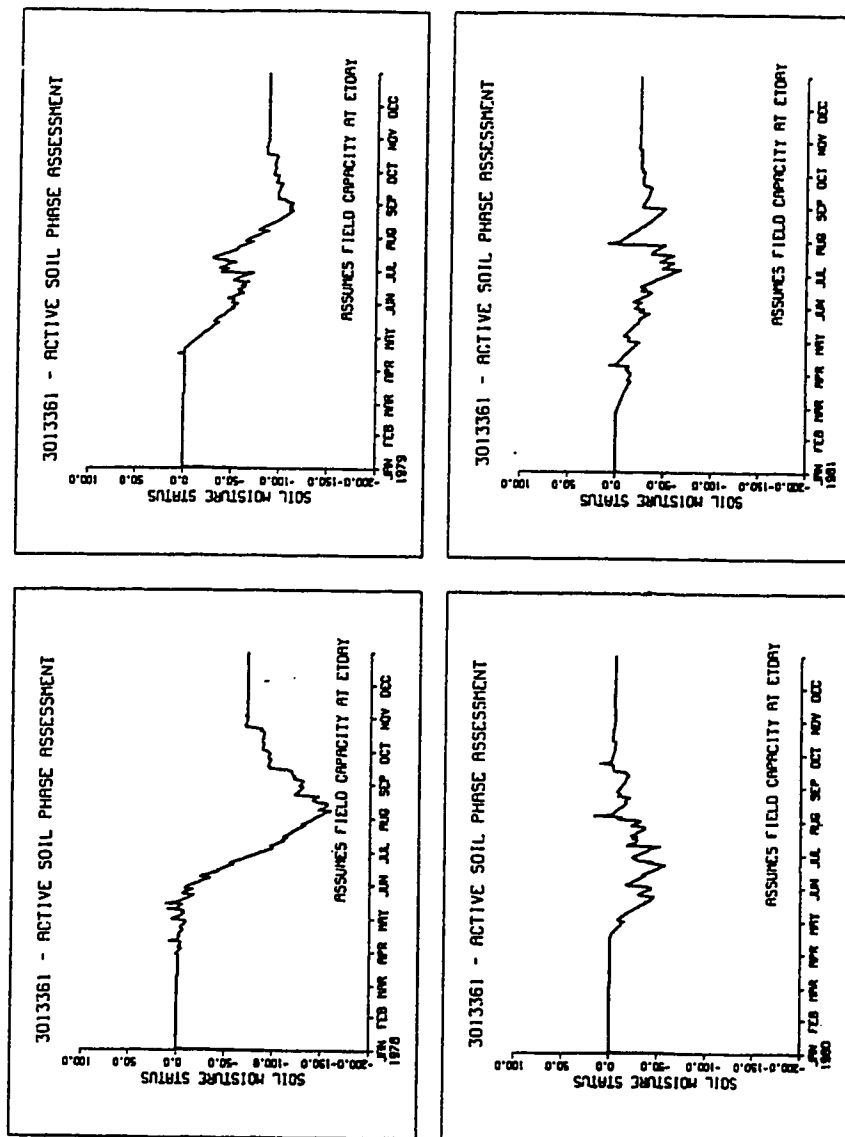


Figure 6-4, - concluded.

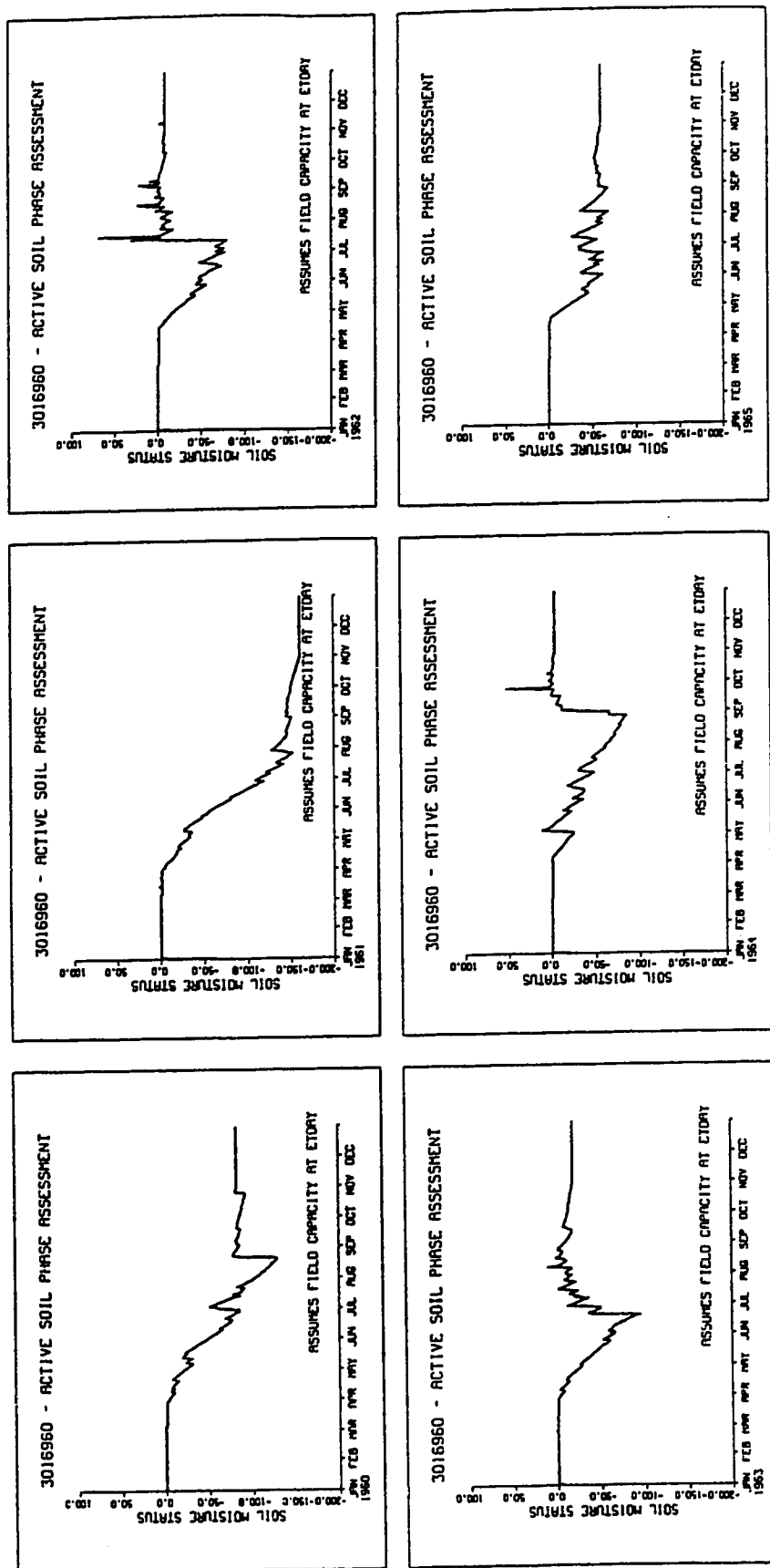


Figure 6-5: Active soil phase plots for Hemaruka.

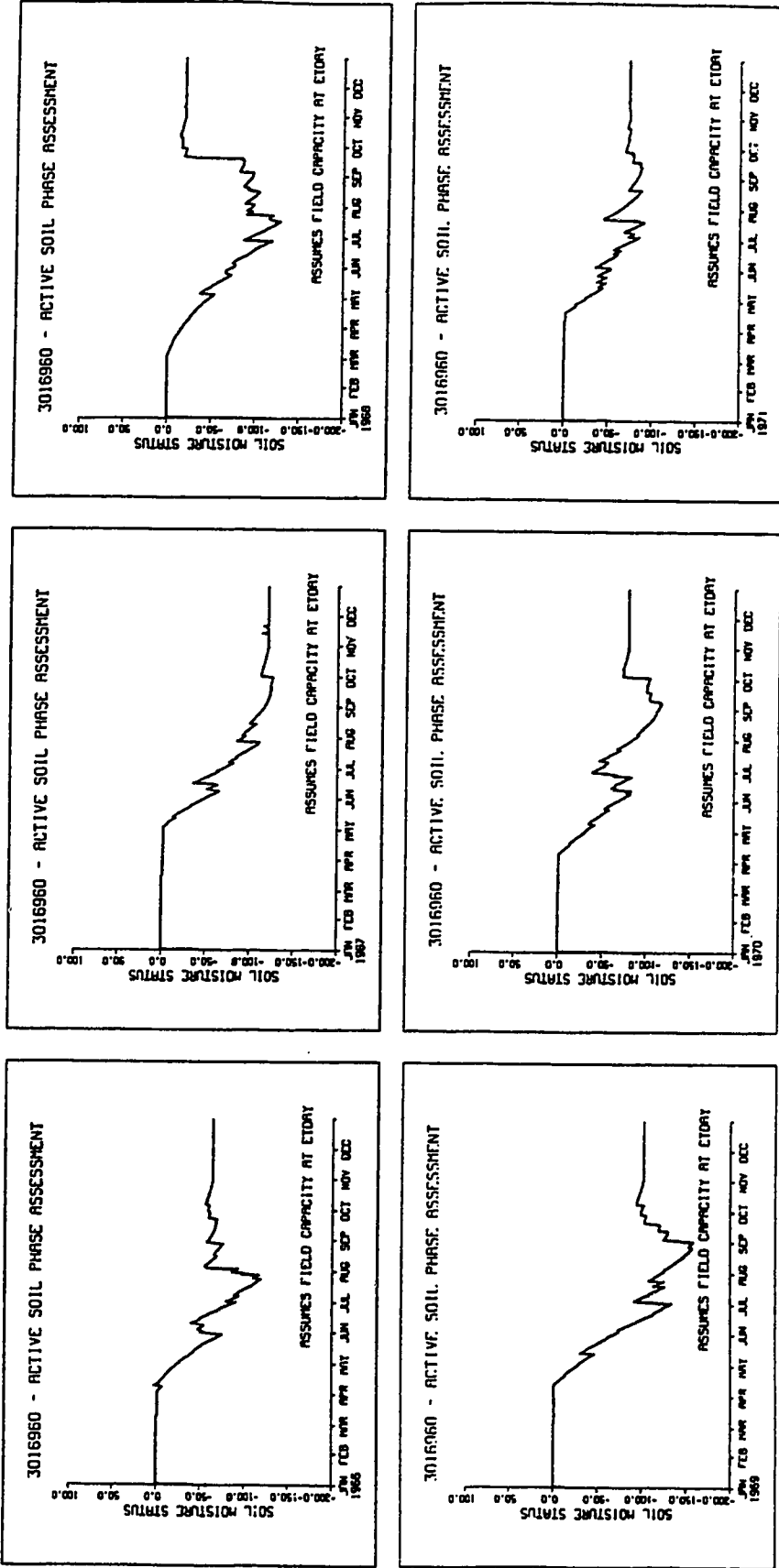


Figure 6-5, - continued.

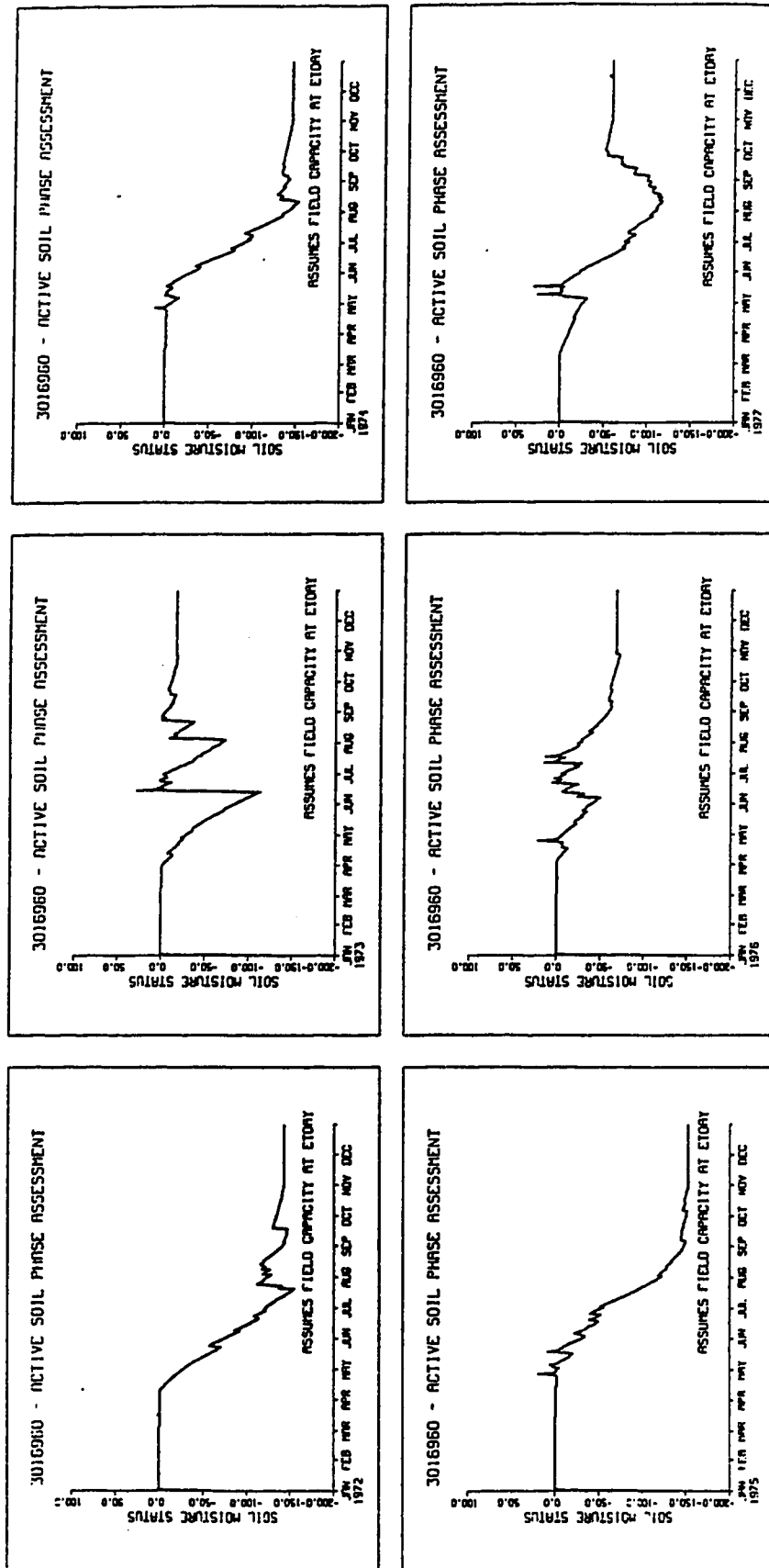


Figure 6-5, - continued.

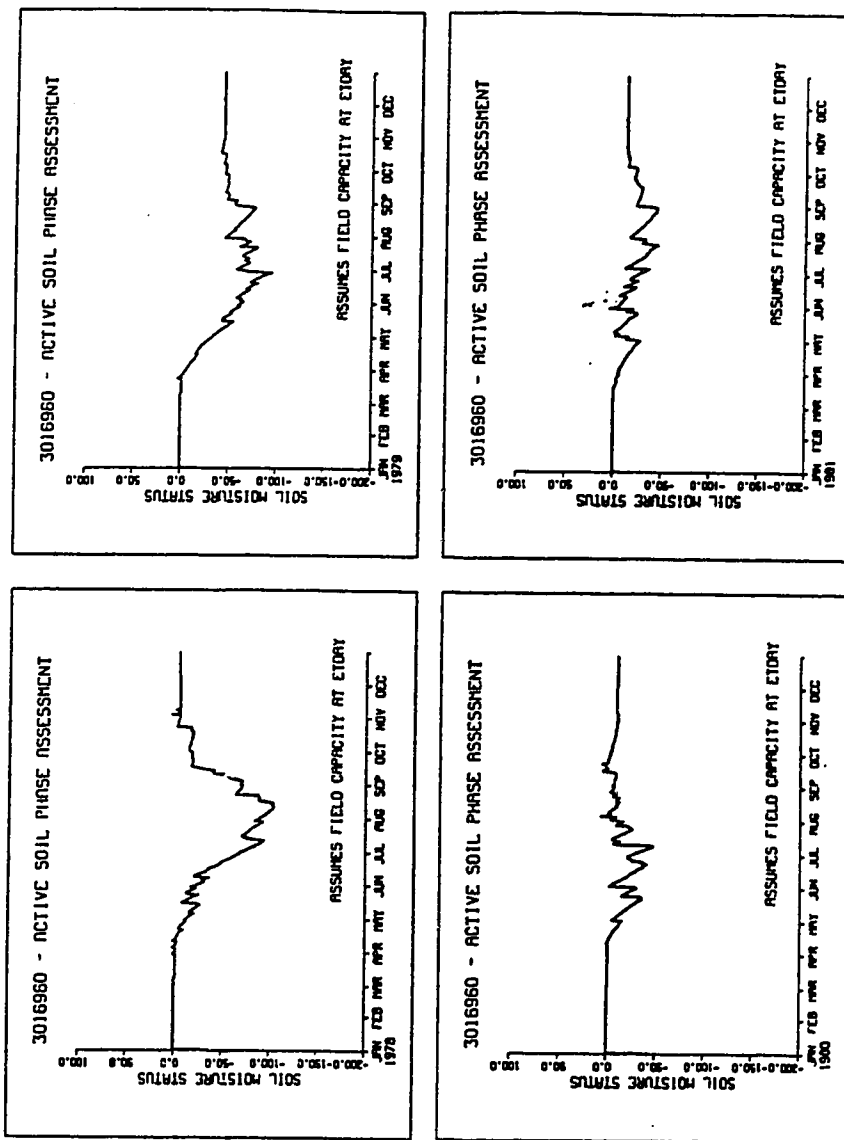


Figure 6-5, - concluded.

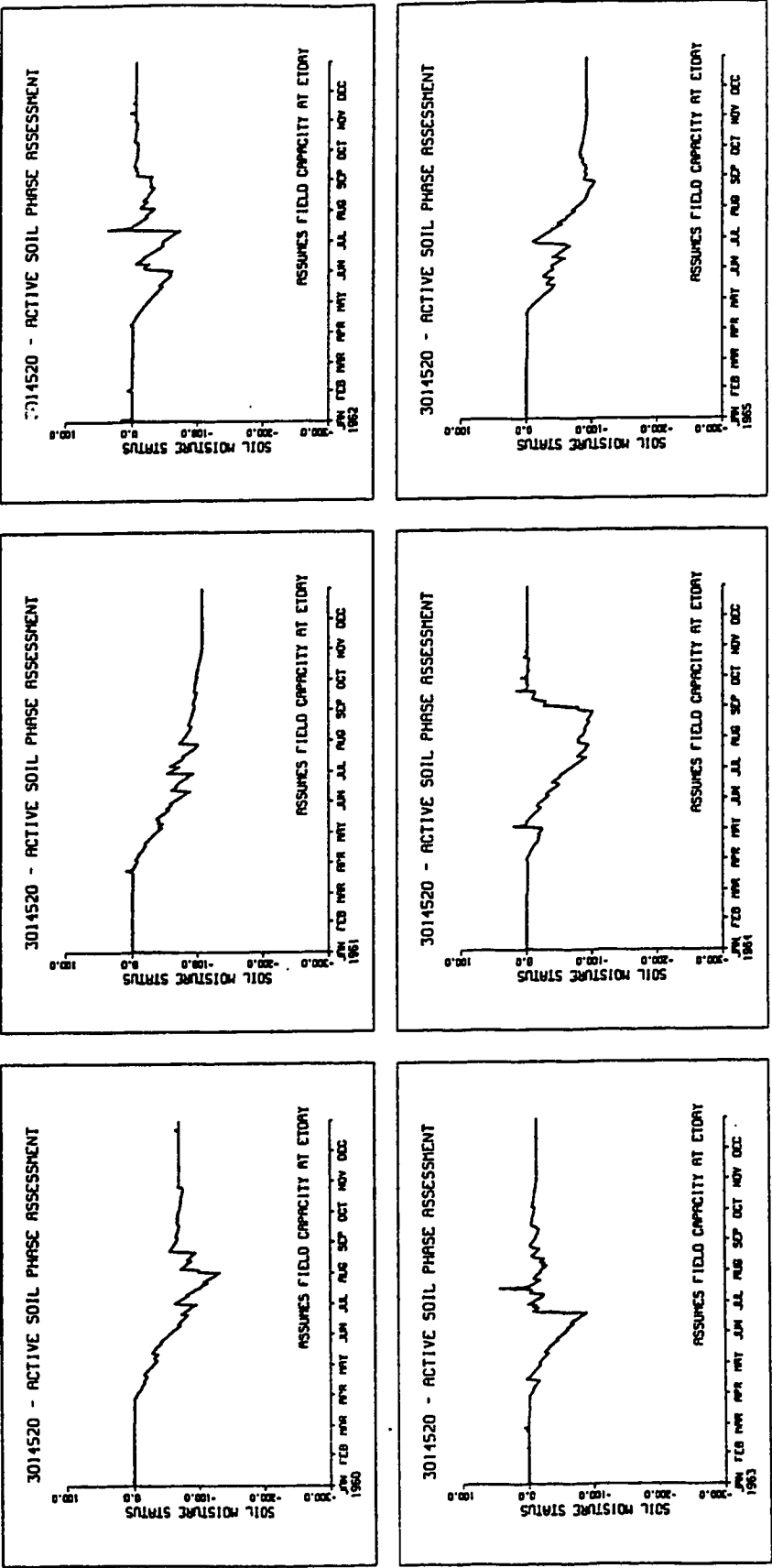


Figure 6-6: Active soil phase plots for Metisko.

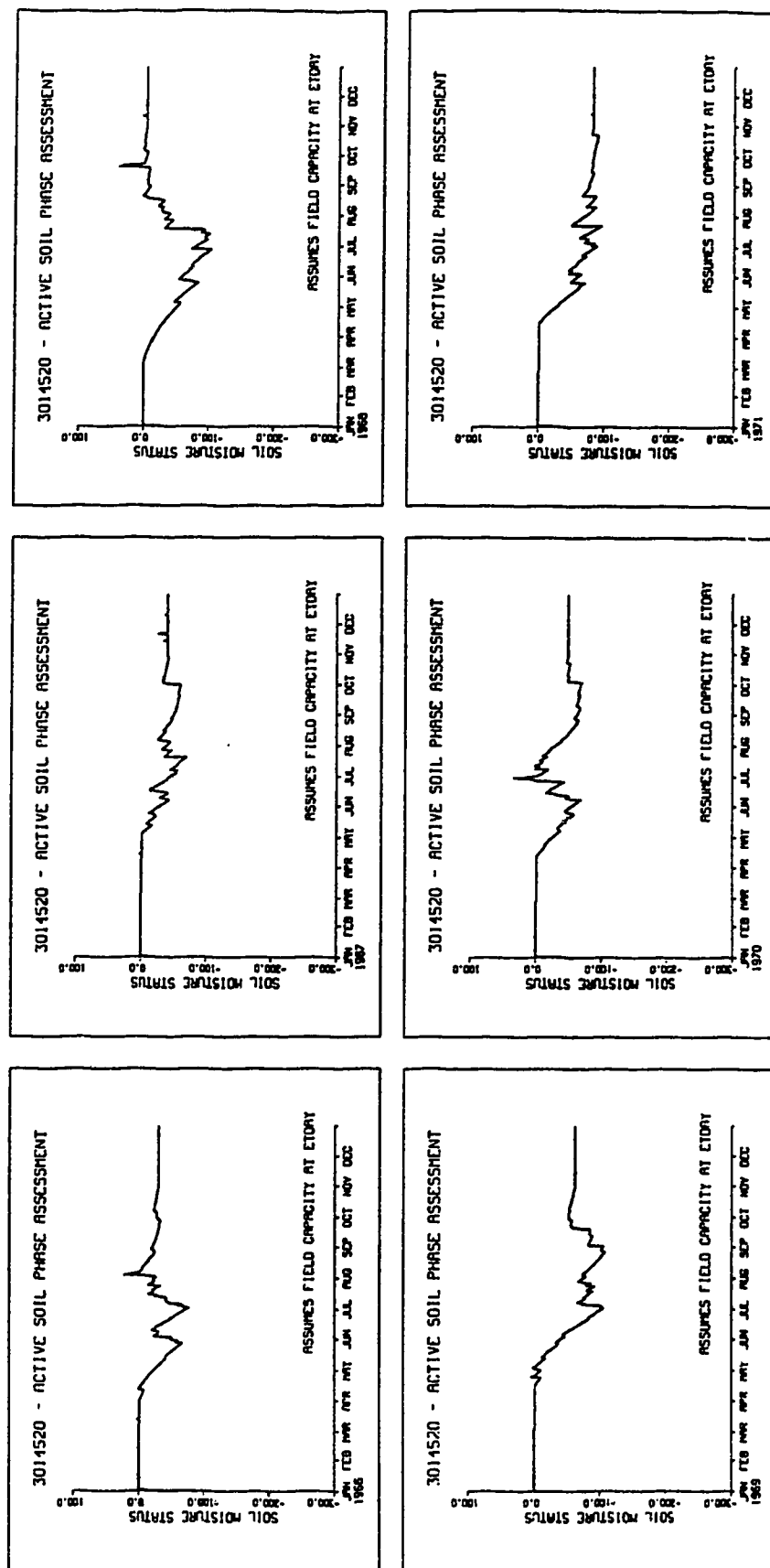


Figure 6-6, - continued.

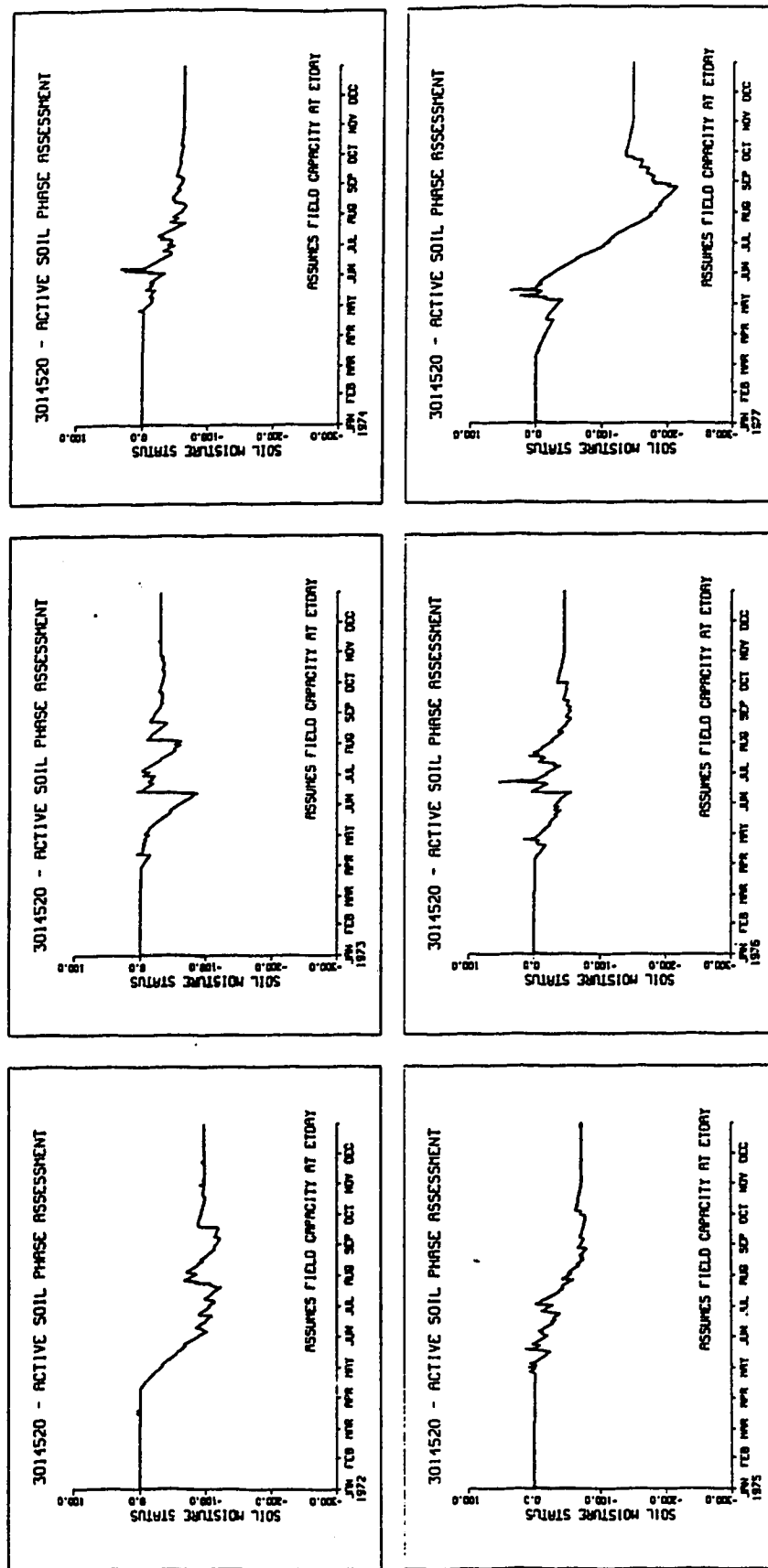


Figure 6-6, - continued.

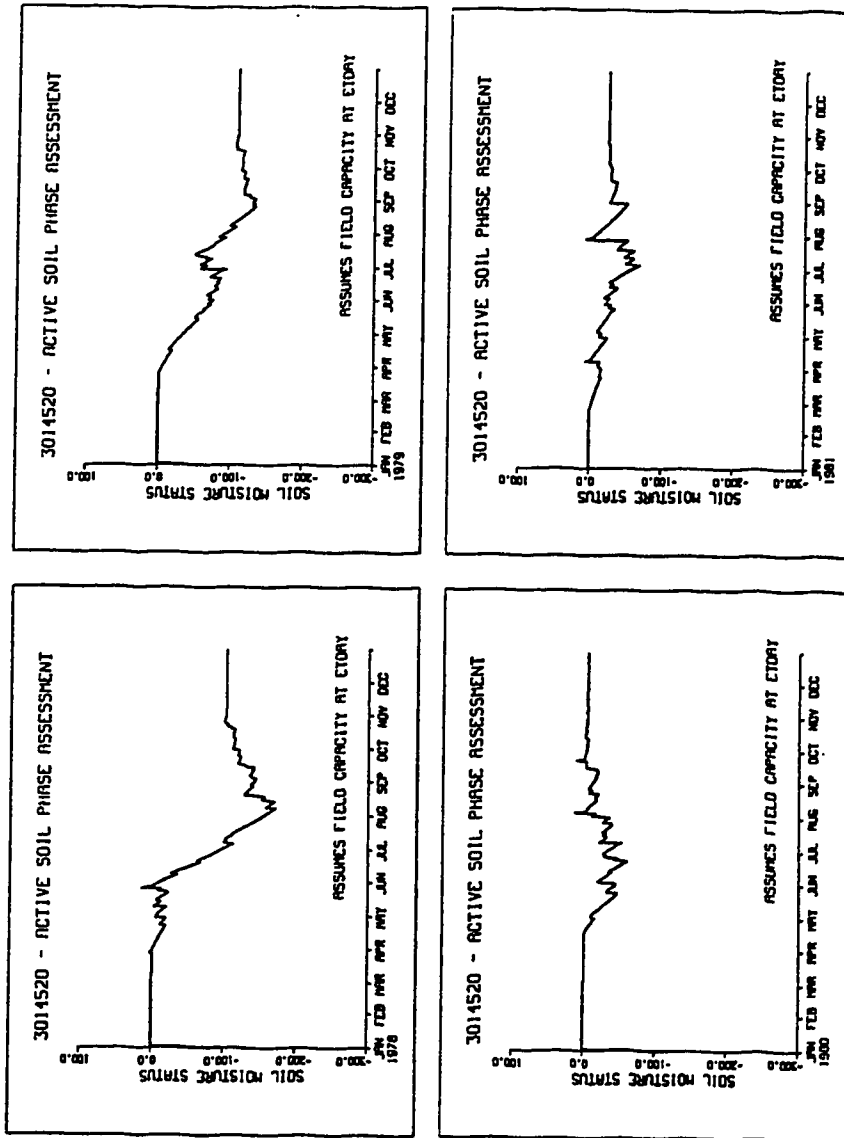


Figure 6-6, - concluded.

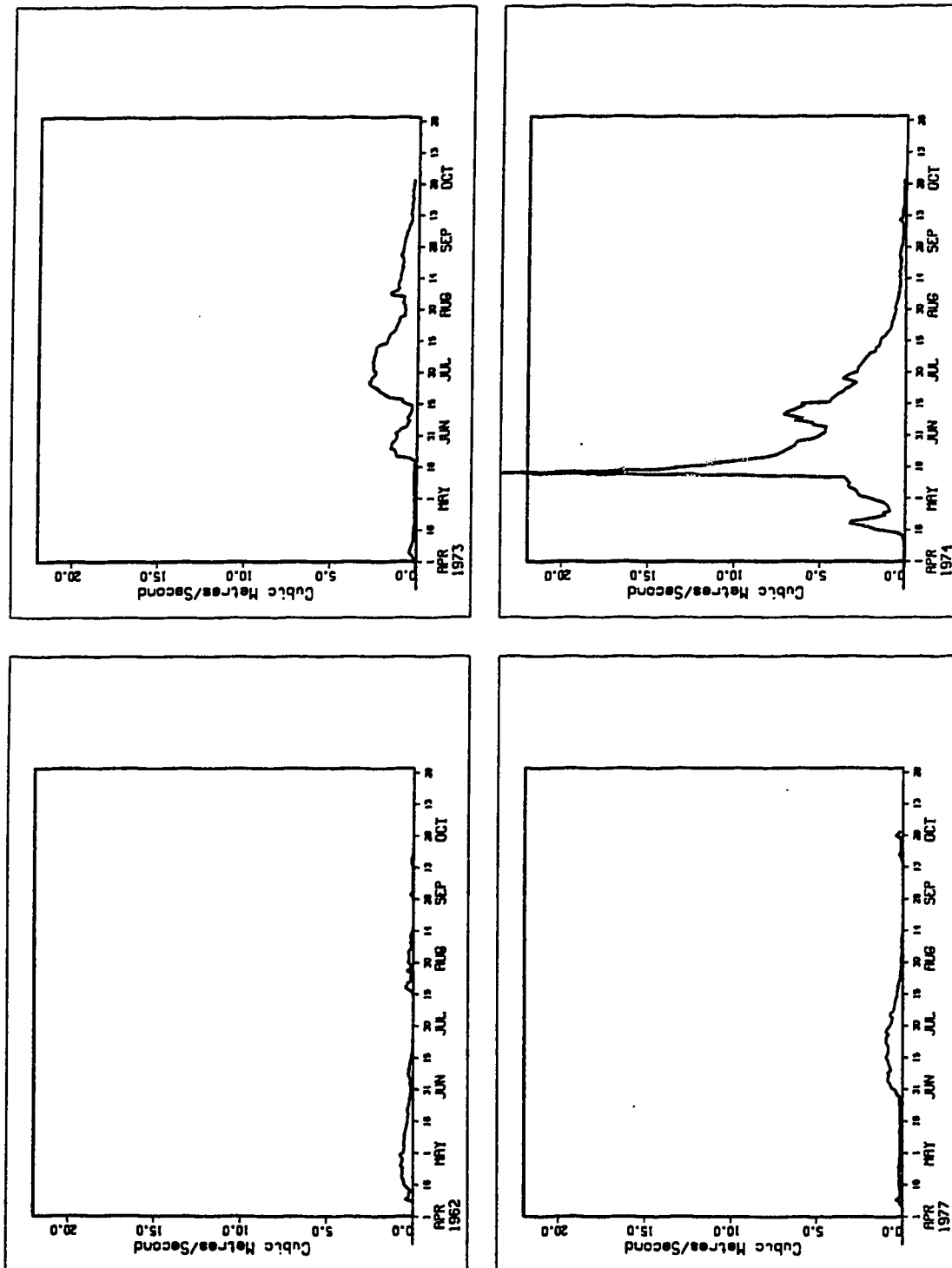


Figure 6-7: Annual runoff hydrographs, Ribstone Creek near Edgarton

Chapter 7

SATURATED SOIL PHASE ASSESSMENT⁷

RIBSTONE CREEK

7.1. Conceptual Model of Prairie Runoff Functions

The runoff from flatland watersheds on the prairies of eastern Alberta is poorly understood. Snow hydrology dominates the runoff picture in virtually all years; rainfall runoff is only notable during time periods when there is a saturated or inundated zone as a result of the spring snowmelt. A conceptual model defining the runoff processes has been developed, and is discussed in some detail in chapter 3. The discussion in this paper presents an analysis of the role of the saturated soil phase. This phase is defined as the saturated (inundated) portions of the basin with direct connections to the stream channel network. In the interest of brevity, only a brief discussion of the conceptual model is presented here.

The Prairie Runoff (PR) Conceptual model represents a three phase theory of prairie river runoff processes. The phases are defined in terms of the soil system: the frozen soil runoff phase deals with snowmelt and rainfall when the soil profile is frozen and, except for initial infiltration losses, essentially impermeable. The second phase, the active soil phase, deals with snowmelt and rainfall as inputs to the soil moisture

⁷A version of this chapter has been published. Byrne, 1989. Canadian Water Resources Journal, 14:3,18-29

system. Inputs are allocated to the soil moisture deficit first, then depression storage and finally, to streamflow runoff. The third phase, the saturated soil area, deals with those areas within the watershed directly connected to the channel network and fully saturated during the runoff season. These areas are assumed to have a runoff coefficient of 1.0; virtually all of the rainfall contributes to streamflow.

Chapter 5 provided an assessment of the relative role of the frozen soil runoff phase, and the impact that depression storage losses have on the annual runoff volume. The discussion here presents an analysis of the role of the saturated soil phase; including estimates of the relative volume of runoff that is derived from the saturated area, and a first approximation of the spatial variation of the saturated area over the runoff season.

7.2. Theory of Saturated Soil Phase Operation

The concept of the saturated soil phase in prairie runoff describes the hydrologic response of inundated or saturated areas directly connected to the surface drainage network. The most notable examples are river valley bottomlands that are inundated during spring snowmelt, and remain in that state for some portion of the runoff season. The actual channel network forms part of the saturated phase.

The saturated soil phase is critical to prairie hydrology because it is the source of virtually all runoff during the open water season. This may appear somewhat incredulous considering the saturated area is, at its greatest extent, only a small percentage of the total watershed area. However, discussion presented previously (Chapter 6 - Active Soil Phase) illustrated the minimal chance of rainfall runoff from the active soil phase, i.e. the soil zone with active vegetative growth. This, combined with the fact the saturated area has a runoff coefficient of 1.0, presents strong support for the concept of the saturated soil phase being virtually the only source of runoff from summer rainfall.

The saturated area is a dynamic factor in the watershed. However, there is very little information available to date on the scale of the area in relation to other basin parameters; or on the variations in the scale of the saturated area over the runoff season. Attempts to model the snowmelt response of Ribstone Creek were generally frustrated by an observed commencement of runoff before sufficient snowmelt had occurred within the model to allow any discharge. This phenomenon is noticeable in Figure 7-1, the 1974 recorded hydrograph. Simulated snowmelt hydrographs would have a similar volume of flow, but with a slightly higher peak than the recorded data, and an abrupt beginning. The simulated hydrograph was based on snowmelt depth and contributing area as determined in chapter 5. It is theorized the observed early runoff response is due to actions of the saturated soil phase. The following explanation is suggested.

The model assumes the entire basin is evenly covered with the simulated snow depth. Under a standard modeling scheme, the snowpack is subjected to simulated melting at the same rate over the basin. Therefore, simulated runoff begins from the entire basin at the same time. However, this is not the most likely situation. The following scenario is more probable: Snowmelt begins, and melt depths in excess of local losses, principally frozen soil infiltration, begin to pool in the areas that will become part of the saturated area once the depression storage deficit is overcome. This input of relatively large volumes of water accelerates the snowmelt process in these areas, principally by lowering the snow albedo, and secondly, by the meltwater heat input. Consequently, there is a quick melt in a constrained area, the saturated contributing area, and runoff begins at a date earlier than snowmelt modeling predicts. Two other factors are important. The saturated area is by definition a topographic low. Therefore, snow depths within the saturated area will be greater than the basin mean depth because of wind transport (drifting) into topographic lows. This deeper

snowpack would have a greater water storage capability and a greater cold storage. These two factors will tend to counteract the rapid melt discussed above. However, data to be presented (section 7.6) demonstrate the maximum extent of the saturated zone for Ribstone Creek is about 25 percent of the snowmelt contributing area. Since the saturated area is receiving runoff from an area much greater in extent, it is reasonable to assume the quick melt process within the saturated zone will still dominate the early spring runoff.

This saturated phase "quick melt" would result in a slightly lower runoff peak because at least some of the saturated phase snowmelt will have already runoff, resulting in a lower peak basin storage value.

The saturated area is at its greatest extent during the period of highest flows. From that point onward, a general decline in the area over summer will occur; interrupted by short term expansion in response to rainfall inputs.

7.3. Developing a Representative Basin Climate File

Assessment of the frozen soil phase was carried out with spatial analysis techniques of modeled spring snow water equivalent SWE data from a number of climate stations. This same approach is not feasible with the assessment of the saturated area, because of the temporal and spatial variability of individual rainfall events. Instead, the modeled estimates of SWE for the basin that were developed in Chapter 5 were related to the individual station SWE values with multiple regression techniques. The regression equations are assumed to be a reasonable reflection of the relative contribution of each the climate stations to the net basin rainfall.

For Ribstone Creek near Czar, the climate stations utilized to determine the net basin rainfall during the open water season are listed in Table 7-1, along with the station values for SWE for each year.

The daily climate data files for the five stations listed in Table 7-1 were combined into a representative precipitation file for Ribstone Creek. No specific information had been developed regarding temperature variation between the stations. Therefore, the daily maximum, minimum and dewpoint temperatures recorded for Coronation were assumed to be representative of the entire basin. However, the regression equation developed in Table 7-1 from the modeled station SWE and the spatially analysed basin SWE was utilized to estimate the net daily basin rainfall for application in the saturated soil phase analysis.

7.4. Basin Storage - Outflow Relationship

A storage outflow curve is required in order to assess the role of the saturated area. The curve was developed using the snowmelt method (Pipes and Quick, 1977) that has been incorporated in the Prairie Runoff Model (PR Model - developed to reflect the Three Phase Conceptual Runoff Model), and the recorded Water Survey of Canada runoff hydrograph. The methodology was straightforward. The snowmelt model was run for the 1974 season, with the snowpack water equivalent that was estimated in Chapter 5. According to that analysis, the total runoff due to snowmelt is

$$RVOL = 1000 [SWE - INF - DP] AREA \quad (7.1)$$

where:

$RVOL$ = runoff due to snowmelt in cubic metres, SWE = spring snow water equivalent in mm, $AREA$ = maximum frozen phase contributing area in sq. km., INF = snowmelt infiltration losses in mm, and DP = depression storage losses in mm.

The net snowmelt runoff in 1974 was:

$$RVOL = 1000 [163 - 61 - 18] 320 = 26,880,000 \text{ m}^3 \quad (7.2)$$

The maximum discharge occurs in response to the peak basin storage value. The snowmelt model determined that snowmelt had finished two days prior to the date of maximum mean daily discharge. Therefore, the peak basin storage value S_j , assuming a two day lag in movement of snowmelt to the saturated storage area; may be estimated as

$$S_j = 26,880,000 - \sum_{i=1}^{(j-1)} Q_i 86400. \quad (7.3)$$

where Q_i = recorded daily runoff in m^3/s , i = the first day of snowmelt, and j = the date of peak basin storage. The second term on the right hand side of Equation (7.3) is simply the volume of outflow from the basin from the beginning of snowmelt to the day previous to peak basin storage. Using Water Survey of Canada data yields

$$\sum_{i=1}^{(j-1)} Q_i = 66.01 \text{ m}^3/\text{s}$$

Therefore, the S_j is

$$S_j = 26,880,000 - 66.01 (86400) = 21,200,000 \text{ m}^3 \quad (7.4)$$

This provides a second point for developing a linear storage-outflow relationship. The first point is (0,0). The storage outflow relationship for Ribstone Creek near Czar, based on this analysis, is

$$Q_i = 9.867E-7 S_i \quad (7.5)$$

7.5. Assessing Saturated Area Variability

The role of the saturated soil phase is assessed on a daily basis; using the storage-outflow relationship, the recorded Water Survey of Canada runoff hydrographs and the basin rainfall data developed from the data in Table 7-1. Table 7-2 contains estimates of the saturated area extent as a function of the basin live storage. These estimates were developed with the following methodology.

First, the storage outflow relationship was used to generate the daily basin storage from the WSC recorded daily hydrograph. The basin storage variation provided a direct reflection of the response of the hydrograph to a rainfall input. Second, dQ , the net change in discharge due to the rainfall input on day $(i+1)$ was determined as

$$dQ_i = (Q_i - Q_{i-1}) + (Q_{i-2} - Q_{i-1}) \quad (7.6)$$

Third, the estimates of dQ were input to the basin storage-outflow relationship to estimate dS , the change in basin storage due to a rain input to the saturated soil phase. The areal extent of the saturated soil phase is then calculated with

$$AREA_i = dS_i / (1000 RAIN_i) \quad (7.7)$$

where rain depth is in mm and the area is in square kilometres.

The above analysis was carried out for rainfall events that fit the following criteria:

1. The rainfall depth was greater than 5 mm. Values of less than 5 mm are subject to greater relative error in measurement, and would therefore introduce a greater error to the analysis.

2. Rain events occurring during a rapid decline in the hydrograph were not used. Attempts to estimate dQ_i in this situation are subject to large error because the daily rate of decline in discharge is much greater than dQ_i .
3. For time periods with basin storage levels below 100,000 m³, only rainfall events in excess of 10 mm were used.
4. Periods of several days of small rainfalls were neglected because of the difficulty in isolating a rain event with a hydrograph response.

Finally, it is important to note that none of the storms were of sufficient magnitude to cause any simulated runoff from the active soil phase. Therefore, it is reasonable to assume the recorded hydrograph response is due to the direct input of rain to the saturated area, rather than to any runoff from the unsaturated zones near the channel system.

7.6. Discussion

Figure 7-2 is a scatter plot of the estimates of saturated area against the total basin storage volume for the same date. The saturated area SAREA varies in a non-linear fashion with increasing basin storage (Table 7-2 and Figure 7-2). The general shape of the data curve indicates a function of the form

$$SAREA_i = a \exp(b S_i) \quad (7.8)$$

would fit the data reasonably well. Equation (7.8) is a semi-logarithmic function that may be linearized by plotting the $\ln(SAREA_i)$ against S_i (Figure 7-3).

The data in Figure 7-3 are reasonably linear for basin storage values in excess of

1,000,000 cubic metres. However, below this value, there is a wide scatter that serves to lower the significance of any statistical analysis. The failure of the data in this range to display any reasonable progression is not unexpected, given the combined error in the input data and the analysis is likely on the same order of magnitude as the estimates values. Two regression analyses relating the live basin storage to the extent of the SAREA are presented in Table 7-2. Comparison of the two analyses reflects the above discussion. The R^2 values for the regressions for all dates and for those dates with storage in excess of 1,000,000 m^3 are 0.635 and 0.865, respectively. The problem with the latter analysis is the relatively small number of data points ($n=8$). However, there was no way to improve the situation. For the period of record available, all storm events that met the criteria presented above have been included in Table 7-2. Nevertheless, the relationship is still instructional.

Figure 7-4 is a scatter plot of the data points with basin storage in excess of 1,000,000 m^3 , with a best fit regression line of the form of equation (7.8). The standard error is 11.6 km^2 . The curve in Figure 7-4 does not provide a complete picture of the variability of the saturated soil zone. For storage values in excess of 3,070,220 m^3 , there is no information. The upper boundary on the saturated zone would be the extent of the floodplain. Once the floodplain is inundated, greater discharges would have little effect on the SAREA because the valley walls are very steep relative to the bottomlands. The saturated zone is therefore limited to the lowlands encompassed by the river valley. This suggests the SAREA function is subject to a limiting sill at some storage level. Extrapolation of the regression line suggests that at a storage level in excess of 5,000,000 m^3 , the SAREA approaches the size of the snowmelt contributing area of 320 km^2 . It is unlikely that the saturated area reaches that extreme - the suggestion here is the upper extent is likely reached at a storage volume in the range of 3,000,000 m^3 .

As live storage approaches 0, the SAREA approaches 5.45 km^2 . The accuracy of this value is open to question. However, theoretically one would expect the residual ponding (depression storage) within the channel system to have a small areal extent once runoff has ceased.

7.7. Modelling Three Phase Runoff Response

This section presents comparisons of daily hydrographs simulated with a hydrologic model based on the Three Phase Runoff system with recorded Water Survey of Canada data. The representative basin climate file is used as input to a simulation program combining the climatic model with a hydrologic model capable of simulating the conditions for each area (soil phase), and of combining the various areal responses with a linear storage routing routine. For Ribstone Creek near Czar, the area of the frozen soil phase (snowmelt runoff area) was set to 320 km^2 (as determined in chapter 5), and several SAREA phase functions were utilized.

Figure 7-5 presents the first of these simulations. The WSC recorded hydrograph is represented by the solid line; the simulated hydrograph is the dotted line. The right hand x axis is a bar chart of basin runoff equivalent depth. This value is calculated as an equivalent runoff depth from the gross area - i.e. the frozen soil runoff area. For example, for a 40 mm rainfall, with a saturated area of 80 km^2 , the basin runoff equivalent depth would be $40 * (80/320) = 10 \text{ mm}$.

The simulated hydrograph in Figure 7-5 is the basin response to runoff from the frozen and active soil phases. This figure has been included to demonstrate the model response to these two inputs. The SAREA function was set to zero for the entire season. There is a very good fit between the two snowmelt peaks, given the approximate methodology used to derive a storage-outflow relationship. The greatest variability in the two hydrographs is in the recessional limbs, where the recorded

runoff shows small peaks in response to rainfall events. No such variation is notable in the simulated hydrograph - therefore, the model is indicating that at no time was there a rainfall depth sufficient to exceed the combined soil moisture and depression storage deficits. The only runoff response is from the snowmelt (frozen) soil phase.

The SAREA phase has been 'turned on' in Figure 7-6. The function used for Figure 7-6 is given in the figure and in Table 7-2, and is the regression line for the data points from Table 7-2 with storage in excess of $1,000,000 \text{ m}^3$. The use of a SAREA function results in the recession limb responding to several small peaks corresponding to those on the recorded hydrograph. However, beyond the middle of June, the simulated hydrograph fails to respond to three distinct peaks that are observable on the WSC hydrograph. For the peak beginning about July 14, there is only a minimal response. This could be due to underprediction of the SAREA, but it is more likely due to inaccuracies in the storage-outflow routing that allows too much outflow from May 1 to 20. Simulated basin storage declines too quickly; is too low after mid-June, and therefore, the SAREA is predicted to be much lower than it would be. An attempt was made to develop a storage-outflow function with a variable K value. However, it is difficult to justify modifying the routing function without supporting data. The model shows a modest response to an input on August 14, but does not react to the second small peak on August 22. The former response is likely somewhat muted by the routing routine. However, the latter recorded peak is somewhat surprising, given the climate data does not report any significant rain. Without a rainfall input, the model could not respond. Regardless, the overall fit of the two hydrographs in Figure 7-6 is very good.

Figure 7-7 presents a simulation with a SAREA curve that neglects the data point for May 18, 1974. This point provided the highest estimate of SAREA in the analysis

(83.5 km²). By eliminating this point, the slope of the curve was flattened somewhat, resulting in a lower peak SAREA value and slightly higher values of SAREA during low flow conditions. Qualitatively, the function results in an expected decline in the quality of early season responses, and improves those later in the summer. However, the only justification that may be offered for eliminating this point is it appears (in Figure 7-4) to have the greatest deviation from the regression line.

Two model simulations for 1969 and 1971 for Ribstone Creek are presented in Figures 7-8 and 7-9. These were two of the major runoff years other than 1974. These simulations were carried out with the basin climate data file as input, and using the SAREA function used to generate Figure 7-6. Both simulations provide a reasonable fit of the recorded hydrograph. In 1971, the WSC hydrograph demonstrates a number of responses to rainfall inputs, and the modeled output mirrors these responses very well. However, it is observable that the simulated small peaks on the recession limb of the simulated output are delayed by one or two days, compared to the recorded responses. In both figures, the main snowmelt modeled peak proceeds the recorded peak. This inequity is principally a routing problem. At this time, the model only has one routing time lag function for all inputs. The figures reflect a lag time of two days - this value is less than the apparent snowmelt lag time, and greater than the saturated area response time. Neither is surprising. One would expect that snowmelt, as a type of porous media flow, would have a relatively slow response time. The saturated area response is likely measurable in portions of the day.

The results presented in Figures 7-6 - 7-9 are subject to a number of uncertainties, including errors related to the very approximate basin storage-outflow analysis presented earlier. Another source of error is the input rainfall depth. Summer rains are typically convective storms in this area, and these are notoriously patchy in areal

coverage. Rainfall recorded at a station may have had little or no impact within distances of a kilometre or less. This is likely the reason for the varied response of the modeled and recorded hydrographs in late April - early May, 1969. The climate data indicates two periods with light rain on several concurrent days. The first period has received a much larger recorded input, and the model reacts with a small peak. However, the recorded flow reacts very little to the first rain, and significantly more to the second. The modeled data shows very little response to the latter rains, yet these were of greater importance to the runoff. The input climate file was obviously not truly representative of the basin climate situation in this particular case.

7.8. Conclusions

An assessment of the relative role of the saturated soil zone in generating runoff from a small prairie river is presented. The analysis argues the variable area concept does not apply to the frozen soil phase - once certain abstractions have been met, runoff occurs from a more or less static area. However, the saturated soil phase is very dynamic, and responds to rainfall inputs in direct proportion to the current extent of the saturated area. A relationship describing the saturated area variability as a function of the basin detention storage has been derived.

A hydrologic model has been developed to reflect the hydrologic functions of the three soil phases: frozen, active and saturated. The model, though still in the development and evaluation stage, has demonstrated an accurate response to inputs that reflects the recorded hydrograph quite well.

7.9. References

Pipes, Anthony and Michael C. Quick, 1977. 'UBC Watershed Model Users Guide'.
Dept. of Civil Engineering, University of British Columbia.

Table 7-1: SWE (mm) values for stations near Ribstone Creek

	1	2	3	4	5	6
1968	66.	70.	24.	45.	27.	48.
1969	59.	91.	77.	96	37	71.
1970	59.	84.	77.	47.	17.	63.
1971	90.	92.	38.	61.	39.	74.
1972	95.	103.	47.	78.	59.	80.
1973	32.	55.	40.	57.	17.	41.
1974	182.	208.	146.	118.	102.	164.
1975	146.	134.	82.	135.	36.	114.
1976	84.	73.	25.	66.	32.	67.
1977	55.	14.	26.	35.	10	32.
1978	90.	56.	36.	45.	58.	59.
1979	98.	50.	56.	34.	50.	54.
1980	66.	34.	87.	87.	35.	53.
X Coef.	.279	.358	.111	.127	.048	
R squared	= .9929					
S.E. of Y estimate	= 3.548 mm					
1 = Brownfield 2 = Coronation 3 = Hughendon						
4 = Metiskow 5 = Wastina Hemaruka						
6 = analysed SWE for Ribstone Creek						

Table 7-2: Assessment of the extent of the saturated area for Ribstone Creek

date	rain(mm)	dQ (m ³ /s)	dS (m ³)	S (m ³)	SAREA (km ²)
690514	6.85	0.08	81062.	1145000.*	11.8
700613	22.65	0.19	192522.	123619.	8.5
700630	28.26	0.25	253319.	37491.	9.0
700701	12.46	0.16	162124.	169217.	13.0
710527	21.88	0.09	91195.	809606.	4.2
710605	17.03	0.13	131726.	639376.	7.7
710623	19.79	0.03	30398.	332534.	1.5
710723	38.92	0.11	111460	166177.	2.9
740518	7.52	0.62	628230.	3070220.*	83.5
740604	20.08	0.41	415442.	1469247.*	20.7
740606	11.23	0.20	202655.	1925220.*	18.0
740705	5.33	0.01	10133.	846084.	1.9
740708	6.85	0.02	20265.	772115.	3.0
740814	22.93	0.05	50664.	24319.	2.2
750518	4.95	0.19	192522.	2624379.*	38.9
750519	13.7	0.46	466106.	2735840.*	34.0
750524	5.99	0.21	207721.	2391236.*	34.7
750603	5.8	0.08	81062.	1013274.*	14.0
750626	21.5	0.17	172257	545141.	8.0
750703	11.7	0.08	81062.	545141.	6.9
750704	5.22	0.05	50664.	596818.	9.2

for all data	for storage >1E6 *
Area=3.63 exp(8.97E-7 Store)	Area=5.45 exp(7.71E-7 Store)
R squared = .6356	R squared = .8694
Degrees of freedom = 19	Degrees of freedom = 7

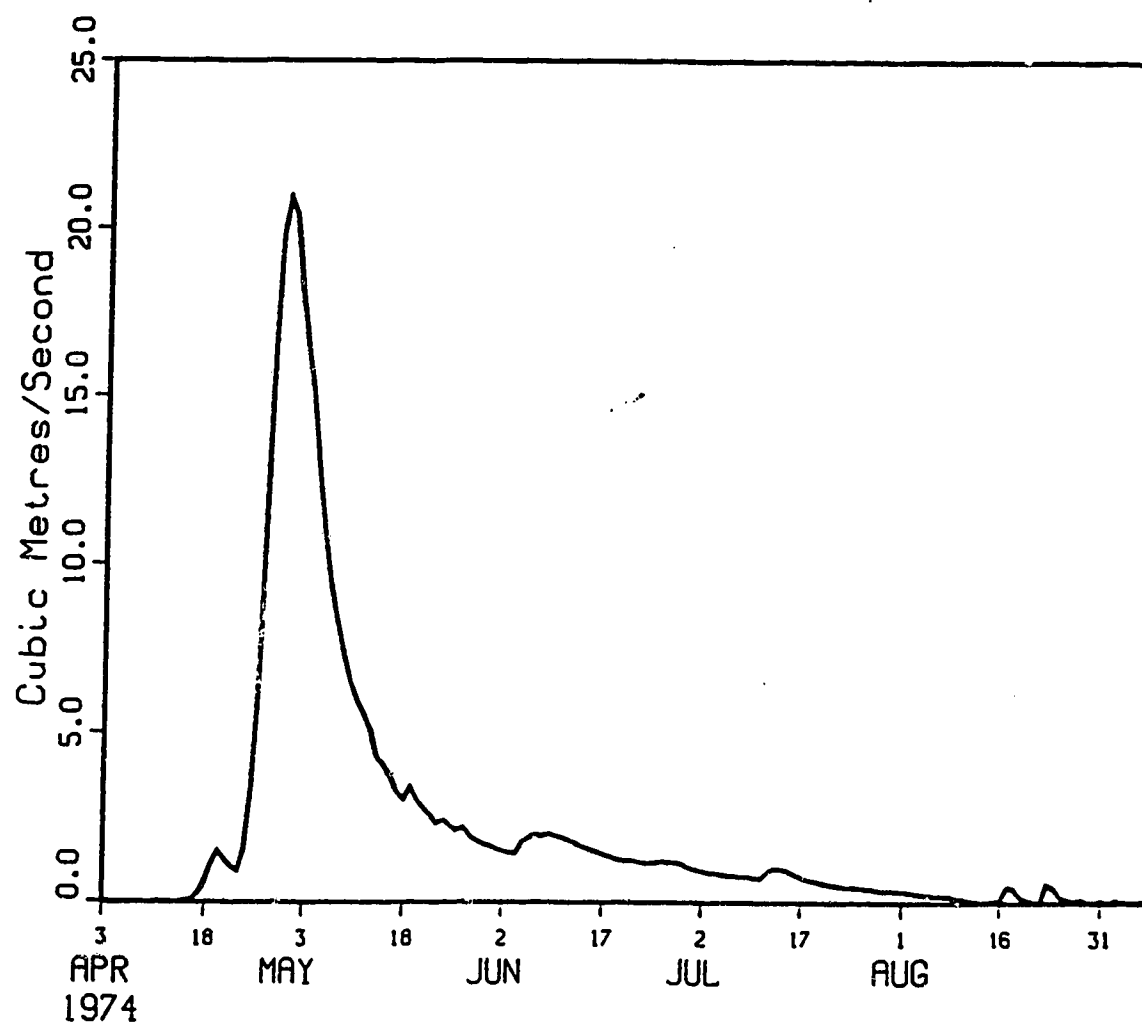


Figure 7-1: Ribstone Creek hydrograph, Water Survey Data.

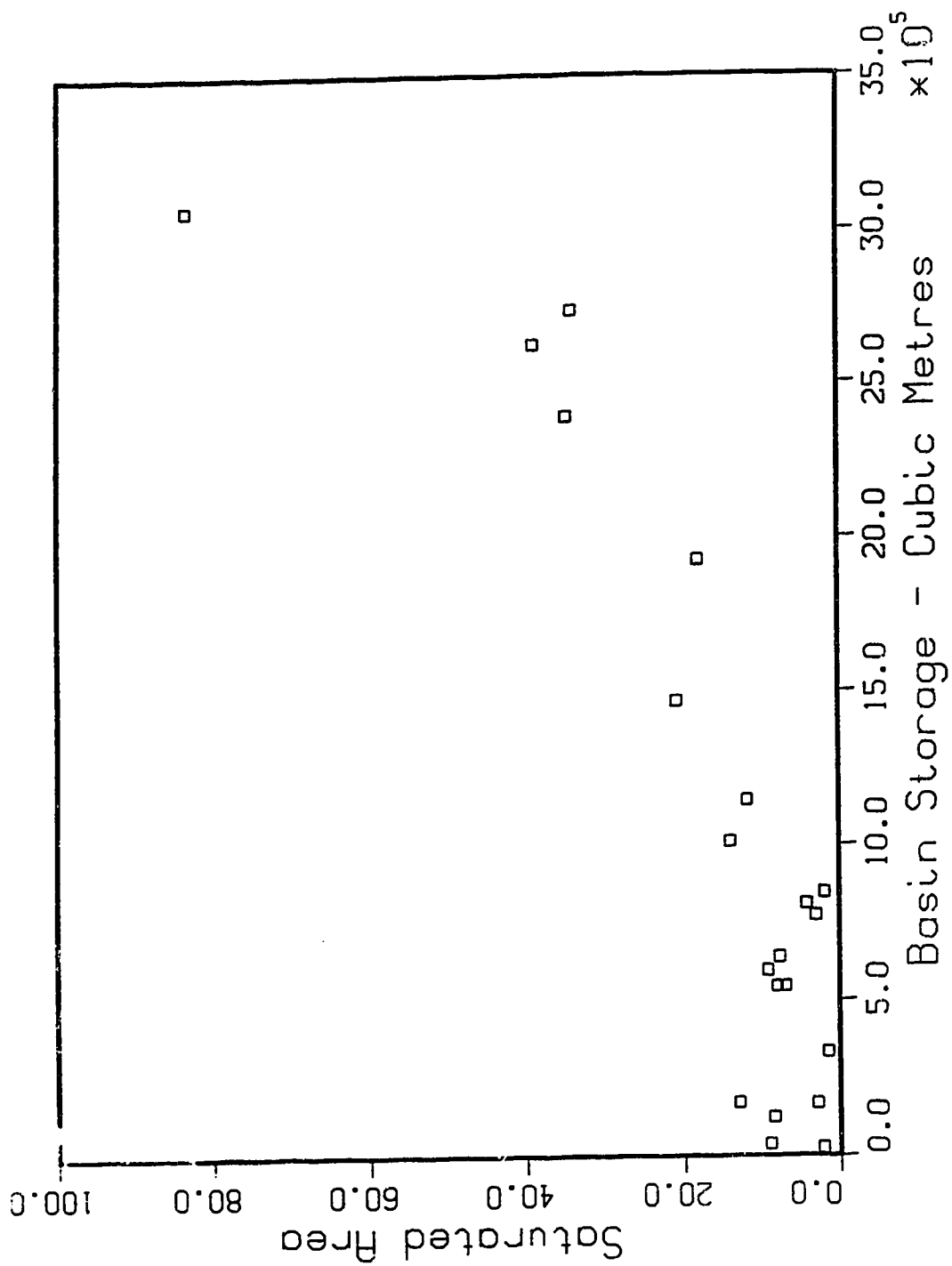


Figure 7-2: Saturated area estimates versus basin storage

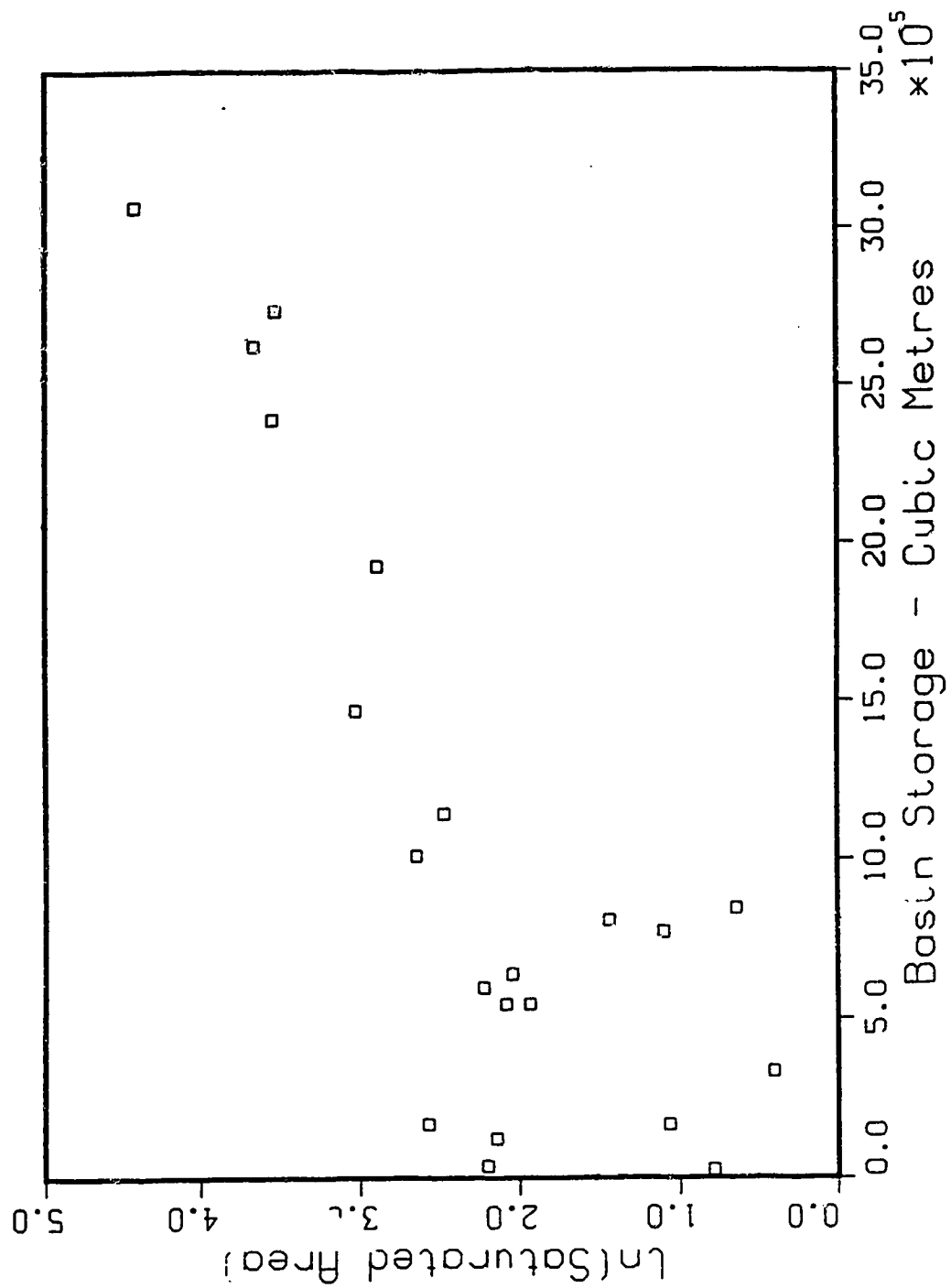


Figure 7-3: \ln saturated area versus basin storage.

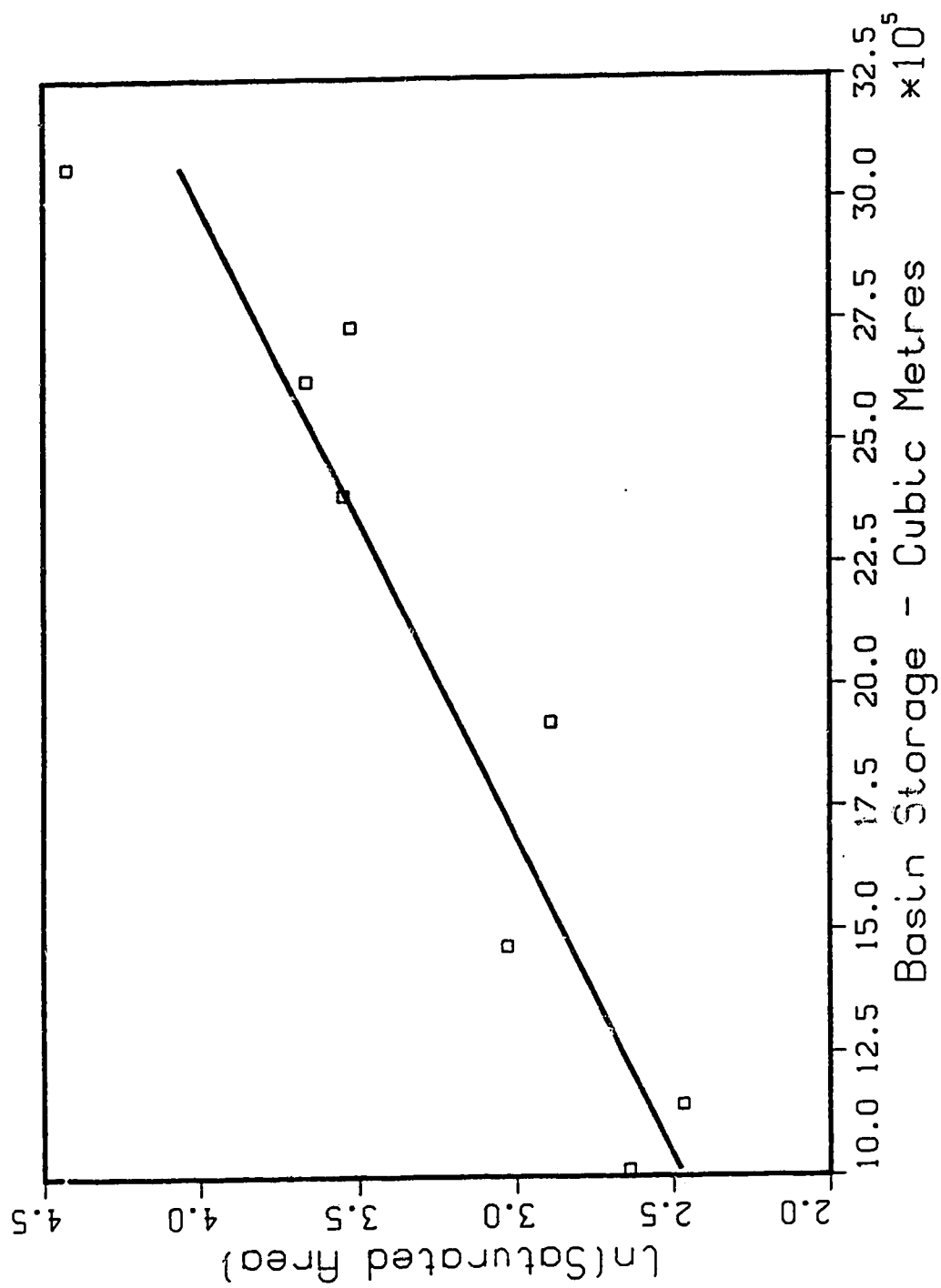


Figure 7-4: Exponential SAREA function.

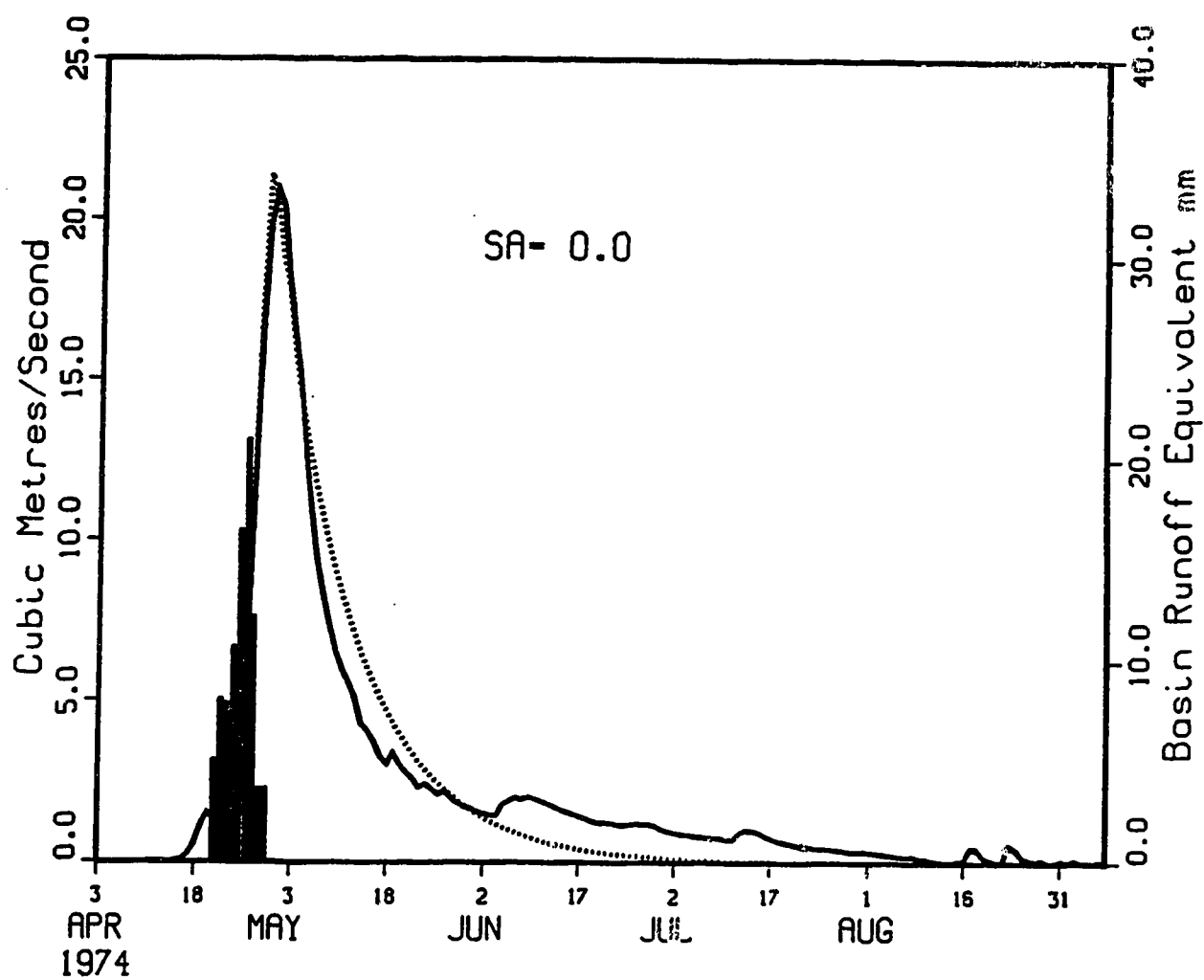


Figure 7-5: Recorded and simulated (broken) hydrographs. The SAREA curve has been turned off, thus the smooth recession limb.

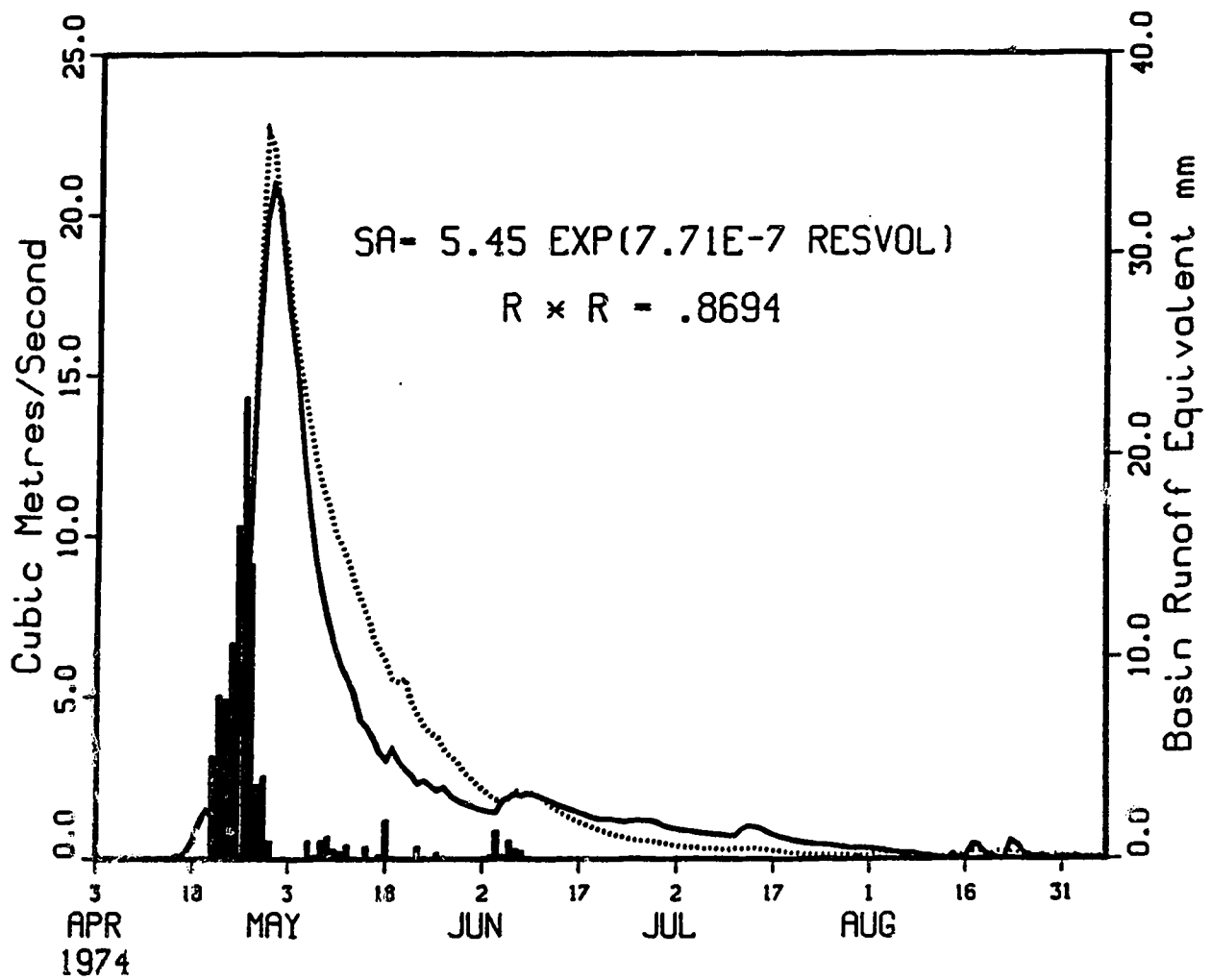


Figure 7-6: Simulation with exponential SAREA function 1.

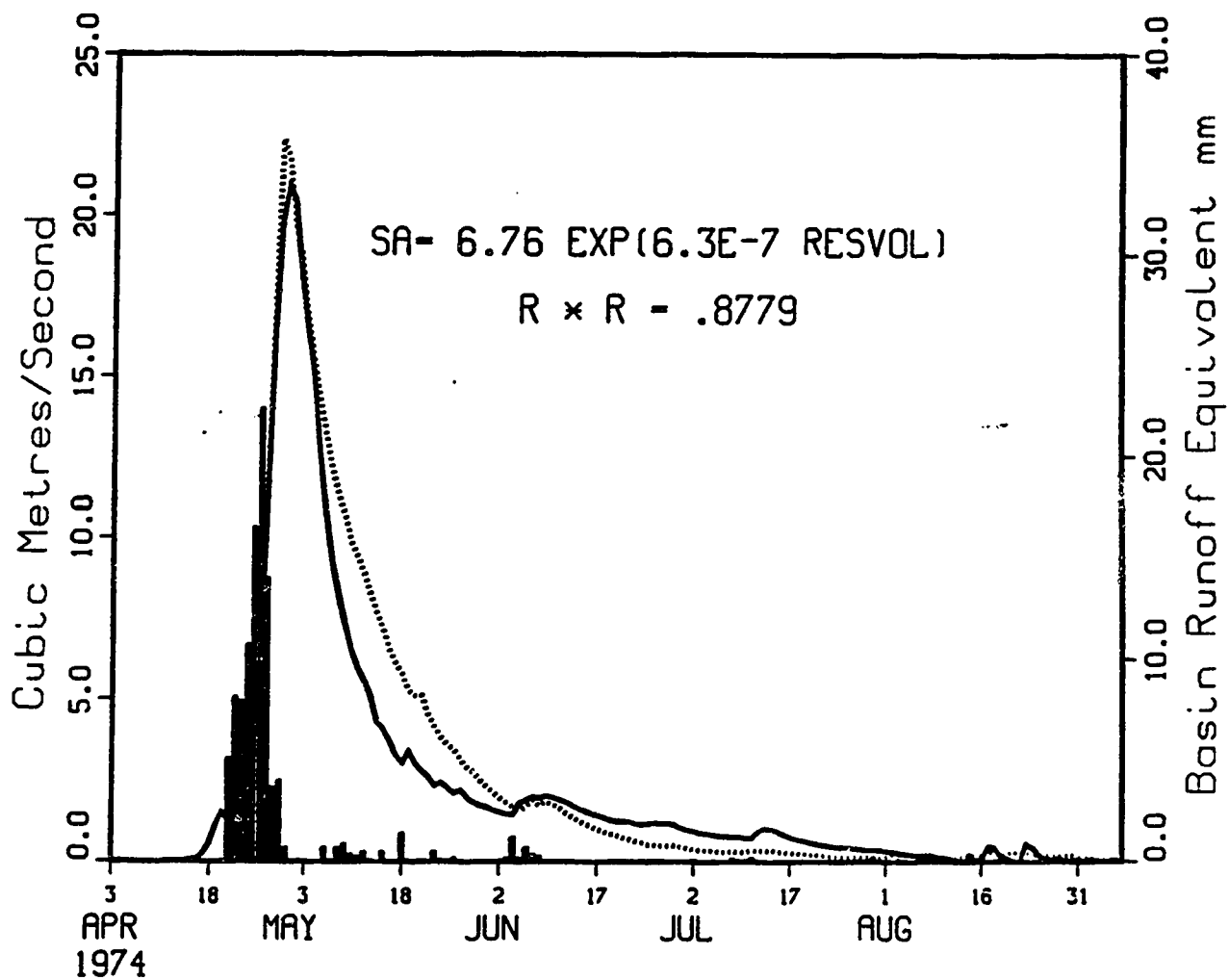


Figure 7-7: Simulation with exponential SAREA function 2.

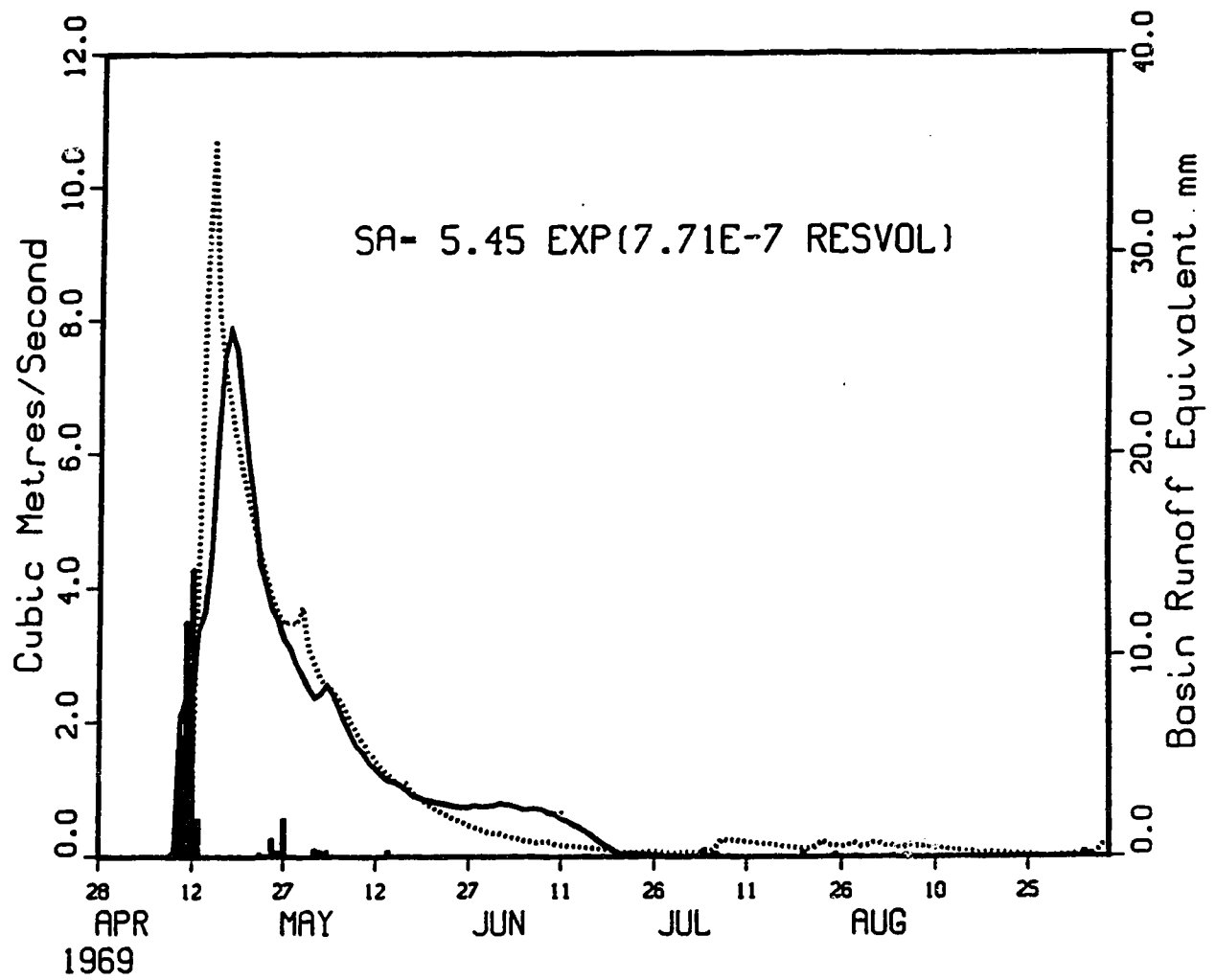


Figure 7-8: SAREA curve 1, 1969 runoff.

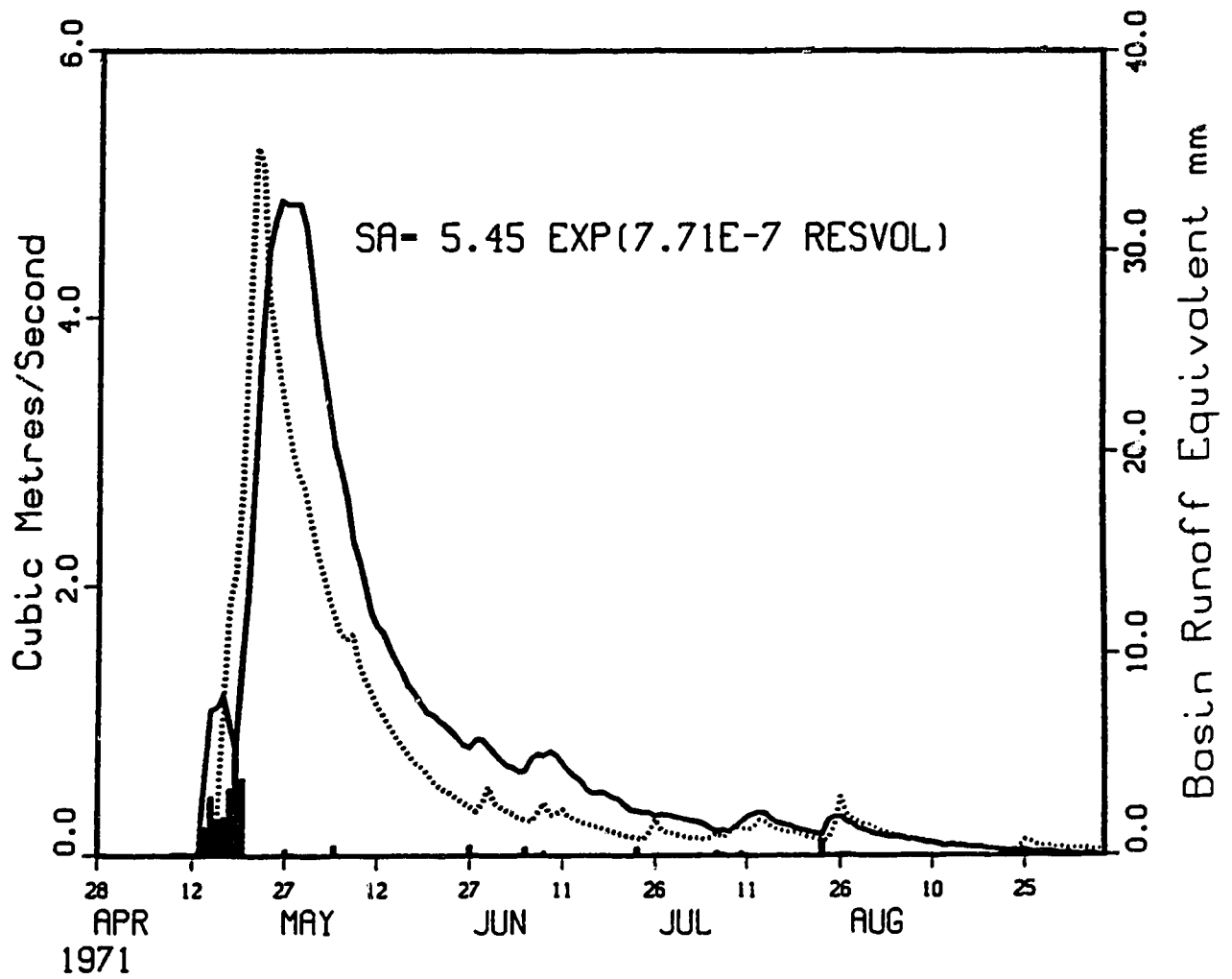


Figure 7-9: SAREA curve 1, 1971 runoff.

Chapter 8

FROZEN SOIL PHASE ASSESSMENT FOR SEVERAL BASINS

8.1. Introduction

The analyses of the hydrologic processes within Ribstone Creek have demonstrated the principal source of streamflow runoff is the spring snowmelt. Quantification of the useable runoff is dependent on knowing the spring snow water equivalent (SWE) and the frozen soil infiltration (INF) over the basin, and the snowmelt contributing area (AREA1). AREA1 was determined for Ribstone Creek using a detailed spatial analysis model to interpolate SWE-INF to one kilometre square elements over the basin. Extensive amounts of computer time and onerous digitizing and data entry were required to define the grid elements to be included in the analysis (see discussion in section "Frozen Soil Phase Assessment - Ribstone Creek near Czar"). This section presents essentially the same analysis for a number of basins, with the only changes being to an element size of ten by ten kilometres for the SWE-INF spatial interpolation, and a simplified hydrograph separation technique. These changes made the application of the techniques more feasible over a number of basins.

8.2. Spring runoff depth - spatial patterns

In order to carry out the AREA1 analysis for a number of basins, two variables must be estimated on an annual basis for each basin; the net spring runoff depth (i.e. SWE-INF as defined earlier) and the snowmelt runoff volume. The climatic model, in combination with the spatial analysis (kriging) program, may be used to determine the SWE-INF values and interpolate them for a grid over any area. In this case, the data was interpolated over the study area, using a grid element size of ten by ten kilometres. The data matrix for each year was contoured within a Geographic Information System (GIS) package produced by TYDAC Technologies of Ottawa. The spatial fields of spring runoff depth over the study area were produced for the years 1960 to 1980. These maps are presented in Figure 8-1.

The runoff shown on the maps in Figure 8-1 demonstrates the extreme variability in runoff depth that may be experienced over relatively short distances. The spring runoff depth is contoured with greater depths of runoff represented by increasingly darker gray shades. Digitized streamflow data over the map, with Water Survey of Canada stations for basins of interest numbered with reference to the legend. Coronation, the only major climate station within the study area, is labeled as well.

The gray scale mapping of spring runoff depth is very useful in that the reader can easily follow the changes. However, one must refer to the legend to establish the relative change for each gray scale change. For example, in 1960 spring runoff depths over the study area ranged from zero in the southeast to peak values of around 30 mm in the southwest. The 1974 map indicates there were very dry areas in the southwest, with runoff depth as low as a few millimetres. Heavy runoff occurred over the north half of the study region, with large pockets of runoff with values in excess of 140 mm northwest of Coronation. Two recognizable patterns are notable: the clearest is that

the southeastern area is almost always within the driest section. The second is that in a number of years, notably 1968, 1970, 1971, 1972, 1974, 1976, 1978, 1979, 1980 and 1981, a tongue of the heaviest runoff extends from the northwest/west out to the region of Coronation. This pattern is weakly discernible in several other years. This observation is somewhat disturbing, since it indicates that Coronation, as the only level one climate station in the region, is not very representative of the surrounding region in many years. A quantitative assessment of the data confirms this. Using Coronation data to represent the Ribstone Creek basin (WSC station number 8 in Figure 8-1) results in an overprediction of about 14 percent in the basin spring runoff depth, as compared to the analysis carried out on a one kilometre square grid.⁸

The grid data used to generate Figure 8-1 is applied in the analysis to calculate the basin spring runoff depth. The relative area of the basin for inclusion was digitized based on the ten km² grid - a grid element was judged to be "within" the basin if a stream channel for the basin was shown with that element on a 1:250,000 NTS map. If the block is "within" the basin, then the runoff depth for that block was included in calculating the basin runoff depth. Each included element was weighted equally in this calculation.

However, the use of a coarse analysis always has the potential to degrade the quality of the results. The relative changes in the error level associated with this analysis over the one km² grid are significant, but not to a level to negate the value of the coarse analysis. The predicted values for basin runoff depth for Ribstone Creek using the ten km² grid relate very closely to the data for the one km² grid. There is an underestimation of about six percent with the coarse analysis (i.e. $1 \text{ km}^2 = 1.059 \{10 \text{ km}^2\} - 0.65$), but the standard error in a regression between the two data sets is very small (< 1 mm) and the correlation is very high ($R^2=0.9988$).

⁸regression analysis $Y = 1.138 X - 1.12$, ($R^2=0.978$)

This presents a question of whether to apply a correction factor for all the watersheds, based on the Ribstone Creek data. Most of this error would be due to the coarse grid - each element of the coarse grid is 100 times the area of the fine grid, therefore, large areas are included that likely do not directly control streamflow runoff. The error may be characterised as random, since the grid overlay may, by pure chance, tend to "fit" more closely to the fine grid representation for some basins than others. Therefore, there is no justification for applying a corrective factor derived from Ribstone Creek to the coarse analysis for any other watershed.

The combination of simplifications in the analysis used in this section results in a small drop in the significance of the relationship of runoff depth and volume for Ribstone Creek. The drop is notable in the change in the R^2 values. Using the detailed analysis for Ribstone produced an $R^2=0.87$, while the R^2 value for the coarse grid analysis is 0.847. This decline is not considered to be a problem; both values are highly significant.

8.3. Simplified hydrograph separation

Analysis of frozen soil contributing area for a number of basins requires an estimate of the spring runoff volume for each year for each basin, utilizing hydrograph separations. For the Ribstone Creek analysis, a computer program was written that approximated the spring hydrograph recession curve with an exponential decline function, and plotted the theoretical recession curve against the Water Survey hydrograph. The placement of the theoretical recession curve could be visually appraised for the best fit to each year, and the spring runoff was calculated as the total runoff minus the volume above the theoretical recession curve. The method used in this section involved penciling in a theoretical recession curve on the hydrograph, and estimating the spring runoff volume with a planimeter.

The question that immediately arises is what level of error may be introduced with the simple planimeter analysis. Again, the Ribstone Creek data may be utilized to verify the results. Regression of spring runoff volumes estimates by the two techniques indicates the simple analysis estimates approximately four percent lower than the computer based technique. There is no justification for declaring either to have greater validity. The very high correlation ($R^2=0.993$) simply confirms that both are likely accurate.

8.4. Multi-basin analysis of frozen soil contributing area

The spring runoff depth ($SRD = (SWE-INF)$) data for the watersheds of consideration is presented in Table 8-1. Table 8-2 contains the estimates of the spring runoff volume for each basin, as developed with the planimeter analysis of the Water Survey of Canada recorded hydrographs.

The results of the regression analyses relating the SWE-INF data to the spring runoff data are presented in Table 8-3. Column 1 is the basin names; columns 2 and 3 are the y intercept and slope for the regression line; column 4 is the square of the correlation coefficient; column 5 is the size of the sample set (dictated by the available Water Survey data); and the column 6 provides the Water Survey of Canada description of the basin flow conditions. Four of the watersheds have been described as regulated and four are streams with natural flow conditions. The regulated streams generally demonstrate a poor relationship to the estimated runoff depths; while three of the four natural flow watersheds have very high correlations. This is not unexpected - during years of low and average streamflow, the recorded streamflow hydrograph for a regulated watershed would not reflect natural conditions since significant percentages of the runoff is undoubtedly stored and/or diverted for other uses. This does not occur for the basins with natural flow, so there is a much stronger relationship.

Alkali creek is the only natural flow watershed that does not have a good correlation with the runoff depths ($r^2=0.131$). Several points may be offered as to why the model appears to fail for Alkali creek, while providing good results for the other natural flow creeks.

1. The Alkali creek region is the driest area in the province, evidenced by the interpolated data images presented in Figure 8-1. The precipitation totals in the region are, on average, the lowest in the province, and the ratio of runoff to precipitation would also be low. Therefore, the relative error in the simulated runoff depth is very high, and may completely obscure the runoff relationship in many years. The data from Table 8-1 for Alkali creek support this contention. No other basin has such consistently low runoff depths.
2. There were no climate stations with a reasonable period of record either within or near Alkali creek. Medicine Hat, Hemaruka and Pollockville were the closest stations, at approximate distances of 200, 160 and 140 kilometres, respectively, from the centre of the Alkali watershed. Extrapolation of the climatic data over such distances is likely invalid.

There are four basins in Table 8-3 that have statistical relationships between simulated runoff depth and recorded volumes with a correlation that justifies estimating AREA1 and basin depression storage losses. These are Buffalo, Iron, Ribstone and Sounding creeks. The Sounding Creek data are not as good as the three natural flow creeks, presumably because of the flow regulation on Sounding Creek. However, the fit is judged to be sufficient to provide some reasonable estimate ($R^2=0.655 \rightarrow R=0.81$). The same argument can be put forward for Monitor creek, if in a much weakened state! Nevertheless, the inclusion of Monitor creek is desirable

since there are only five data points in total, and exclusion of twenty percent of the useable data points is not practical at this time.

The Monitor creek regression plot of runoff depth versus spring runoff volume demonstrates a significant scatter of the data points. However, the 1965 data point has by far the greatest deviation from the regression line, with a runoff volume of greater than 12.6 million cubic metres and a very low runoff depth of 28 mm. This deviation could be due to any of the following potential problems:

1. Water Survey data errors;
2. climate data error;
3. error in the modeling program.

Initial discussions with Water Survey of Canada staff in Calgary regarding the 1965 runoff year for Monitor creek indicated the data had been reviewed several times and were felt to be a good estimate of the flow volumes. However, the peak discharges that were recorded exceeded bankfull discharges, with significant volumes of water flowing over the bridge and road at the survey station site (pers. comm., John Anderson, WSC, 1989). The technician indicated the discharge in excess of bankfull was measured. However, measurement under these conditions would have been difficult, and quite possibly subject to error.

There is very little chance the climatic data could be in error since the analysis is not dependent on a single station, but is built upon interpolated data from a number of stations.

One other source of error may be the modeling process. Three major phases are incorporated in the modeling process: fall soil moisture determination; overwinter moisture transfers (represented by Morton ET); and spring snowmelt infiltration to

frozen soils. Figures 8-1 (1965), 8-3 and 8-4 represent the output steps for each modeling phase.⁹ The overwinter precipitation (WP) for Monitor creek was about 120 mm of water equivalent (Figure 8-3) and the spring SWE value was approximately 47 mm of water (Figure 8-4). The data in Table 8-1 has a SRD of 28 mm for Monitor creek, therefore, the spring snowmelt infiltration was 19 mm (since $SRD = SWE - INF$). Reference to the values of WP, SWE and SWE-INF in Table 5-2 indicates the range of possible values for each parameter. The values of WP and INF for Monitor in 1965 fall well within these ranges. However, the Morton ET is very high for 1965 for Monitor. This is a second possible area of error.

Neither of these possible sources of error may be explicitly checked. Prior to 1968, the climatic data is not as dependable simply because more data was missing or unrecorded, and substantial data transposition was carried out in order to have a complete record at all stations. However, the stations nearest to Monitor creek did have relatively complete records for the 1964-65 time period. The sunshine data used prior to 1968 is also suspect. Only three stations in the province, the Edmonton Municipal airport, the Lacombe Research Station and Suffield were collecting sunshine data prior to 1968. The 1960-67 sunshine data for all other stations was estimated using post 1968 regression relationships between these three stations and the other thirty one stations. No glaring error is noticeable in the sunshine data for these three stations, and hence, there is no justification for any type of adjustment.

The above discussion presents a weak argument for exclusion of 1965 from the Monitor creek analysis. This exclusion would be disconcerting, since 1965 is an important year for flow discharge. Exclusion does increase the fit of the Monitor creek data to the rest of the analysis, but that is no justification whatsoever. The

⁹The maps of winter snowfall and SWE depth for all years are included in Appendix B.

conclusion was drawn there is not sufficient grounds for excluding the 1965 data year from the analysis for Monitor creek.

The depression storage DP and AREA1 estimates for the five basins are presented in Table 8-4. The table also includes estimates of the gross and effective areas as defined by the PFRA (1985). There is no strong relationship between the AREA1 values and either PFRA area.

8.5. Relating AREA1 to basin geomorphology

The analysis in the previous section provides estimates of AREA1 for five basins. An immediate question that arises is whether there is any method for predicting AREA1 with some characteristic geomorphic variable that may be measured easily from a map or airphoto. The logical parameter to consider is the basin drainage density.

Drainage density (DD) is defined as the quotient of the sum of the channel lengths and the total drainage area; ie. a length of channel per unit area. Typically, drainage density is defined using the area of the basin as established by apparent regional drainage divides on contour maps. This treatise has already disputed this method of determining area for a basin on the prairies, and in so doing, implicitly argues that drainage density may not be defined in the "usual" manner. Instead, drainage density must be defined by using a good estimate of the contributing area for the basin, such as the AREA1 values developed here.

Drainage density is a function of the climatic, soil, vegetative and topographic characteristics of a region. For the five basins of interest here, one may safely state the vegetative and topographic characteristics are quite consistent. Soil conditions over the study area typically demonstrate a high degree of local variation, but are quite

consistent on the macro scale. The soils are formed largely of glacial till deposits with thicknesses ranging up to sixty metres or more (Hardy, 1967). Local deposits of loess, sand and gravel overlay the till in some areas. However, these local deposits do not impact seriously on any of the basins of interest here. Therefore, the drainage density variations between the study basins will be attributable in large part to variations in the climatic conditions that result in the major runoff events; principally, the spring runoff. This hypothesis is tested in the following analysis.

8.5.1. Determining drainage density

In order to calculate drainage density, a method for determining the total length of channel within a basin was required. This analysis initially planned to use a small map measuring device with a revolution counter for a small wheel that could be run along a line of interest, with the resulting number of revolutions being scaled to estimate the distance covered. This device proved clumsy to operate on the 1:250,000 scale maps that were initially selected for channel measurement (criteria for selecting this scale is discussed below). The task was onerous, and application to a number of basins would result in severe eye strain. Typically, one would need to repeat the process for a basin a number of times, and then take the average of the trials. The availability of a 300 dot per inch (dpi) computer scanner and software allowed for developing an accurate and efficient method for measuring channel length. The method operated as follows.

An experienced draftsman with a high quality drafting pen and paper would trace the basin channels on a clean sheet of paper. The traced image was run through the scanner at high resolution (300 dpi) and stored in POSTSCRIPT format. The image clarity was always checked with the scanner software editor. This image, after interpretation by a simple program, was transferred to the University of Lethbridge

VAX mainframe system. At that point, a Fortran program was used to interpret the hexadecimal POSTSCRIPT code to determine the total number of pixels that were part of the channel system.

Several problems had to be dealt with before the method could be used with confidence. First, the drafting pen was supposed to be 0.35 mm, which would theoretically be 4.13 pixels wide. The width was consistently wider than this due to ink bleeding outwards slightly from either side of the line. Further, the scanner would turn on a pixel if any small portion of the pixel crossed a line. A number of trials were carried out to study the variation in line width, depending on line orientation to the scanner grid. For a large number of lines, with random orientation to the scanner grid, the average pen width was 8.36 pixels, with a variation of about 1 pixel.

Once the average pen width was determined, the channel length could be calculated in the following manner. The program interpreted the hexadecimal code to count the total number of pixels that had been activated in the image. Dividing the total number of pixels by the average line width in pixels resulted in a mathematical representation of the channel length, one pixel wide. For a 1:250,000 map, a pixel length represents 21.17 metres. Therefore, the channel length is this value times the number of pixels left after division. Mathematically stated, the channel length is

$$L = [\text{Total pixels} / 8.36] \times 21.17 \quad (8.1)$$

This method was used to determine the channel lengths for the five basins being analysed. These values are presented in Table 8-5.

The choice of 1:250,000 maps for measuring channel length may appear to be incorrect, since a map scale of 1:50,000 is available and would provide much greater detail on small and intermittent channels that may exist within the basin. The feeling

here is these channels are only in existence due the control exerted by the larger channels that dominate flow. Each major channel is flanked by a contributing band or corridor, and minor channels are incorporated within this area. The 1:50,000 maps were felt to contain an almost confusing amount of detail; while the 1:250,000 maps would probably provide a more accurate representation of the main channel system.

8.5.2. Drainage density and runoff depth relationship

The discussion above theorized that AREA1 values and the drainage density should be a function of the runoff depth SRD. The drainage densities for the five basins, and the parameters utilized to calculate them, are presented in Table 8-5. A fourth parameter, SRD-DS is also included. This parameter is the average runoff depth for each basin (Table 8-1) minus the depression storage deficit for the basin in mm (Table 8-4). The Monitor and Monitor2 rows represent the output data for Monitor creek with 1965 data included and excluded, respectively, as discussed earlier.

The analysis that may be carried out on the data in Table 8-5 is somewhat limited by the number of points. A rigorous analysis is not justified and would be open to questions of statistical significance. Nevertheless, it is beneficial to plot the drainage density and (SRD-DS) data, and perform basic statistical analyses, keeping in mind the small data set and including a definitive significance test. The data plots do provide a functional relationship.

Figure 8-5A is a plot of drainage density and SRD-DS from Table 8-5, with Monitor creek included. The plot demonstrates a strong linearity of the two parameters, with the Monitor creek point having the greatest divergence from the general trend. The retention of Monitor creek data to this point has been with the intention of maintaining as many data points as possible. However, the evidence in Figure 8-5A indicates the data point is not adding to the relationship; in fact a large error is added by retaining it.

The data plot in Figure 8-5B demonstrates a good linear relationship between SRD-DS and drainage density. However, the fact there are only four data points bring the significance of the fit into question. In order to deal with this, a students t test of the correlation coefficient R was adopted (Guttman et al., 1971):

$$t = \frac{|r| [(n-2)^{0.5}]}{[(1-r^2)^{0.5}]} \quad (8.2)$$

This value for the correlation coefficient here is $t = 7.63$, a value that indicates R is statistically significant at the 1 percent level.

The relationship in Figure 8-5B may be used to estimate the drainage density for any basin in the study area, and from that value, the AREA1 parameter may be approximated. This would allow a water manager to estimate the natural spring water yield for any of the regulated basins in the study area, and to a limited degrees, for similar physiographic areas adjacent to the area from modeled values of SRD if some method were available to determine the micro depression storage of the basin. The next section addresses possible methods for determining the micro depression storage of a basin.

8.5.3. Determining micro-depression storage for any study area basin

The micro depression storage of a basin is a function of the micro topography, as discussed earlier. There is no practical method for mapping the topographic variation at the contour level that would be required for explicitly determining depression storage for a number of basins. The question that is dealt with here is whether any relationship may be developed from parameters that may be measured off a standard topographic map.

An obvious parameter to consider in investigating depression storage is the channel

slope. Mitchell and Jones (1976, 1978) and Gayle and Skaggs (1978) indicated micro-depression storage was a function of the local micro-relief. This concept may not be directly transferable to this study, but it does provide a starting point. Most of the depression storage that is notable on 1:50,000 NTS maps and on 1:60,000 airphotos is not connected to the channel system. The depressions that are linked to the drainage network are always within the lowland sections of the basin. Therefore, the depression storage should be related to the local relief of the main channel in the lower sections of the basin. In order to test this hypothesis, the main channel slope (S_0) was measured on a 1:250,000 map for the lowest section of the channel network. The S_0 for the lowest section was assumed to be the slope between the two lowest contours to cross the channel prior to the basin outlet. The slope data for the four basins is presented in column 2 of Table 8-6. There was no strong relationship between S_0 and the calculated values of depression storage. A second empirical parameter, the area of depressions (A_{DS}) connected to the channel network, was added to the analysis. This parameter could be estimated very easily with the use of the 300 dpi scanner. Traced images of the depression storage areas were scanned at 300 dpi. For a map scale of 1:250,000, each pixel represented an area of 448.07 m². The program written for the channel length analysis was modified to simply count pixels and multiply by the area per pixel. No adjustment was made for pen bleeding, since the areas were wide blocks of black, and any thickness added by bleeding would be negligible in comparison.

There was no strong relationship between the A_{DS} and depression storage; but a multiple regression of S_0 and A_{DS} to DS resulted in the equation given in Table 8-6, with an apparently strong correlation coefficient. Relating DS to these two parameters is certainly justified on a theoretical basis. Again, the concern is whether the correlation is actually significant, given the small number of cases ($n=4$). The basis of standard significance tests is that the sample be large enough to represent the

population. The t test statistic used above is not directly applicable for a multiple regression, and most statistics reference texts implicitly suggest a standard significance test may not be applied below $n=5$ for one degree of freedom, and $n=6$ for two degrees of freedom (as is the case here). There is no way to increase the n value; therefore a more robust test that does allow the use of smaller samples is needed. The test that has been selected is a randomization test, fashioned somewhat after Edgington (1980) and Costanzo (1983).

Randomization theory allows one to assess the probability of a given set of results occurring by chance from a random sample of the population. An order test is applied to the data after randomization. The ranking of the observed statistic in the ordered data provides an estimate of the probability of the observed statistic having occurred by chance.

The hypothesis that will be tested here is whether one or more randomly chosen sets of S_0 and A_{DS} might generate results at least as good as those in Table 8-6. Consider the current pairing of A_{DS} and S_0 to be random. This pairing is one of 24 possible ways to pair these variables; the notation here labels the original pairing 1234. If one variable is kept in this order, then the second may be arranged in 23 other ways - basic probability states for N different variables, there are $N!$ arrangements (permutations). The permutations are presented in Table 8-7.

The two variables, paired in all possible permutations, were used to generate DS' , an estimate of the depression storage for each of the four basins, using the multiple regression equation. The randomly generated sets of DS' were tested against the input values of DS , with the intention of minimizing $Q = \sum_{i=1}^4 (DS_i - DS'_i)$, for all permutations. The results of this analysis are presented in Table 8-7. The original pairing 1234 appears first in the table, and has the lowest value of the test statistic Q .

The tabulated results provide the following conclusions. First, the probability of a random sample generating a set with greater significance than the regression equation is less than 4.2%. Second, the regression equation has a significance level $P \geq 95.8\%$.

The application of the regression equation in Table 8-6 allows one to predict the depression storage deficit for any basin in the study area. The method may be extended beyond east central Alberta if the user is satisfied the climatic, soil and vegetative characteristics are consistent with the study area.

8.6. Summation

The spring runoff depth for eight watersheds in eastern Alberta was simulated for a grid with 10 x 10 kilometre elements. This distributed data was utilized to estimate the runoff river basin runoff depth for a number of watersheds. These data were related to the spring runoff volume attributable to snowmelt. The results were used to estimate the frozen soil phase (snowmelt) contributing area for the basins; and the basin micro depression storage capability.

The analysis could not provide functional results for watersheds that were listed as regulated by the Water Survey of Canada. This is expected since the WSC data that is available would not reflect natural runoff conditions in many years. The basis of the the analysis assumes a natural relationship between the spring runoff depth and the runoff volume.

The results of the analysis for three of four basins with natural runoff conditions were very positive. Estimated values of snowmelt contributing area and depression storage deficit were utilized to develop relationships for estimating each from geomorphological data recorded from standard National Topographic Survey maps. These relationships may be utilized to estimate the two parameters for any watershed

with climatic and physiographic conditions similar to those of the study area. These estimates may be applied with estimates of the SRD to determine the amount of spring runoff that would be derived from the watershed.

8.7. References

Costanzo, C. M., 1983. *Statistical inference in geography: modern approaches spell better times ahead*. Professional Geographer, 35:158-165.

Edgington, E. 1980. Randomization Tests. New York: Marcel Dekker, Inc.

Gayle, G.A. and R.W. Skaggs, 1978. *Surface storage on bedded cultivated lands*. Transactions of the ASAE. 21:101-109.

Hardy, W.G., ed. 1967. Alberta, A Natural History. Edmonton: M.G. Hurtig, Publishers.

Knudsen, Daniel C., 1987. *Computer-intensive significance testing procedures*. Professional Geographer, 39(2):208-214.

Mitchell, J. K. and B. A. Jones, 1976. *Micro relief surface depression storage: analysis of models to describe the depth storage function*. AWRA Water Resources Bulletin, 12, 6.

Mitchell, J. K. and B. A. Jones, 1978. *Micro relief surface depression storage: changes during rainfall events and their application to rainfall-runoff models*. AWRA Water Resources Bulletin, 14, 4.

Table 8-1: Spring runoff depth (SRD) in mm for eight watersheds.

	Alkali	Berry	Buffalo	Bullpound	Iron	Monitor	Ribstone	Sounding
1960	0	1	6	2	7	1	4	0
1961	2	6	8	8	8	6	5	7
1962	0	2	25	1	17	11	18	7
1963	5	5	60	4	47	25	32	17
1964	0	1	8	0	6	4	6	3
1965	14	20	44	21	56	28	38	23
1966	26	32	18	35	21	24	23	26
1967	5	22	10	30	10	7	12	12
1968	0	2	22	2	20	6	15	5
1969	20	28	33	27	35	31	44	27
1970	0	8	22	12	33	12	29	12
1971	16	26	29	28	37	24	38	23
1972	12	22	38	27	45	26	34	27
1973	1	5	19	7	17	6	13	6
1974	29	34	80	34	111	64	97	57
1975	12	20	19	24	31	29	58	28
1976	11	9	16	10	18	20	26	17
1977	0	3	10	5	9	2	8	3
1978	14	21	24	21	40	27	29	26
1979	11	14	22	14	33	19	24	19
1980	12	17	27	20	31	16	20	18
1981	12	12	17	11	17	16	13	15
mean	9	14	25	16	30	18	27	17

Table 8-3: Regression data for nine Alberta basins.

basin	A	B	R ²	N	Flow Condition
Alkali	304,562	203.	0.131	17	Natural
Berry	-4,467,574	892.	0.381	17	Regulated
Blood In.	-102,412	206.	0.226	16	Regulated
Buffalo	-2,231,862	247.	0.853	10	Natural
Bullpound	-2,553,692	326.	0.174	17	Regulated
Iron	-13,000,000	878.	0.786	17	Natural
Monitor	-852,824	196.	0.496	22	Regulated
Ribstone	-5,535,396	315.	0.847	14	Natural
Sounding	-2,236,176	241.	0.655	13	Regulated

A = basin micro-depression storage (m³), B = AREA1 (km²), R² = correlation statistic and N = years of data.

Table 8-4: AREA1 and depression storage deficit estimates.

basin	depression m	storage mm	AREA1 <- - - - ->	PFRA areas*	
				gross km ² - - - - ->	effective - - - - ->
Buffalo	-2,231,862.	9.	248.	709.	247.
Iron	-13,000,000.	15.	878.	3489.	976.
Monitor	-852,824.	4.	196.	1438.	326.
Monitor2	-847,052.	5.	175.	1438.	326.
Ribstone	-5,535,396.	18.	315.	1830.	697.
Sounding	-2,236,176.	9.	242.	2996.	868.

*PFRA (1985) data.

Monitor2 is output data with 1965 data eliminated.

Table 8-5: Drainage density and runoff depth relationships.

basin	channel length km	AREA1 km	drainage density 1/km	SRD-DS mm
Buffalo	61.	248.	0.246	16
Iron	300.	878.	0.342	15
Monitor	169.	196.	0.862	14
Monitor2	169.	175.	0.966	13
Ribstone	254.	315.	0.806	9
Sounding	260.	242.	1.074	8

Monitor2 is output data with 1965 data eliminated.

Table 8-6: Depression storage, area and channel slope data.

basin	slope	water area km²	DS mm	DS' mm
Buffalo	0.004354	0.972	9	9
Iron	0.00145	22.34	15	16
Ribstone	0.000725	26.15	18	17
Sounding	0.000967	17.58	9	9
DS' = -13.1 + 4758.3 slope + 1.007 area				
R² = .941,				

Table 8-7: AREA1 and depression storage deficit estimates.

Permut. of X2	Buffalo		Iron		Ribstone		Sounding		Sum DS-DS'
	DS'	DS	DS'	DS	DS'	DS	DS'	DS	
1234	8.60	9.	16.30	15.	16.68	18.	9.20	9.	3.22
1243	8.60	9.	16.30	15.	8.05	18.	17.83	9.	20.48
1324	8.60	9.	20.13	15.	12.85	18.	9.20	9.	10.89
1342	8.60	9.	20.13	15.	8.05	18.	14.00	9.	20.48
1423	8.60	9.	11.50	15.	12.85	18.	17.83	9.	17.89
1432	8.60	9.	11.50	15.	16.68	18.	14.00	9.	10.22
2134	30.11	9.	-5.22	15.	16.68	18.	9.20	9.	42.86
2143	30.11	9.	-5.22	15.	8.05	18.	17.83	9.	60.12
2314	30.11	9.	20.13	15.	-8.67	18.	9.20	9.	53.12
2341	30.11	9.	20.13	15.	8.05	18.	-7.52	9.	52.71
2413	30.11	9.	11.50	15.	-8.67	18.	17.83	9.	60.12
2431	30.11	9.	11.50	15.	16.68	18.	-7.52	9.	42.45
3124	33.95	9.	-5.22	15.	12.85	18.	9.20	9.	50.53
3142	33.95	9.	-5.22	15.	8.05	18.	14.00	9.	60.12
3214	33.95	9.	16.30	15.	-8.67	18.	9.20	9.	53.12
3241	33.95	9.	16.30	15.	8.05	18.	-7.52	9.	52.71
3412	33.95	9.	11.50	15.	-8.67	18.	14.00	9.	60.12
3421	33.95	9.	11.50	15.	12.85	18.	-7.52	9.	50.12
4123	25.32	9.	-5.22	15.	12.85	18.	17.83	9.	50.53
4132	25.32	9.	-5.22	15.	16.68	18.	14.00	9.	42.86
4213	25.32	9.	16.30	15.	-8.67	18.	17.83	9.	53.12
4231	25.32	9.	16.30	15.	16.68	18.	-7.52	9.	35.45
4312	25.32	9.	20.13	15.	-8.67	18.	14.00	9.	53.12
4321	25.32	9.	20.13	15.	12.85	18.	-7.52	9.	43.13

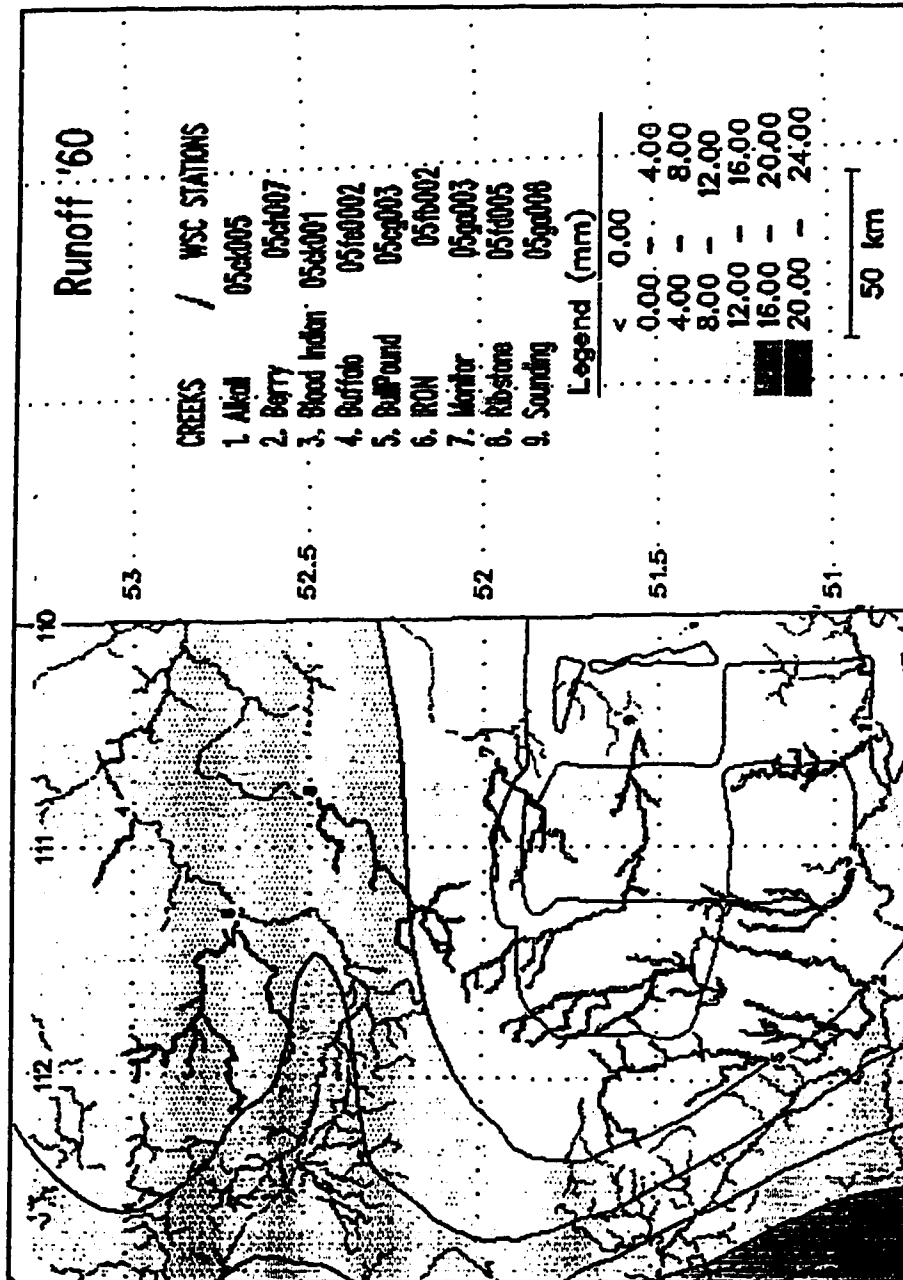


Figure 8-1: Spring runoff depth over the study area, water equivalent

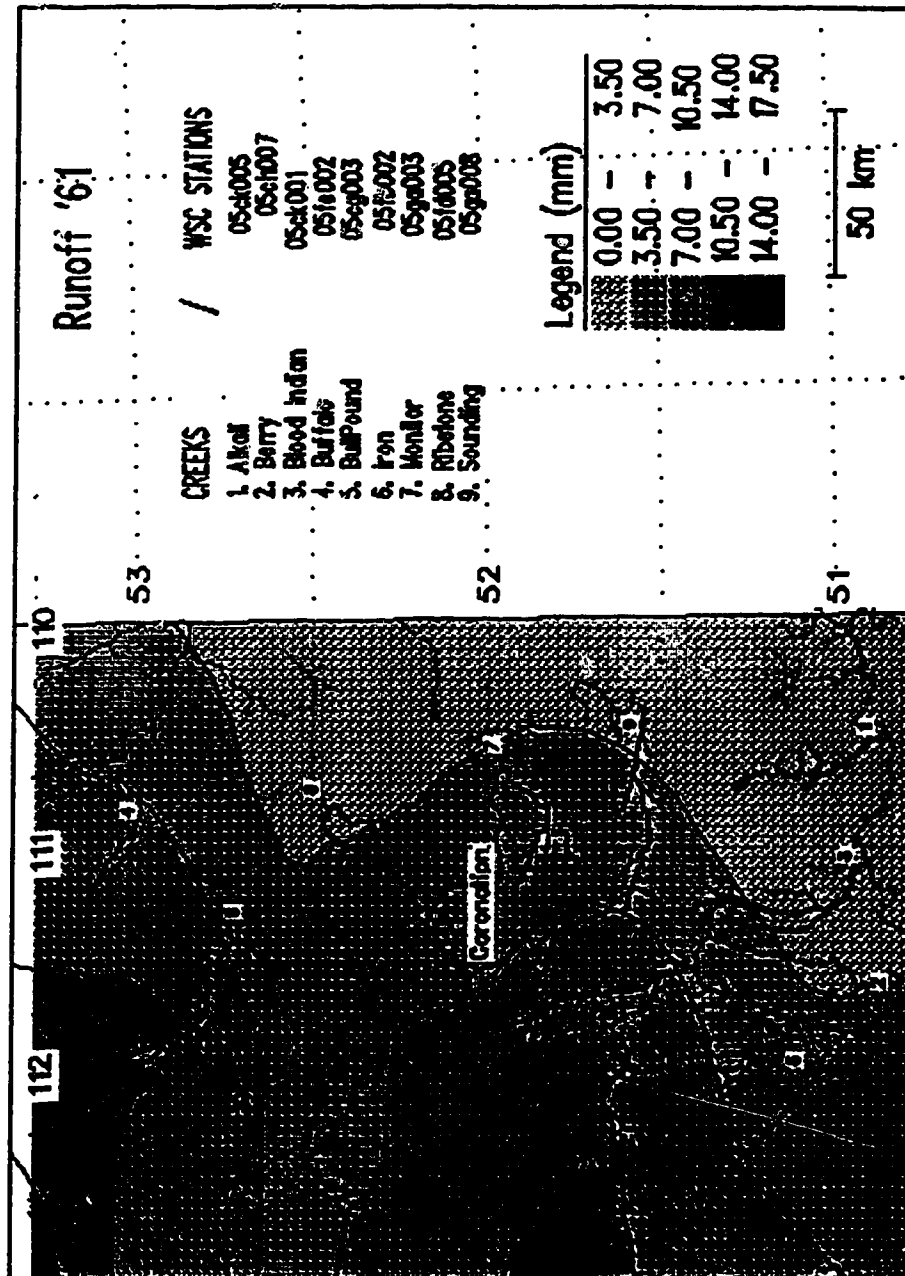


Figure 8-1, - continued.

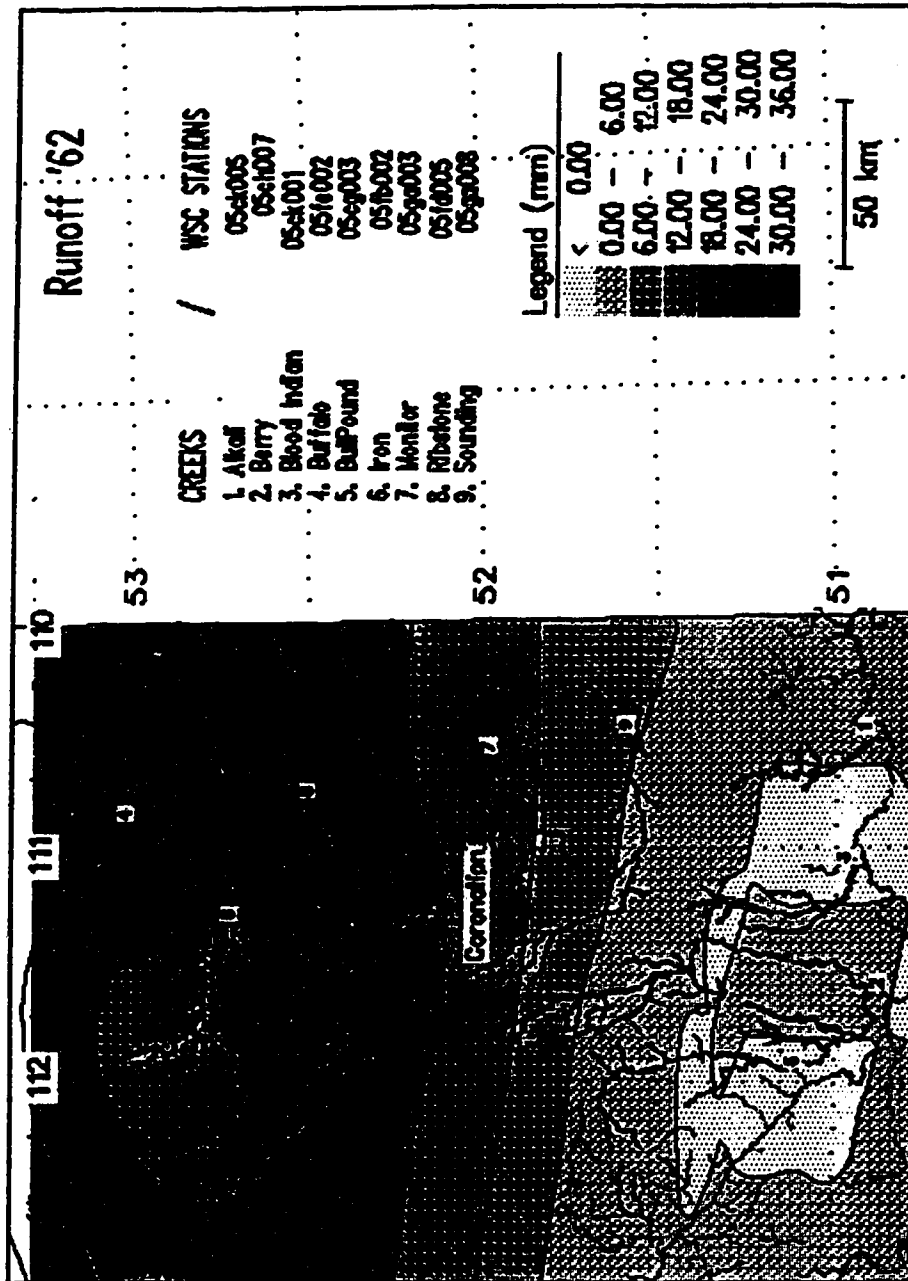


Figure 8-1, - continued.

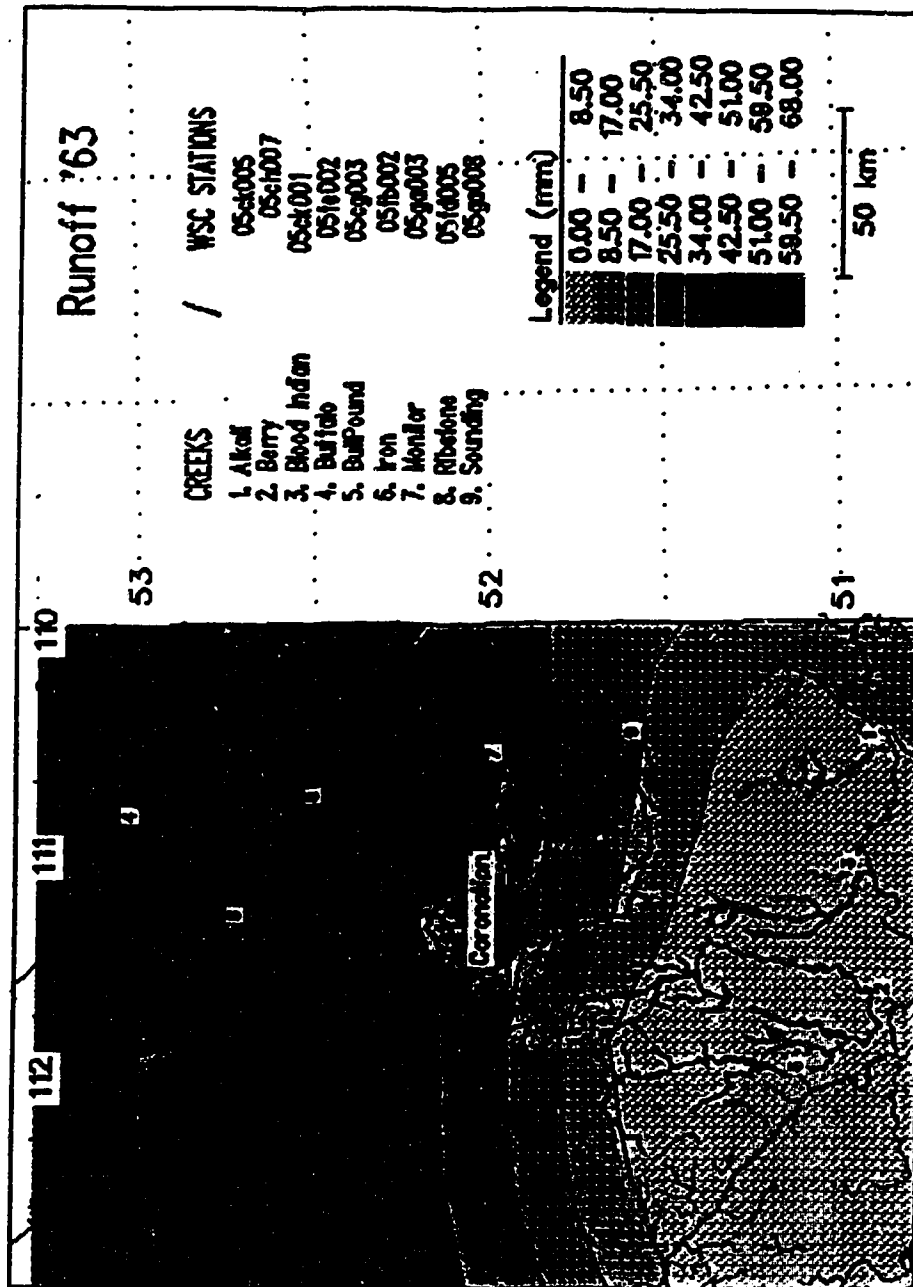


Figure 8-1, - continued.

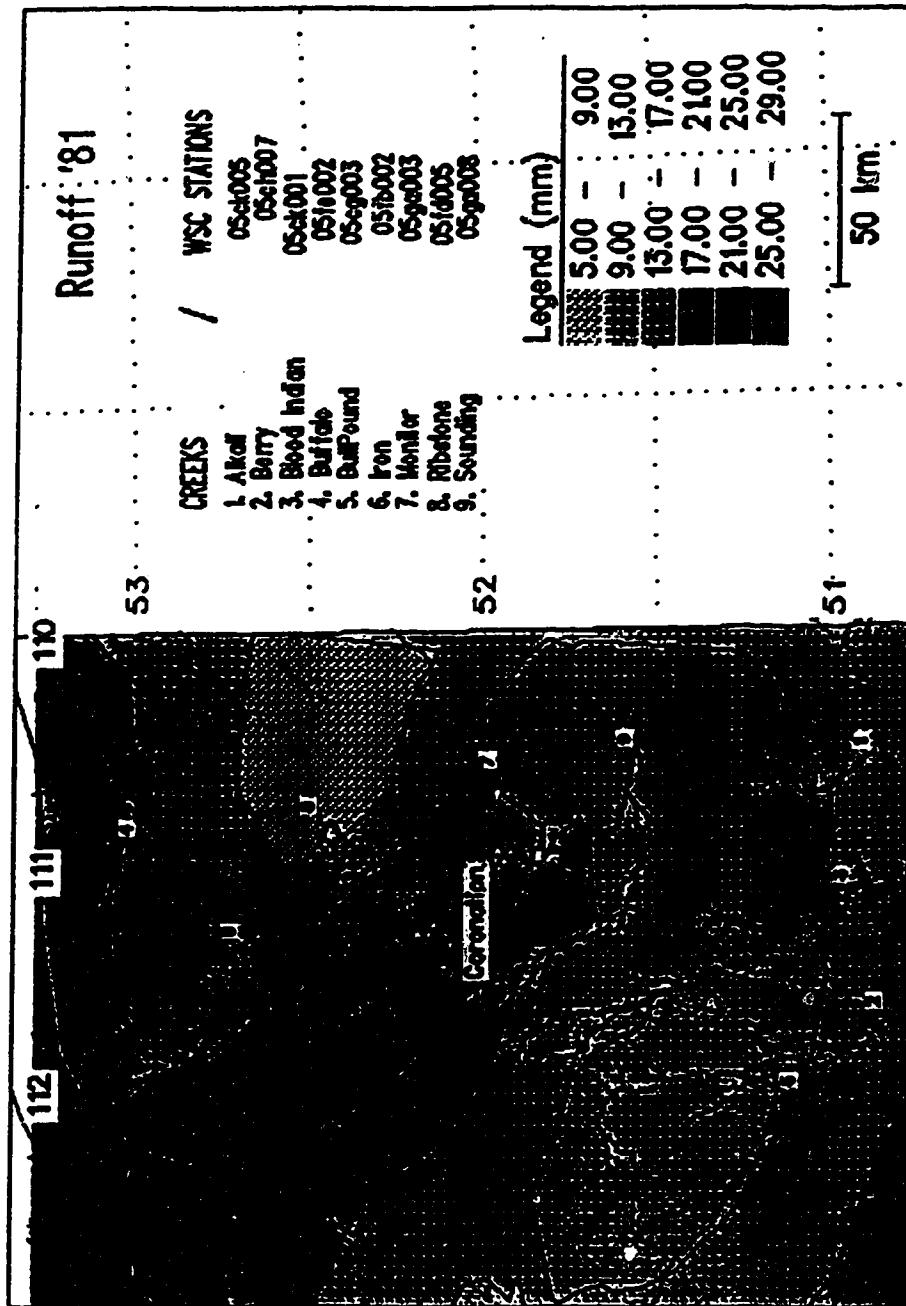


Figure 8-1, - continued.

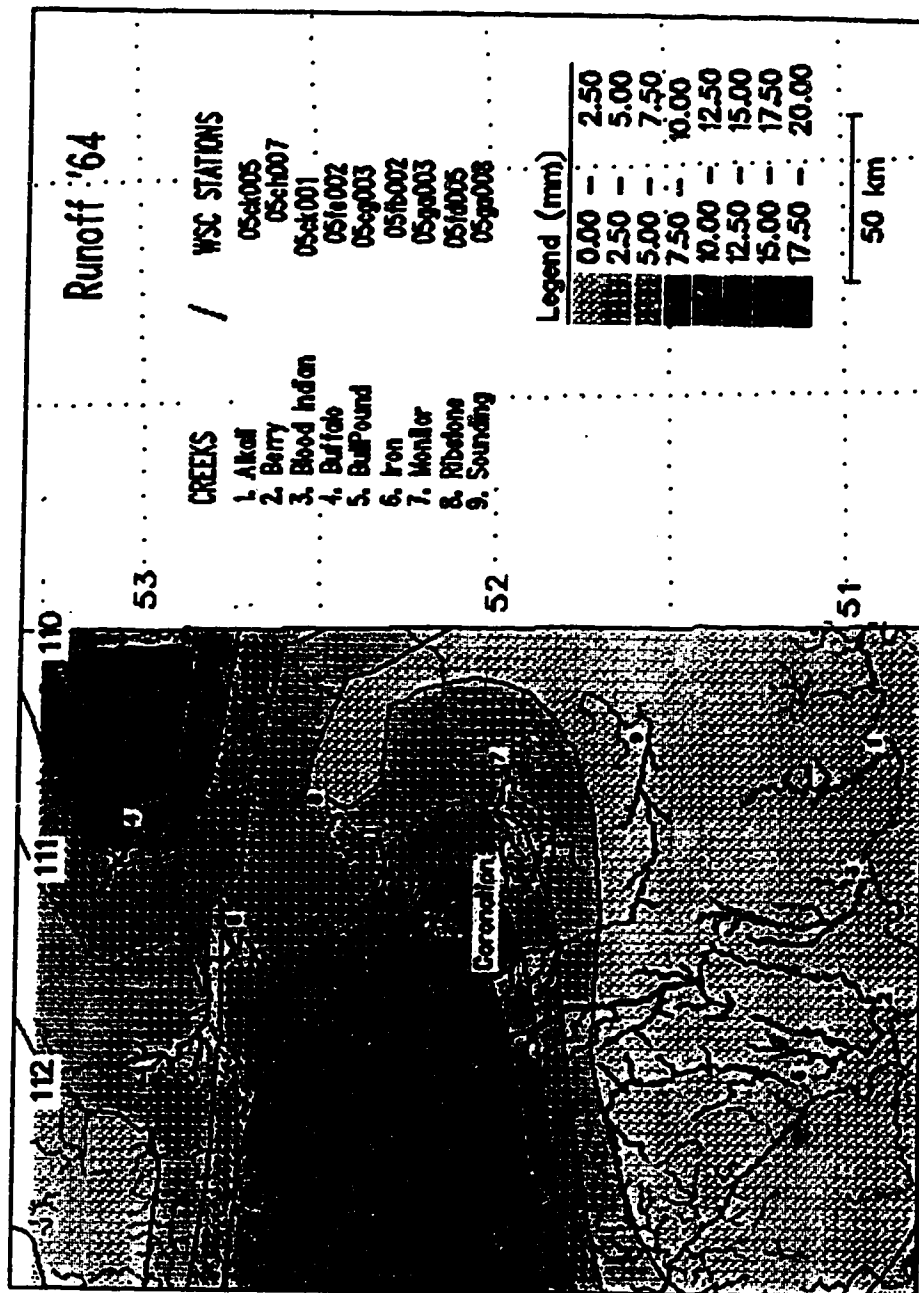


Figure 8-1, - continued.

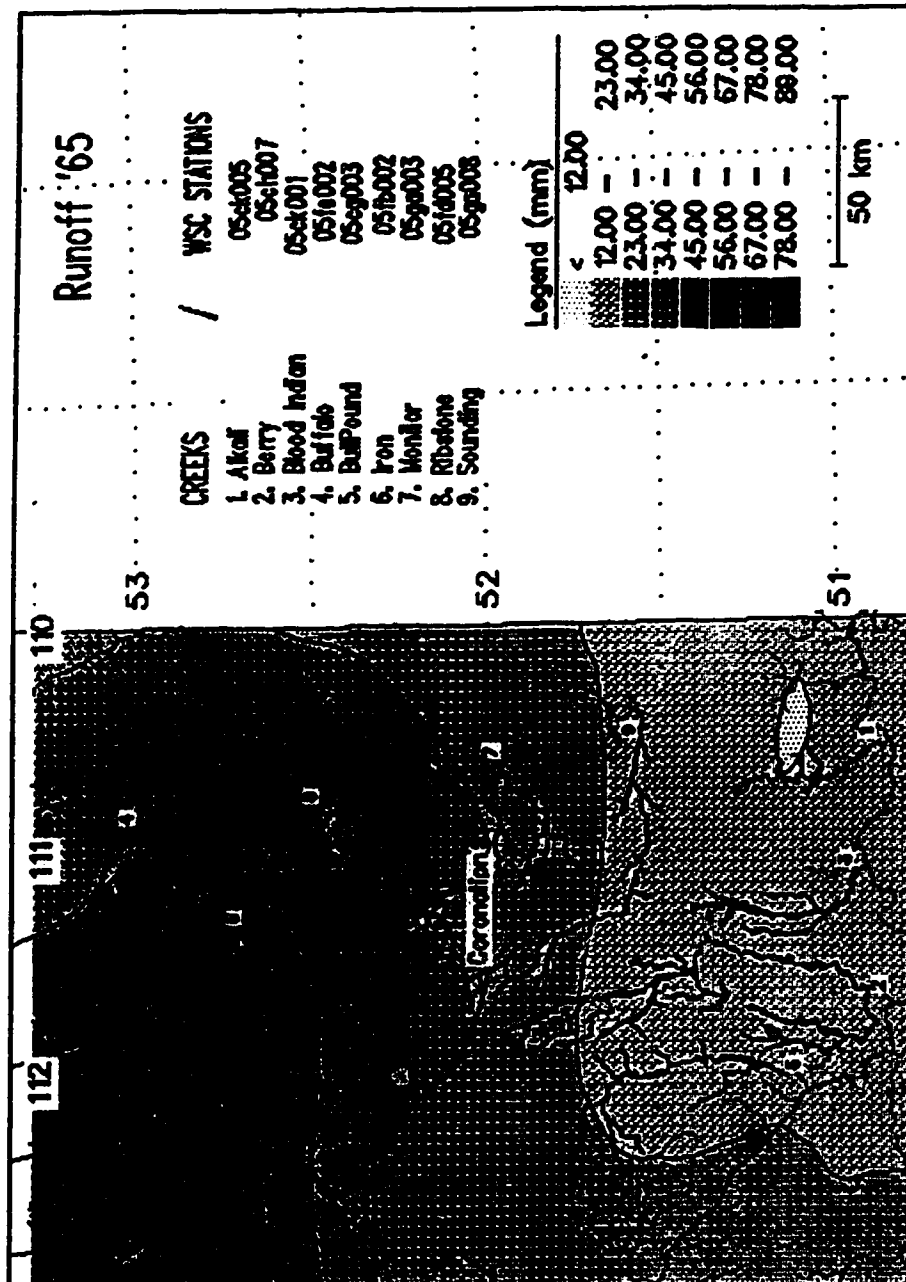


Figure 8-1, - continued.

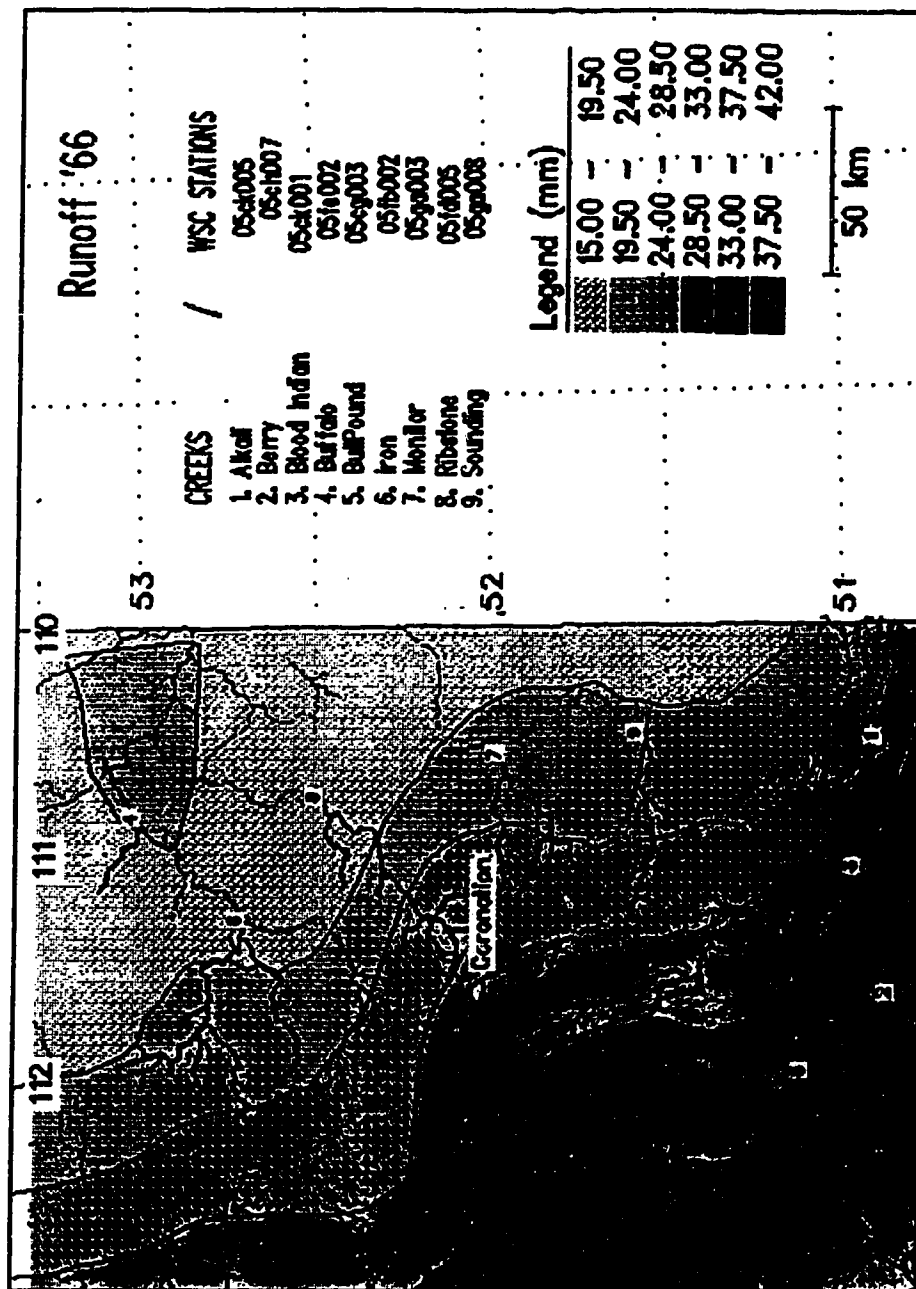


Figure 8-1, - continued.

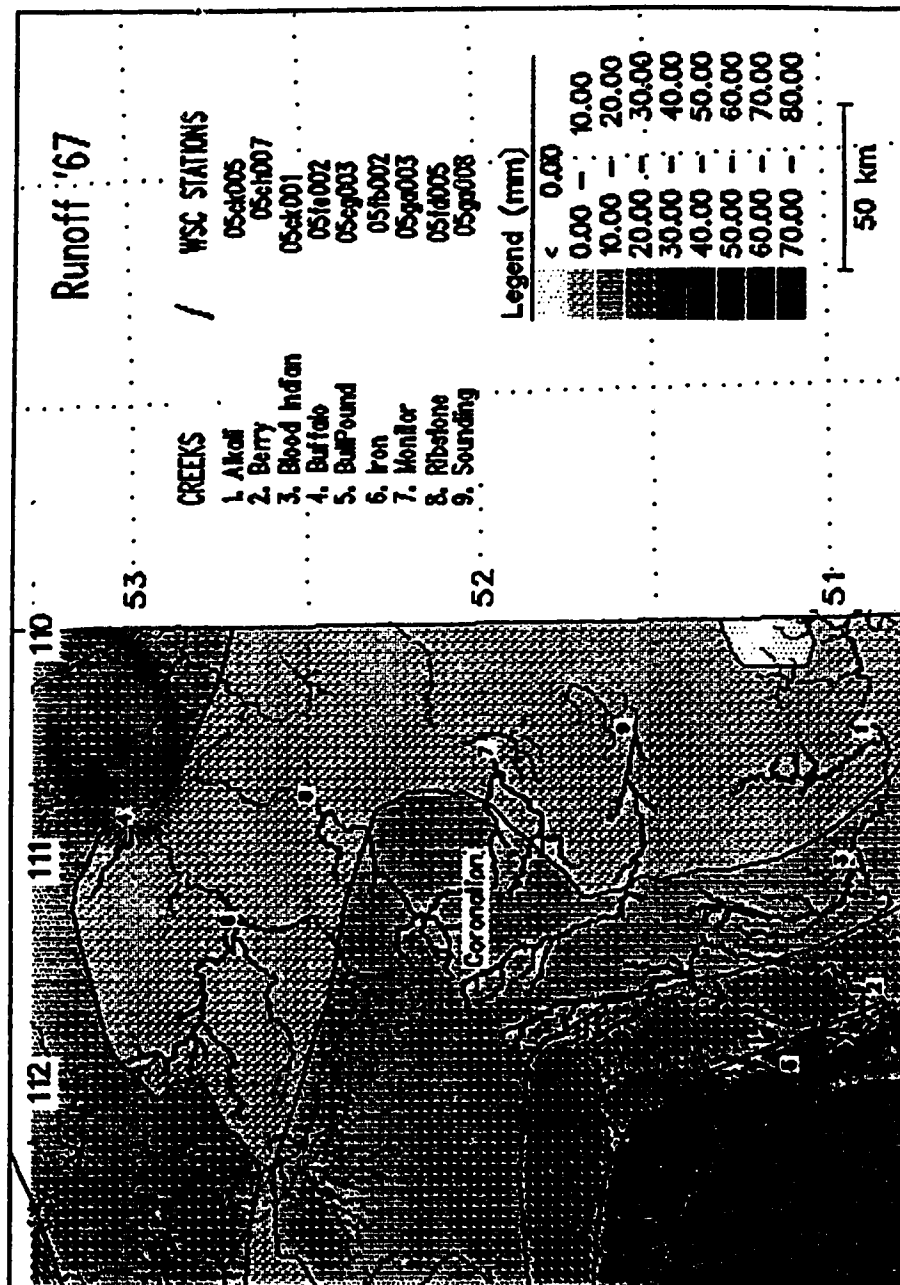


Figure 8-1, - continued.

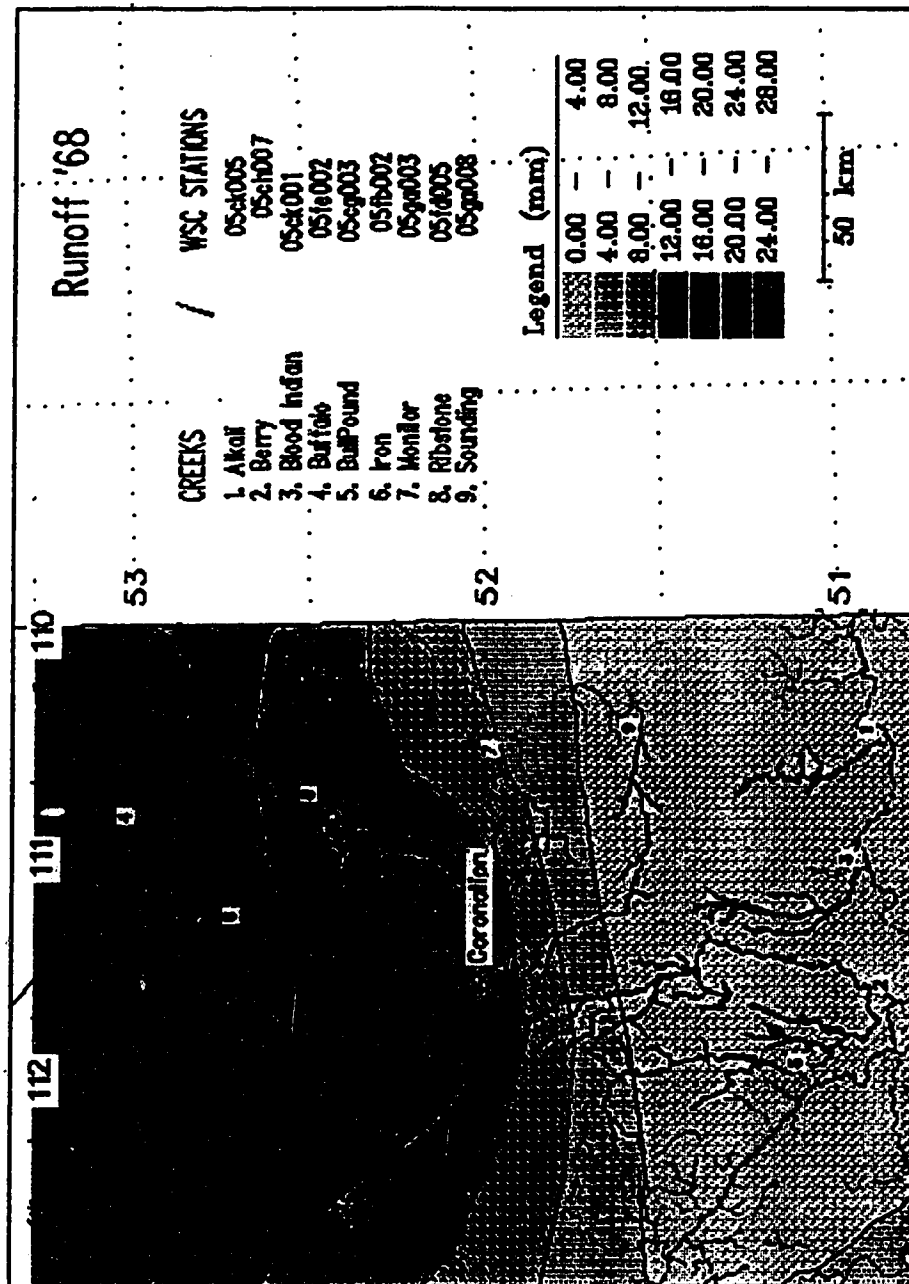


Figure 8-1, - continued.

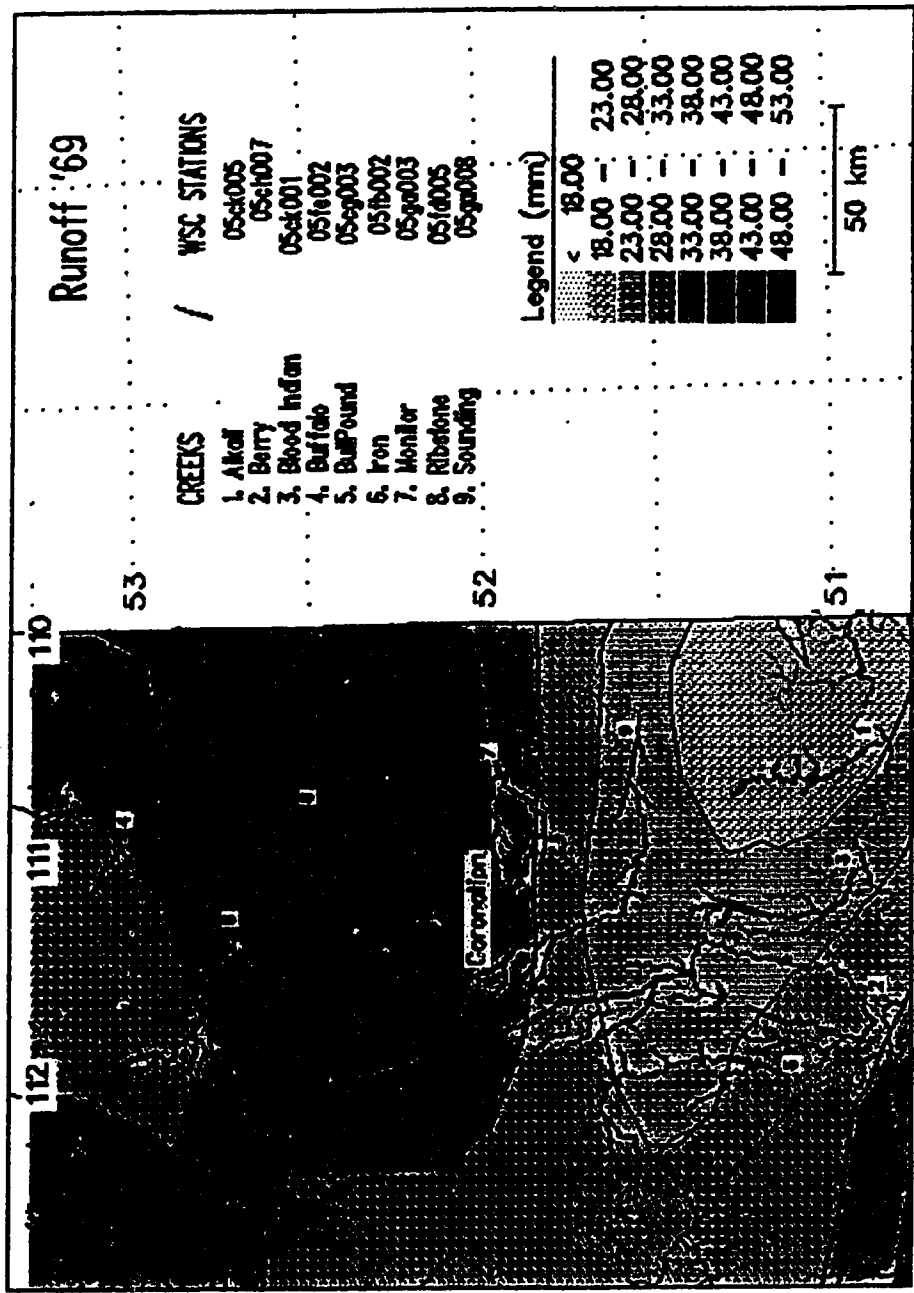


Figure 8-1, - continued.

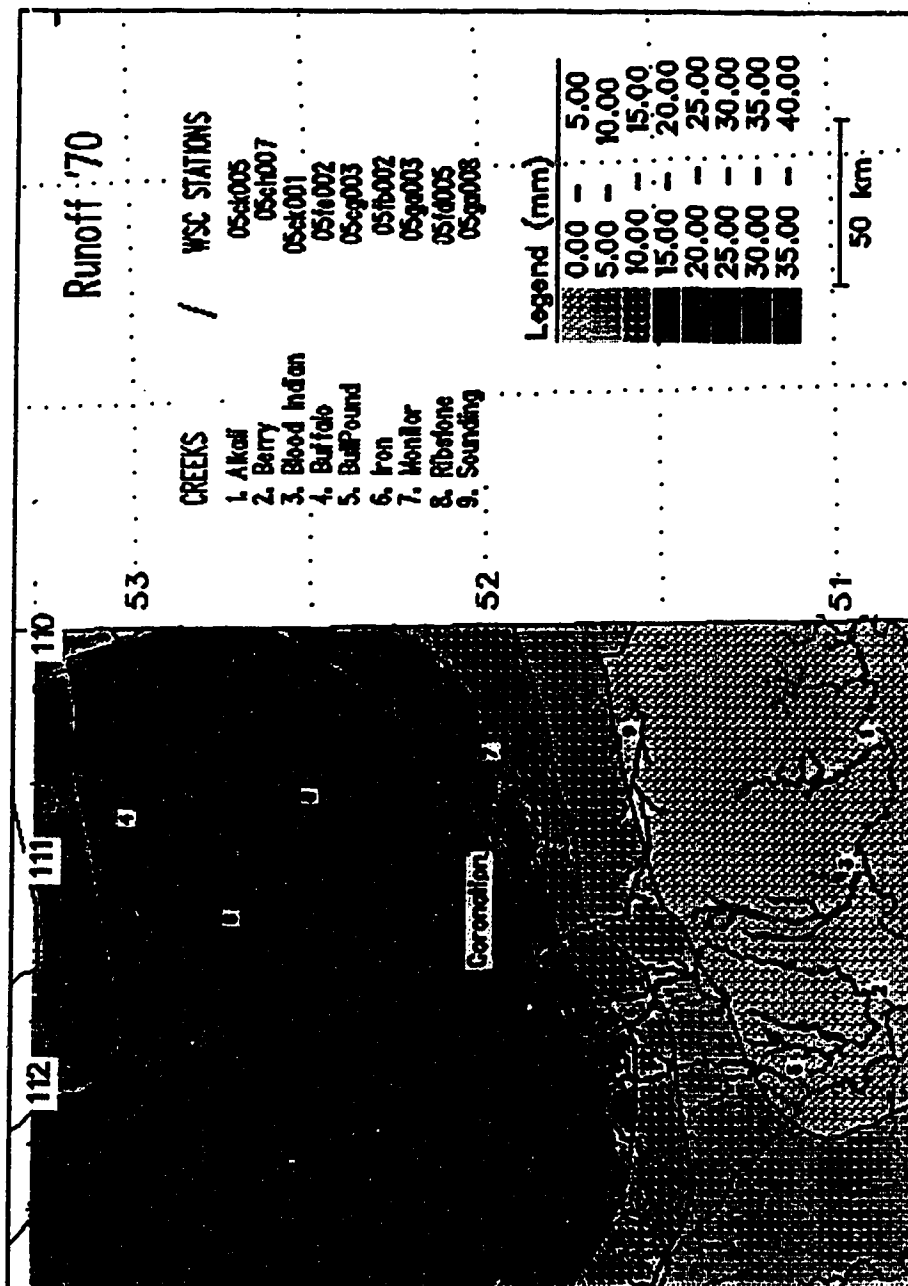


Figure 8-1, - continued.

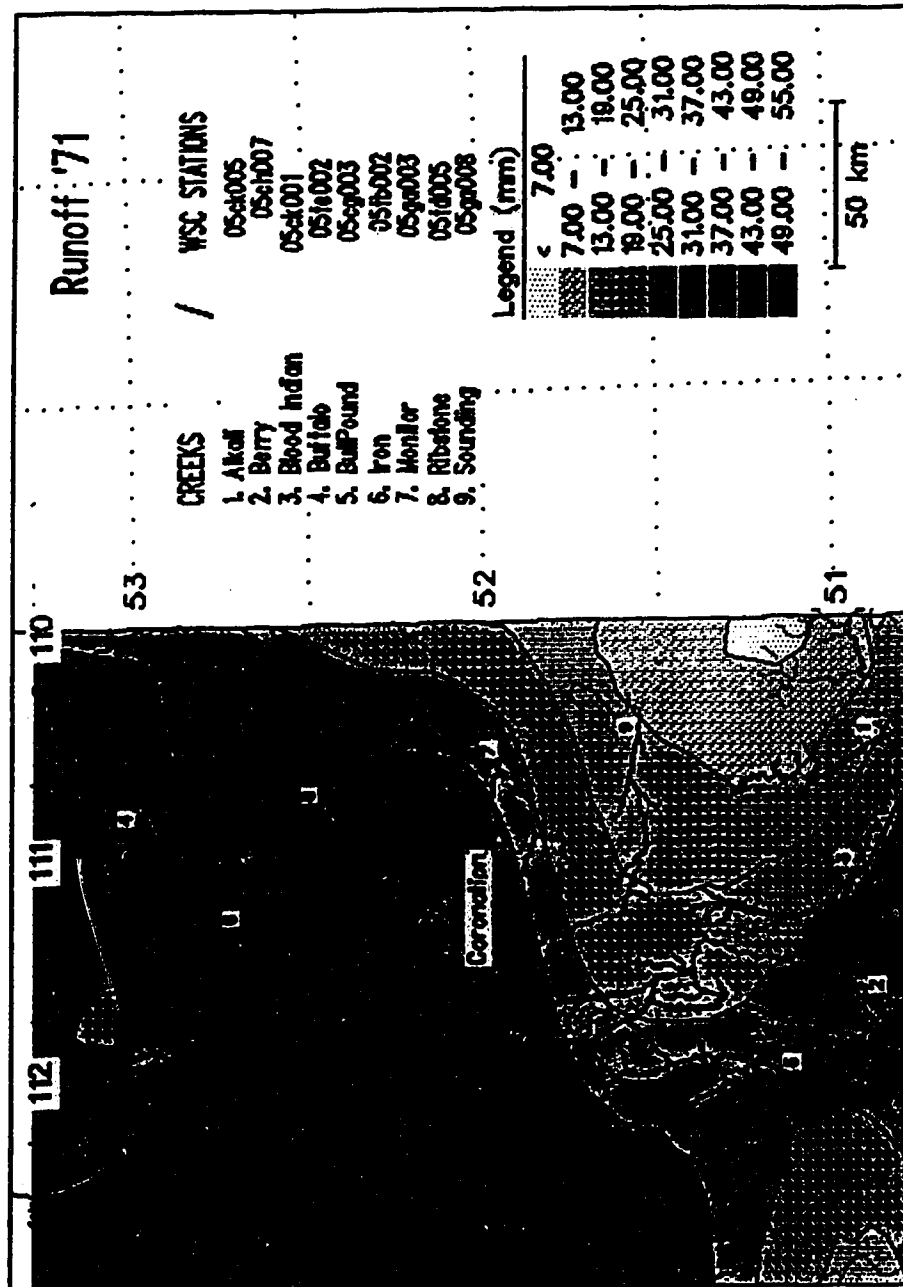


Figure 8-1, - continued.

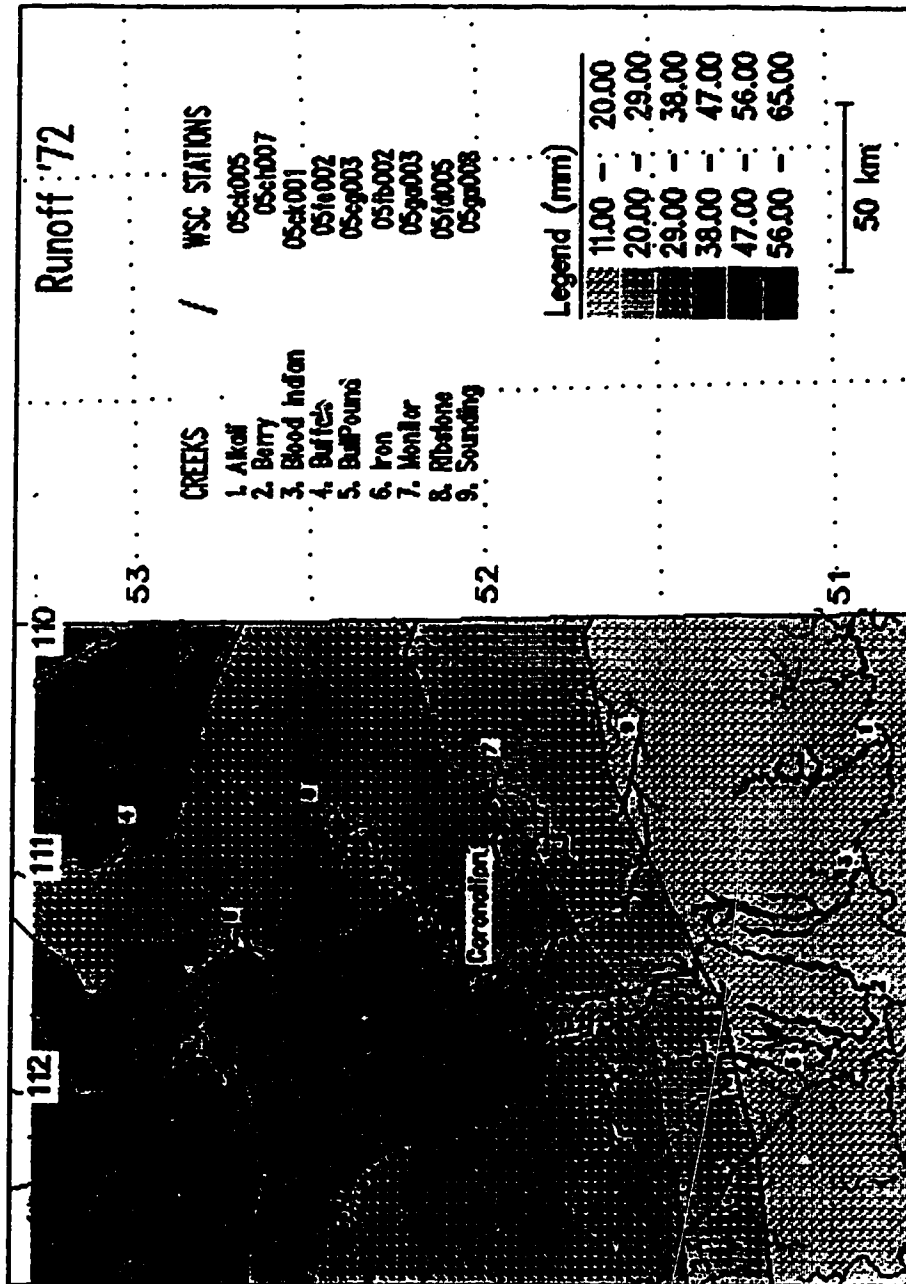


Figure 8-1, - continued.

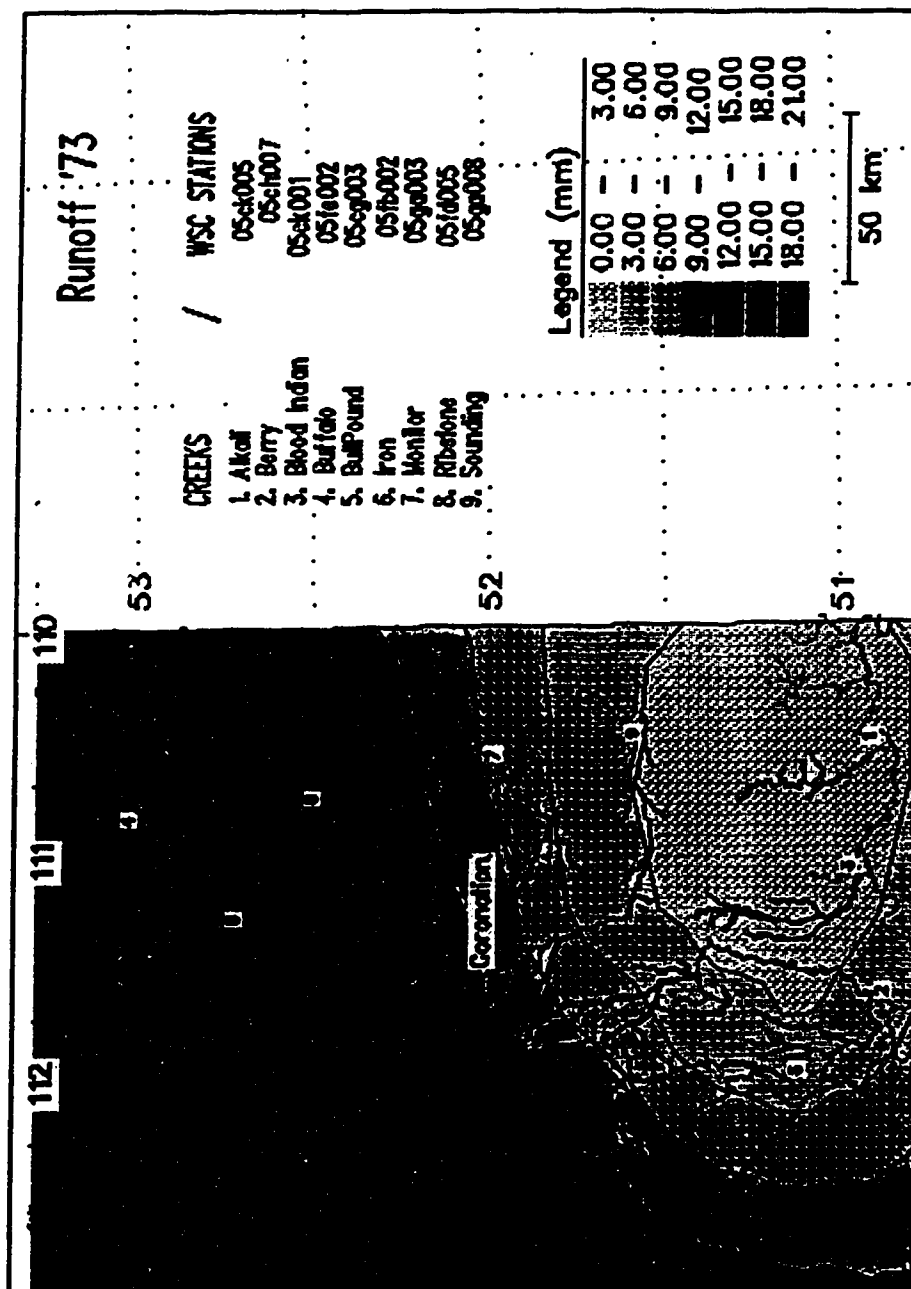


Figure 8-1, - continued.

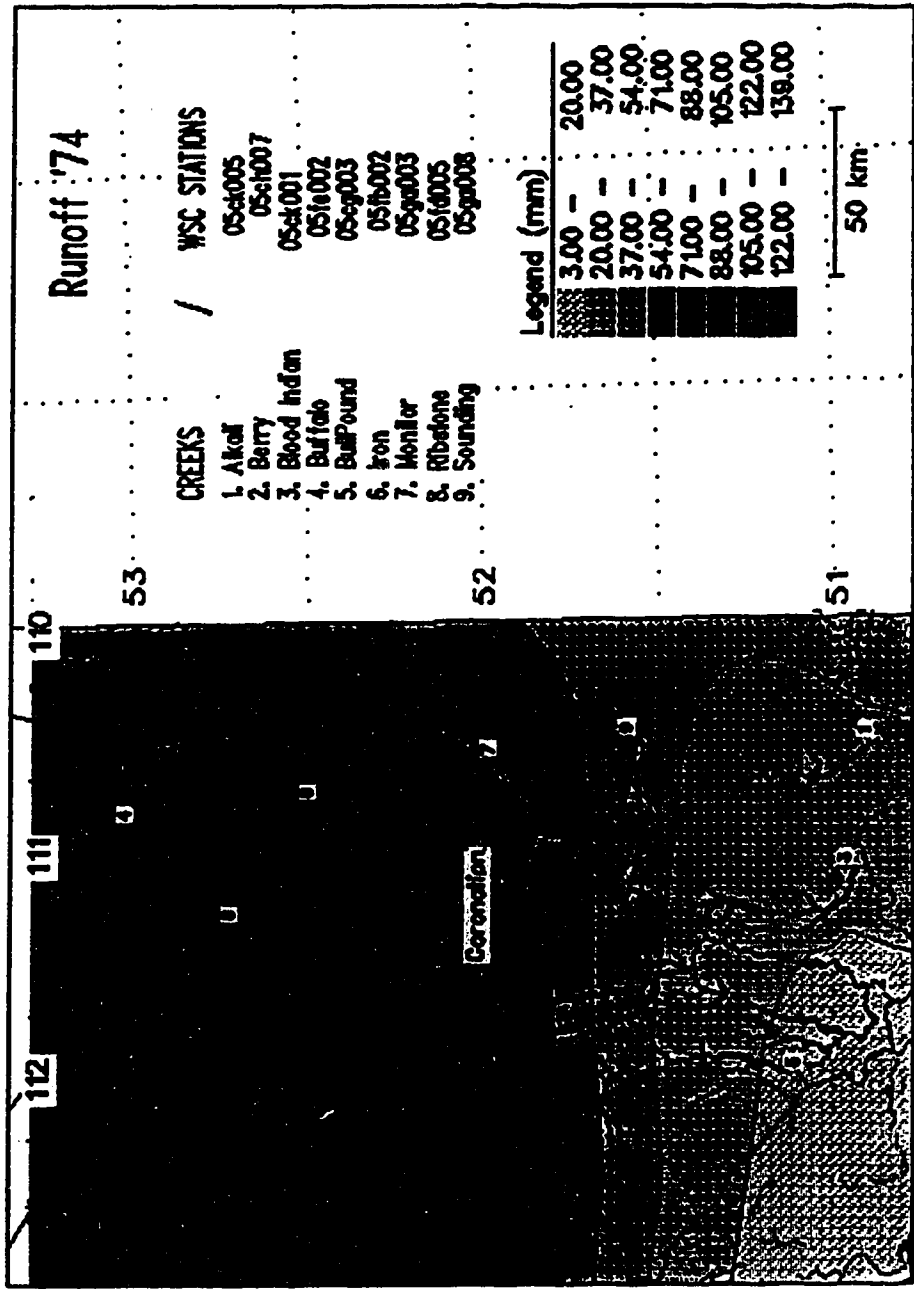


Figure 8-1, - continued.

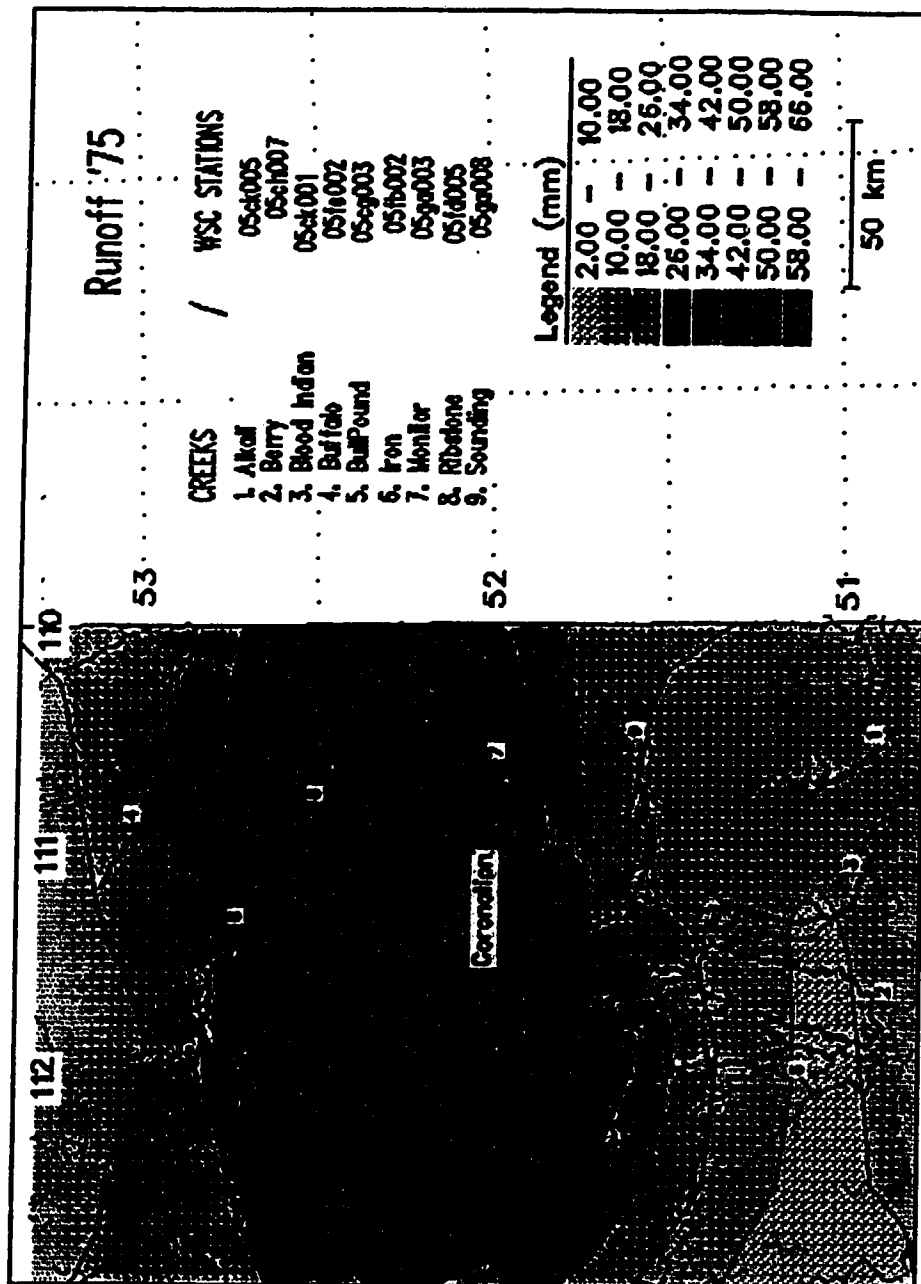


Figure 8-1, - continued.

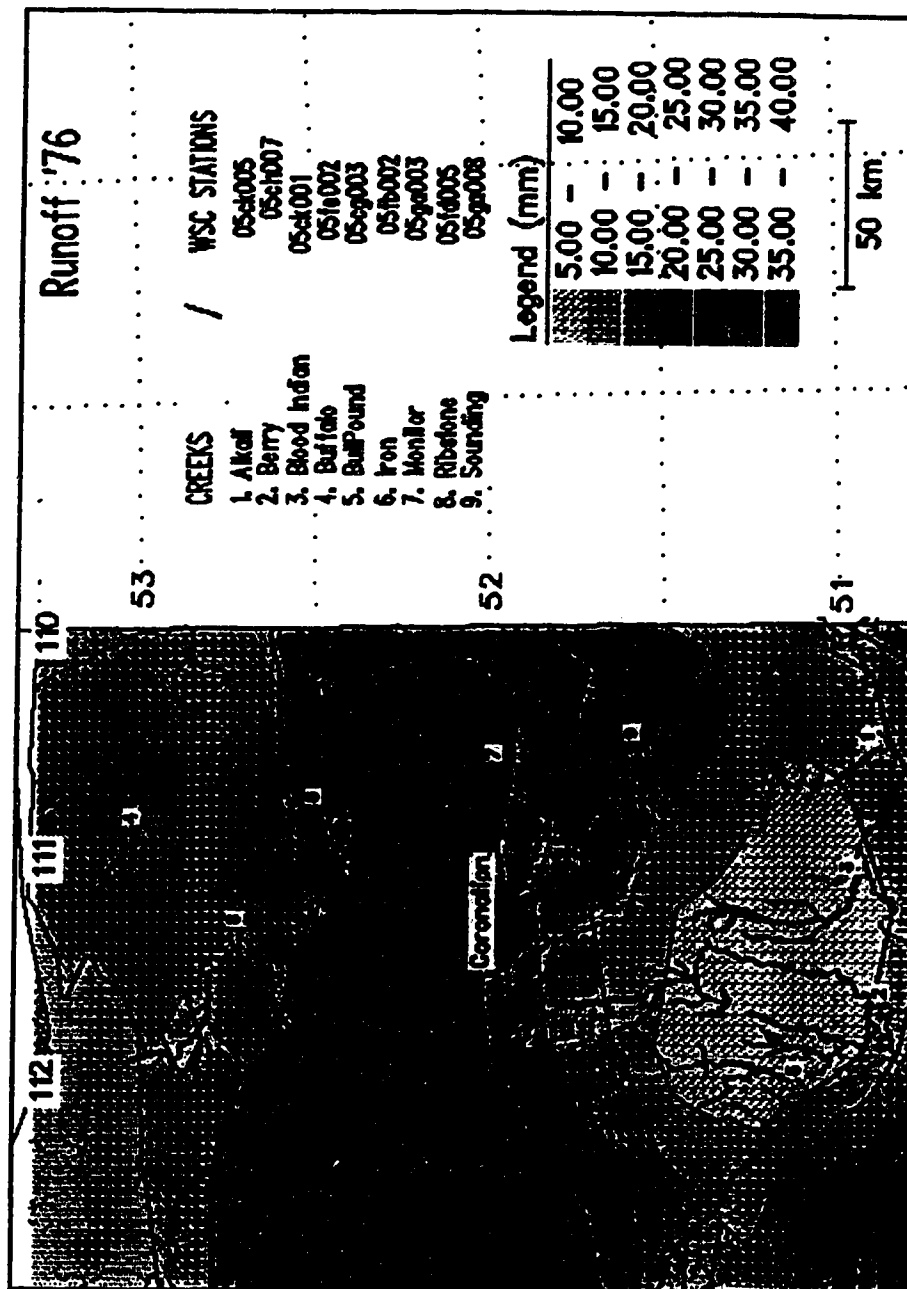


Figure 8-1, - continued.

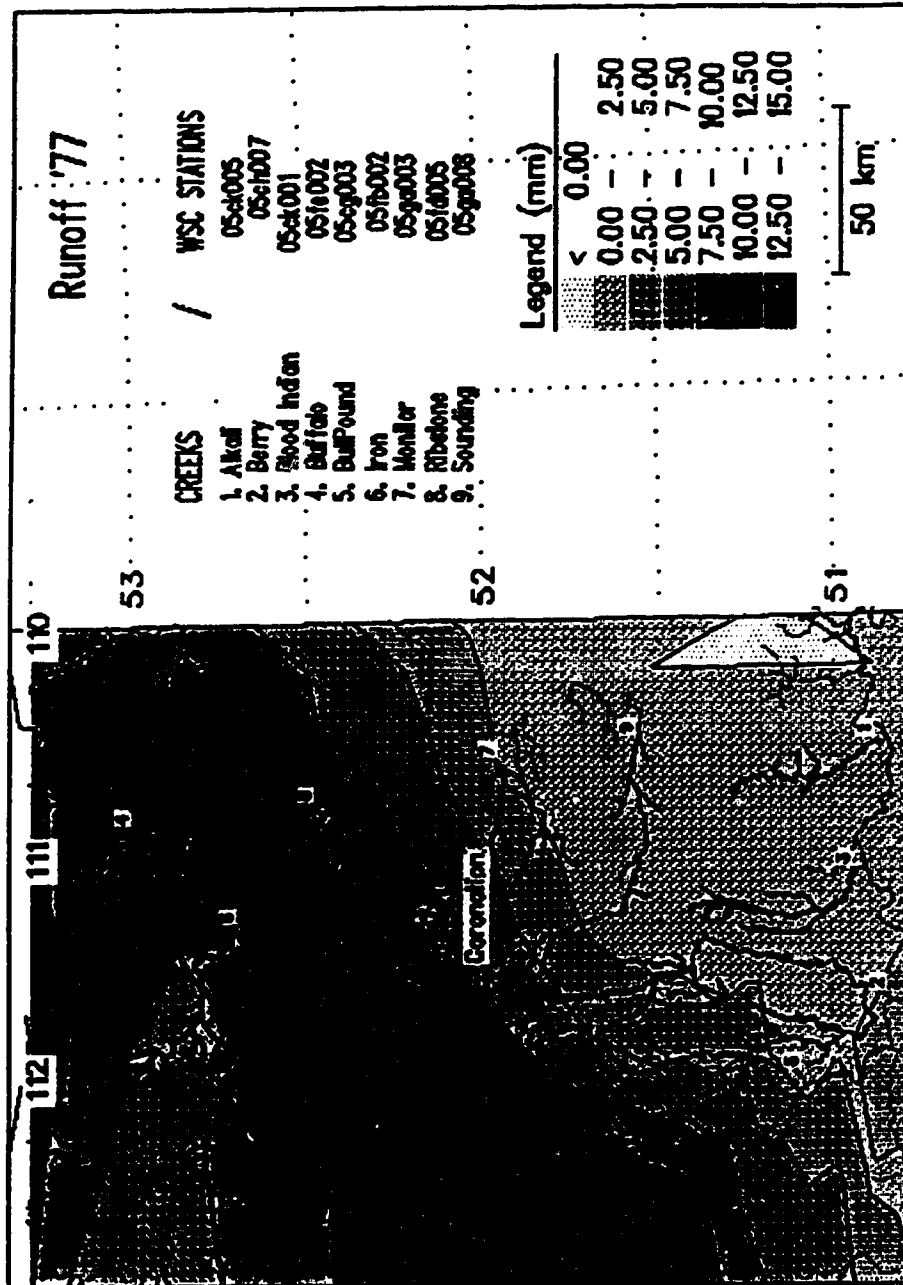


Figure 8-1, - continued.

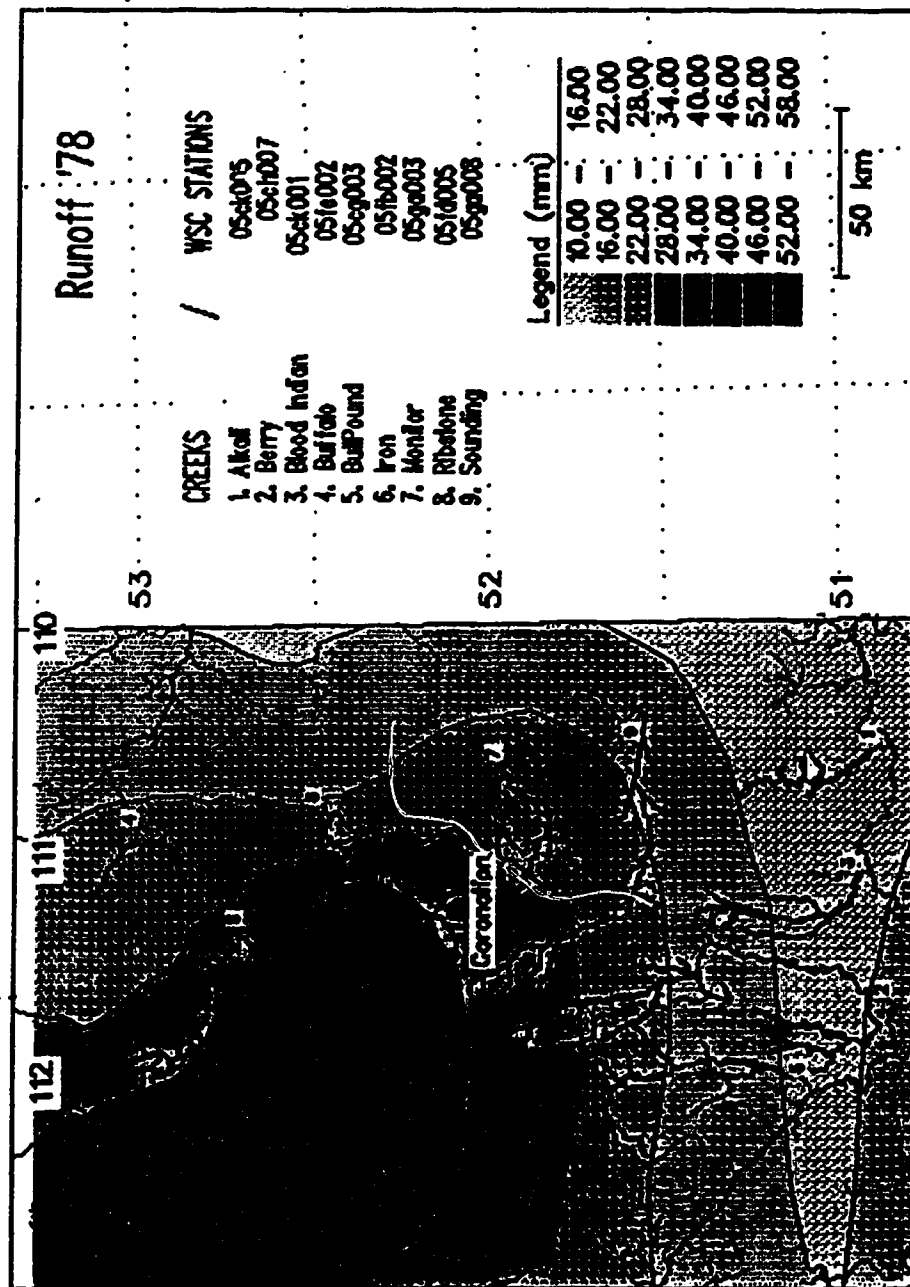


Figure 8-1, - continued.

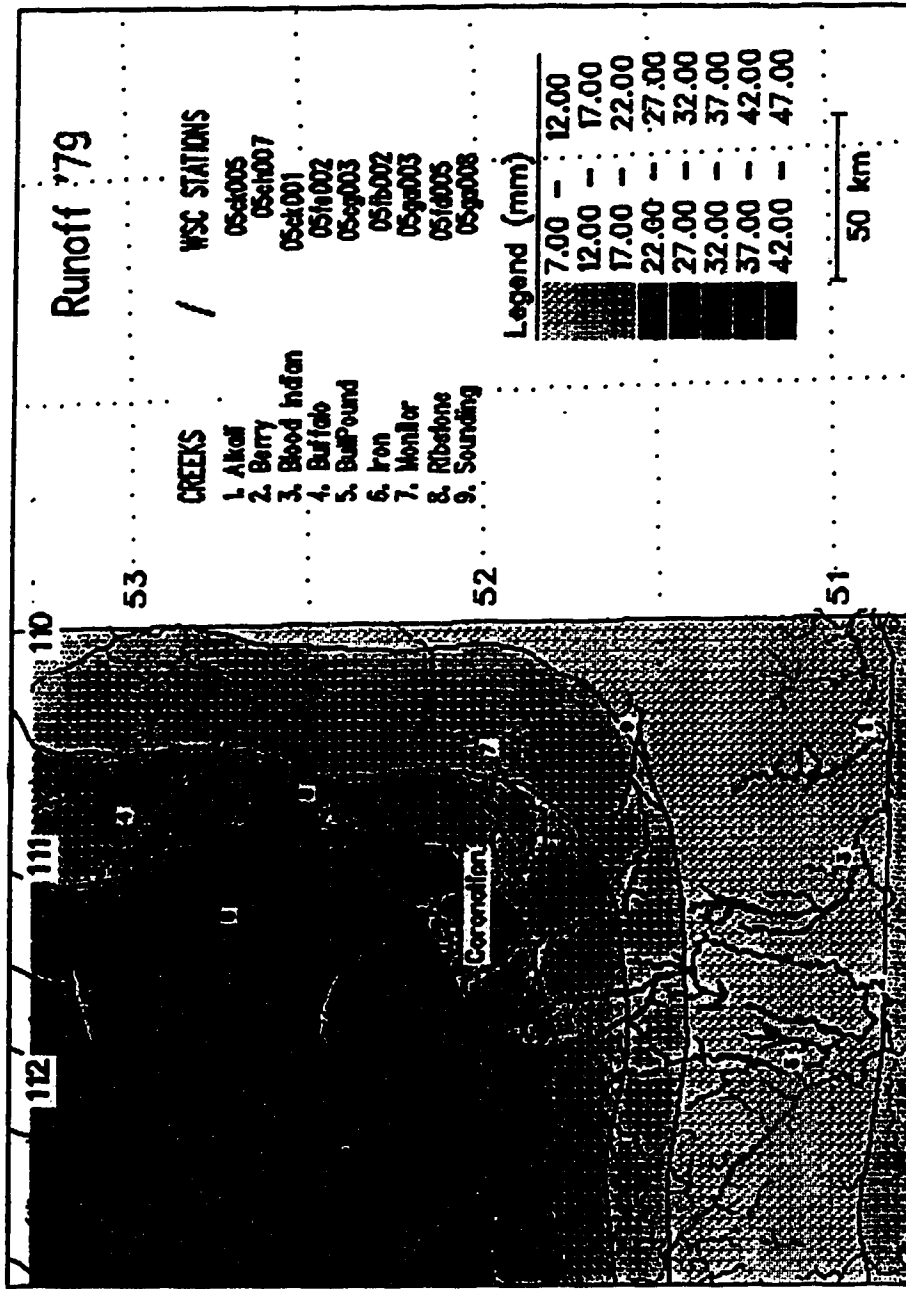


Figure 8-1, - continued.

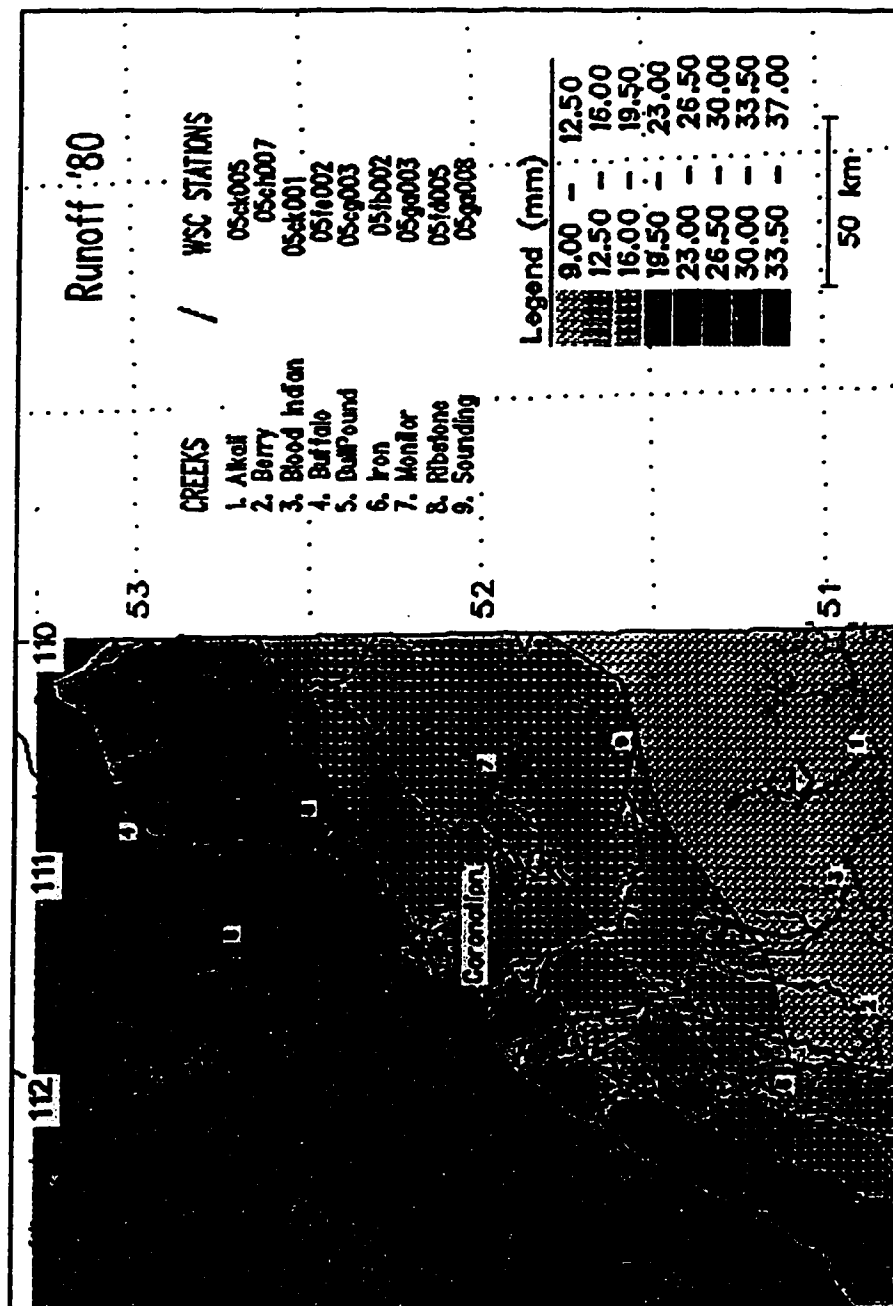


Figure 8-1, - continued.

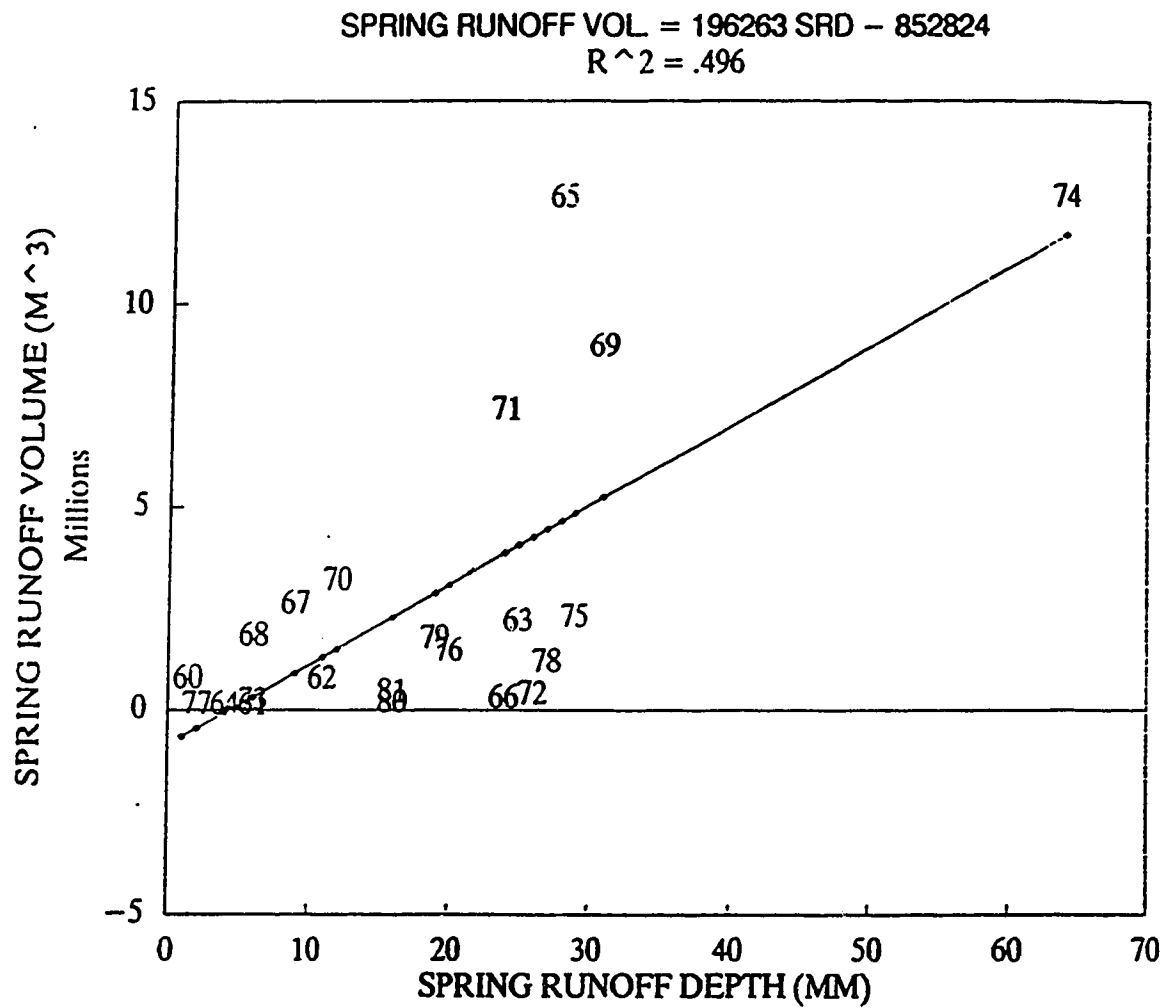


Figure 8-2: Monitor creek regression plot, AREA1 analysis.

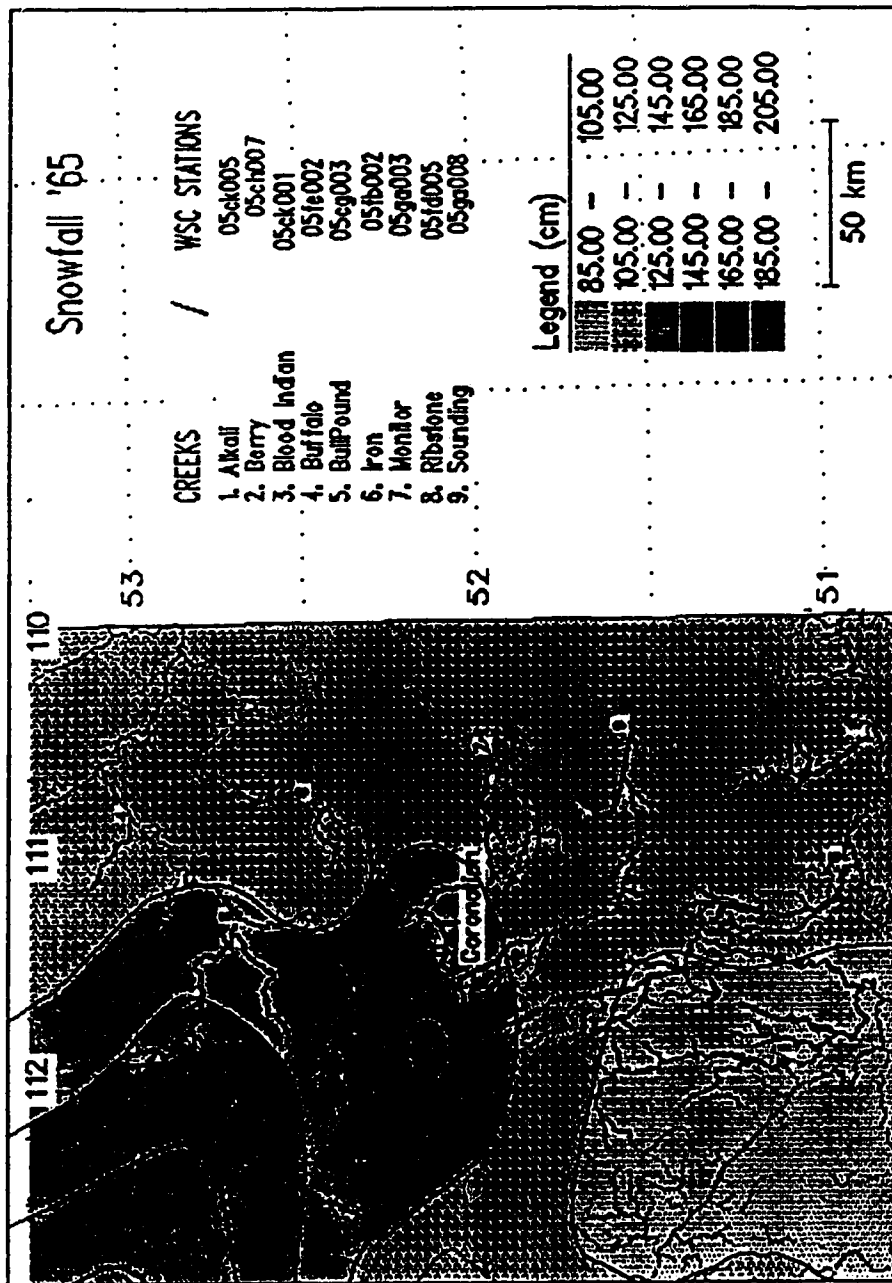


Figure 8-3: 1964-65 snowfall over the study area.

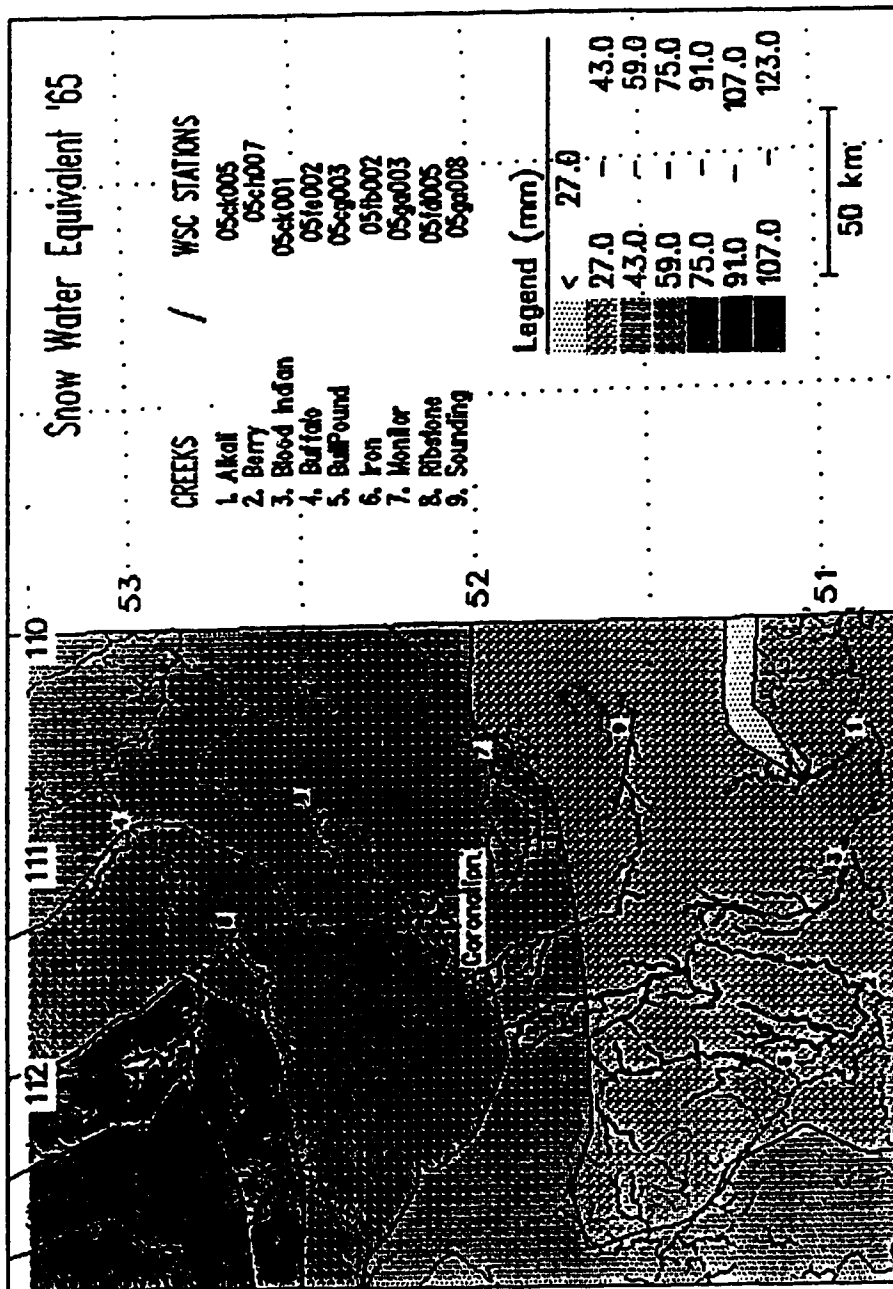


Figure 8-4: 1964-65 SWE depth for the study area.

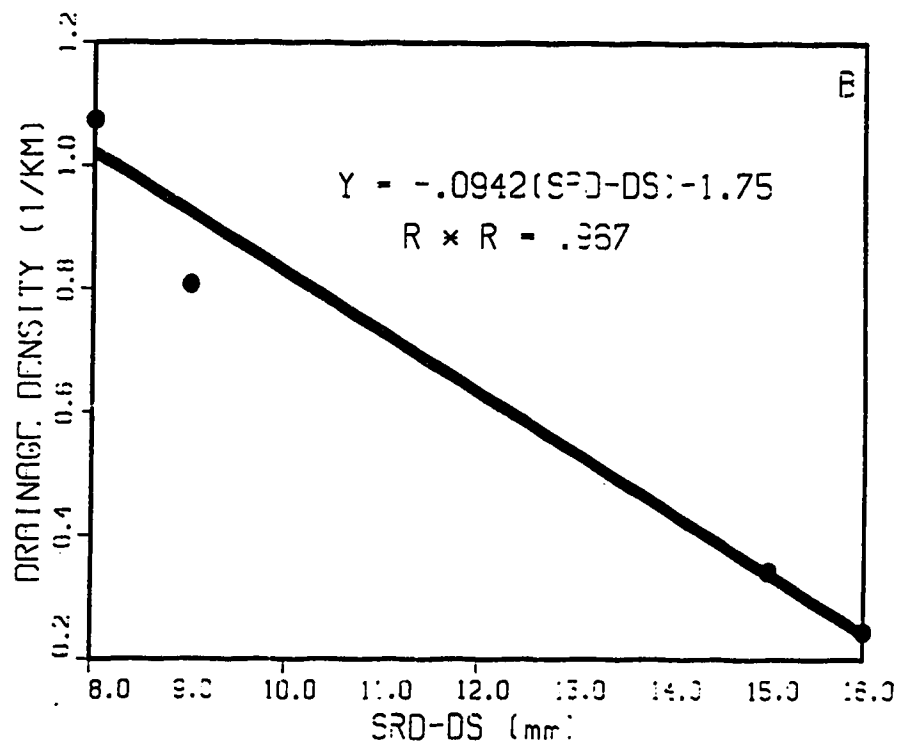
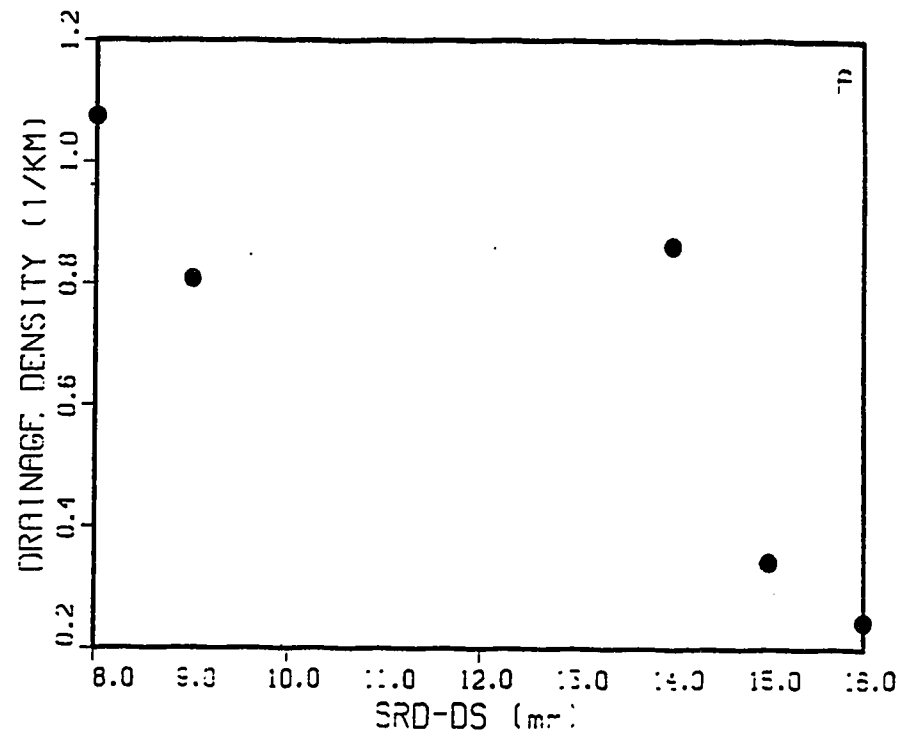


Figure 8-5: Scatter plot of SRD-DS and drainage density.

Chapter 9

SYNTHESIS

9.1. Introduction

The preceding chapters provided several analyses of the hydrologic processes on the prairies of eastern Alberta. The intent was twofold: first, to address the objectives stated in chapter 1; and second, to test the hypothesis of a three phase soil system being the critical control mechanism for runoff for the watershed in the study area. In effect, these two intentions were complementary. The objectives focused on the precipitation phase, and the resulting snowmelt and/or rainfall runoff; and the soil system and contributing area, two parameters that are strongly related under the conceptual discussion of the three phase system. The role of detention and depression storage in the runoff process was addressed. These two processes combine to create the saturated soil phase that is theorized to be so critical to the possibility of any runoff beyond the snowmelt runoff period.

The three phase model was introduced in section 3.3 with the following discussion.

The Prairie Runoff (PR) Conceptual model represents a three phase theory of prairie river runoff processes. The phases are defined in terms of the soil system: the frozen soil runoff phase deals with snowmelt and rainfall when the soil profile is frozen and, except for initial infiltration losses, essentially impermeable. The second phase, the active soil phase, deals with snowmelt and rainfall as inputs to the active soil moisture system. Inputs are allocated to the soil moisture deficit first, then depression storage and finally, to streamflow runoff. The third phase, the

saturated soil area, deals with those areas within the watershed directly connected to the channel network and fully saturated during the runoff season. These areas are assumed to have a runoff coefficient of 1.0;

9.2. Conclusions

1. The frozen soil phase area that contributes to runoff in most years varies little, and may be assumed to be a constant. Several points support this contention. First, the soil is frozen, and incapable of interacting with the snowmelt runoff (after initial infiltration). The variable area concept is based on the soil infiltration/storage functions interacting to reduce runoff potential on a distributed basis as a function of the soil properties and moisture storage levels. Since snowmelt infiltration into frozen soils is limited, the controlling mechanism for contributing area is depression storage and thus, topography. Second, the quantitative arguments developed from the analyses in Chapters 5 and 8 demonstrate a strong linear relationship between snowmelt runoff depth (SWE-INF) and spring runoff volume. The linearity of this relationship imposes a constant area on the frozen soil phase.

2. There is no runoff from the soil system beyond snowmelt that contributes to the streamflow recorded in the study basins in the vicinity of Ribstone Creek or to the south and east of Ribstone, within the study area. The extent of this lack of runoff to the north and western sectors is unknown, but is theorized to be a significant distance. Chapter 6 presents a series of analyses of the active soil phase for a number of climate stations near Ribstone creek. The analyses, based on assumptions that favoured the generation of runoff, failed to demonstrate any occurrence of runoff from historical climatic data. At the very least,

this analyses supports the contention that there is minimal runoff to streamflow from the active soil phase; and in that case, only in very rare events, and insignificant quantities relative to snowmelt runoff.

3. The saturated soil phase is virtually the only source of runoff in addition to snowmelt. The analyses in Chapter 7 support this contention; as do the occurrences of relatively small runoff peaks associated with summer rainfall. The volume of runoff typically does not relate directly to the depth of rain. Instead, the volume relates to the current discharge level in the basin. If the rainfall occurred shortly after snowmelt, the volume would be greater than that from a similar storm occurring later in the season. There would typically be no runoff associated with rainfall on the basin once streamflow had ceased, even in the case of very heavy storms. Therefore, the occurrence of summer runoff would have to be related to antecedent moisture conditions; and in this case, to the extent of the saturated phase in the basin.

4. Depression storage is a dominant factor in controlling runoff volumes from all soil phases; and, the mode of depression storage interaction with runoff is assumed to be micro-depression storage. Two magnitudes of depression storage were identified; micro and macro. The macro storage had been assumed by many researchers to exert a dominant control over the streamflow runoff on the prairies, and this is the case to some degree. However, macro depression storage is typical of closed drainage basins that do not interact with the stream channel network. Large depressions within a channel network would be destroyed as a major storage depression by erosion of the outlet. Most of the larger depressions are

low points that serve as the focal point of a closed drainage basin. The water level in these depressions would be a function of the evaporation rate, groundwater interaction (net influent or effluent) and the size of the closed basin. The analyses in Chapters 5 and 8 show that depression storage losses in every snowmelt runoff event are significant; and constant. This is inconsistent with the nature of major depressions, since they will have varied available storage, depending on groundwater interaction and seasonal evaporation. Therefore, the depression storage losses associated with snowmelt must be sufficiently small to be completely depleted before the next snowmelt. This depression storage has been termed micro depression storage here, and is defined as storage that is depleted in each year by evapotranspiration and percolation to the regional groundwater system. Therefore, the storage is always empty in the spring, and depression storage losses are always constant.

Appendix A

WP, SWE and θ_p Spatial Fields for Ribstone Creek, 1968-80

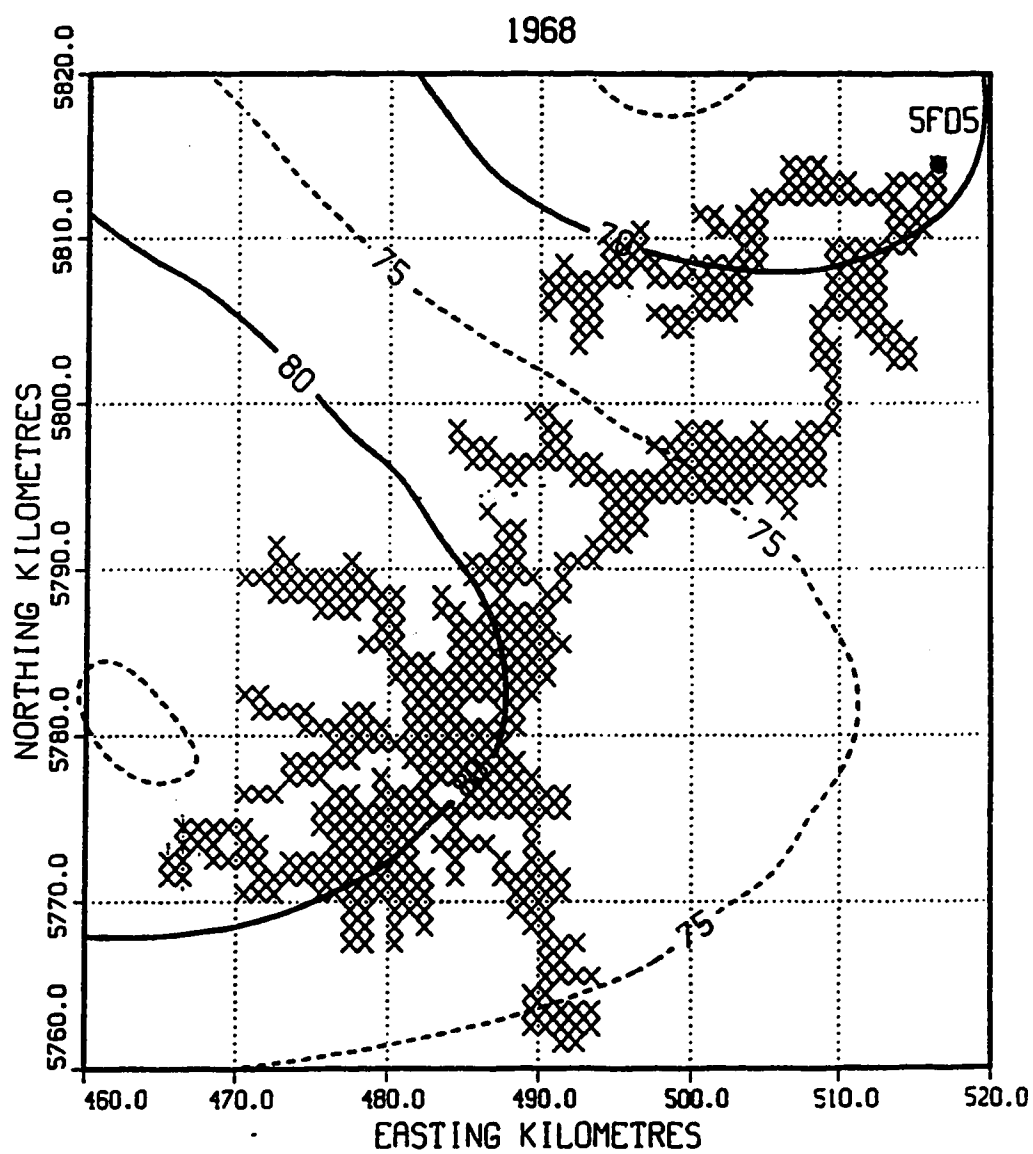


Figure A-1: 1968 WP spatial field in mm H₂O equivalent.

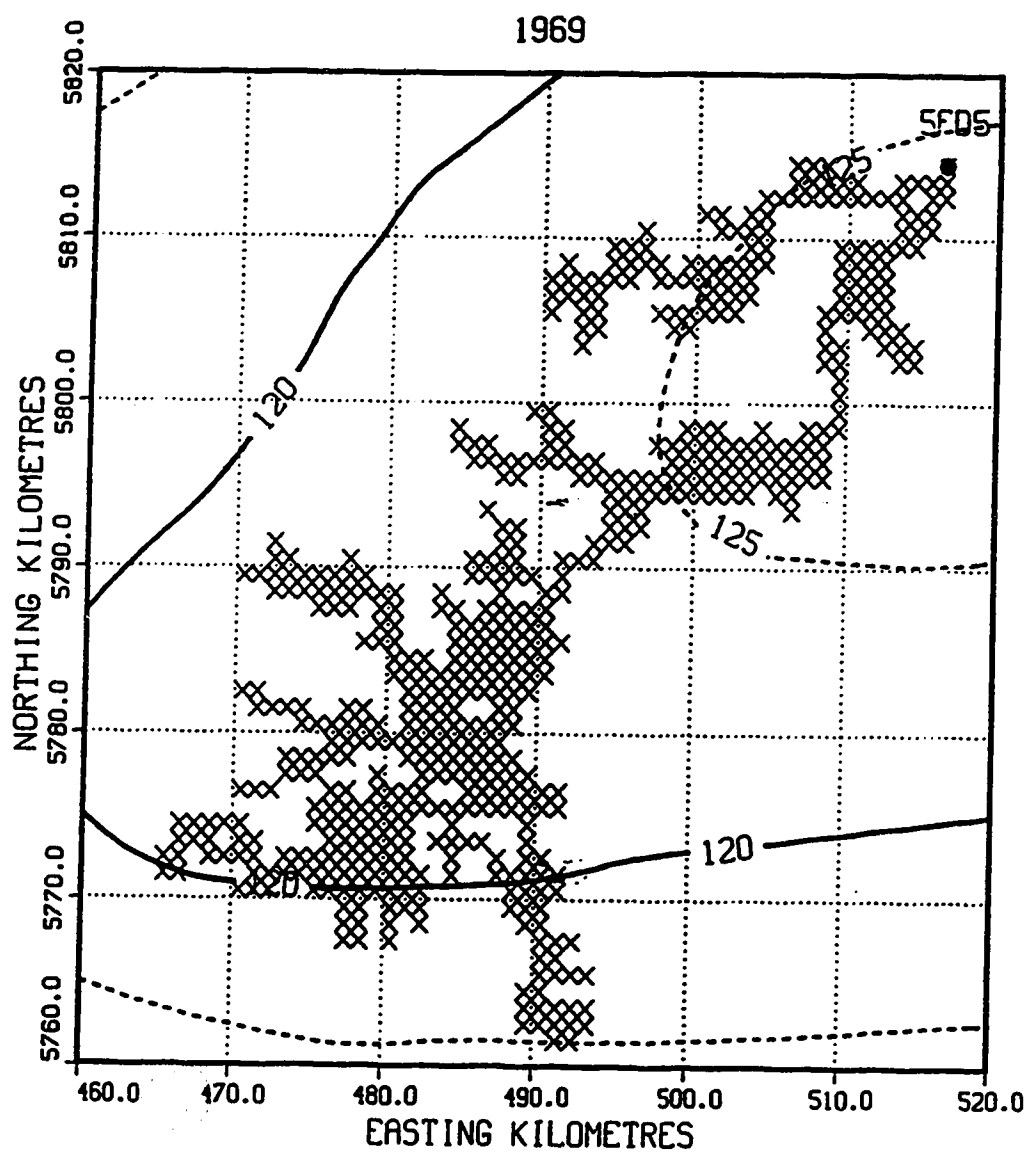


Figure A-2: 1969 WP spatial field in mm H₂O equivalent.

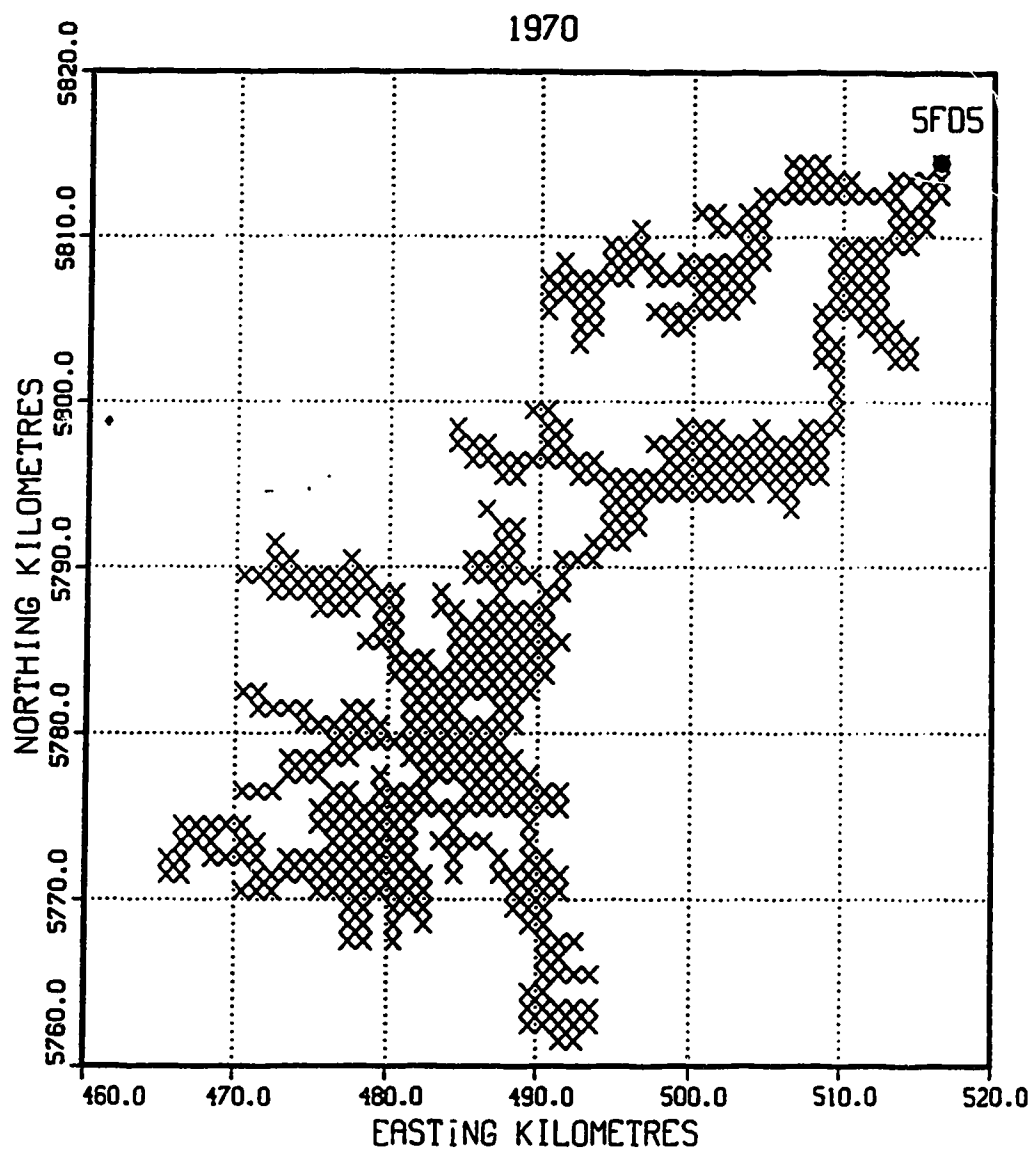


Figure A-3: 1970 WP spatial field in mm H₂O equivalent.

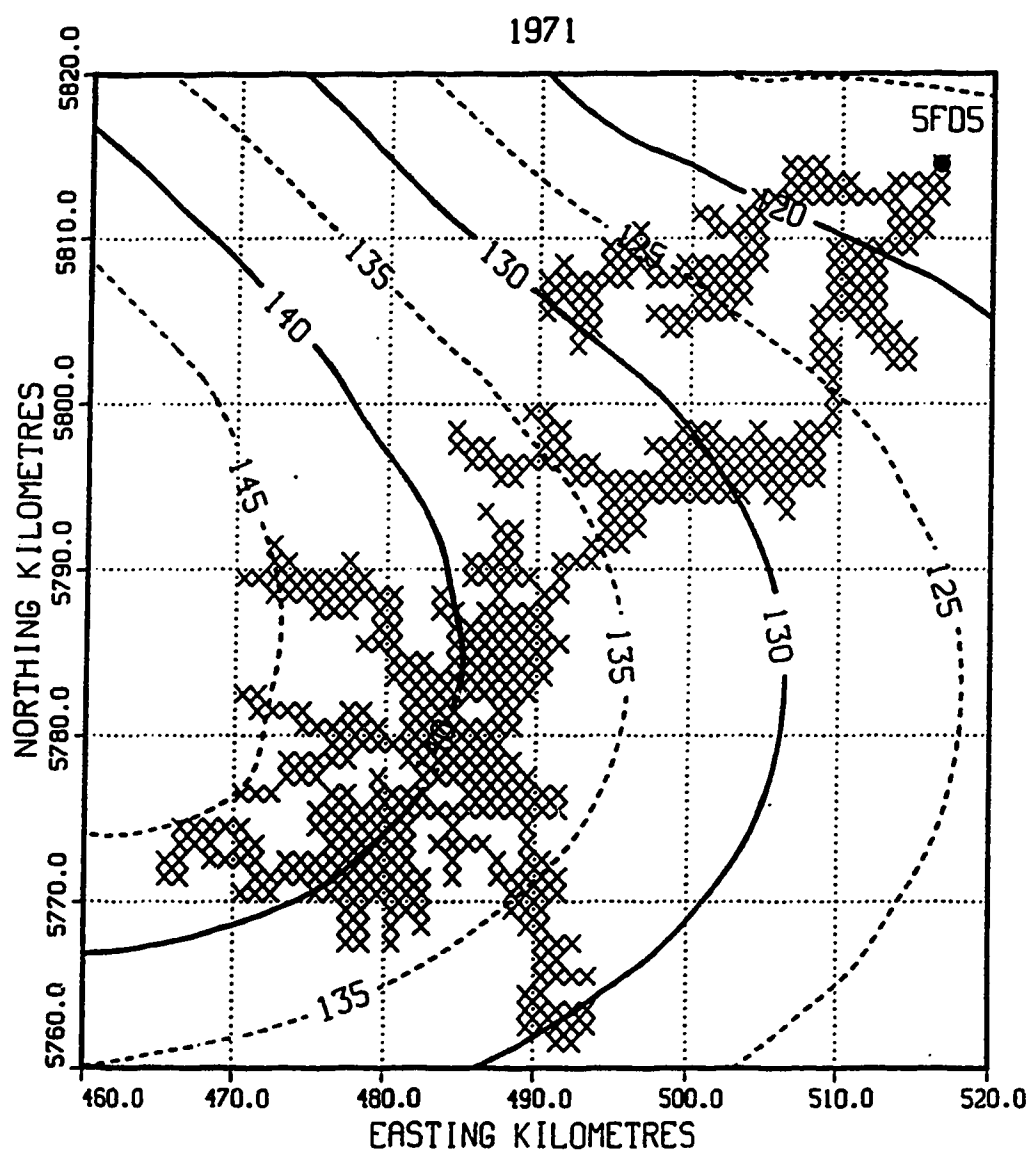


Figure A-4: 1971 WP spatial field in mm H₂O equivalent.

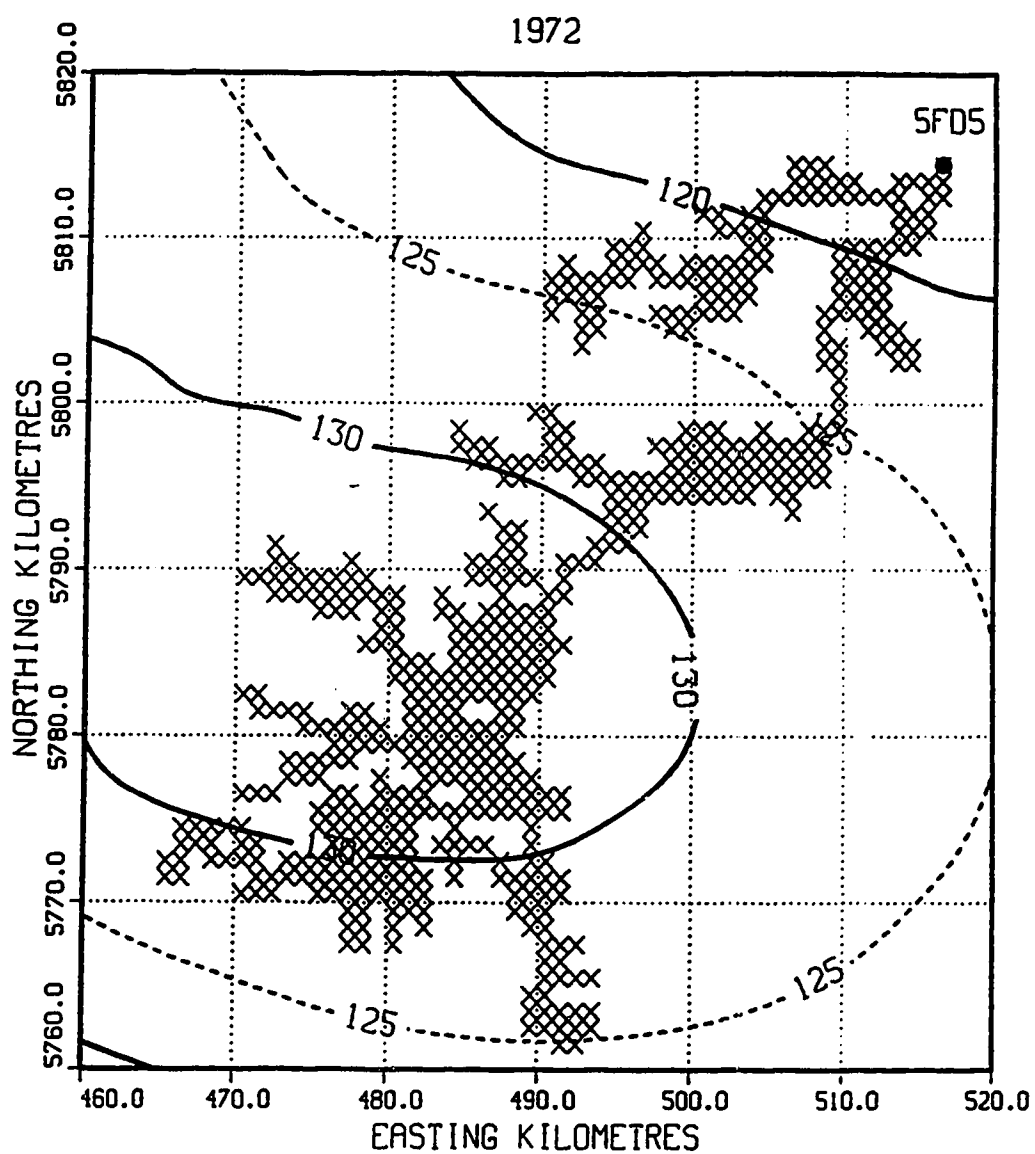


Figure A-5: 1972 WP spatial field in mm H₂O equivalent.

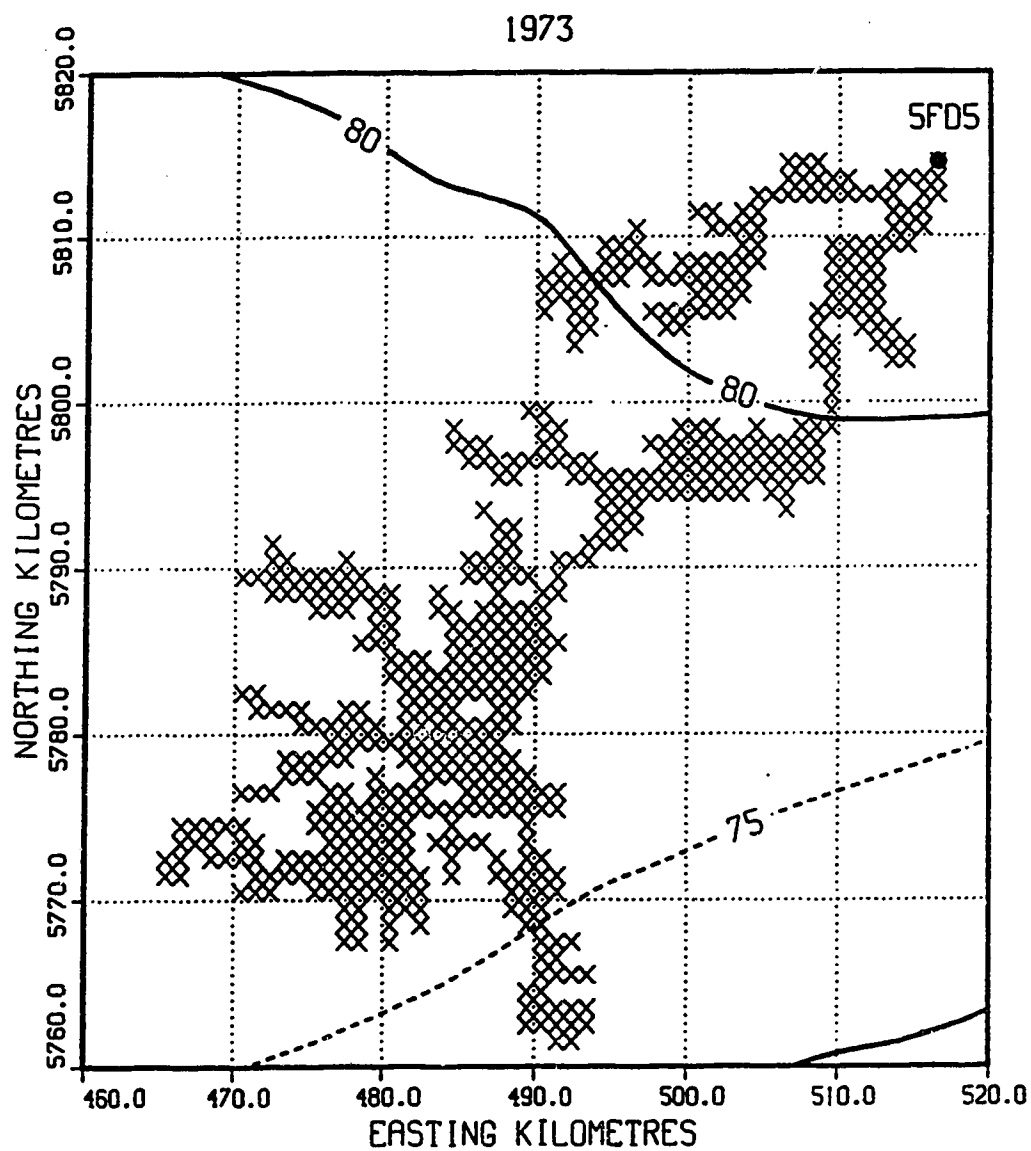


Figure A-6: 1973 WP spatial field in mm H₂O equivalent.

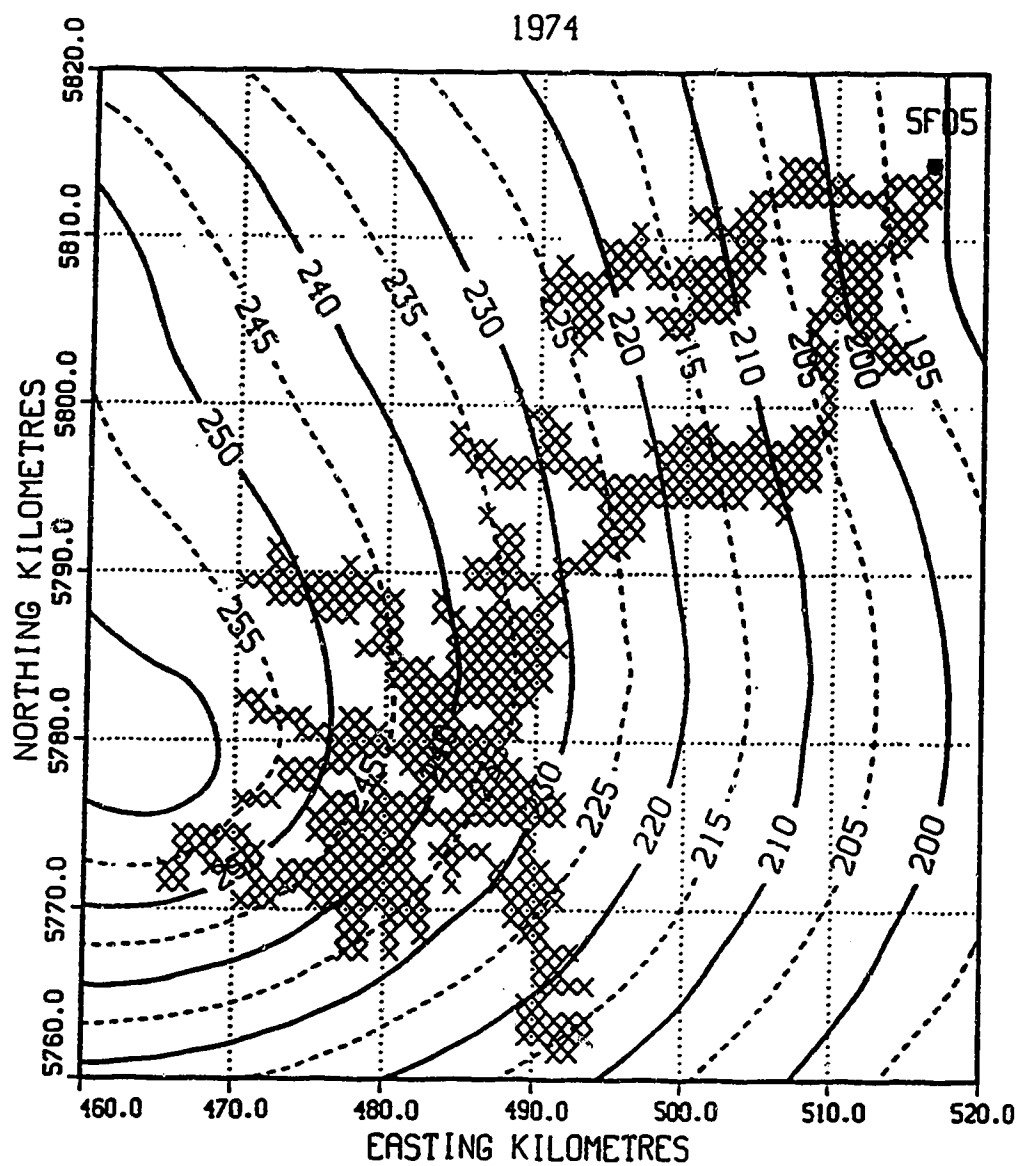


Figure A-7: 1974 WP spatial field in mm H₂O equivalent.

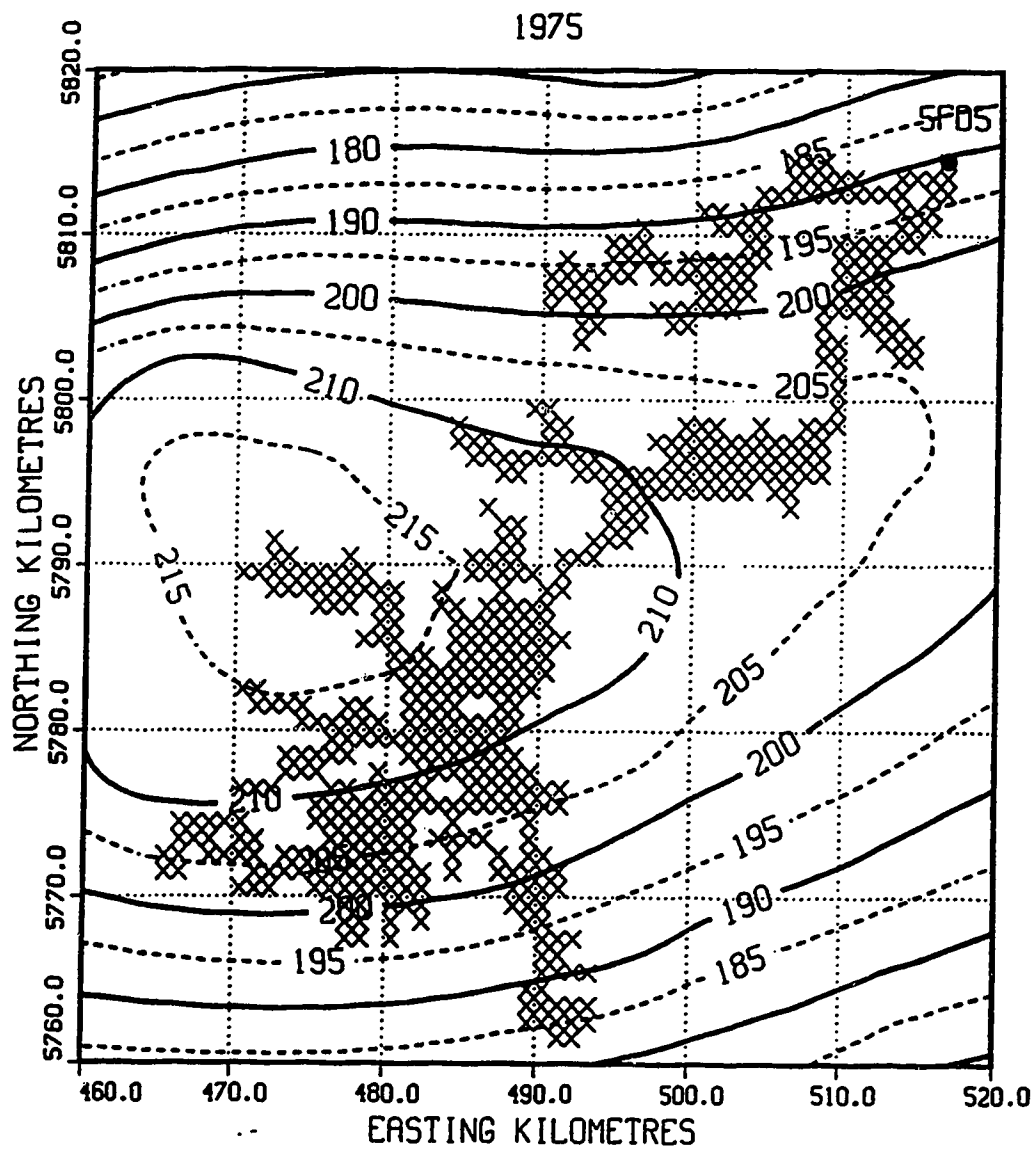


Figure A-8: 1975 WP spatial field in mm H₂O equivalent.

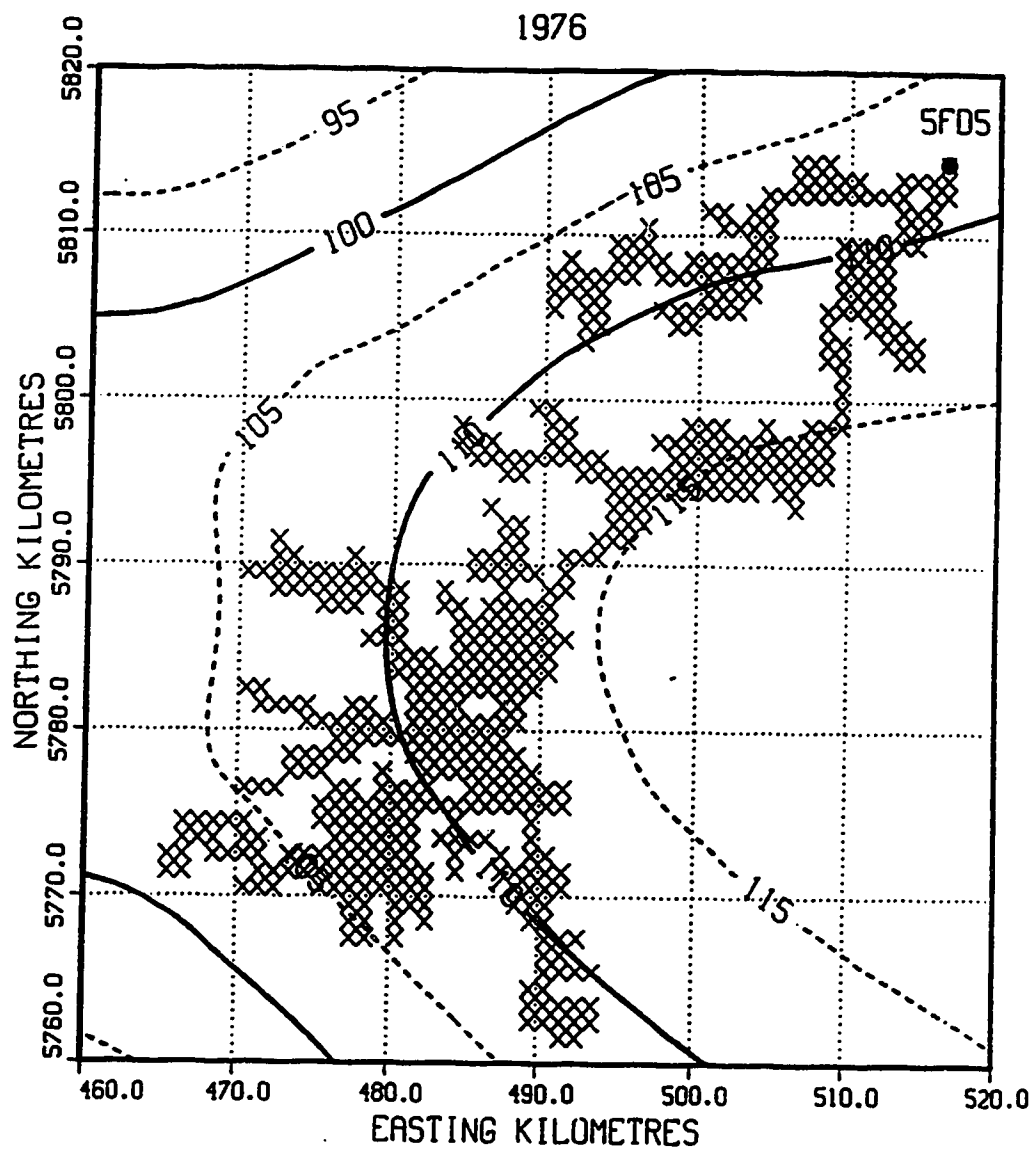


Figure A-9: 1976 WP spatial field in mm H₂O equivalent.

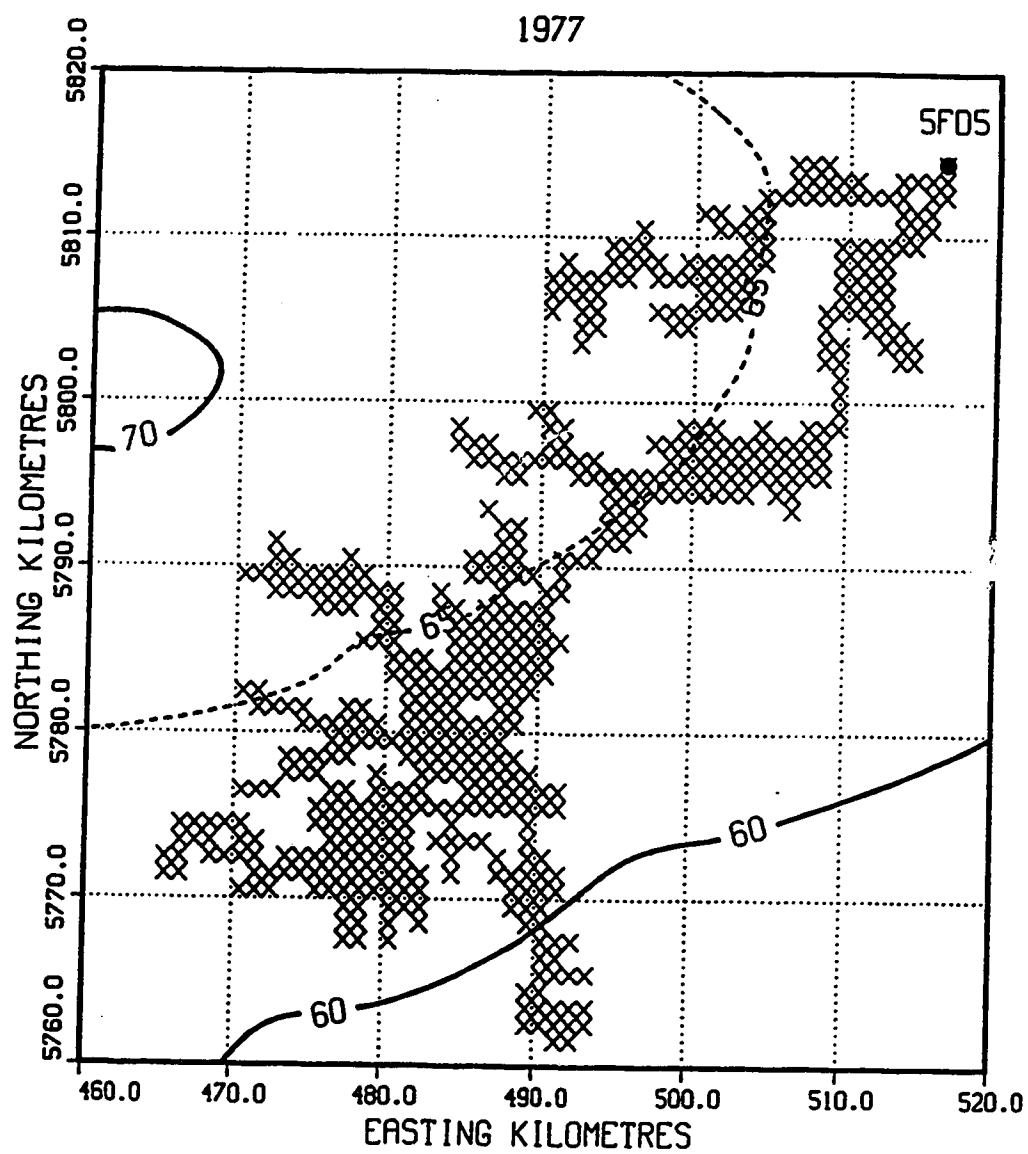


Figure A-10: 1977 WP spatial field in mm H₂O equivalent.

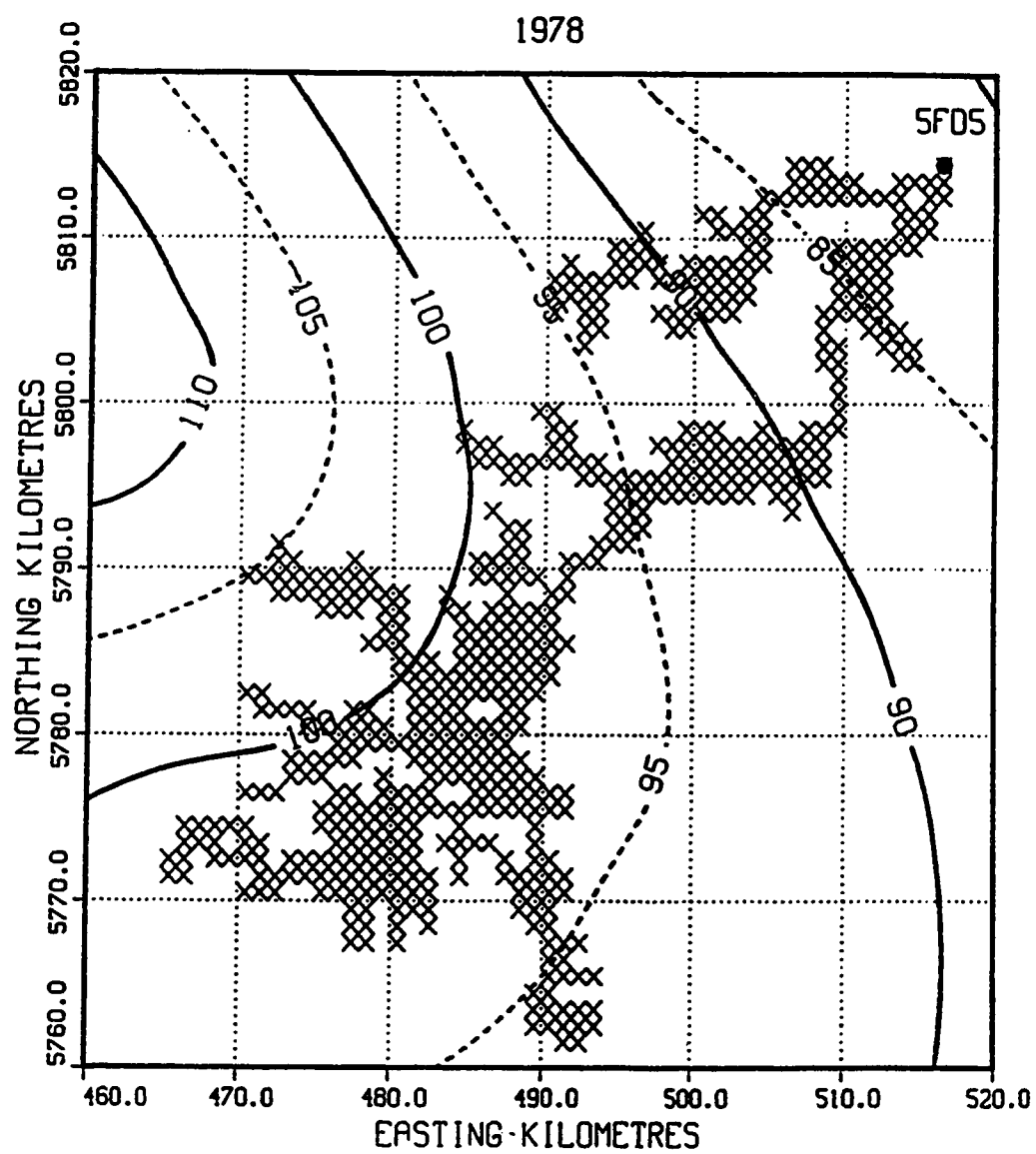


Figure A-11: 1978 WP spatial field in mm H₂O equivalent.

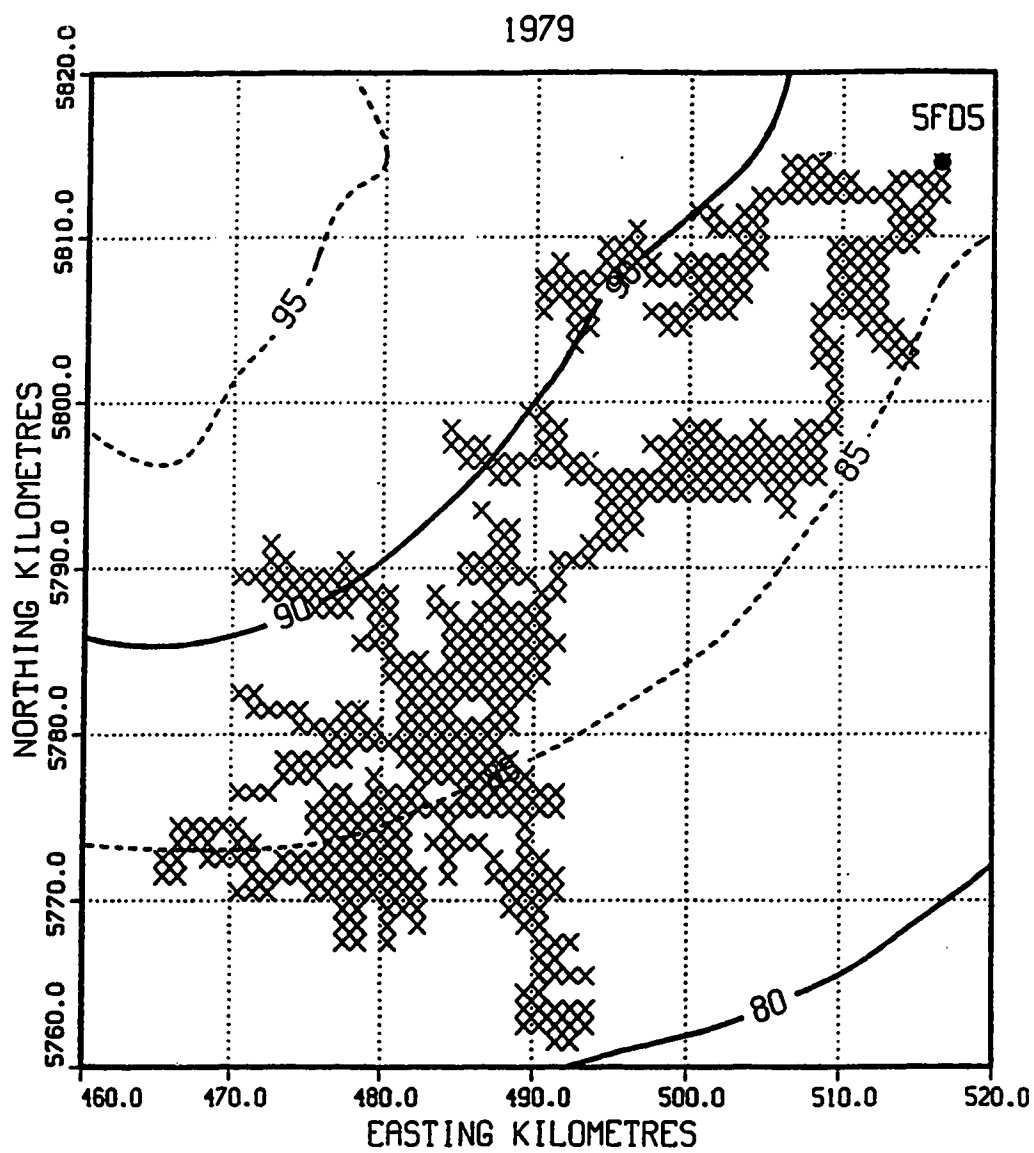


Figure A-12: 1979 WP spatial field in mm H₂O equivalent.

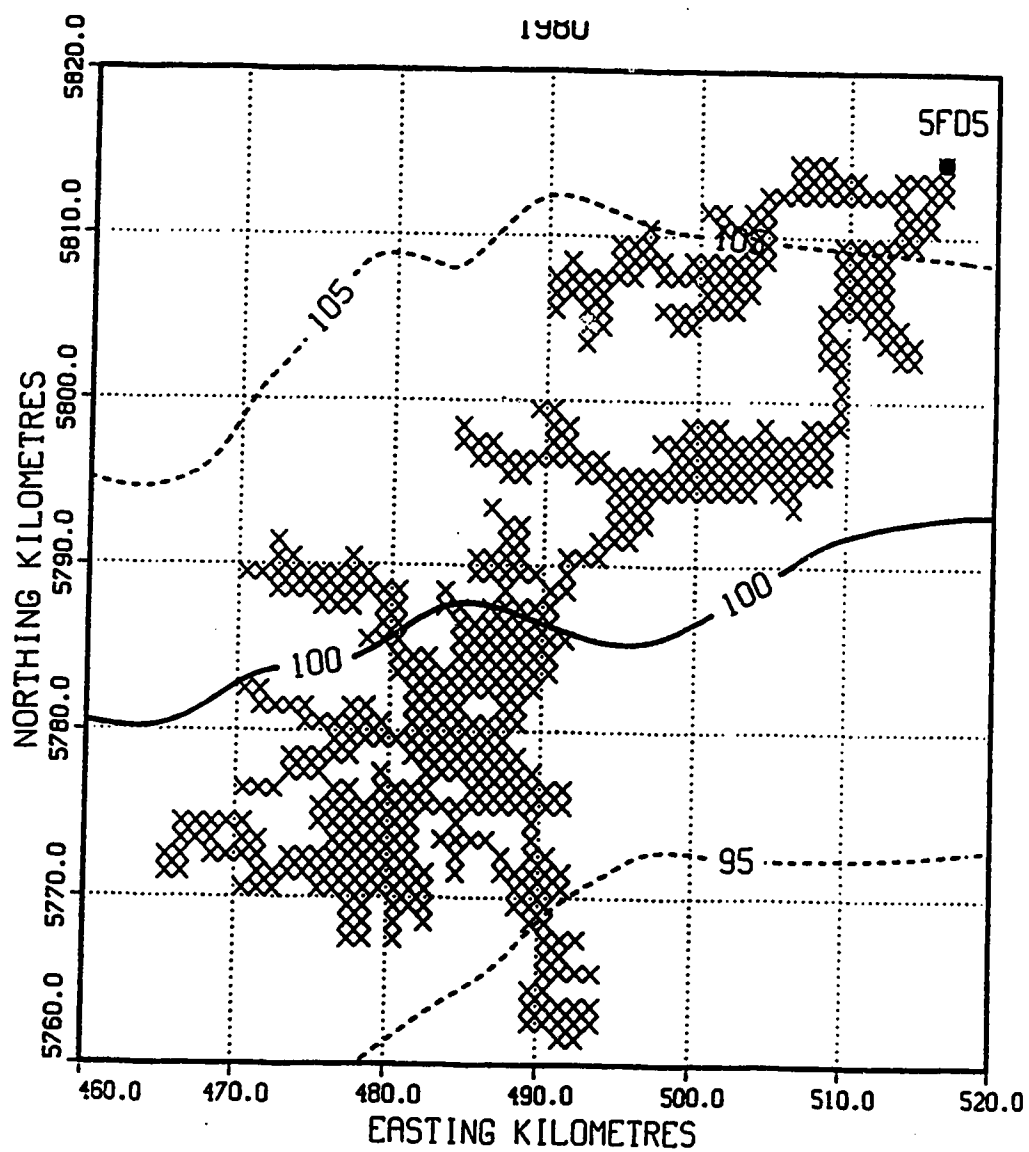


Figure A-13: 1980 WP spatial field in mm H₂O equivalent.

WINTER PRECIP. - ET
RIBSTONE CREEK NEAR CZAR

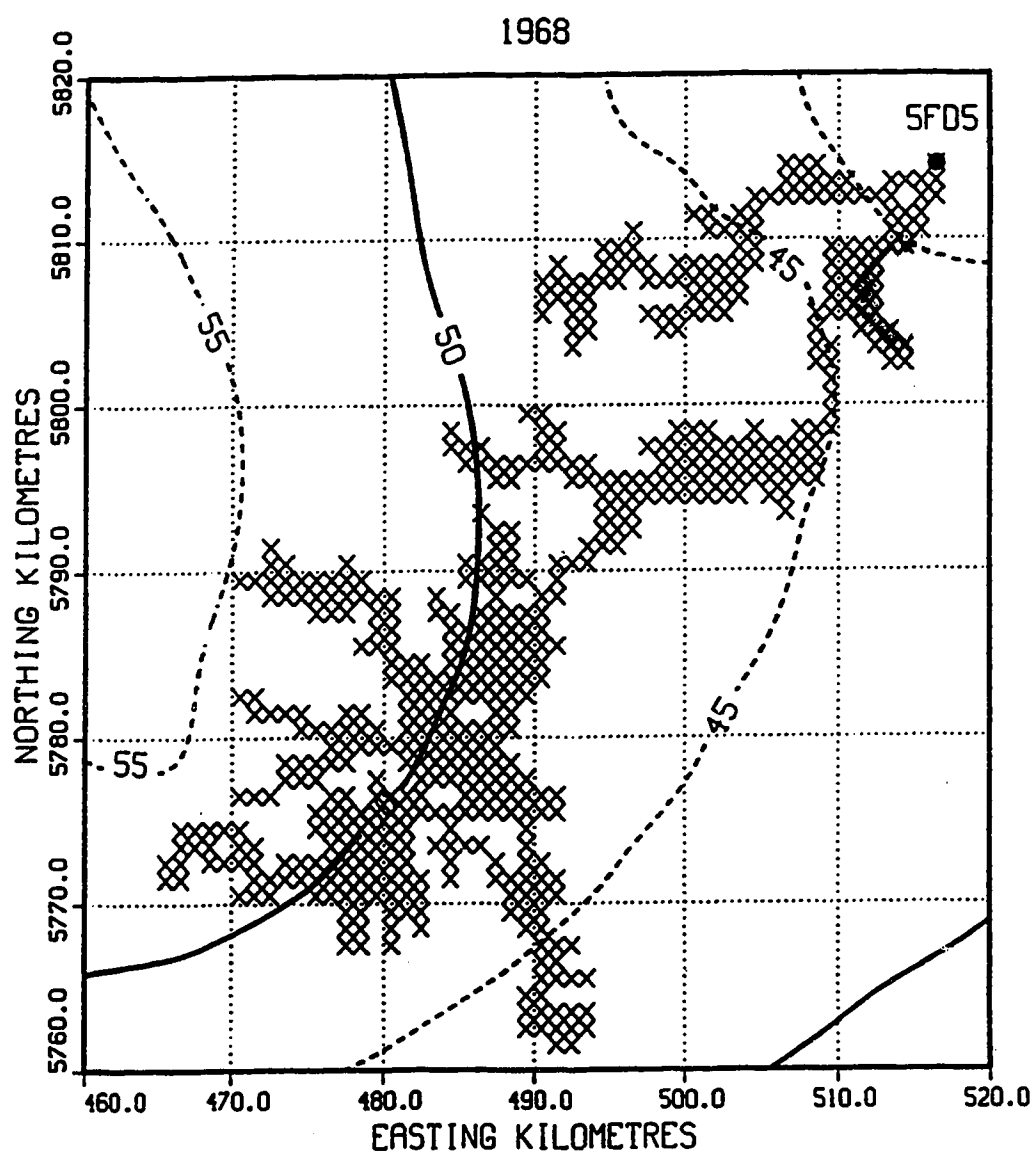


Figure A-14: 1968 SWE spatial field in mm H₂O equivalent.

WINTER PRECIP. - ET
RIBSTONE CREEK NEAR CZAR

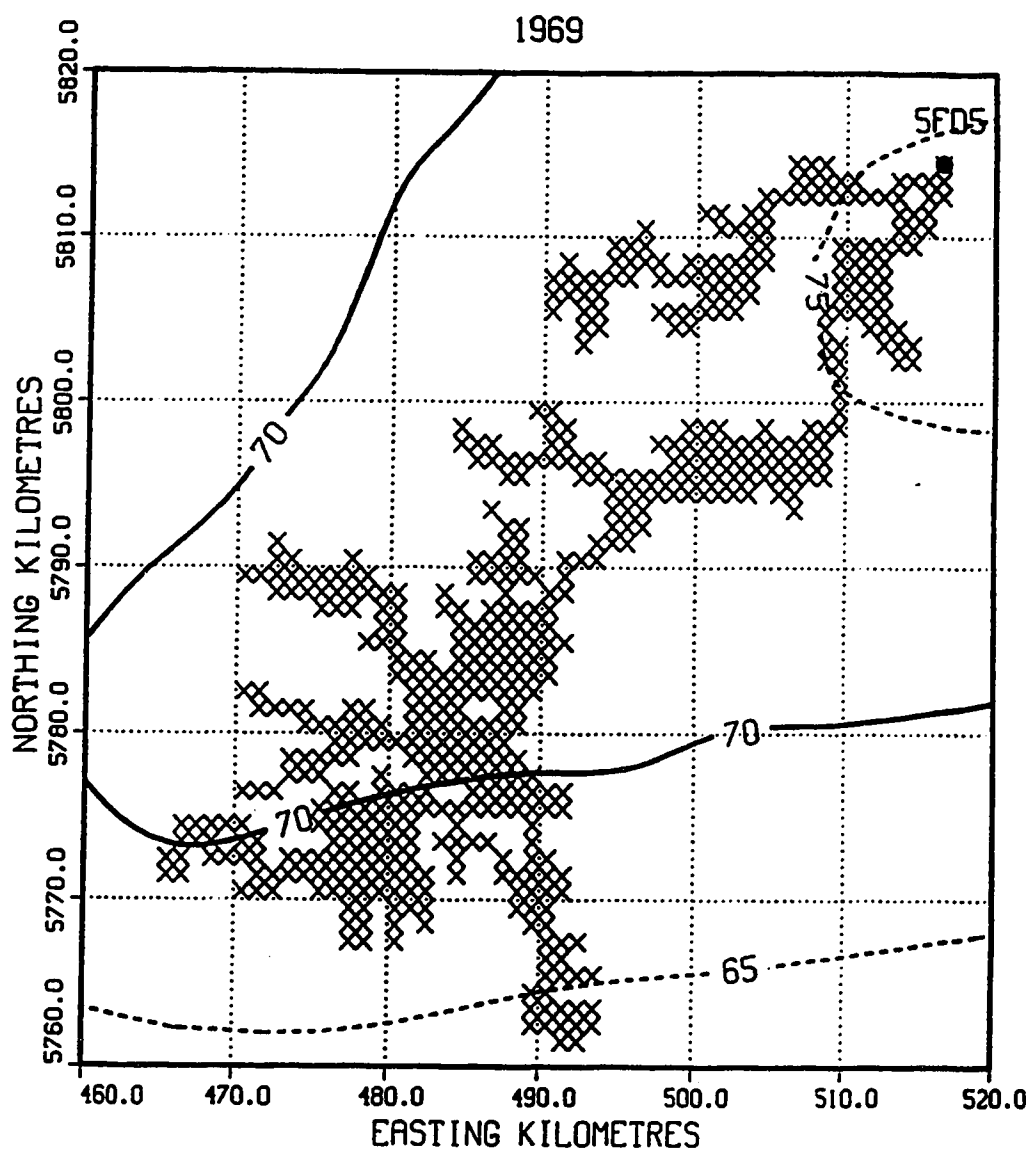


Figure A-15: 1969 SWE spatial field in mm H₂O equivalent.

WINTER PRECIP. - ET
RIBSTONE CREEK NEAR CZAR

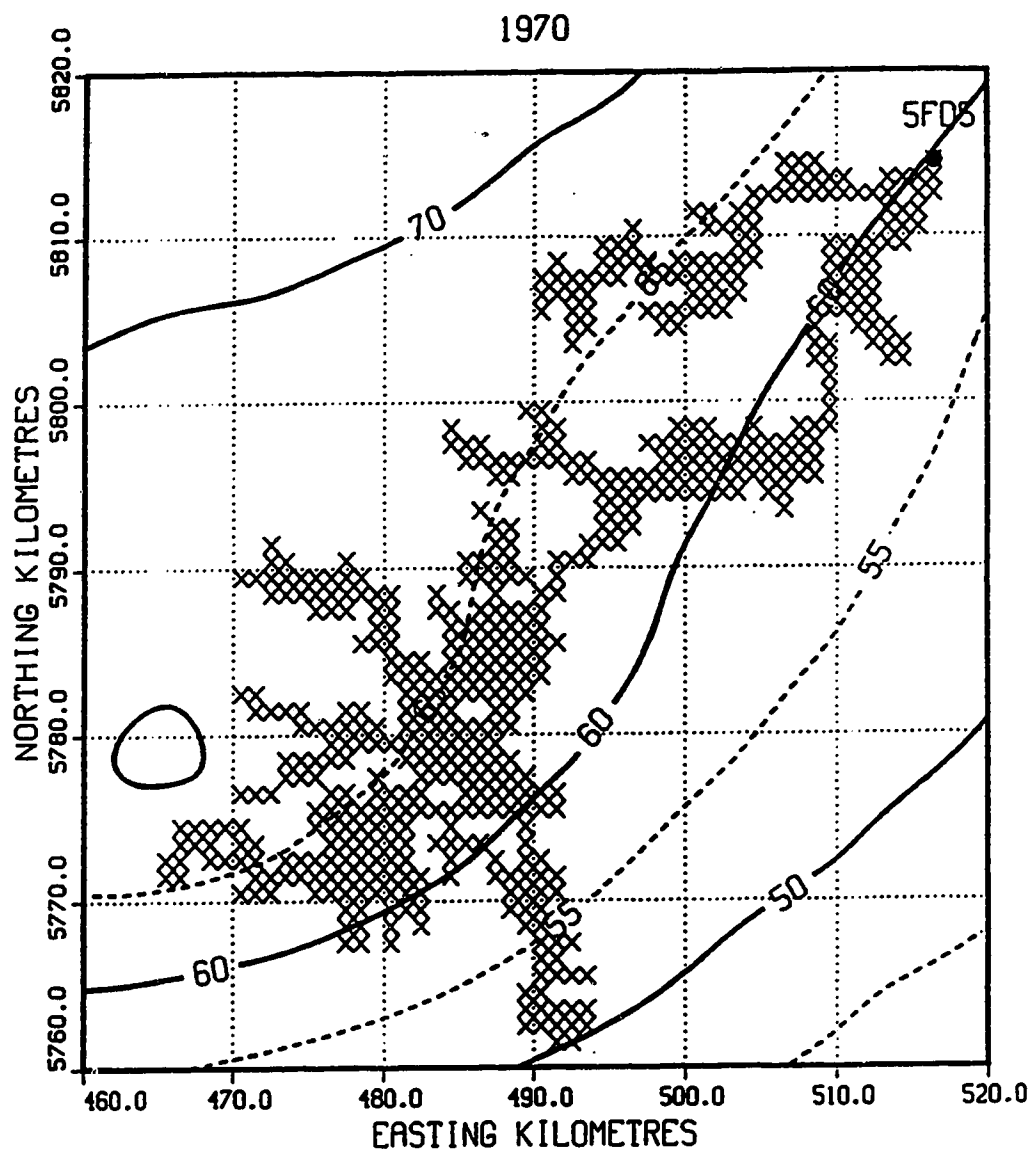


Figure A-16: 1970 SWE spatial field in mm H₂O equivalent.

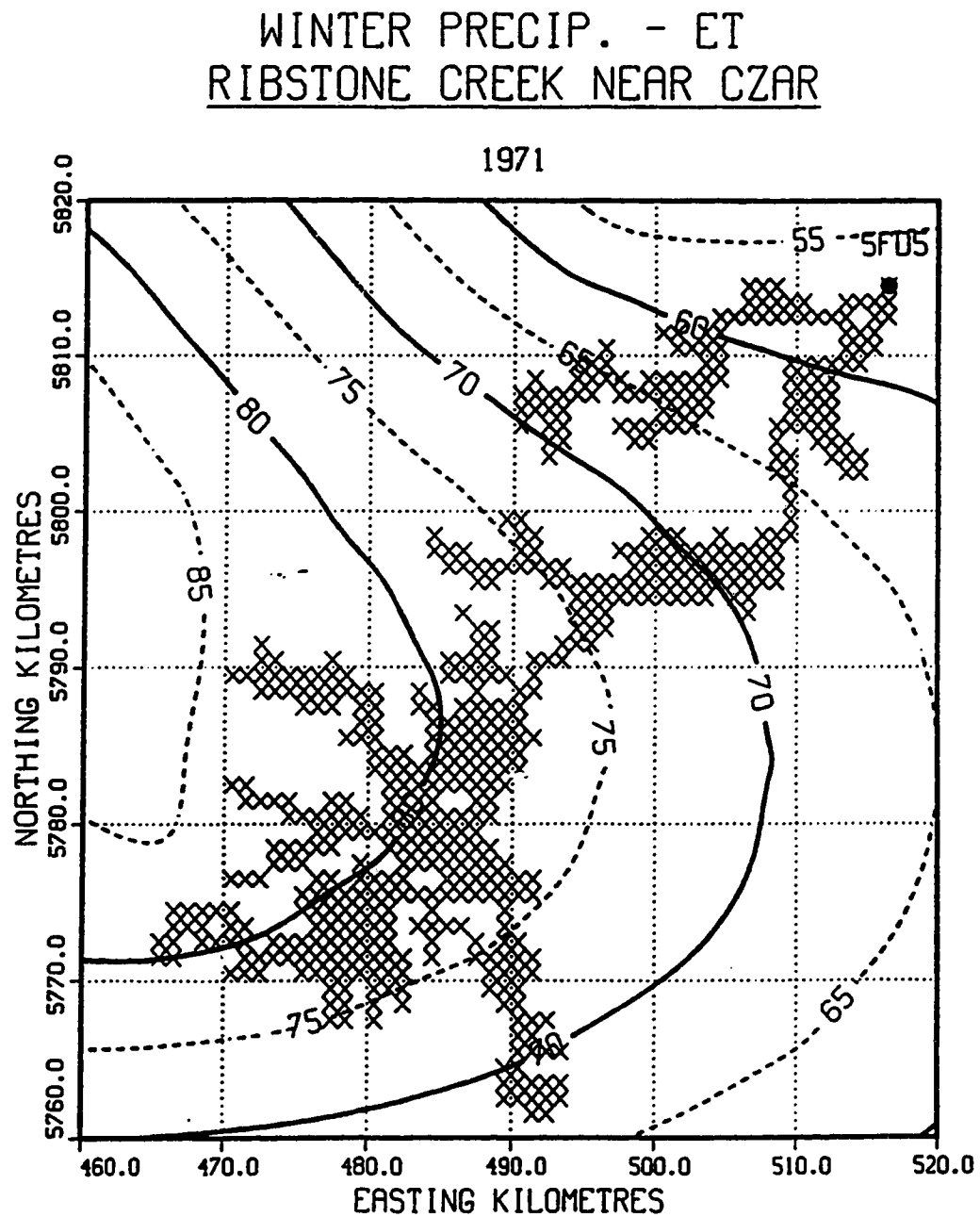


Figure A-17: 1971 SWE spatial field in mm H₂O equivalent.

WINTER PRECIP. - ET
RIBSTONE CREEK NEAR CZAR

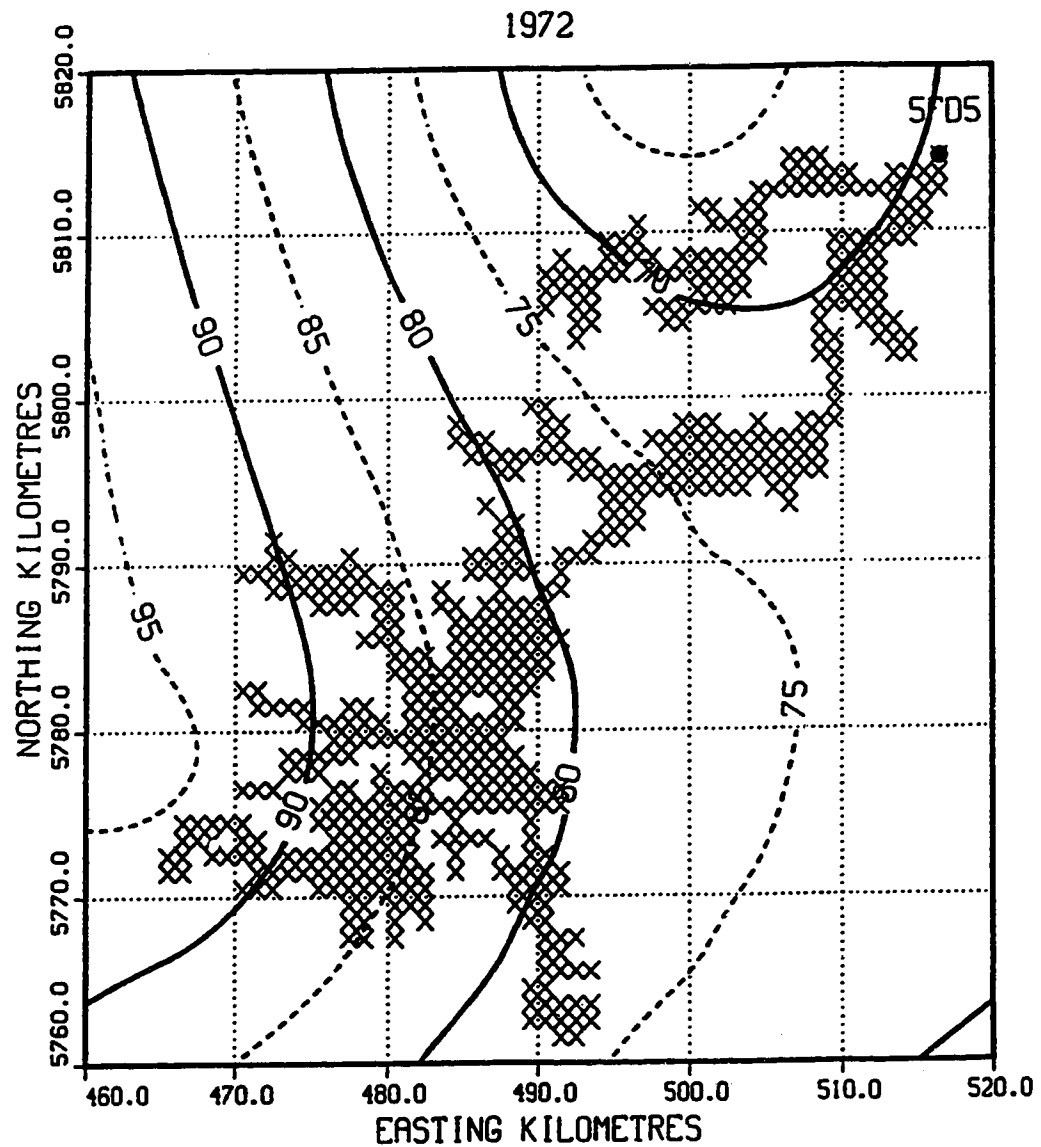


Figure A-18: 1972 SWE spatial field in mm H₂O equivalent.

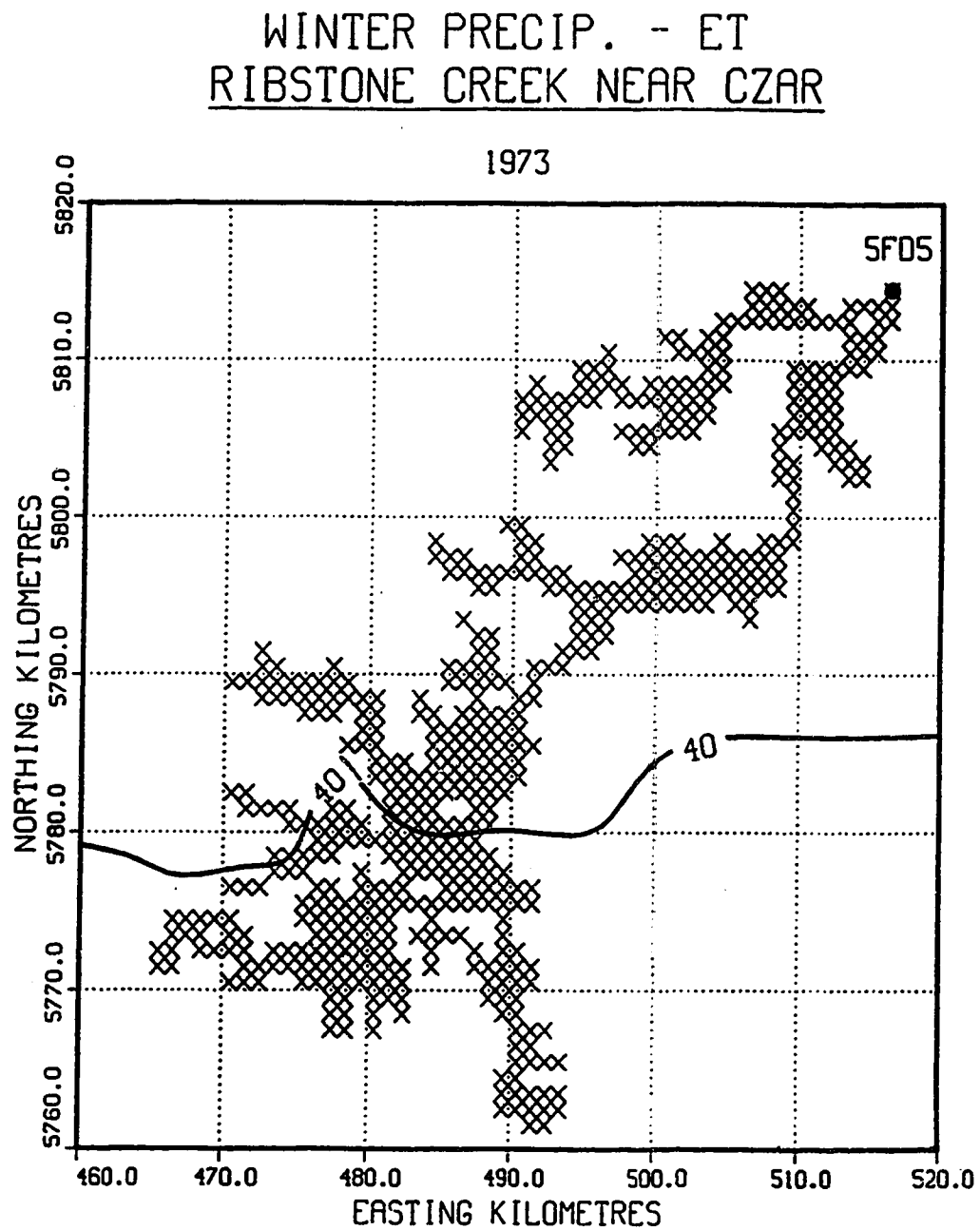


Figure A-19: 1973 SWE spatial field in mm H₂O equivalent.

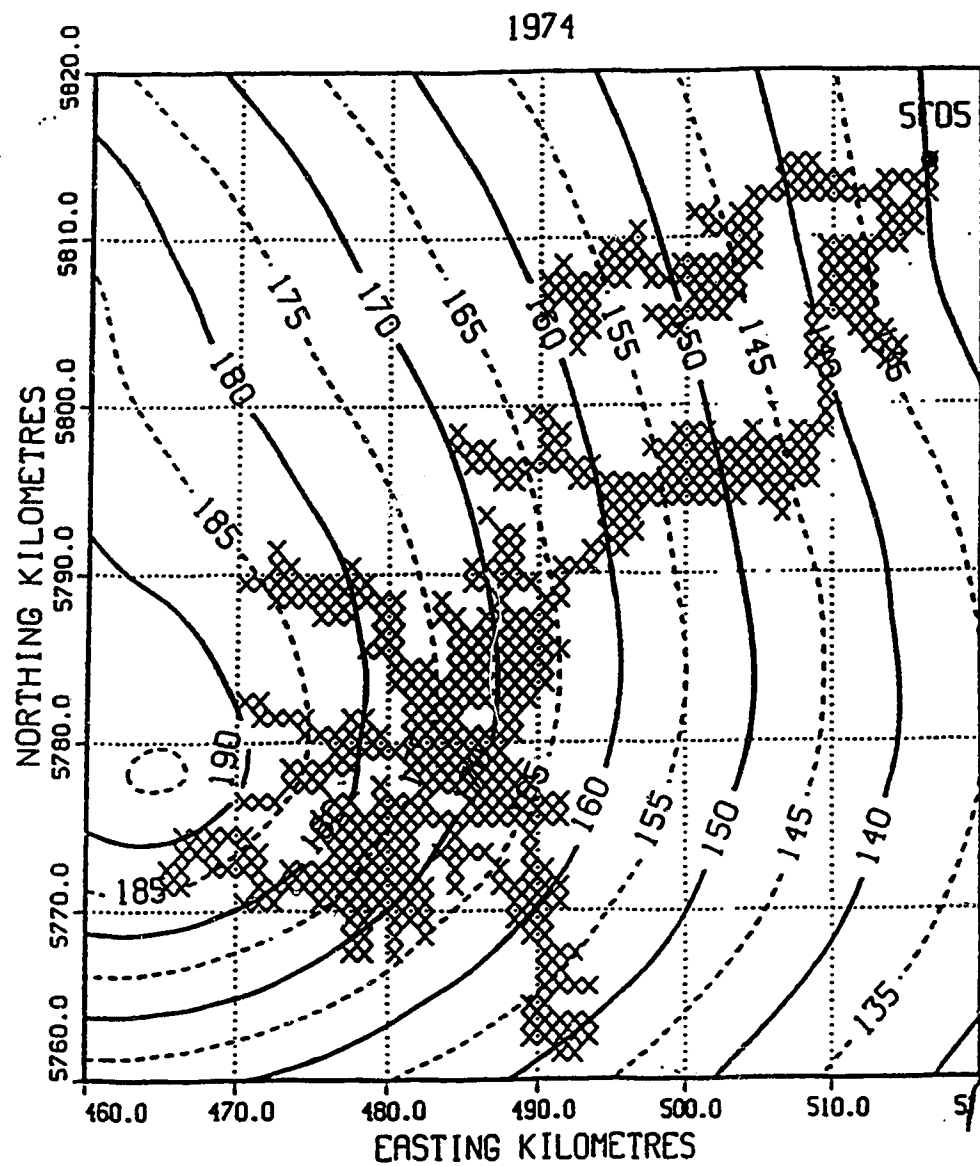


Figure A-20: 1974 SWE spatial field in mm H₂O equivalent.

WINTER PRECIP. - ET
RIBSTONE CREEK NEAR CZAR

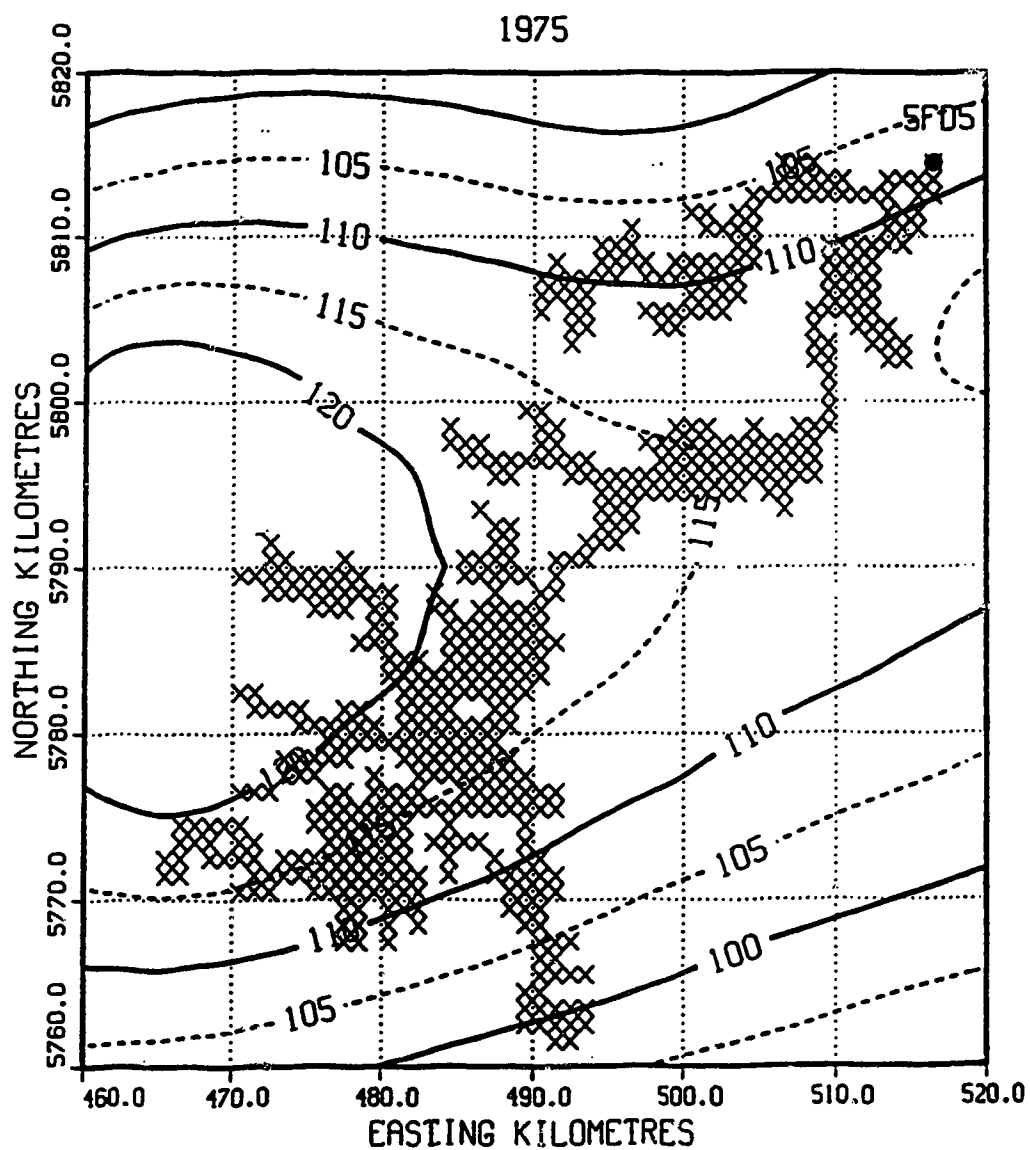


Figure A-21: 1975 SWE spatial field in mm H₂O equivalent.

WINTER PRECIP. - ET
RIBSTONE CREEK NEAR CZAR

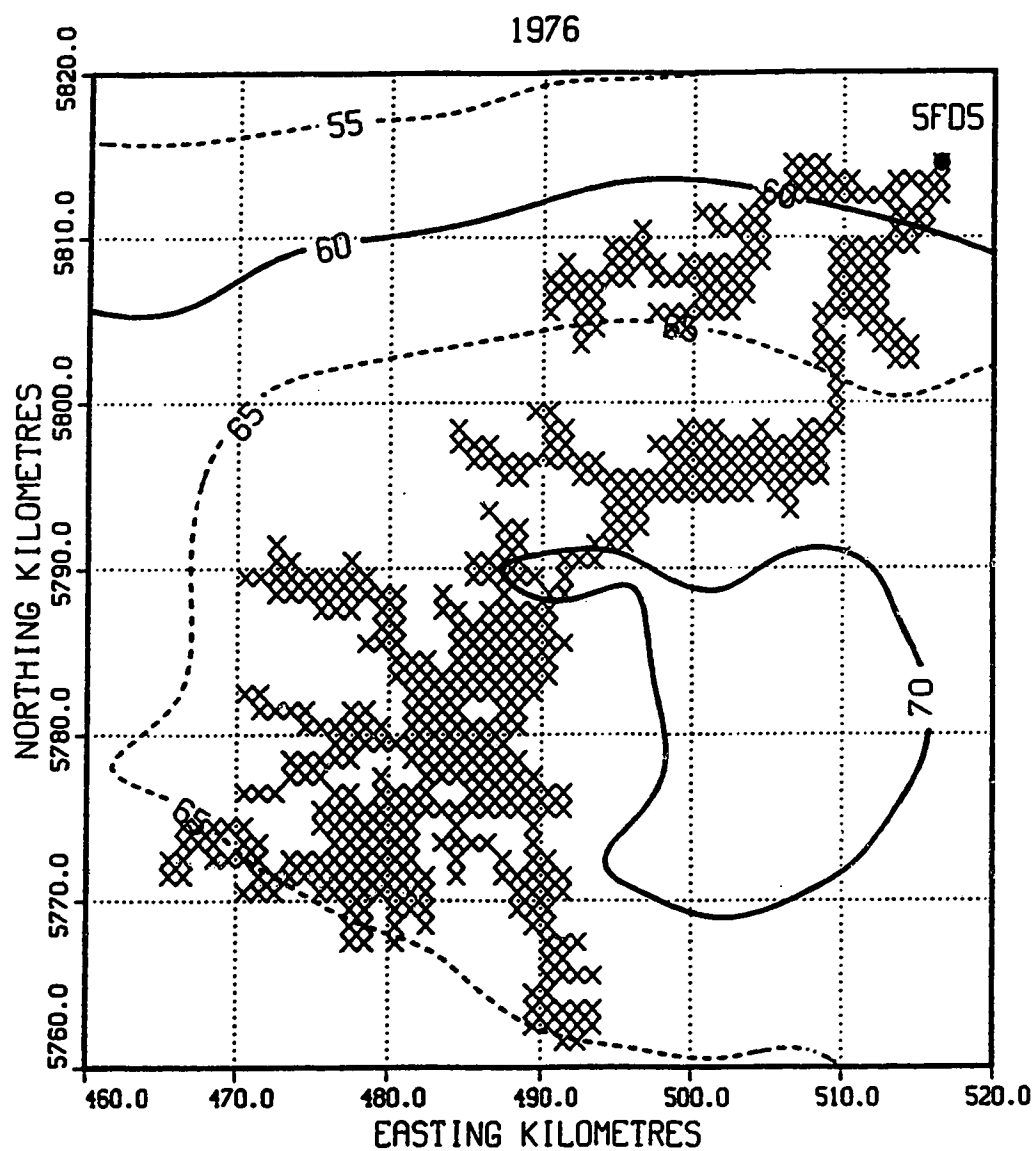


Figure A-22: 1976 SWE spatial field in mm H₂O equivalent.

WINTER PRECIP. - ET
RIBSTONE CREEK NEAR CZAR

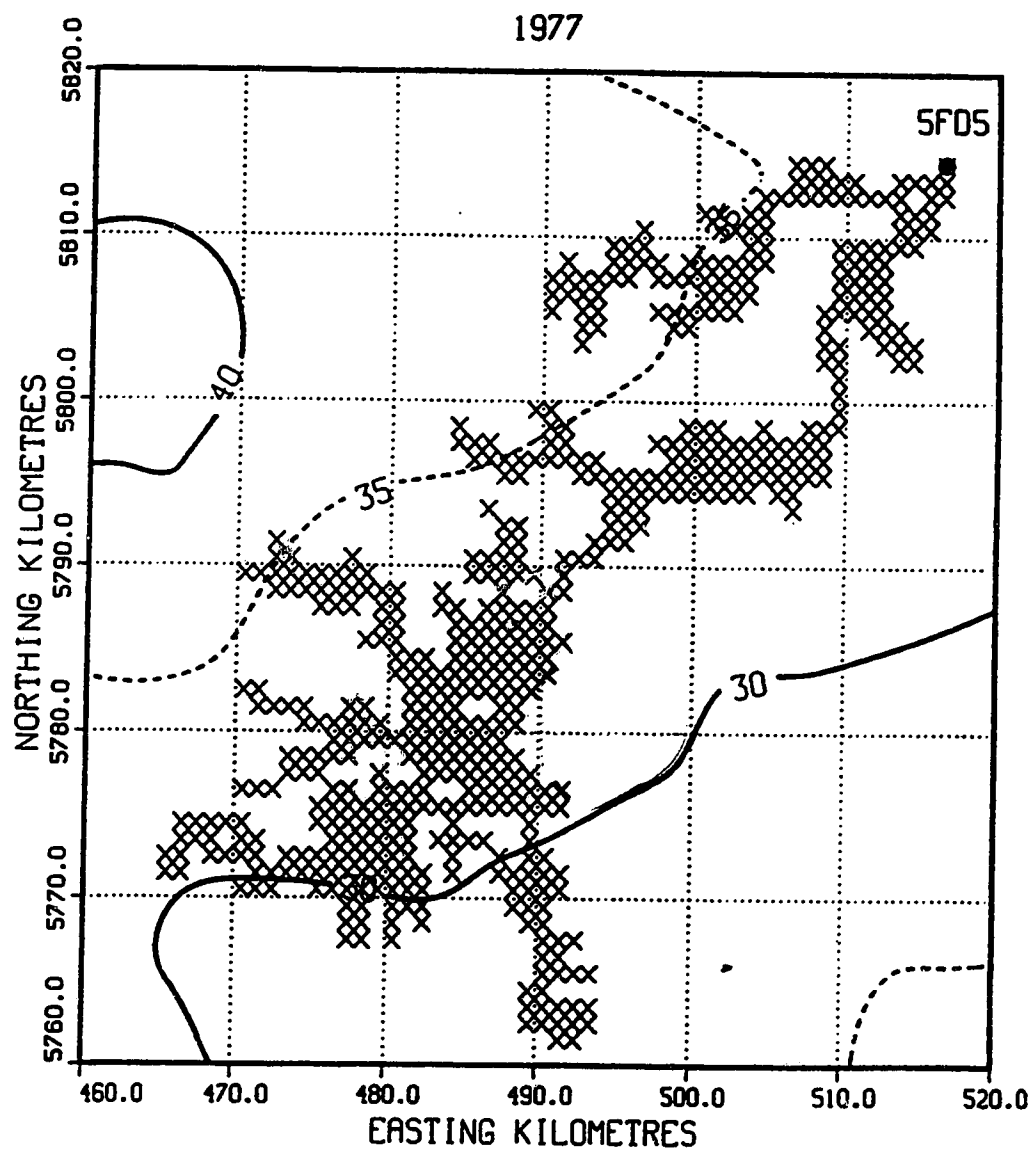


Figure A-23: 1977 SWE spatial field in mm H₂O equivalent.

WINTER PRECIP. - ET
RIBSTONE CREEK NEAR CZAR

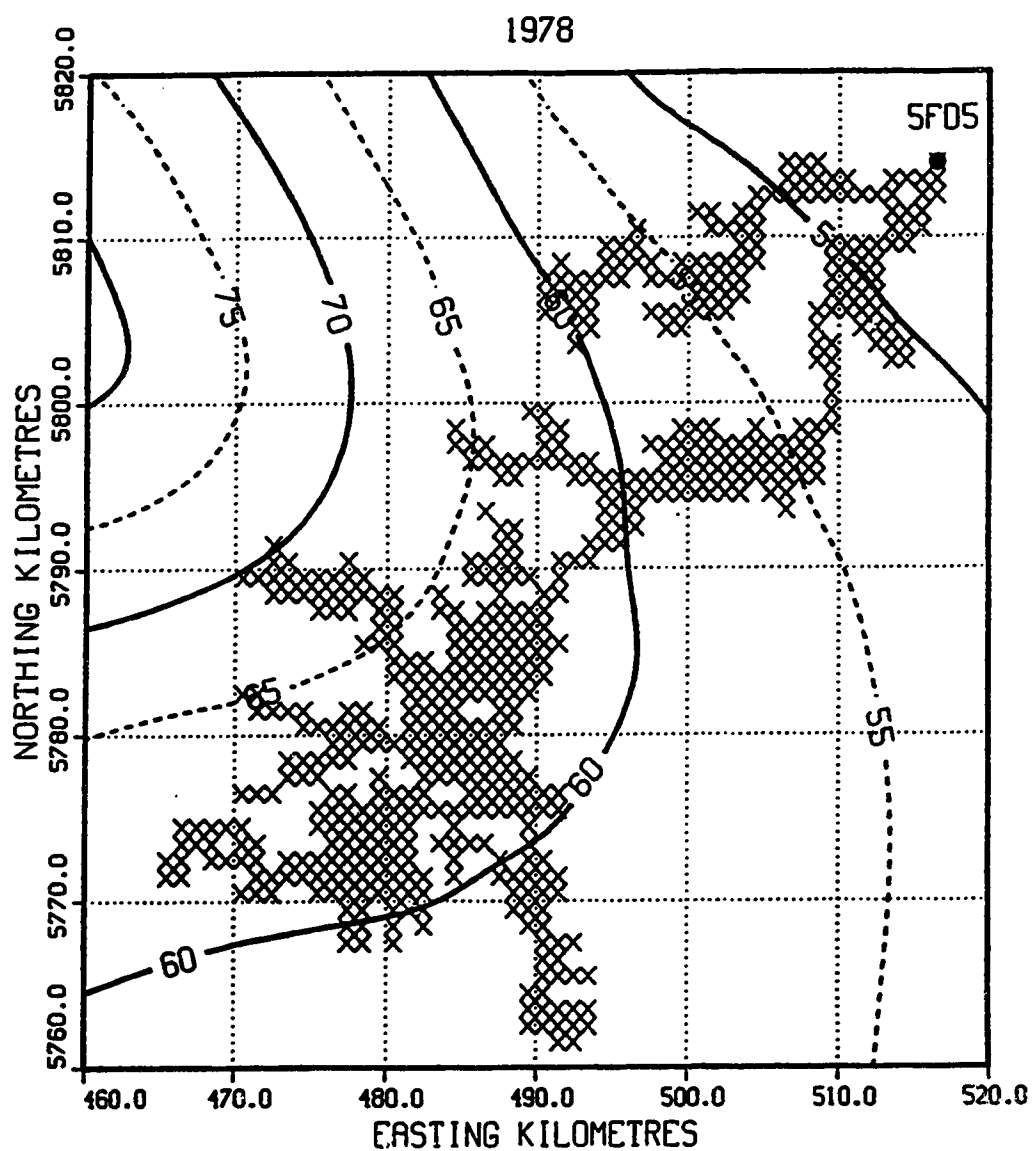


Figure A-24: 1978 SWE spatial field in mm H₂O equivalent.

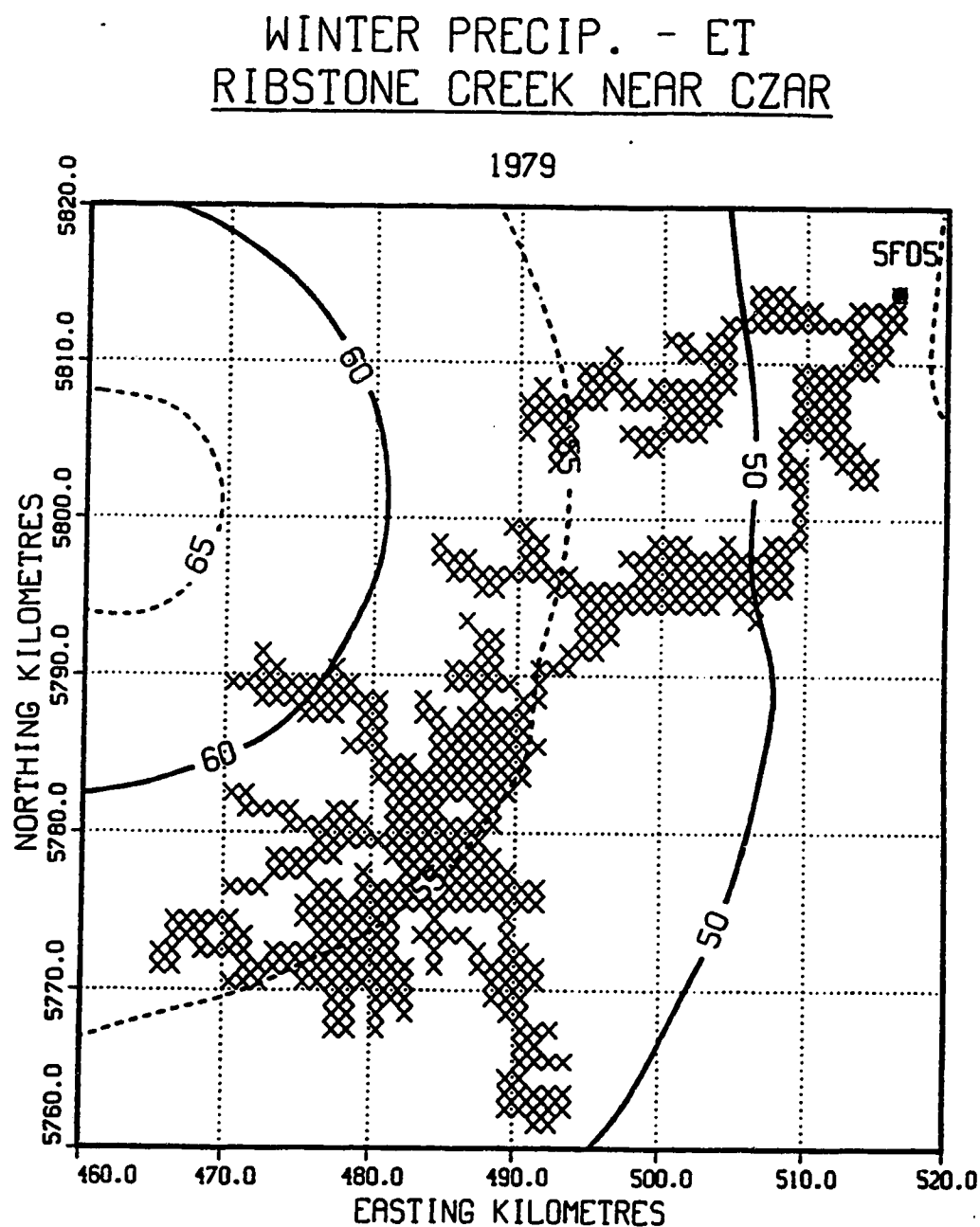


Figure A-25: 1979 SWE spatial field in mm H₂O equivalent.

WINTER PRECIP. - ET
RIBSTONE CREEK NEAR CZAR

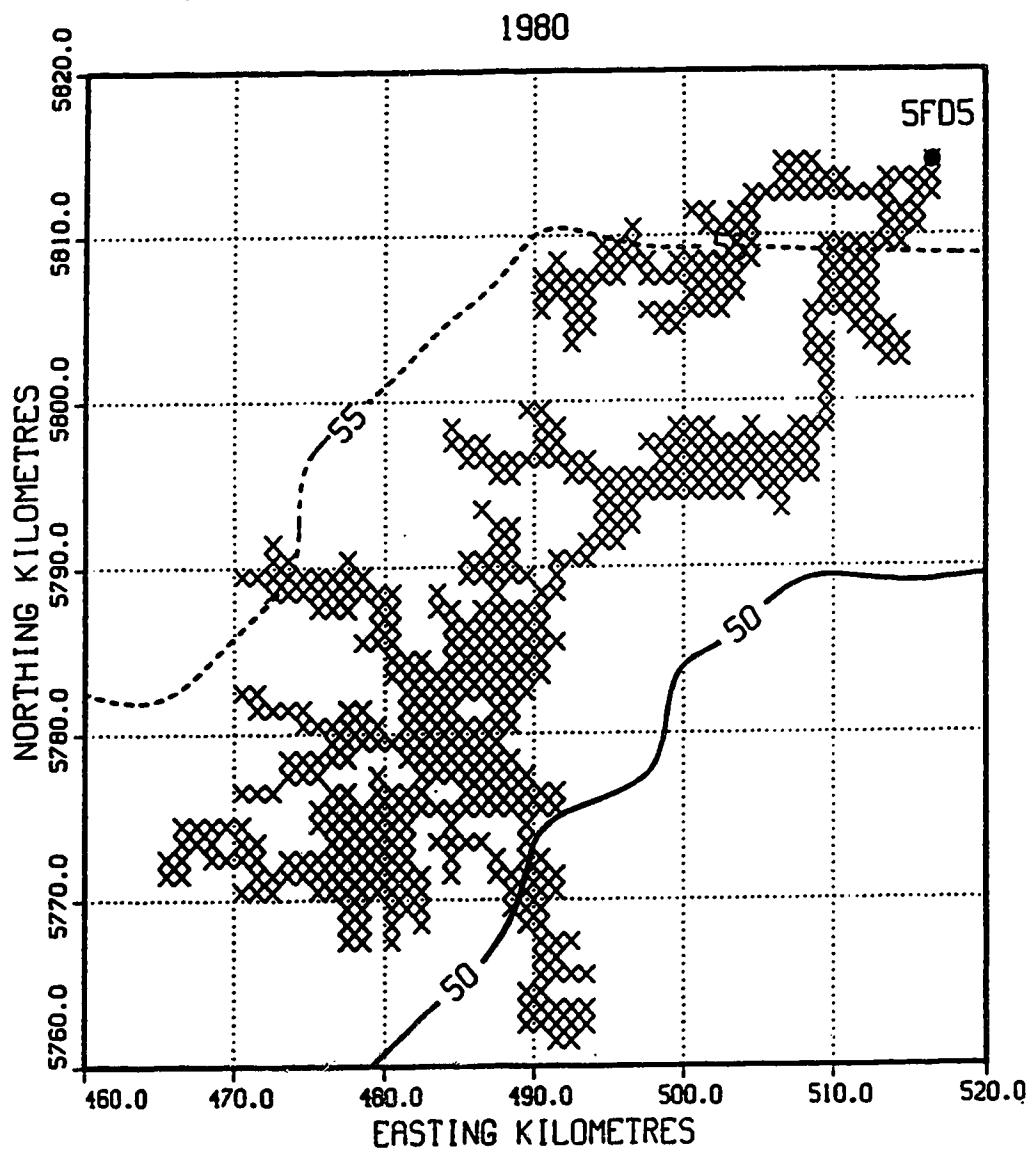


Figure A-26: 1980 SWE spatial field in mm H₂O equivalent.

THETA % - RIBSTONE CREEK

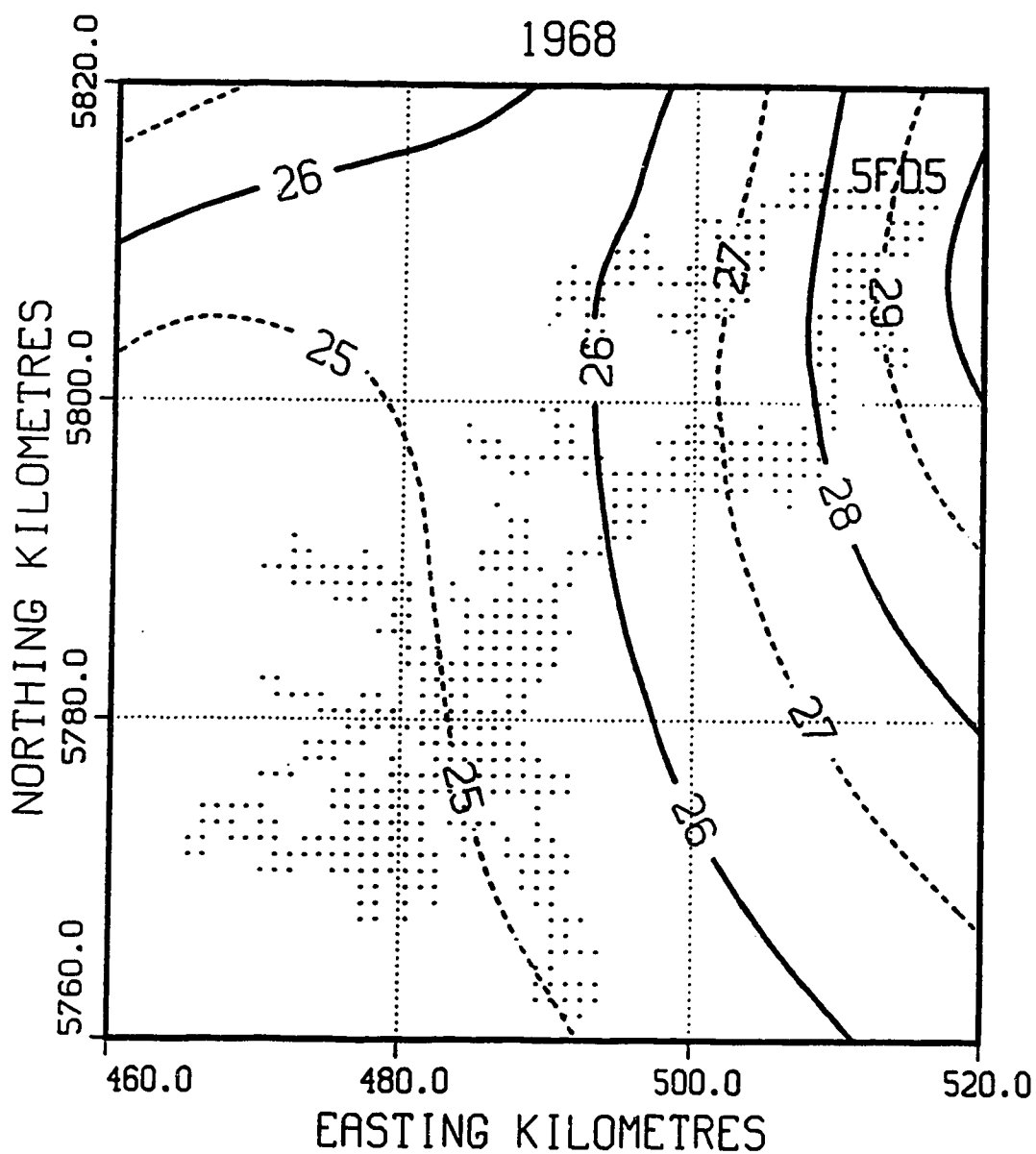


Figure A-27: 1968 θ_p spatial field in mm H₂O equivalent.

THETA % - RIBSTONE CREEK

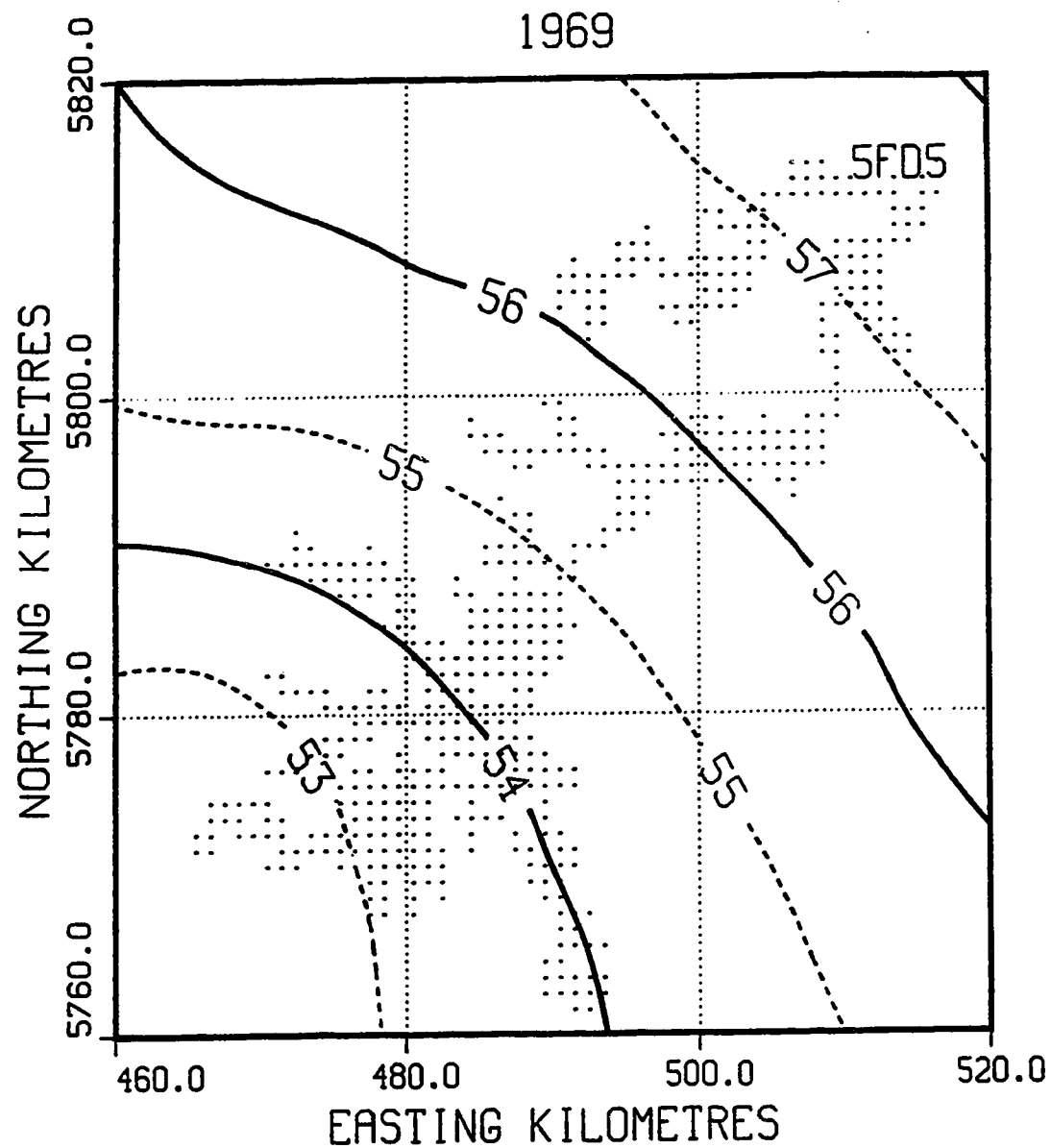


Figure A-28: 1969 θ_p spatial field in mm H₂O equivalent.

THETA % - RIBSTONE CREEK

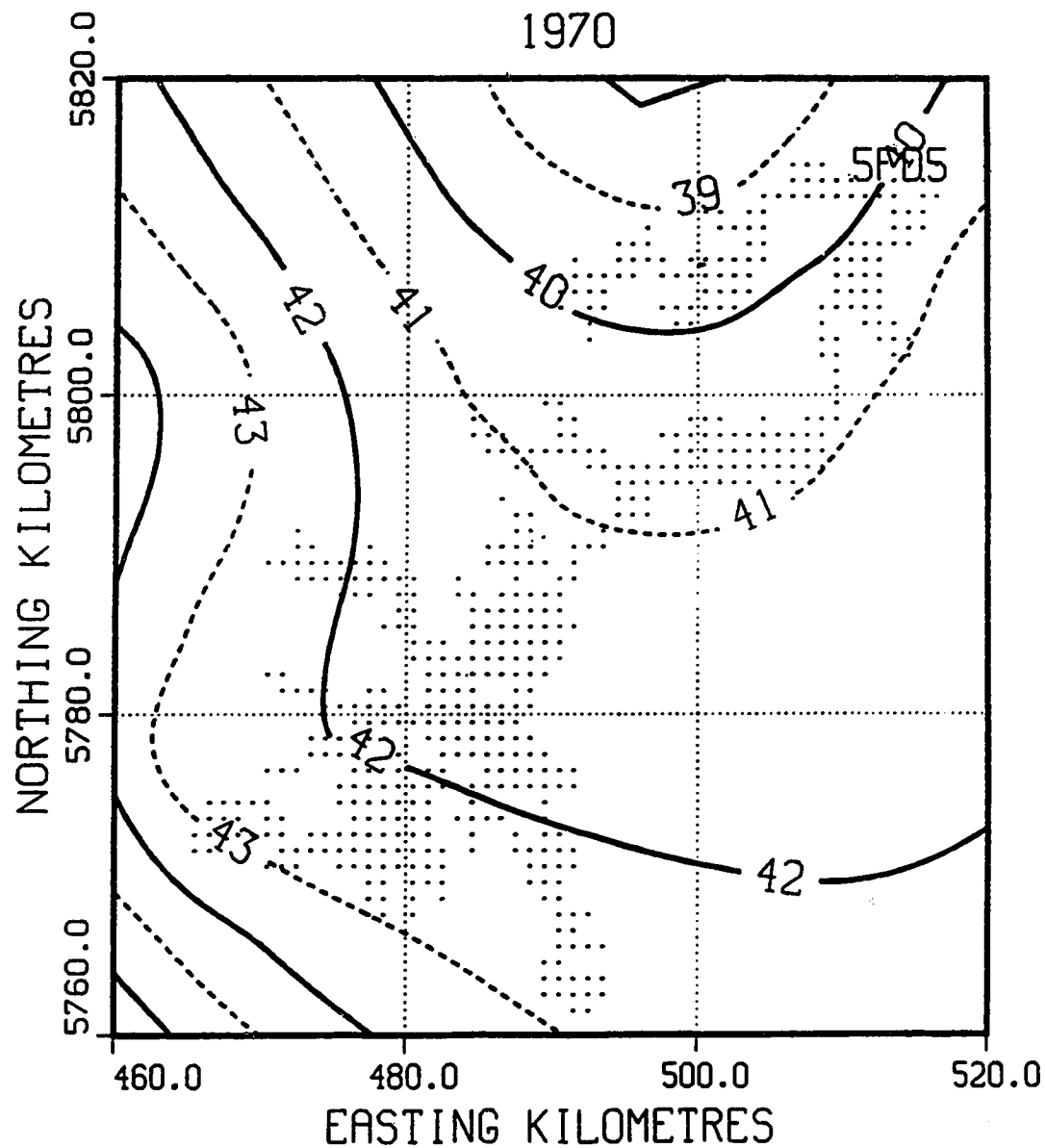


Figure A-29: 1970 θ_p spatial field in mm H₂O equivalent.

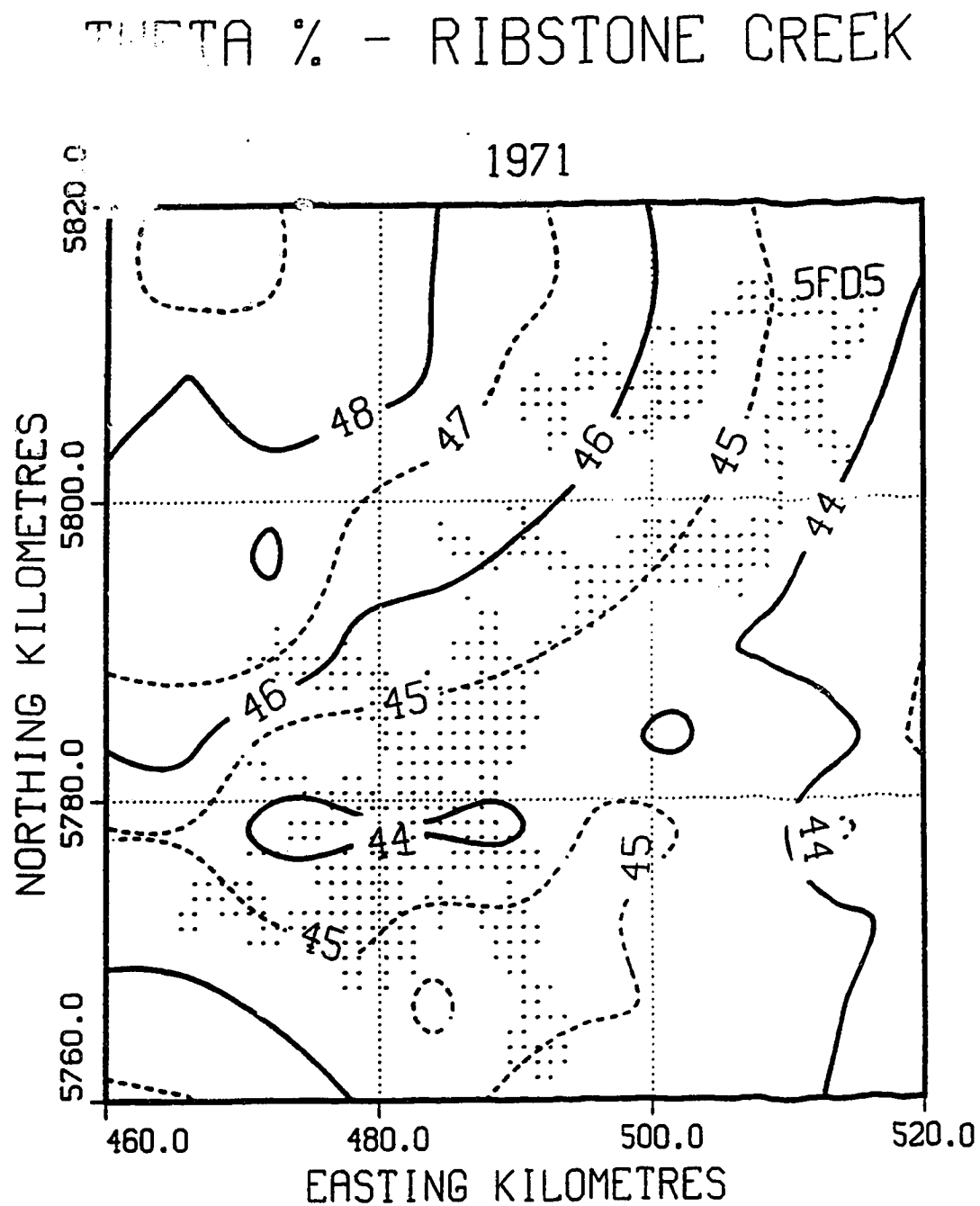


Figure A-30: 1971 θ_p spatial field in mm H₂O equivalent.

THETA % - RIBSTONE CREEK

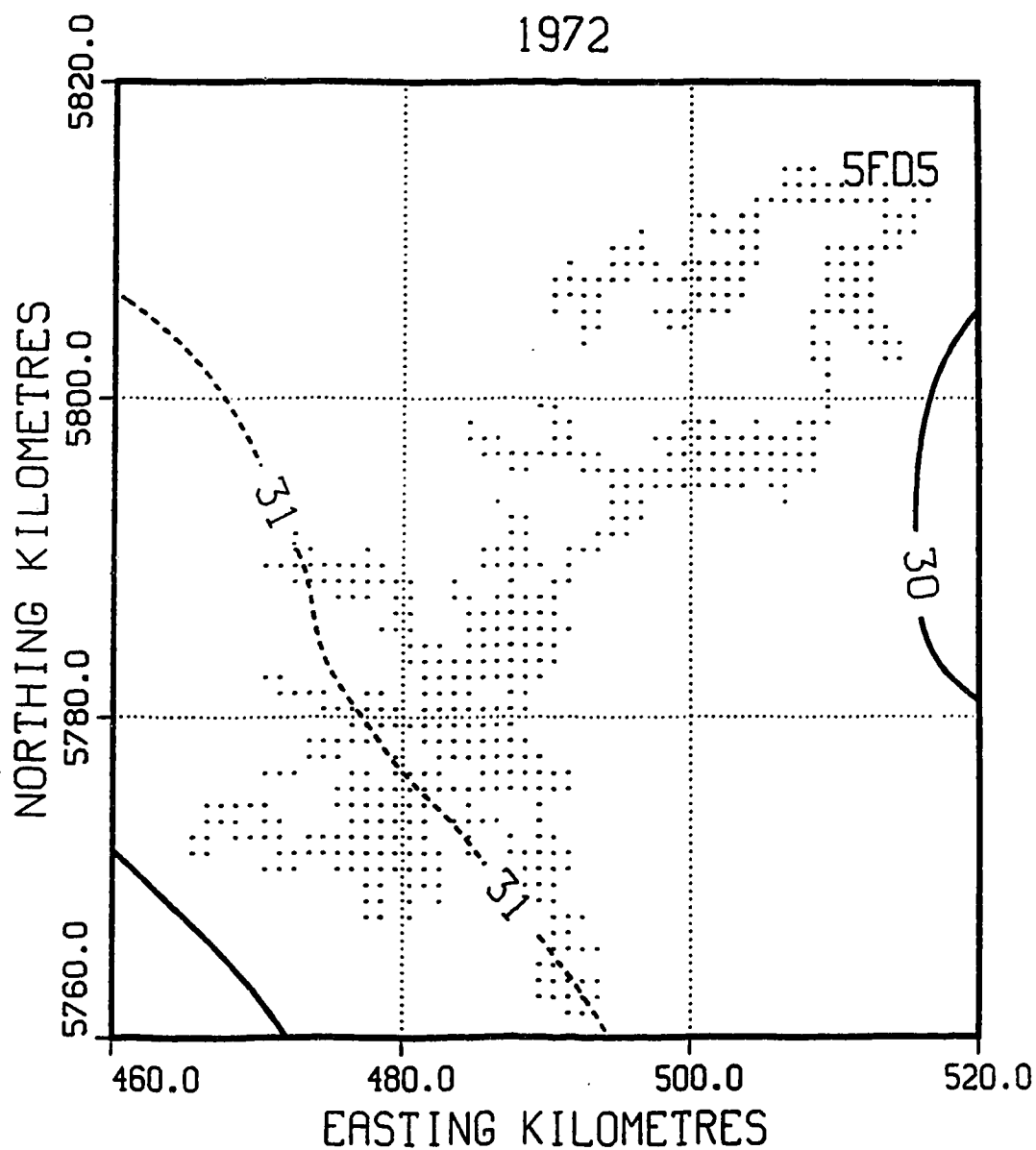


Figure A-31: 1972 θ_p spatial field in mm H₂O equivalent.

THETA % - RIBSTONE CREEK

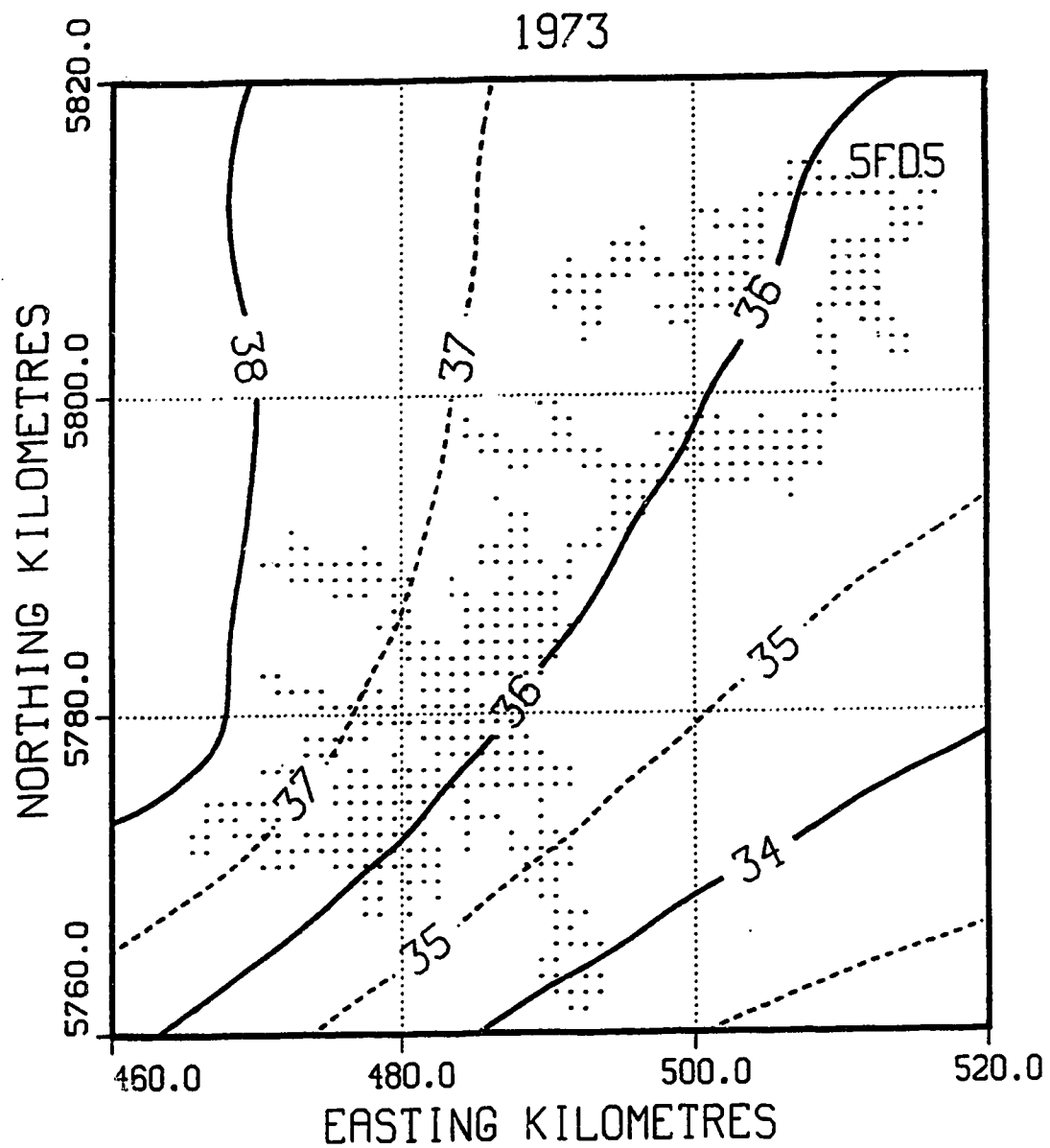


Figure A-32: 1973 θ_p spatial field in mm H₂O equivalent.

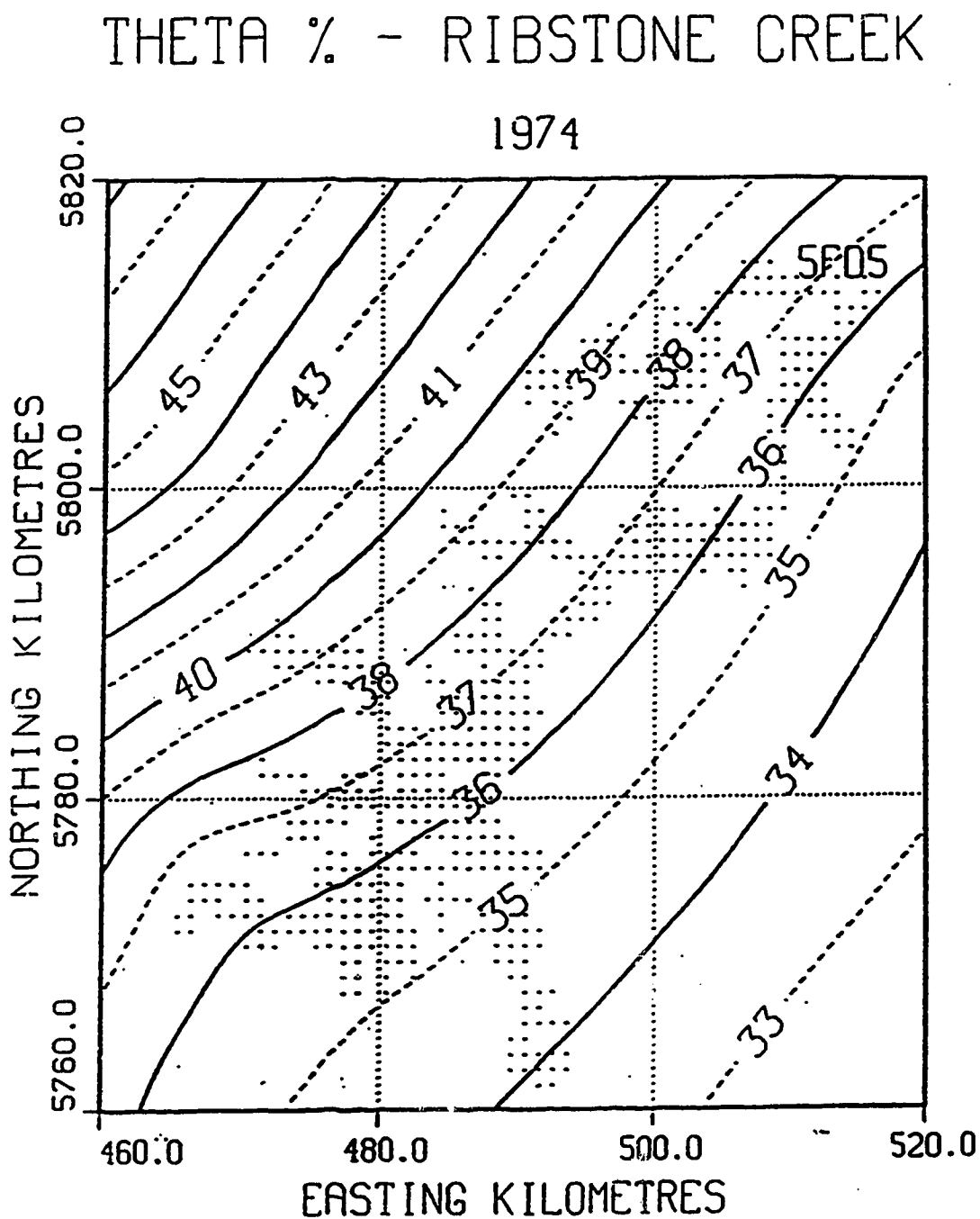


Figure A-33: 1974 θ_p spatial field in mm H_2O equivalent.

THETA % - RIBSTONE CREEK

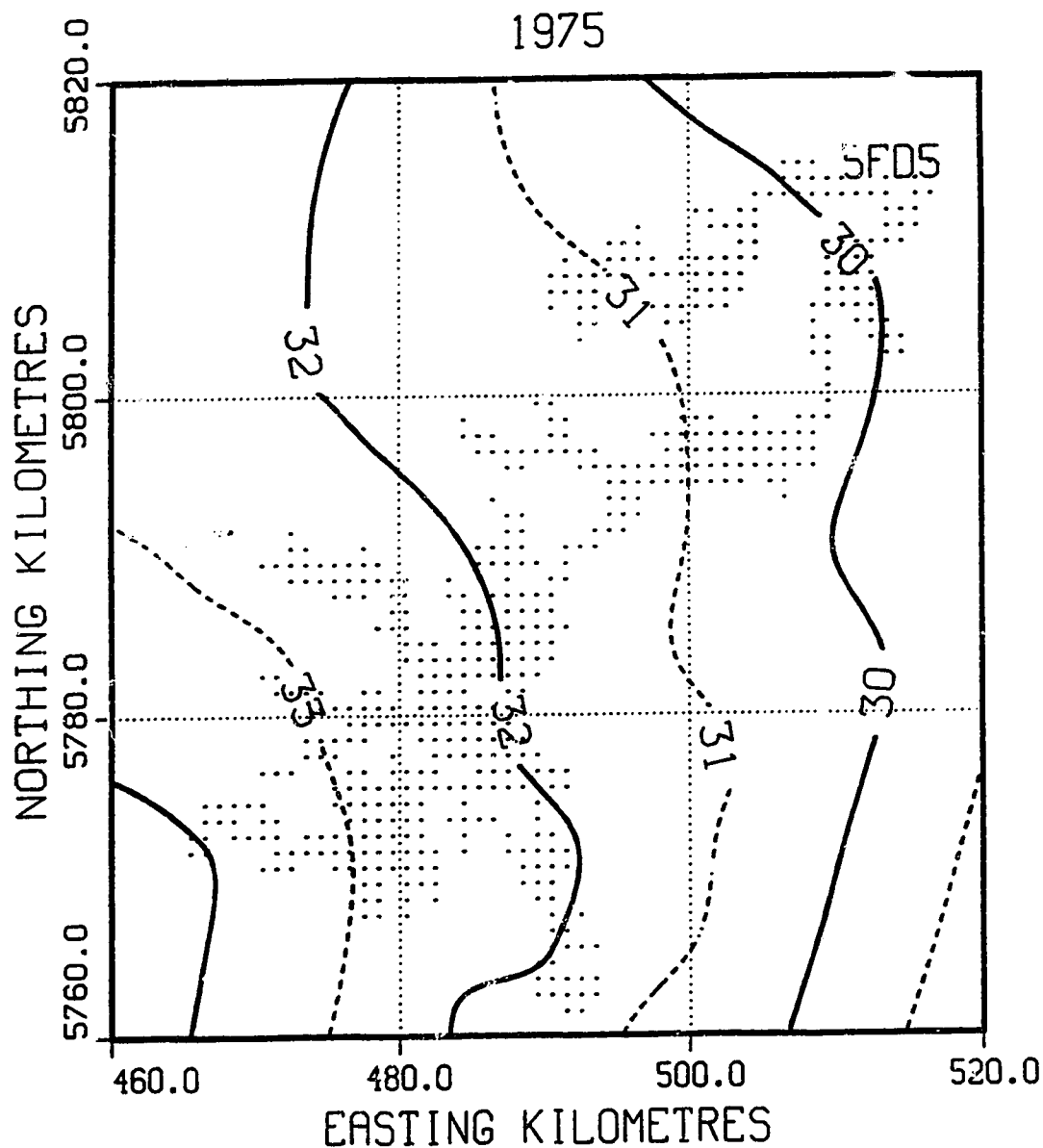


Figure A-34: 1975 θ_p spatial field in mm H₂O equivalent.

THETA % - RIBSTONE CREEK

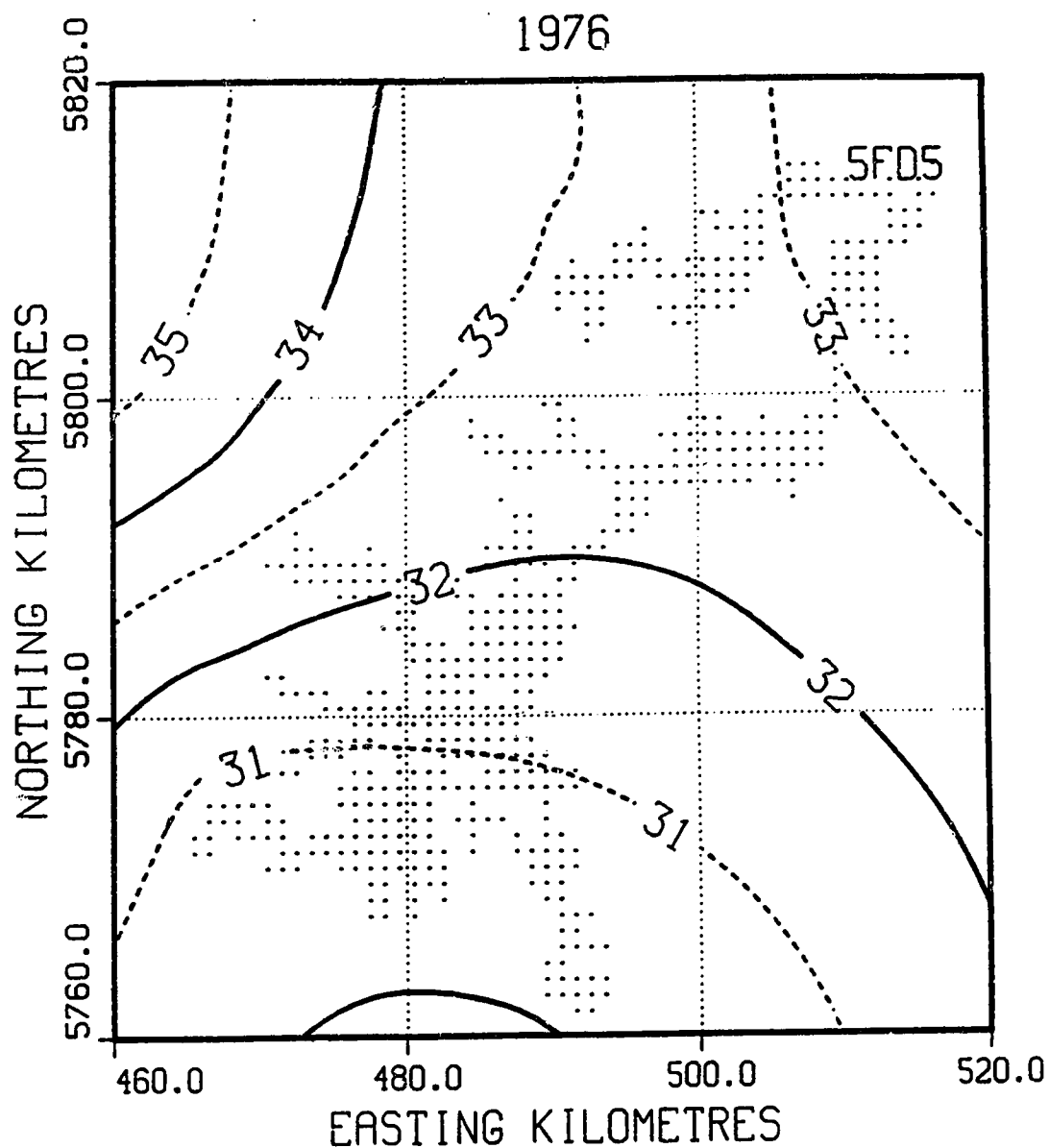


Figure A-35: 1976 θ_p spatial field in mm H₂O equivalent.

THETA % - RIBSTONE CREEK

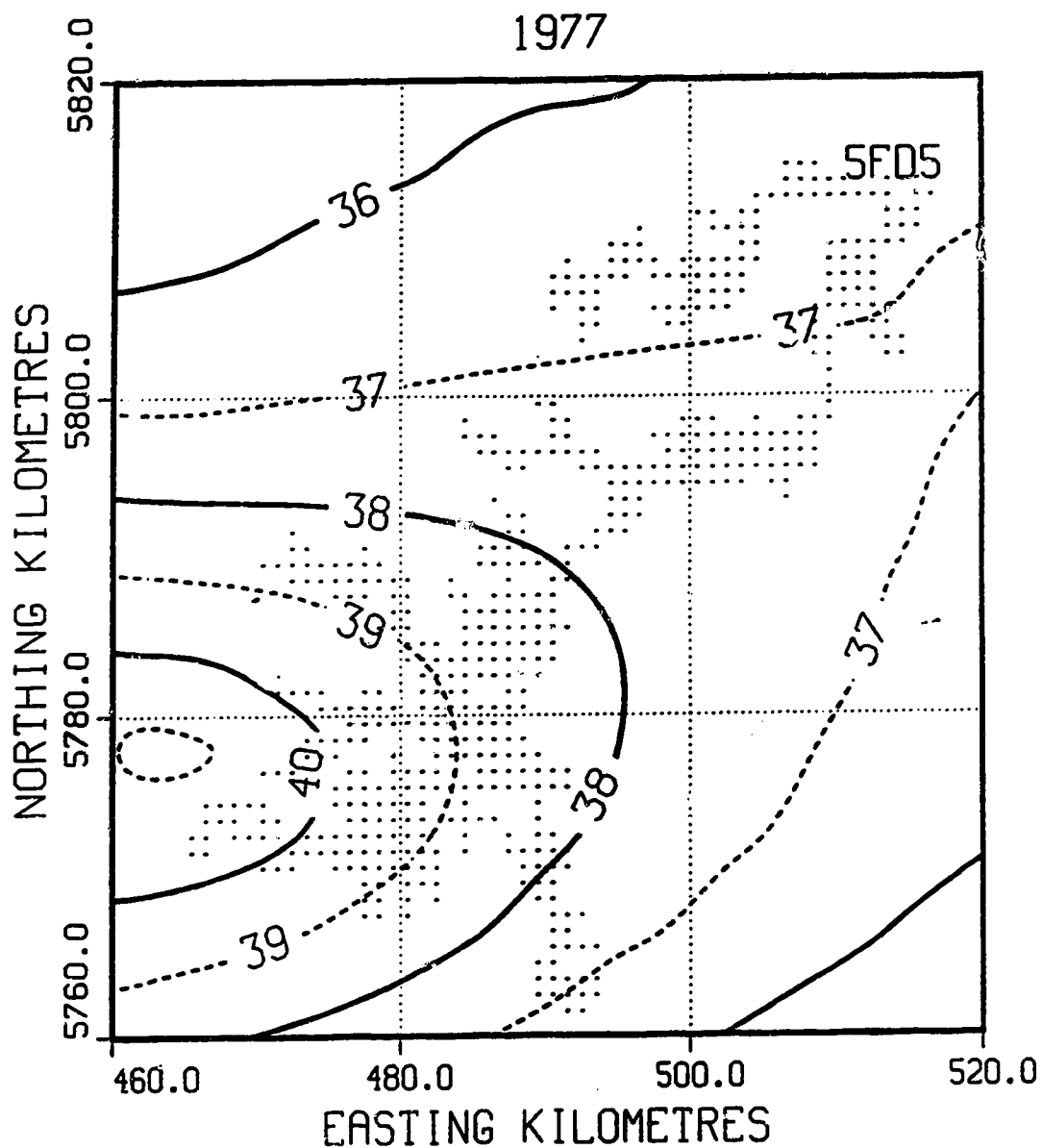


Figure A-36: 1977 θ_p spatial field in mm H₂O equivalent.

THETA % - RIBSTONE CREEK

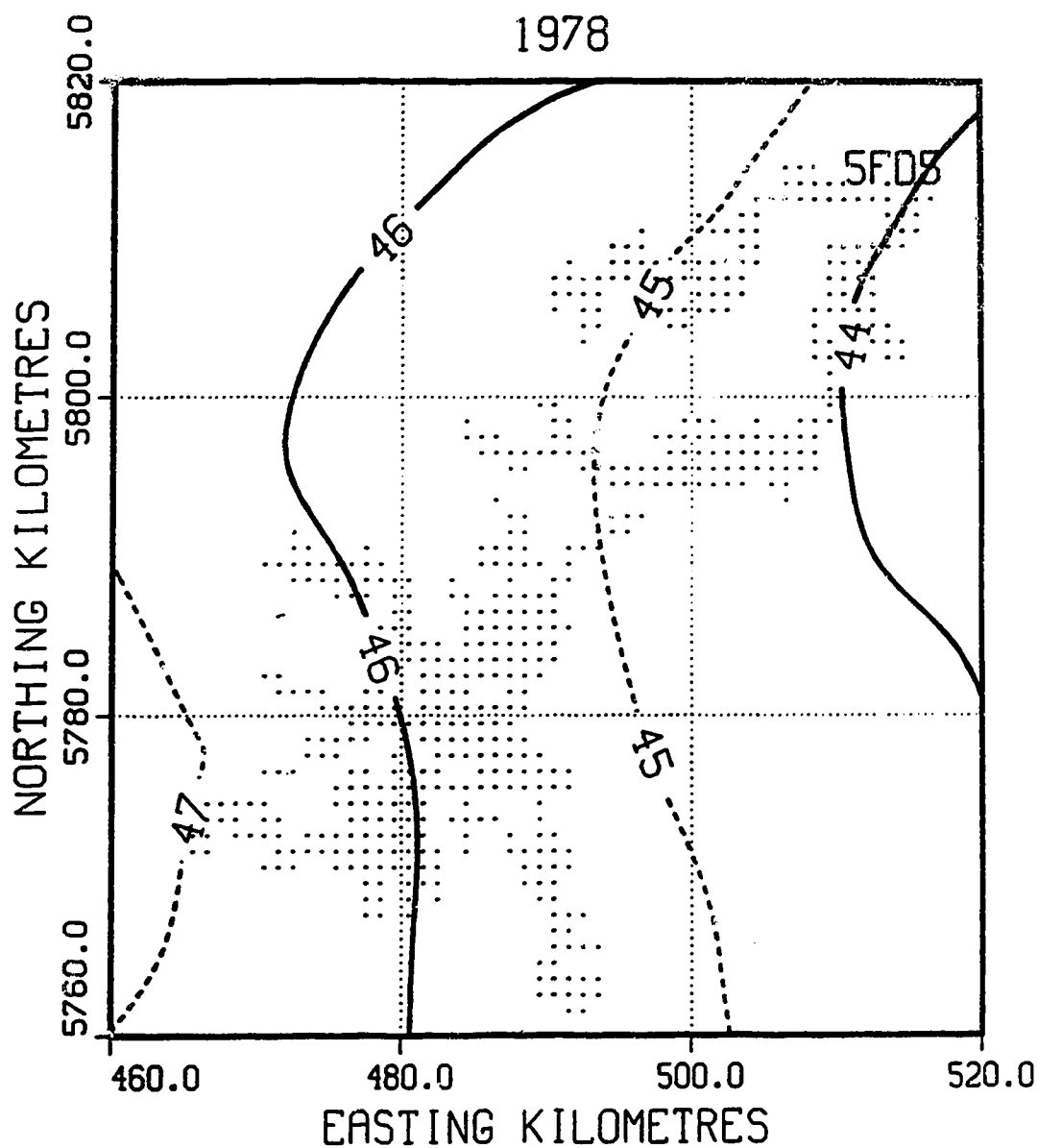


Figure A-37: 1978 θ_p spatial field in mm H_2O equivalent.

THETA % - RIBSTONE CREEK

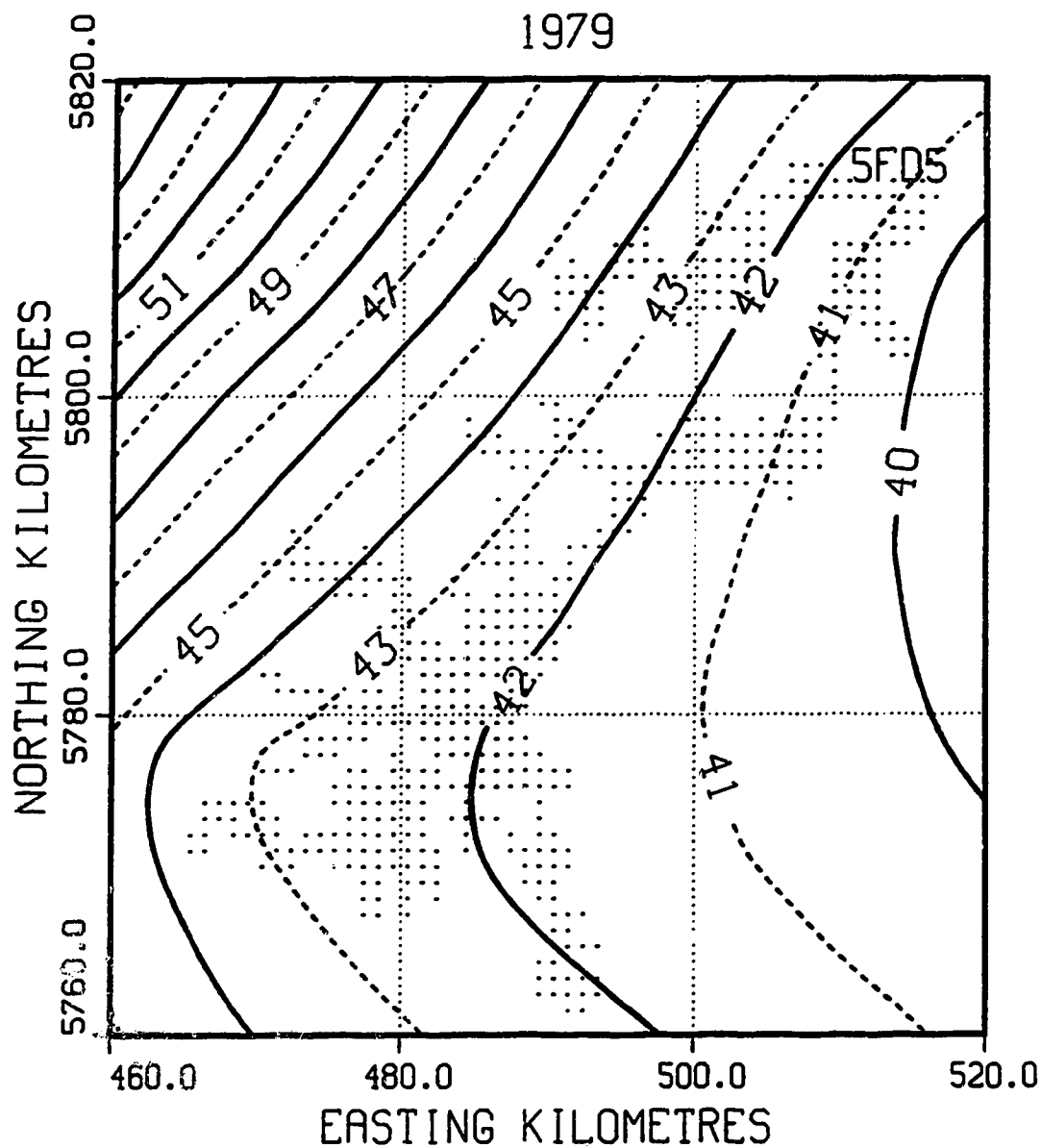


Figure A-38: 1979 θ_p spatial field in mm H₂O equivalent.

THETA % - RIBSTONE CREEK

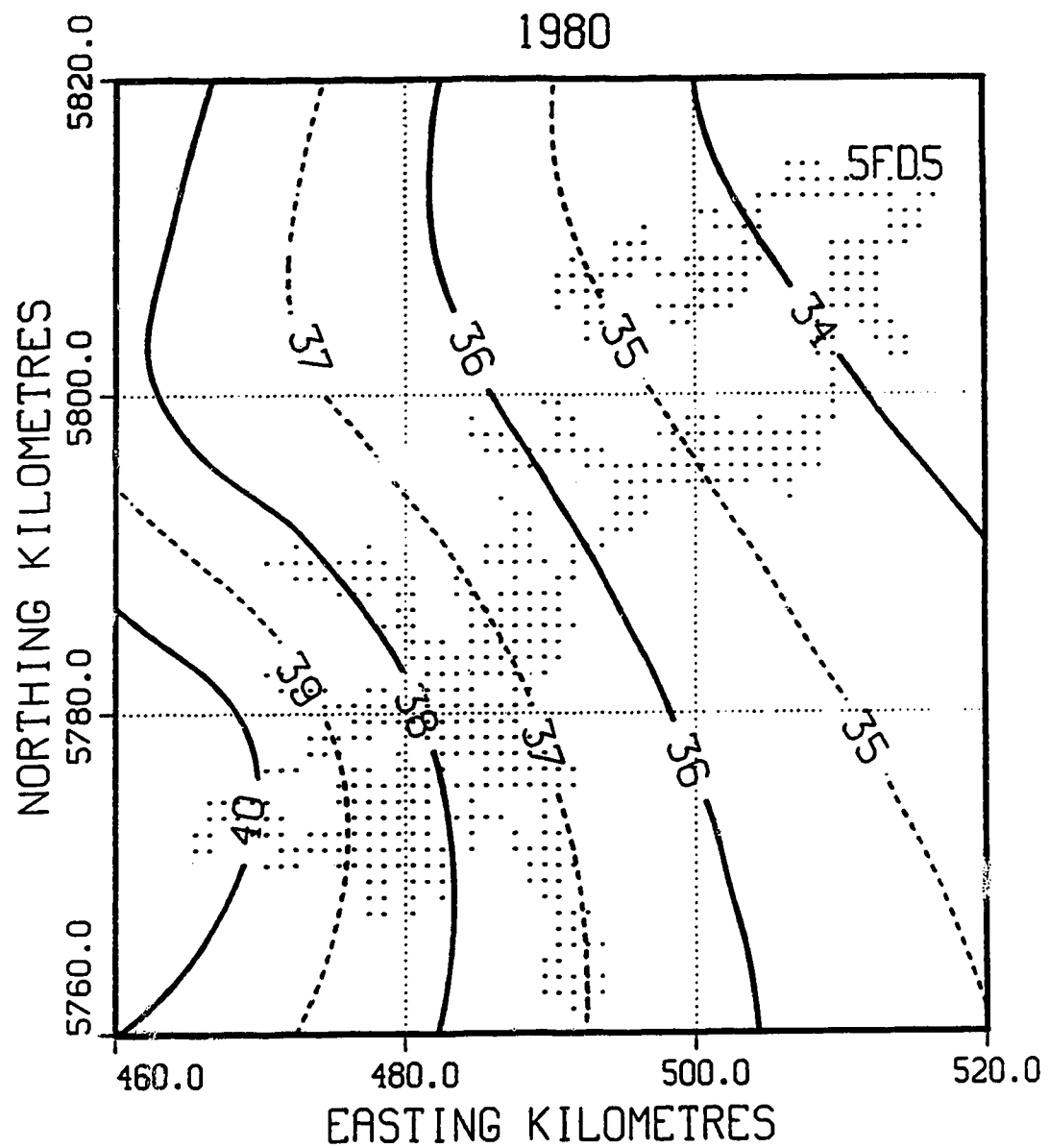


Figure A-39: 1980 θ_p spatial field in mm H₂O equivalent.

Appendix B

STUDY AREA WP AND SWE SPATIAL FIELDS, 1960-81

The WP and SWE spatial patterns over the study area are highly varied on a spatial and temporal basis from year to year, and demonstrates a significant spatial variation within each year. This appendix contains the grey level contour maps for both of these parameters for the period 1960-81.

Ocassionally, an image may have several contours with very erratic or square shapes. These are due to large areas having values approaching 0. Roundoff error in the programs would result in there being no distinct pattern; hence the contouring routine would produces an erratic image.

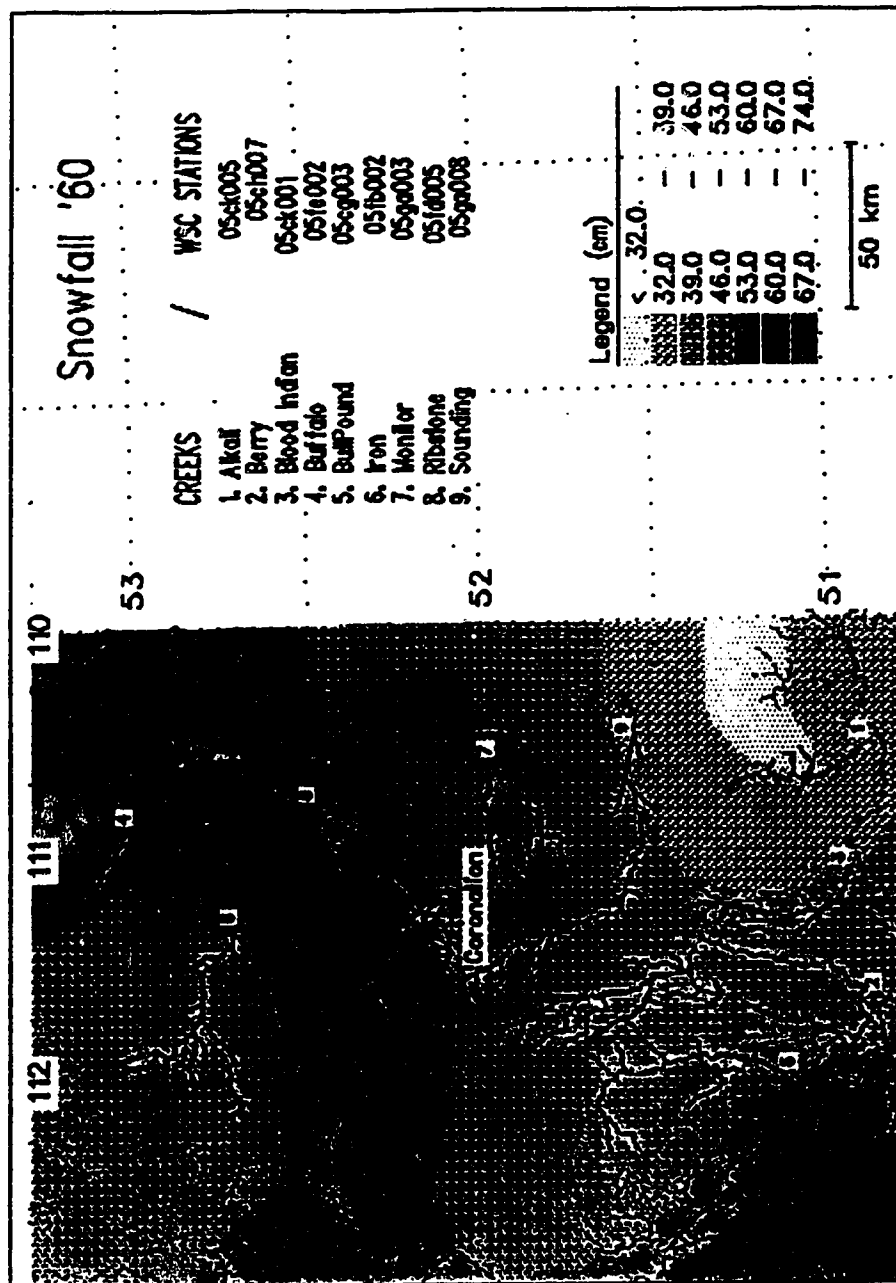


Figure B-1: 1960 - Study area winter precip., mm H₂O.

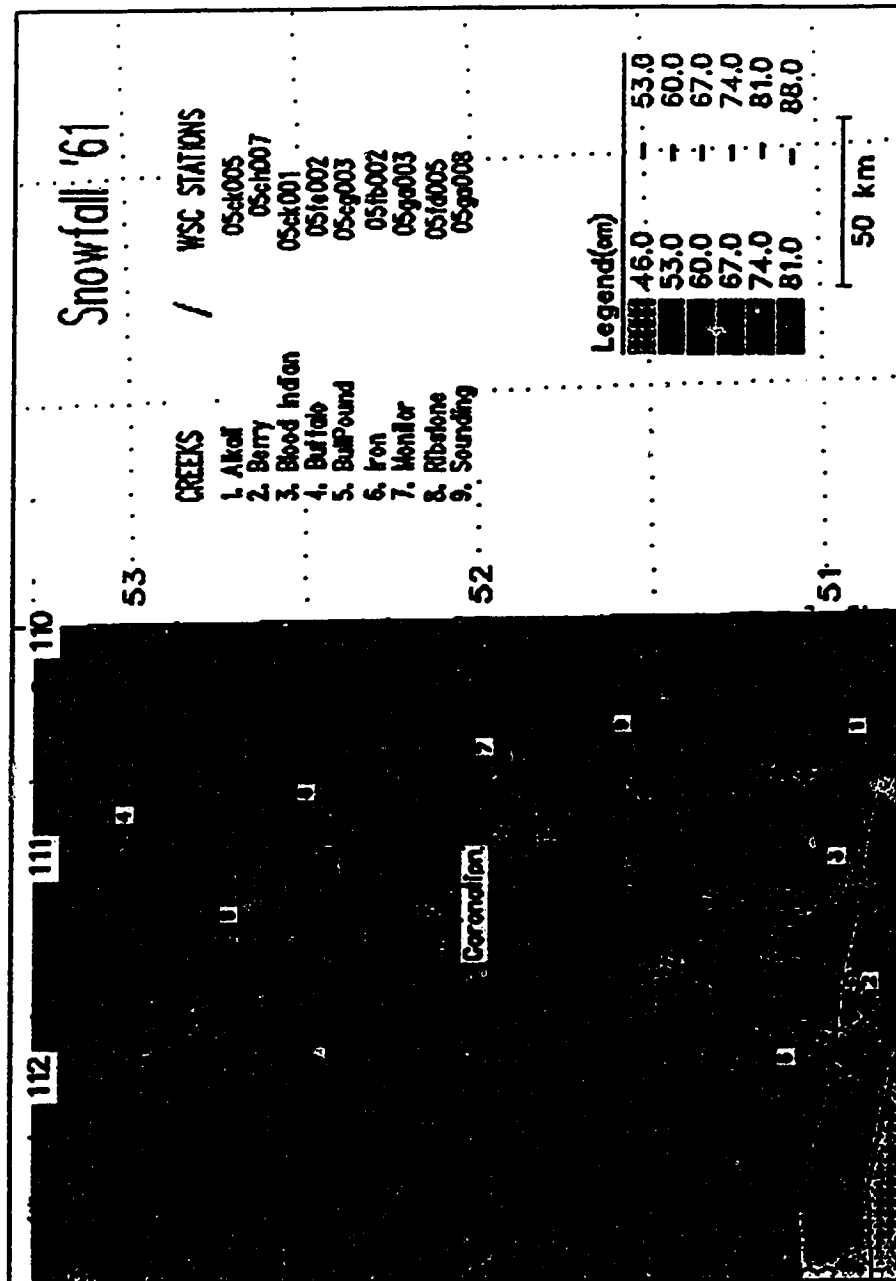


Figure B-2: 1961 - Study area winter precip., mm H₂O.

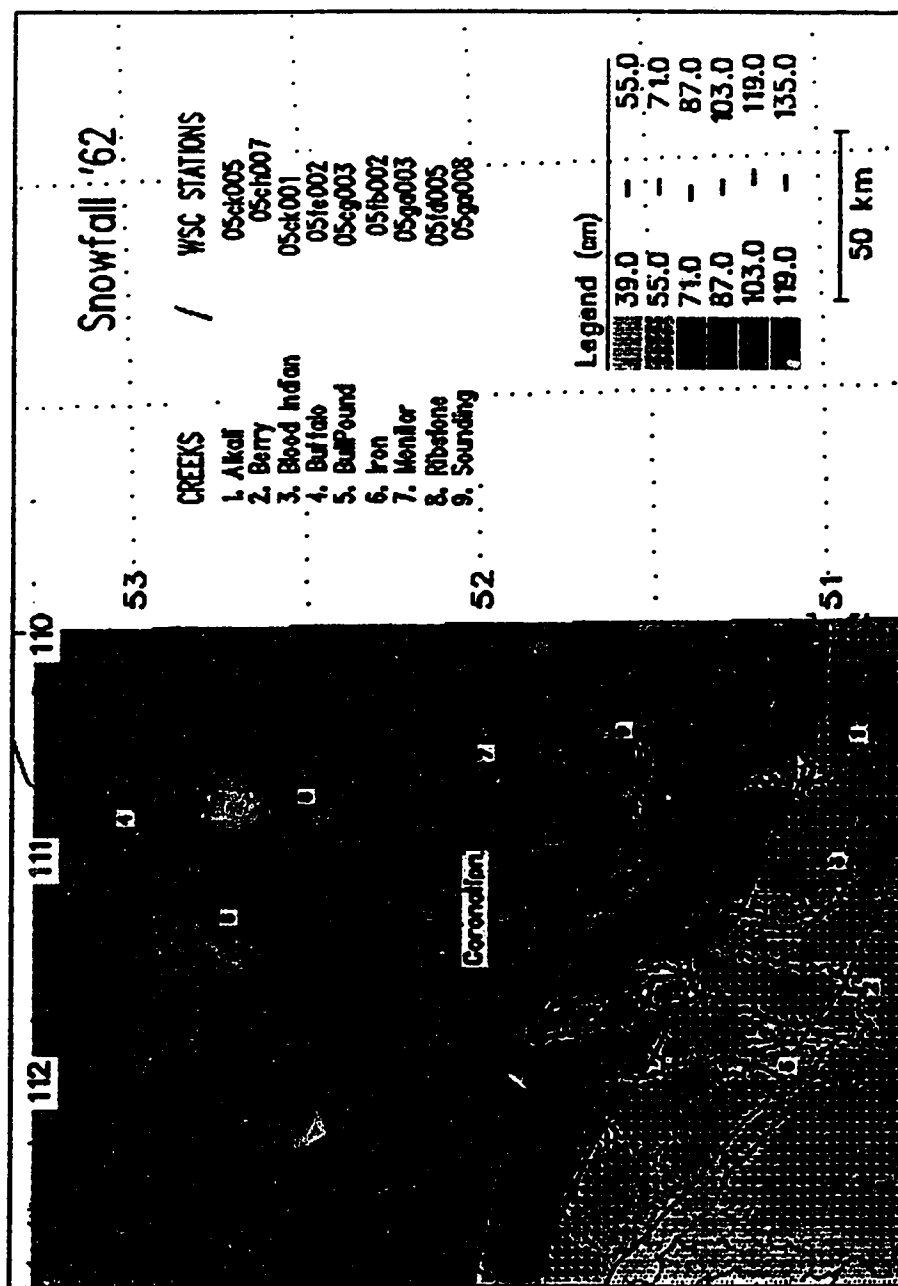


Figure B-3: 1962 - Study area winter precip., mm H₂O.

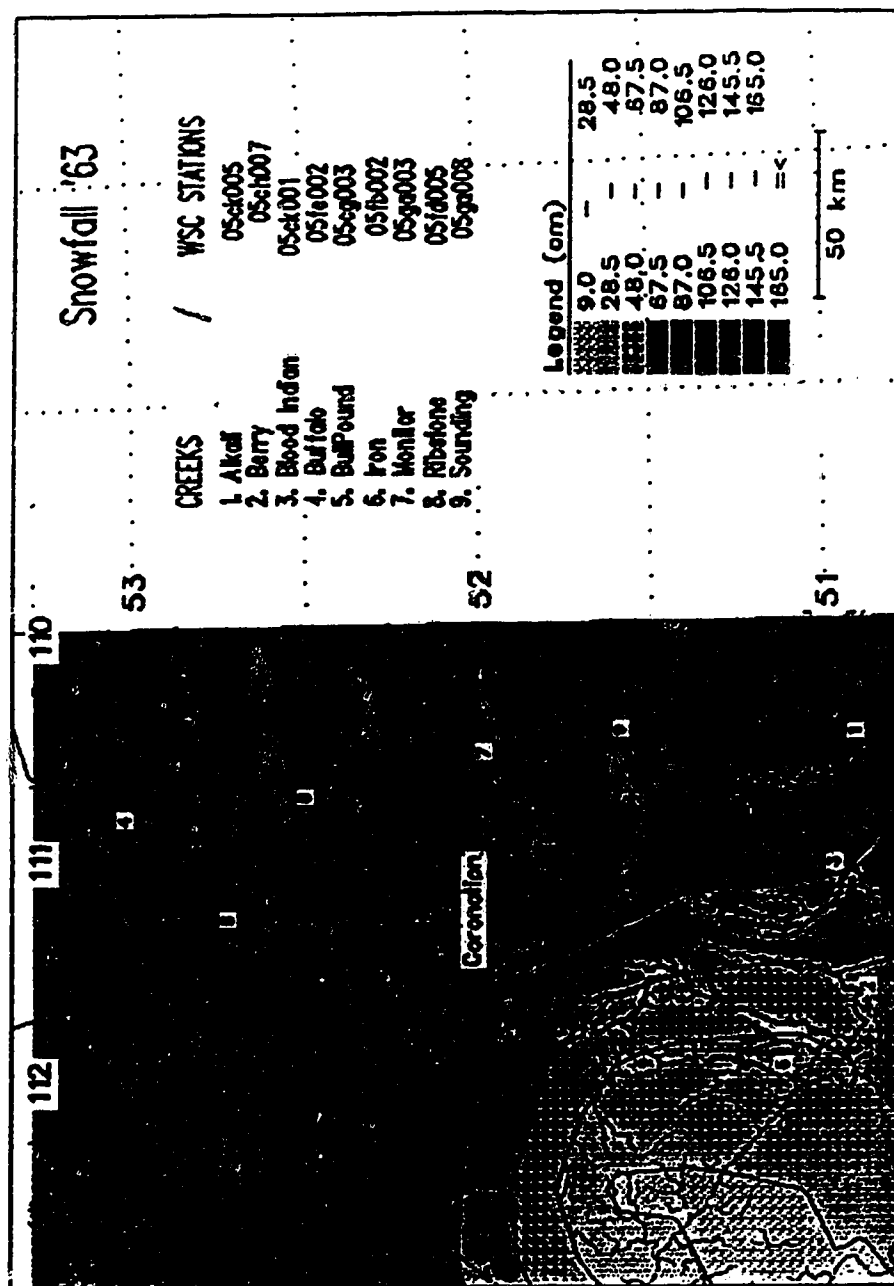


Figure B-4: 1963 - Study area winter precip., mm H₂O.

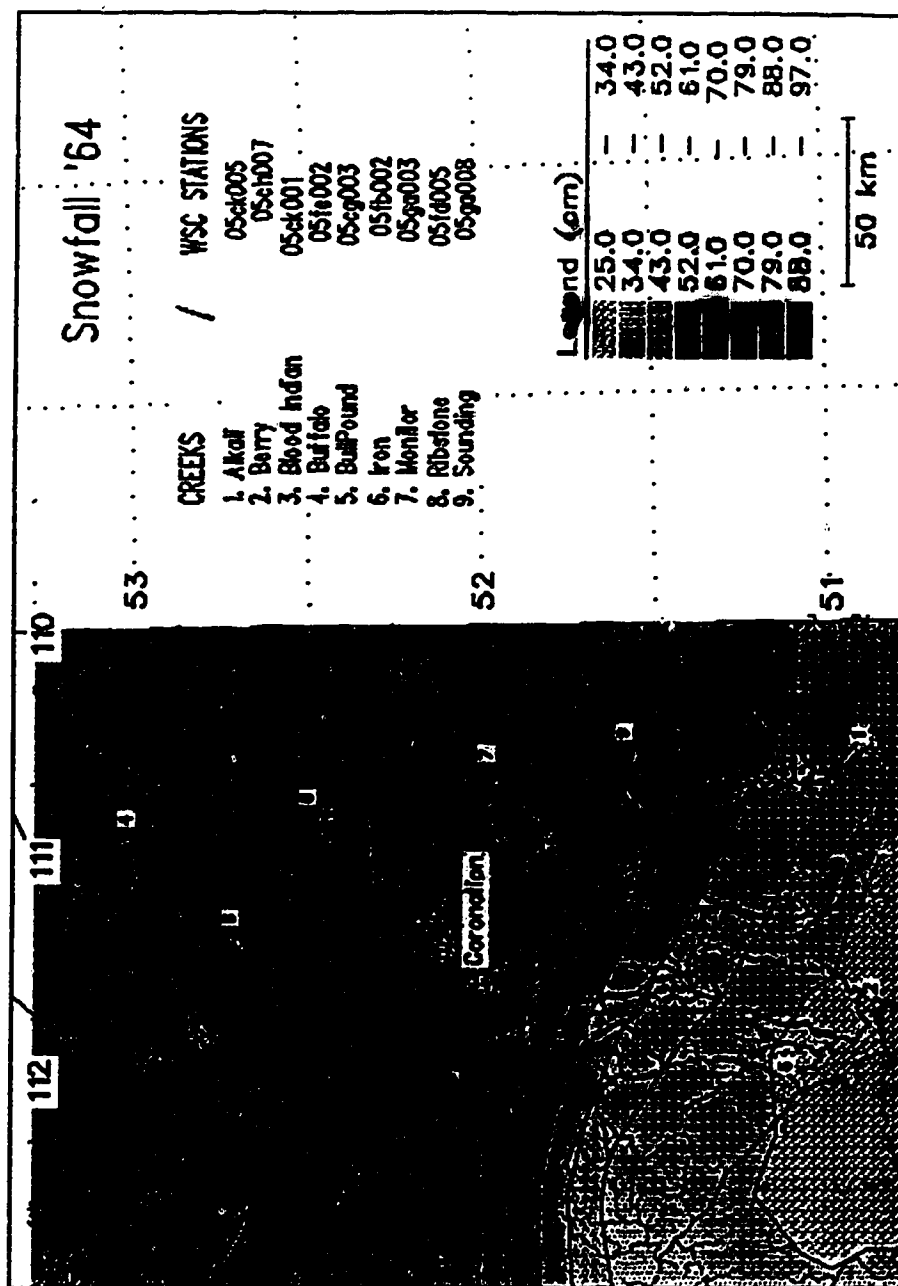


Figure B-5: 1964 - Study area winter precip., mm H₂O.

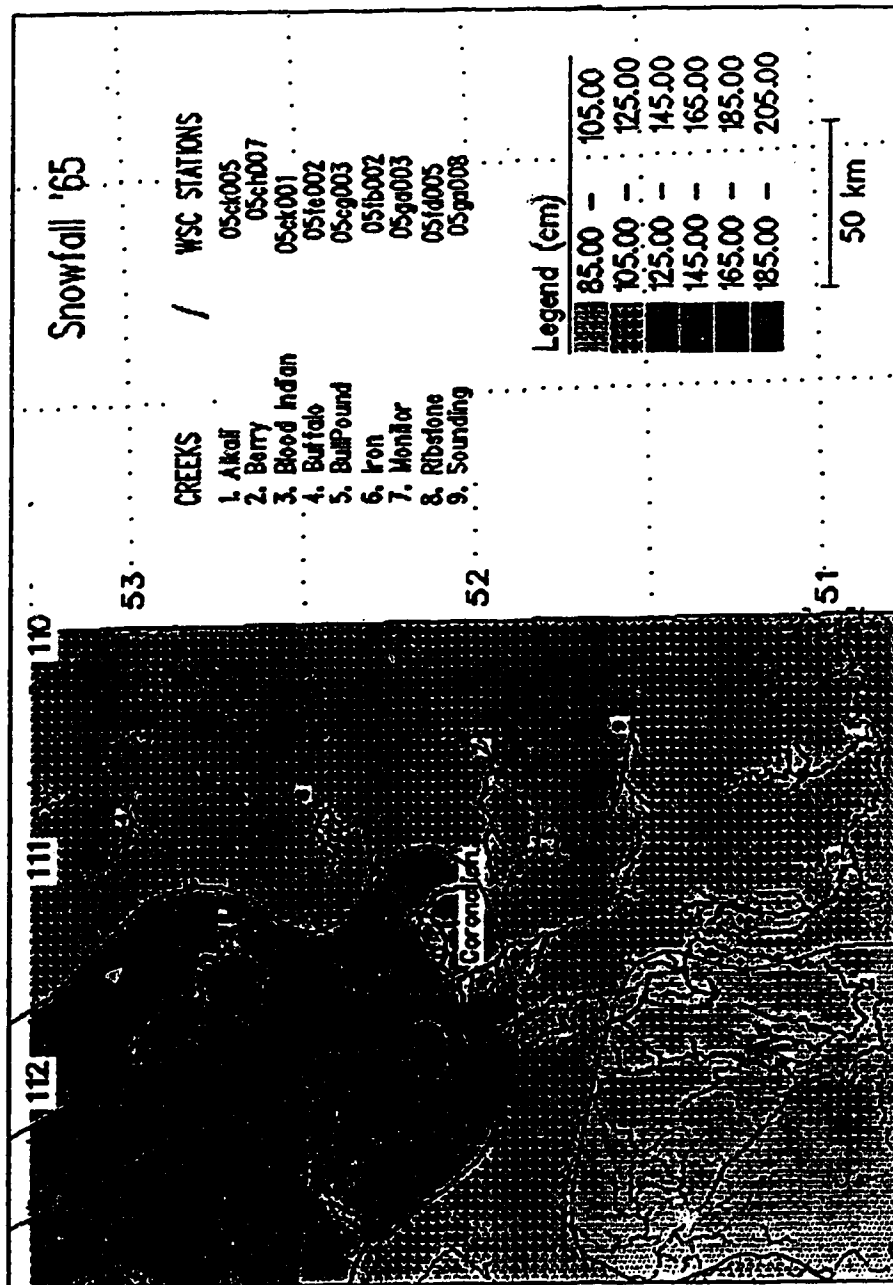


Figure B-6: 1965 - Study area winter precip., mm H₂O.

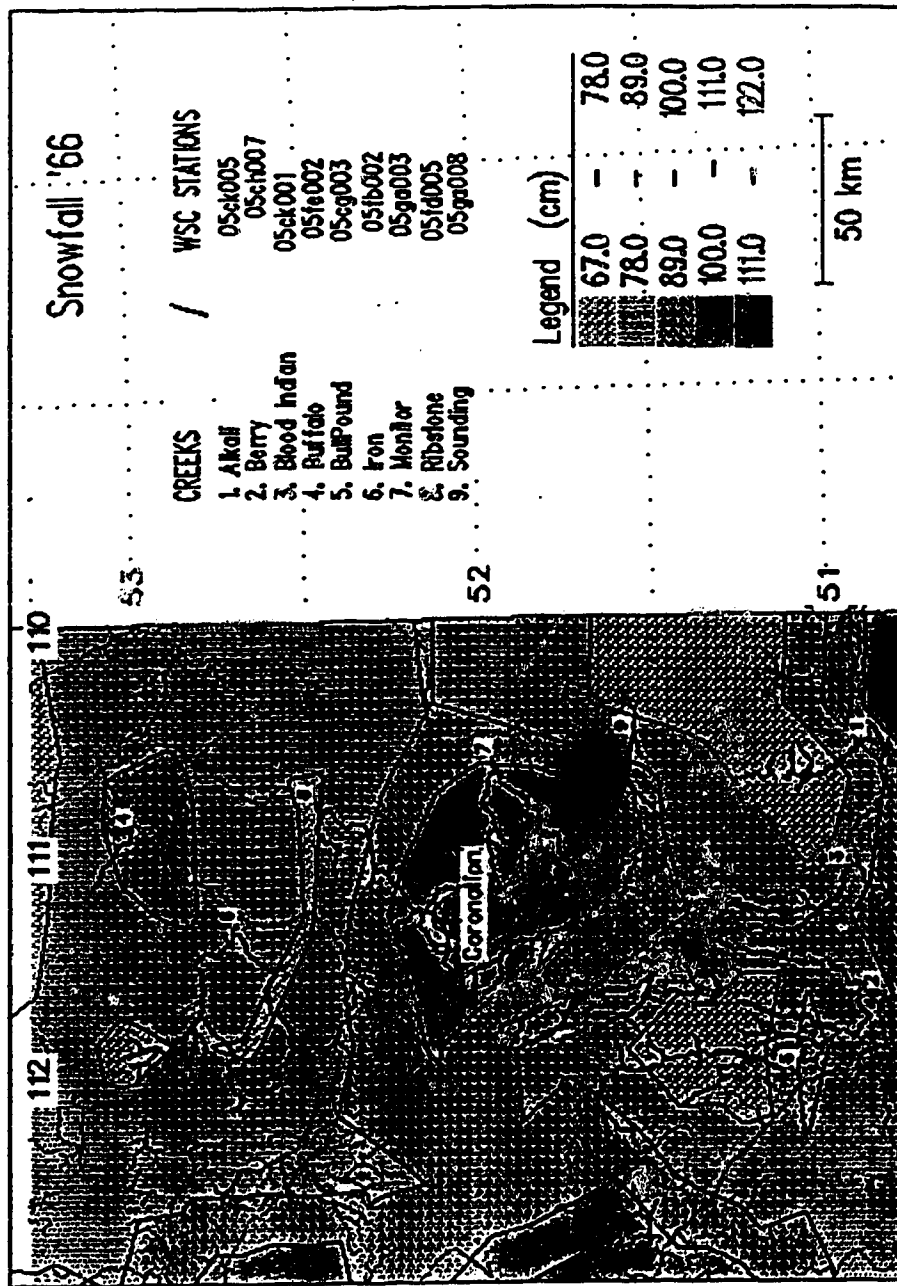


Figure B-7: 1966 - Study area winter precip., mm H₂O.

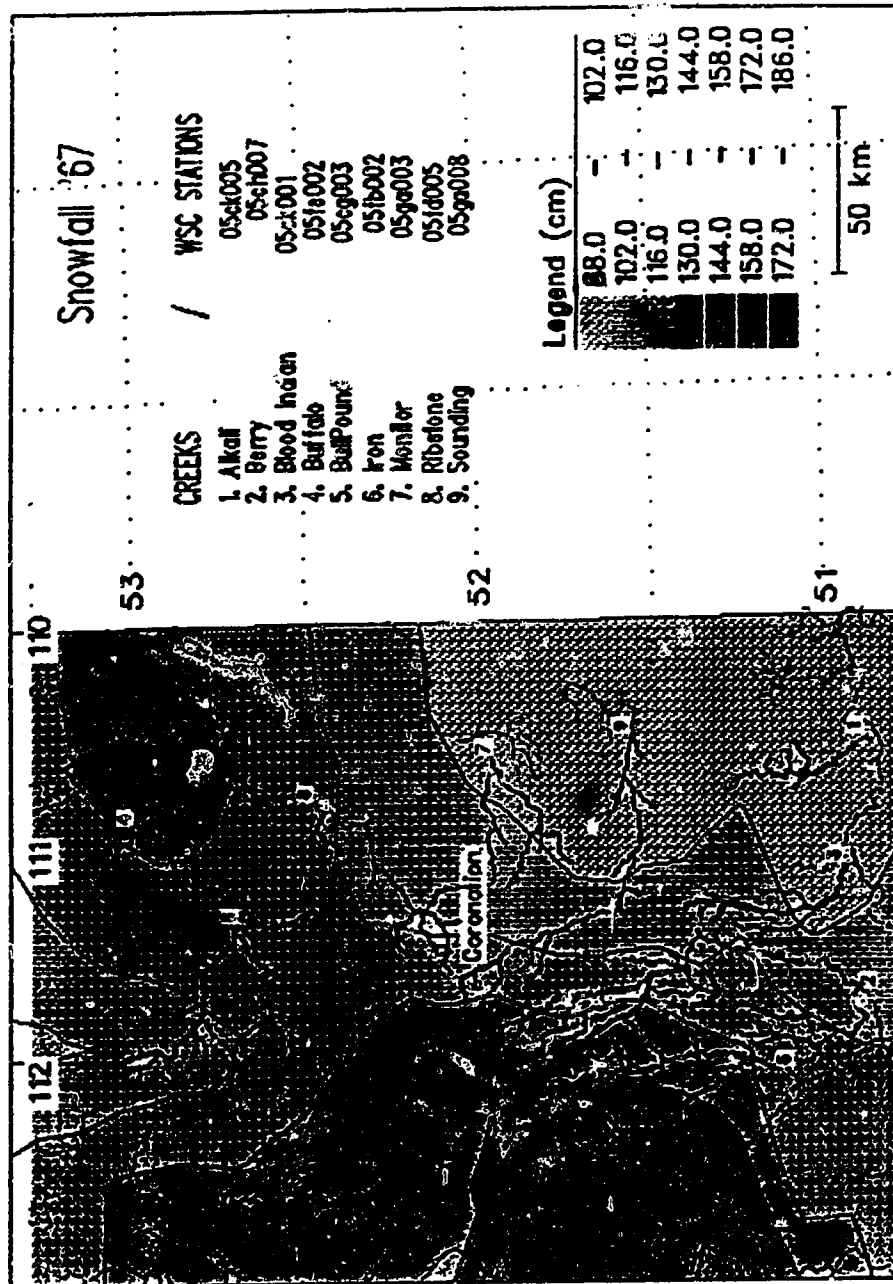


Figure B-8: 1967 - Study area winter precip., mm H₂O.

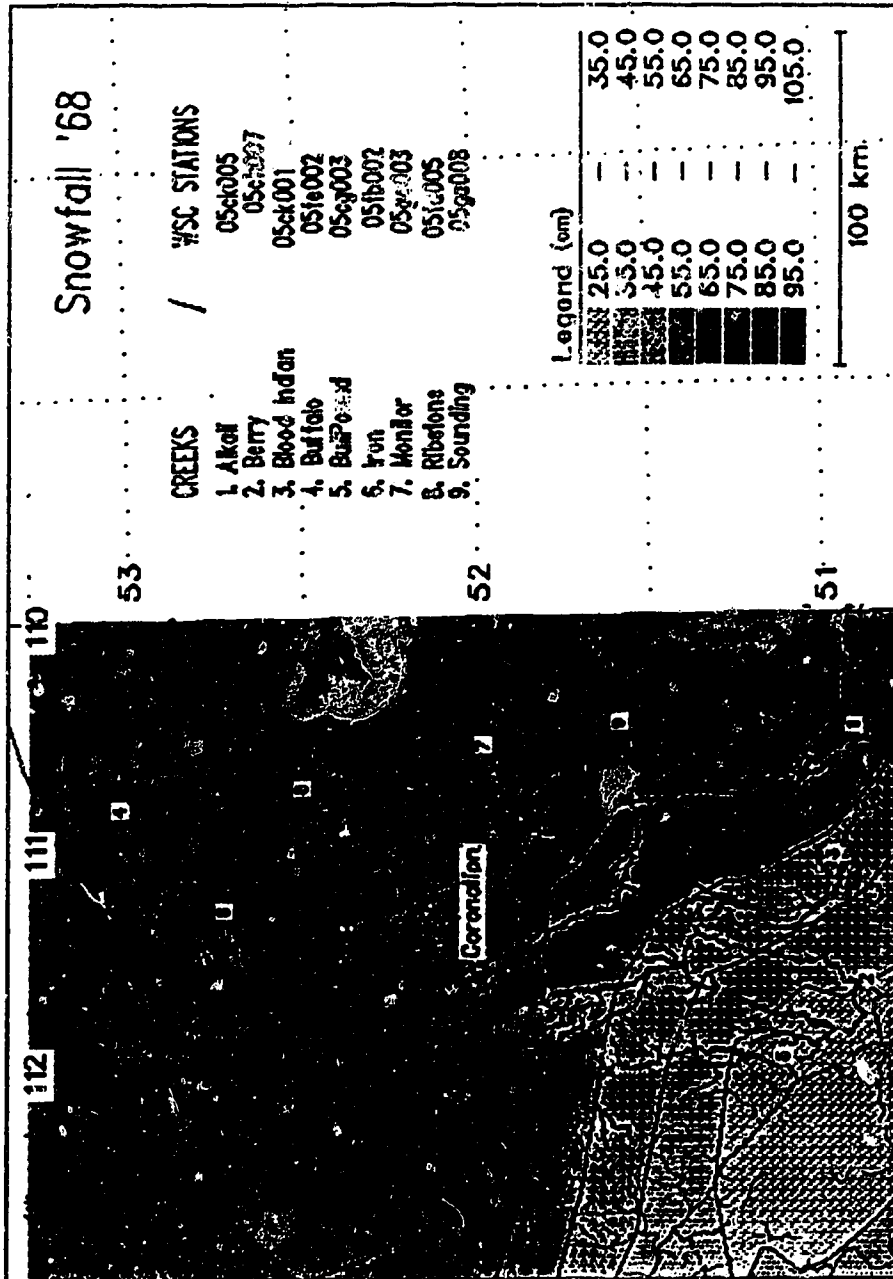


Figure B-9: 1968 - Study area winter precip., mm H₂O.

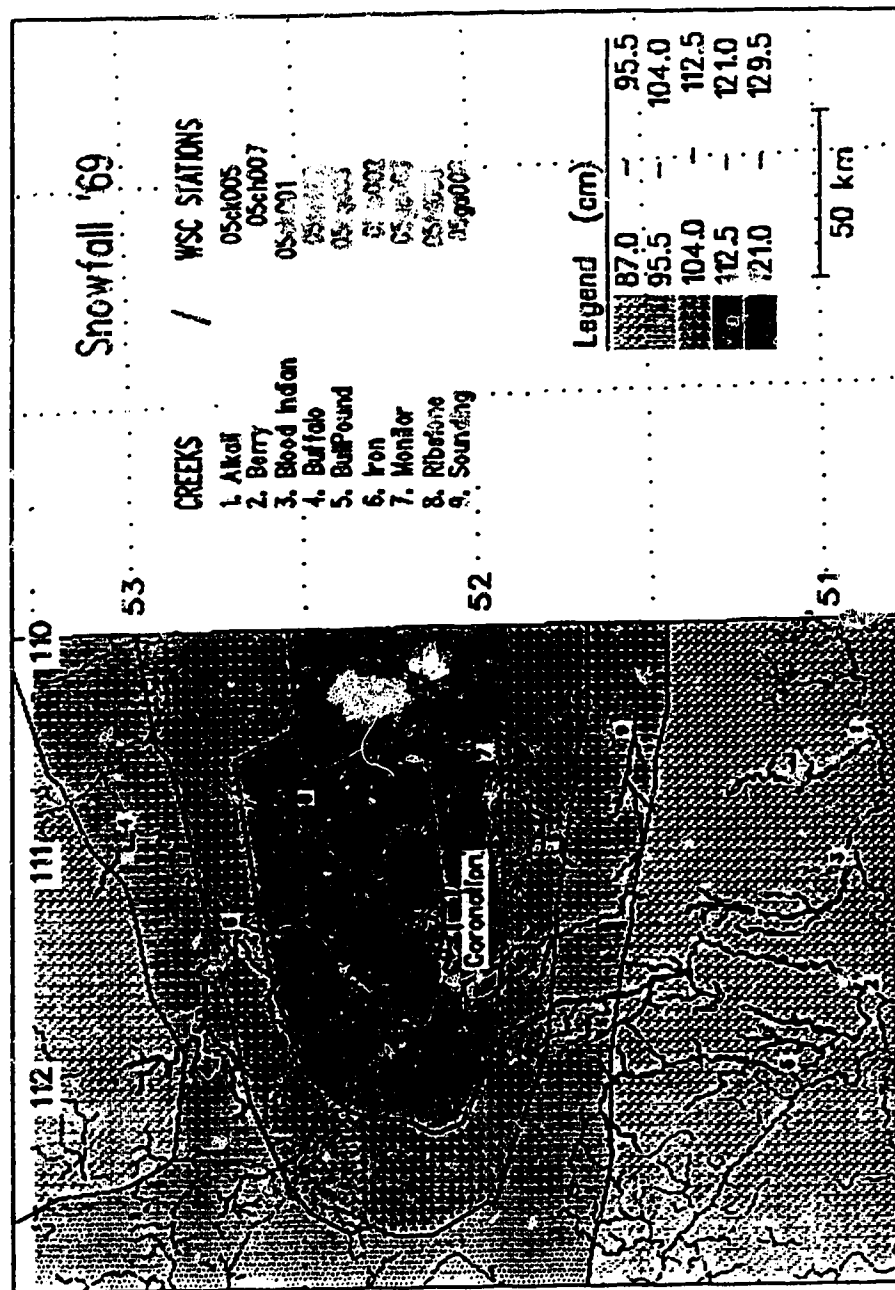


Figure B-10: 1969 - Study area winter precip., mm H₂O.

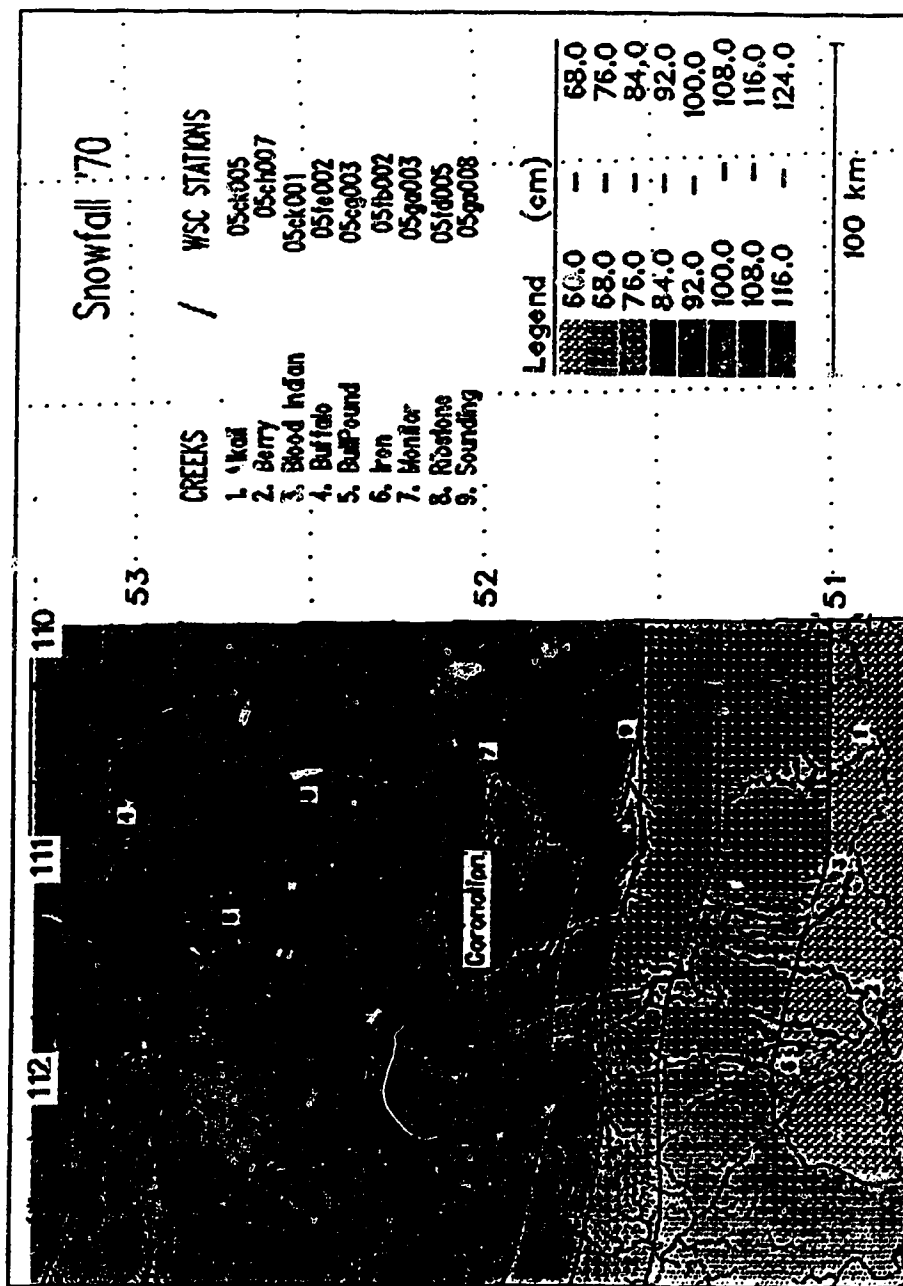


Figure B-11: 1970 - Study area winter precip., mm H₂O.

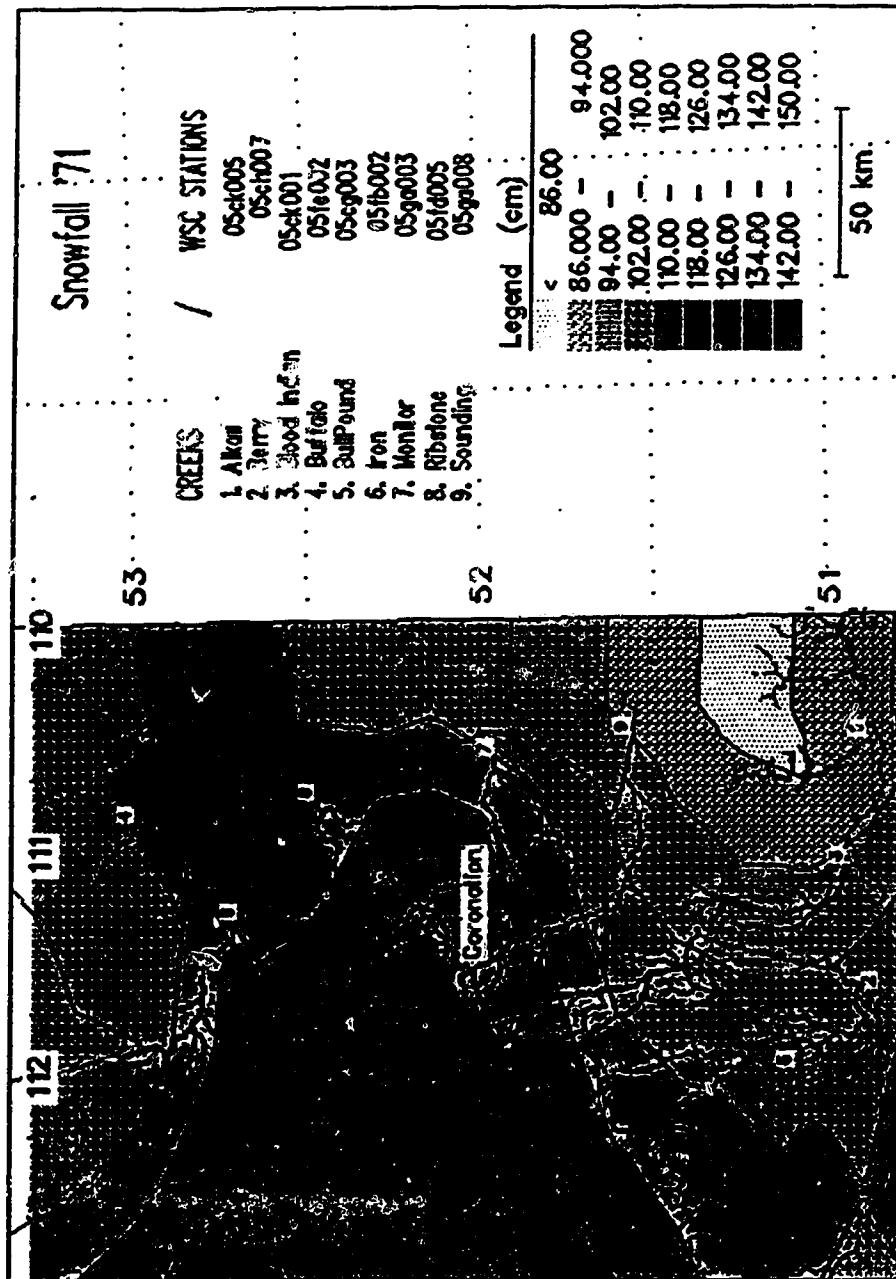


Figure B-12: 1971 - Study area winter precip - mm H₂O.

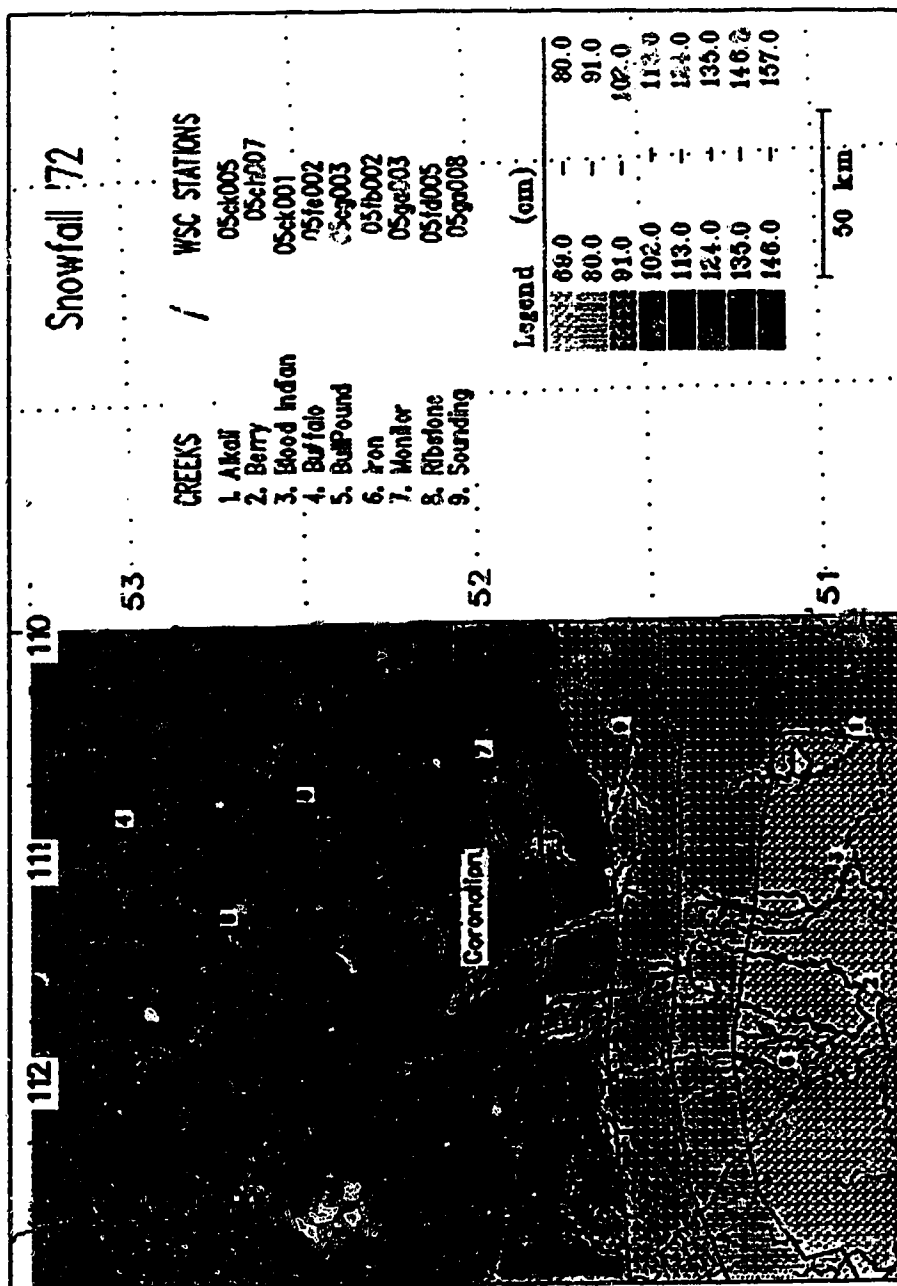


Figure B-13: 1972 - Study area winter precip., mm H₂O.

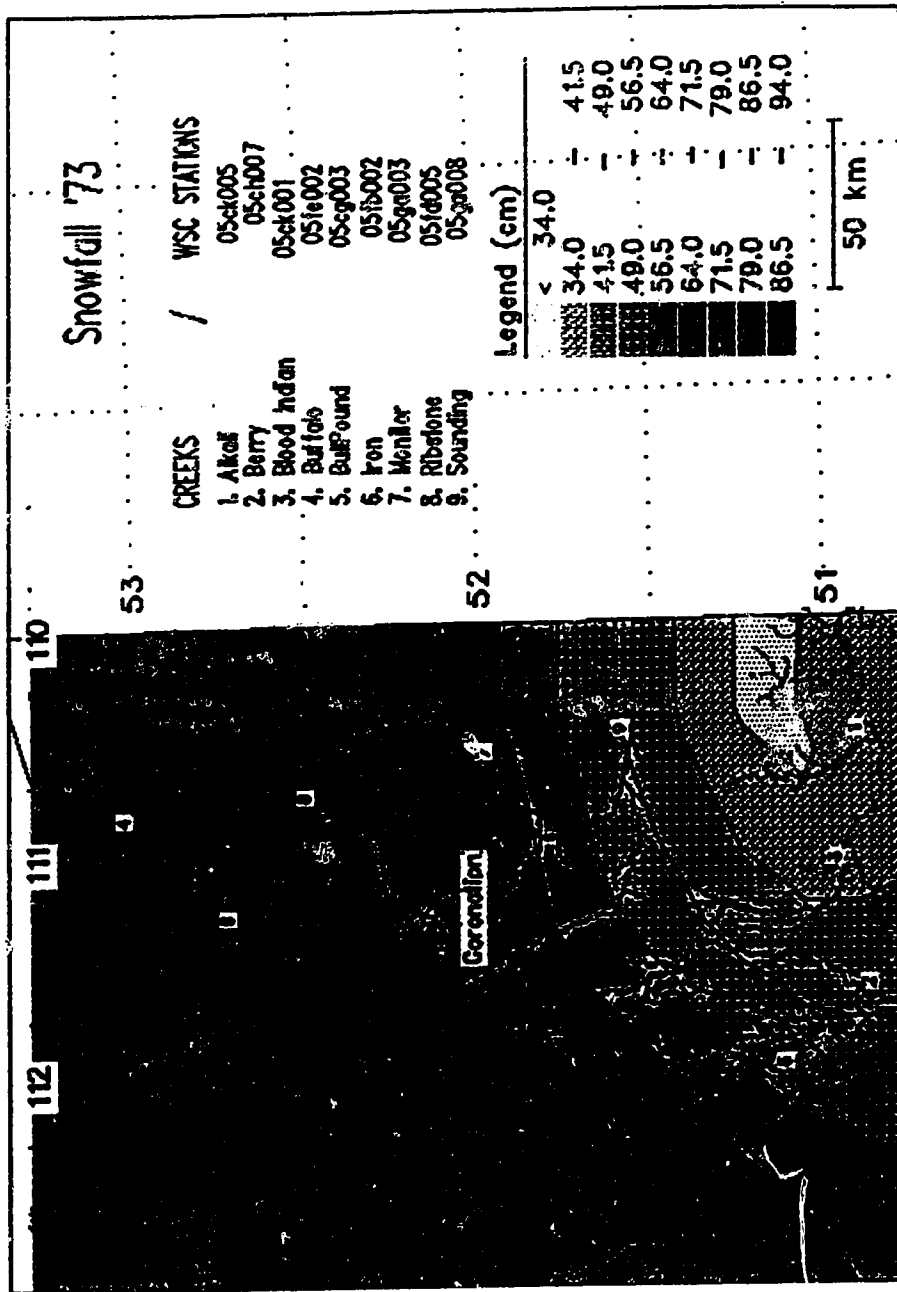


Figure B-14: 1973 - Study area winter precip., mm H₂O.

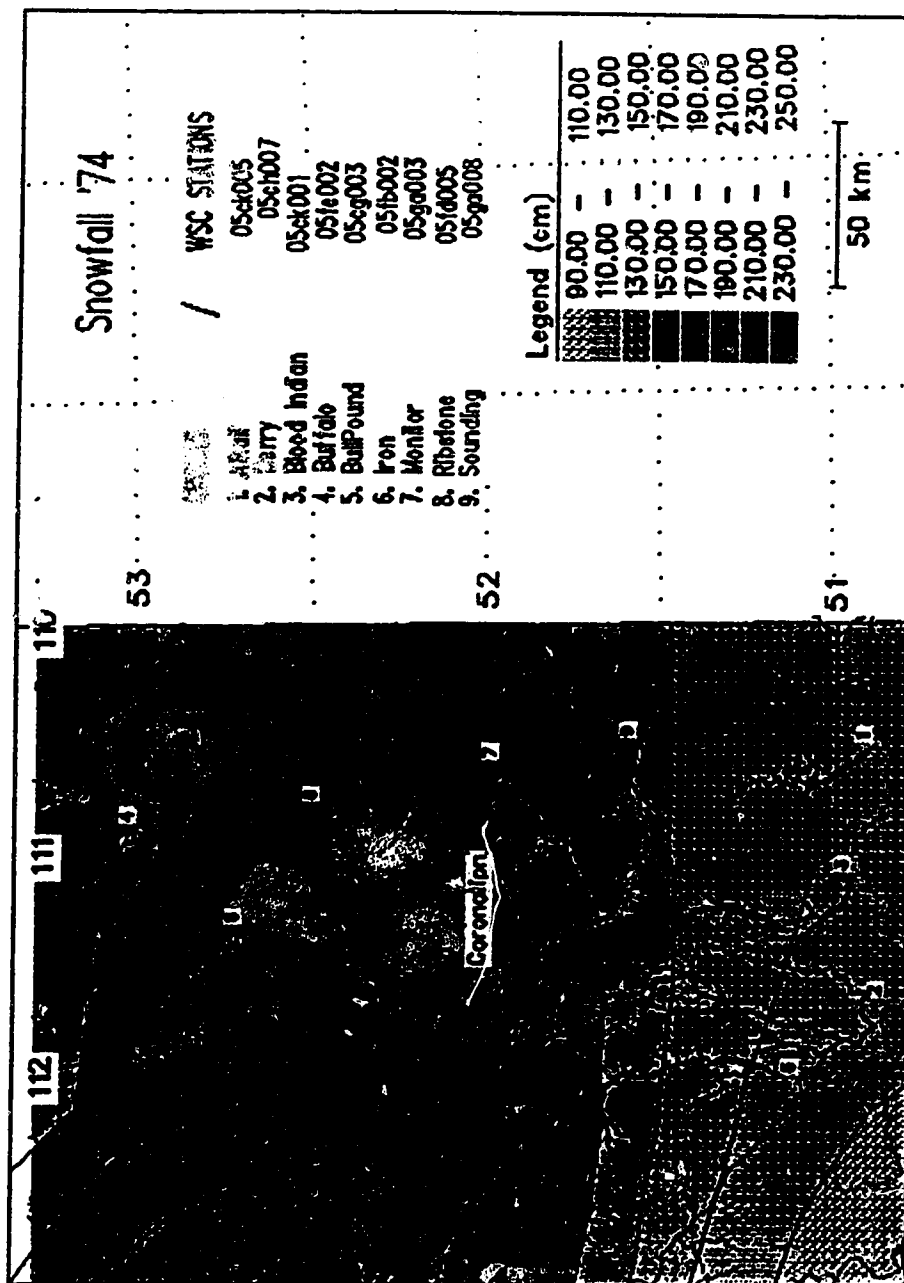


Figure B-15: 1974 - Study area winter precip., mm H₂O.

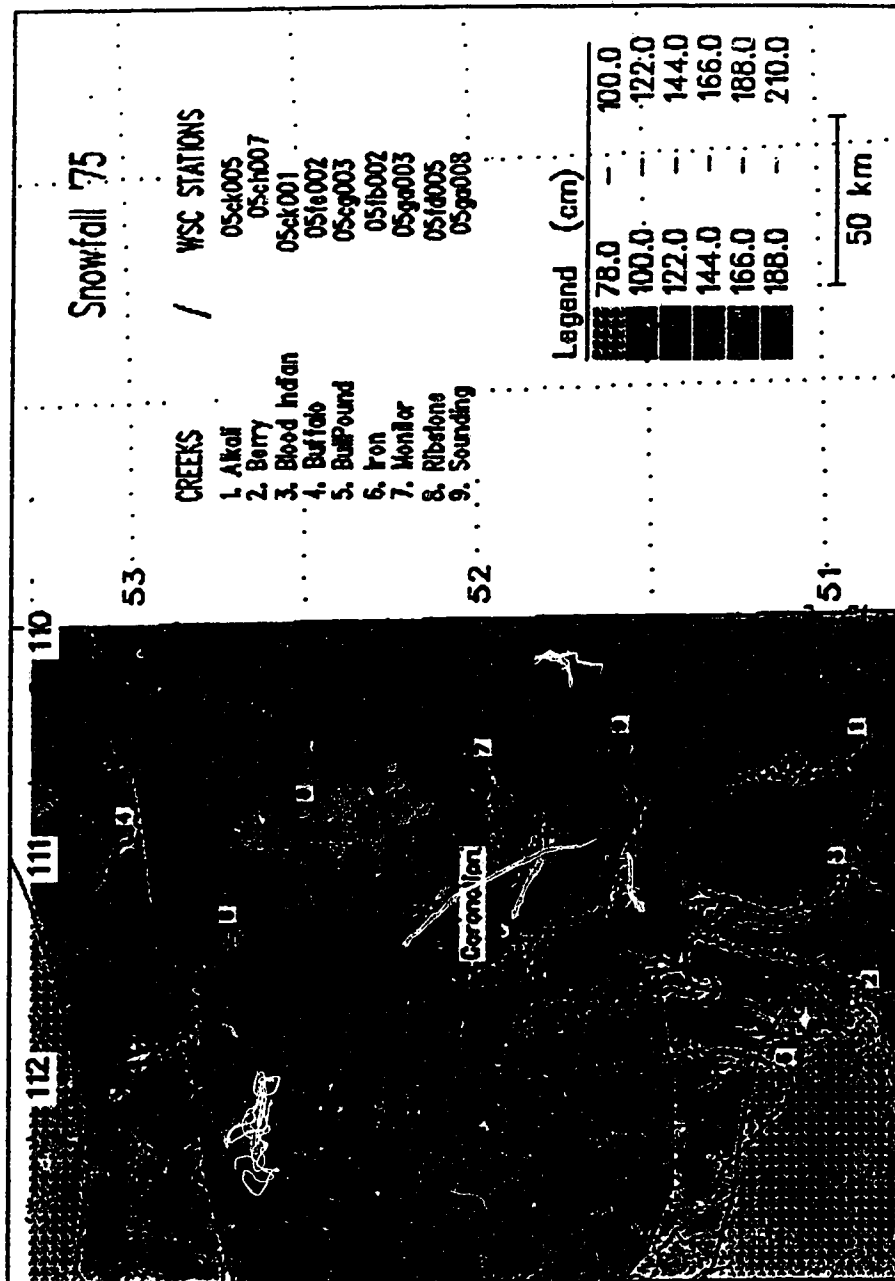


Figure B-16: 1975 - Study area winter precip., mm H₂O.

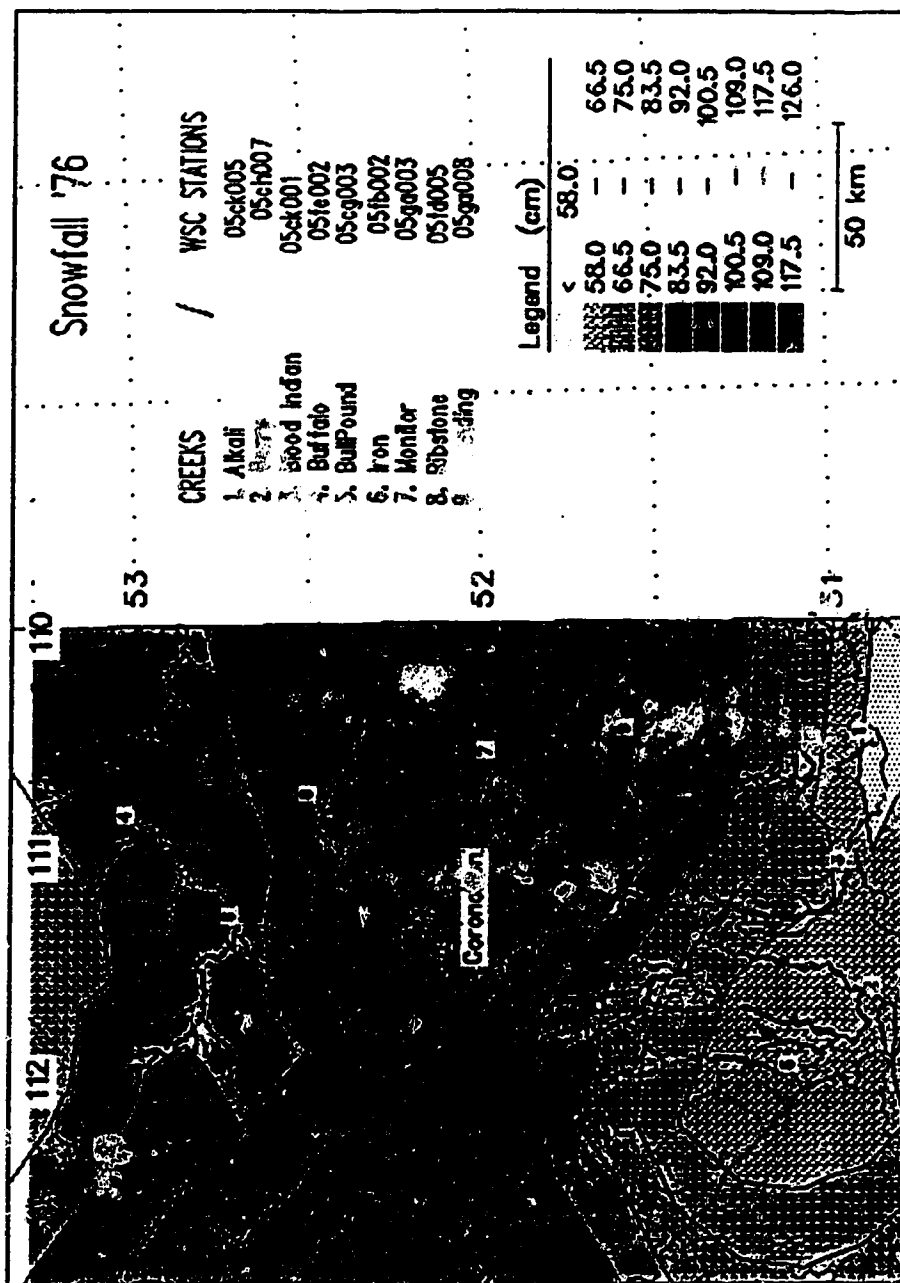


Figure B-17: 1976 - Study area winter precip., mm H₂O.

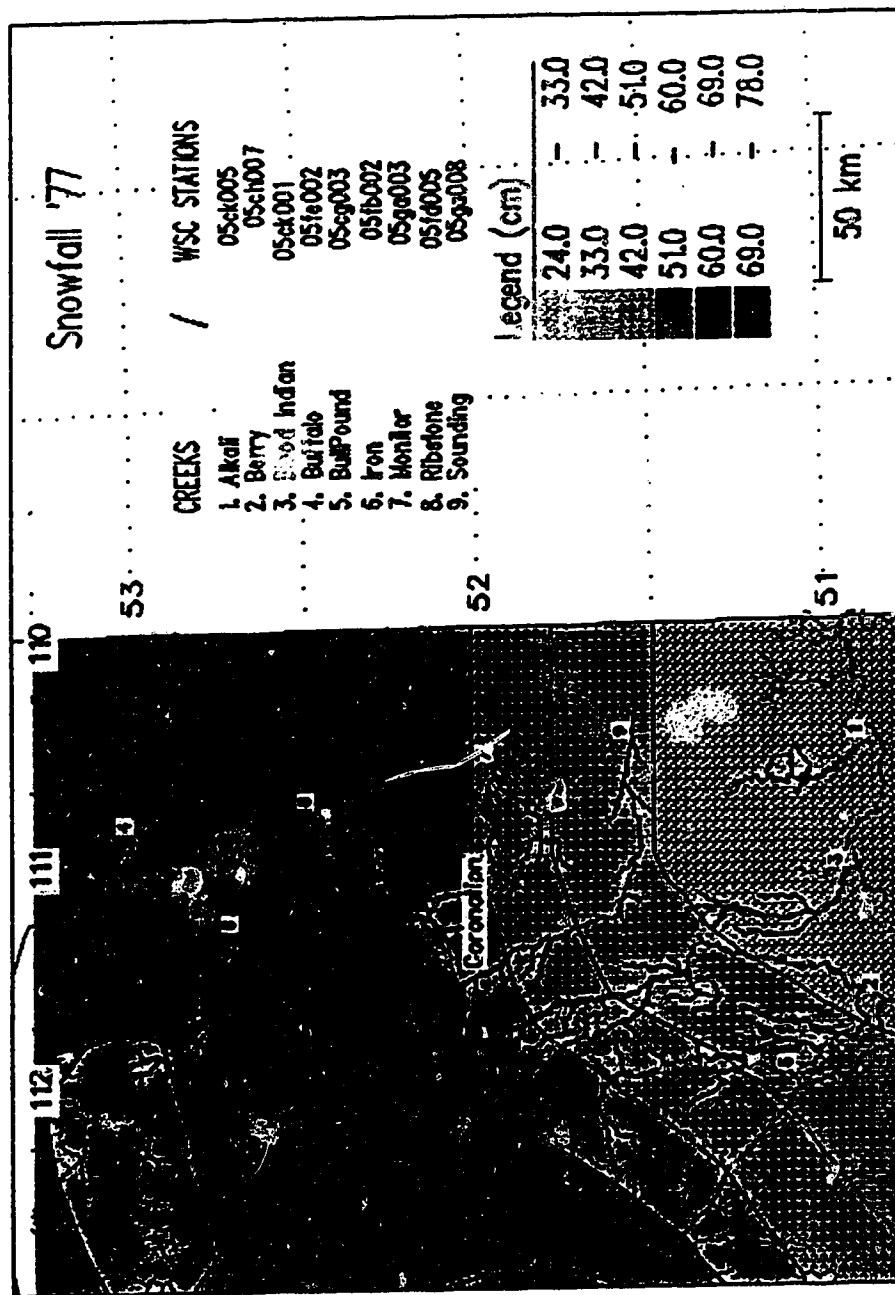


Figure B-18: 1977 - Study area winter precip., mm H₂O.

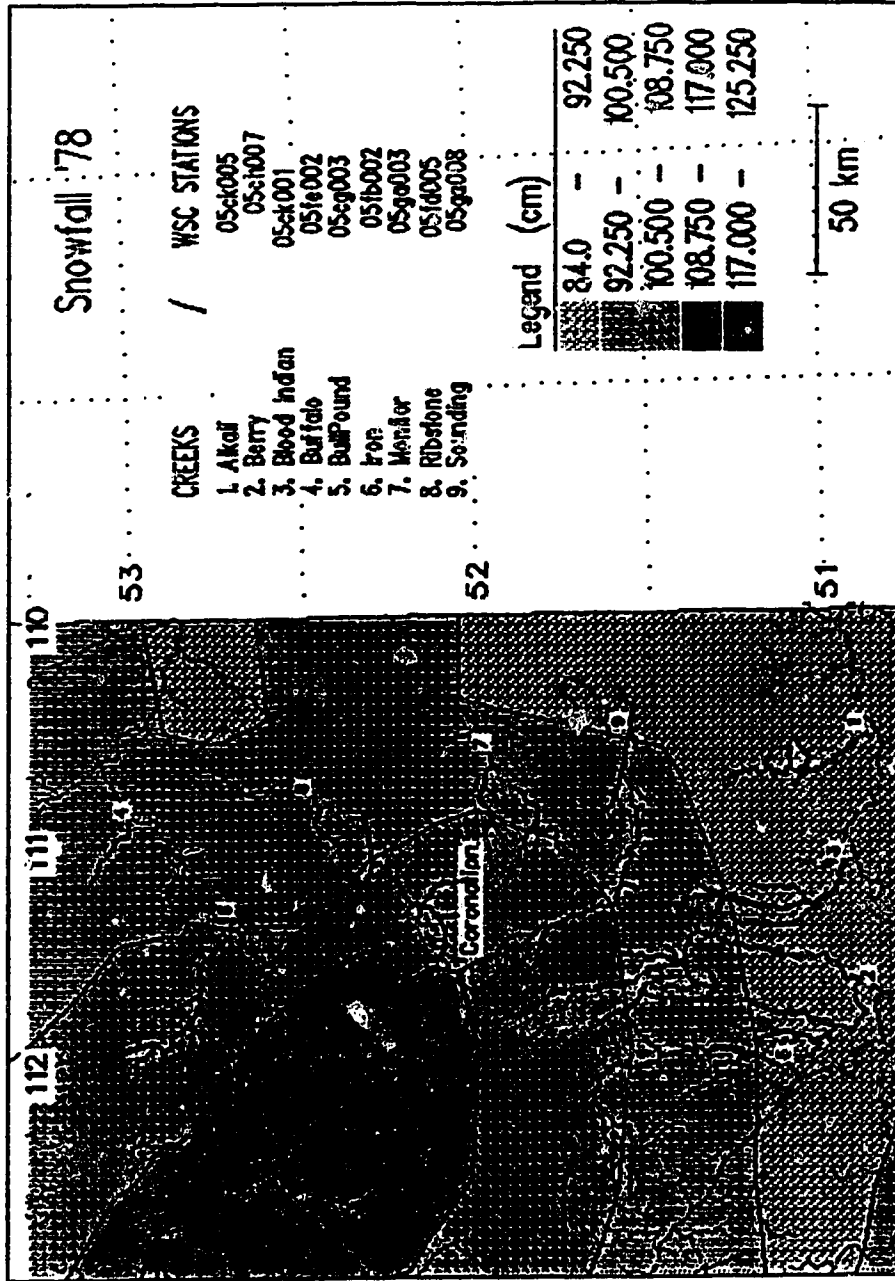


Figure B-19: 1978 - Study area winter precip., mm H₂O.

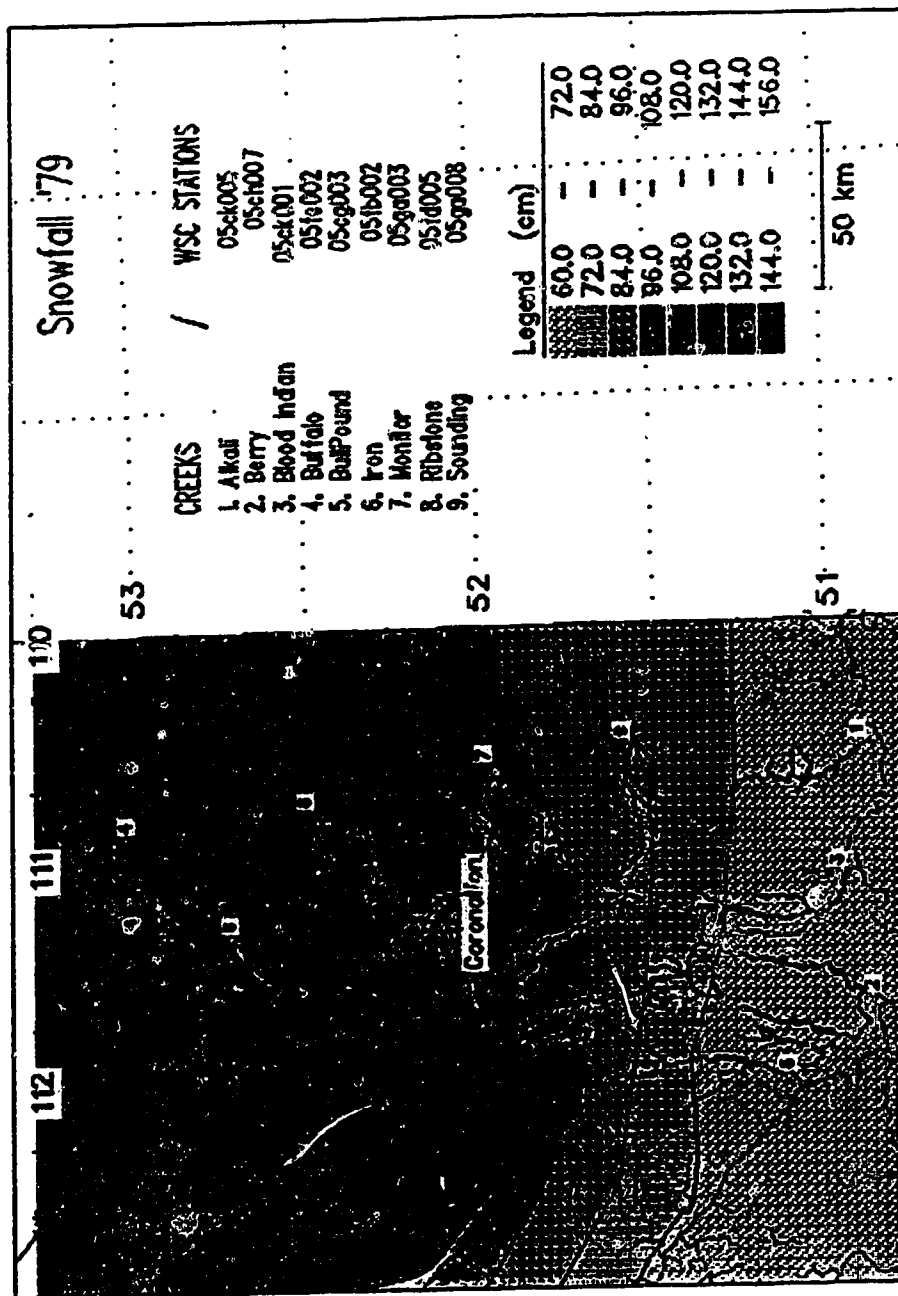


Figure B-20: 1979 - Study area winter precip., mm H₂O.

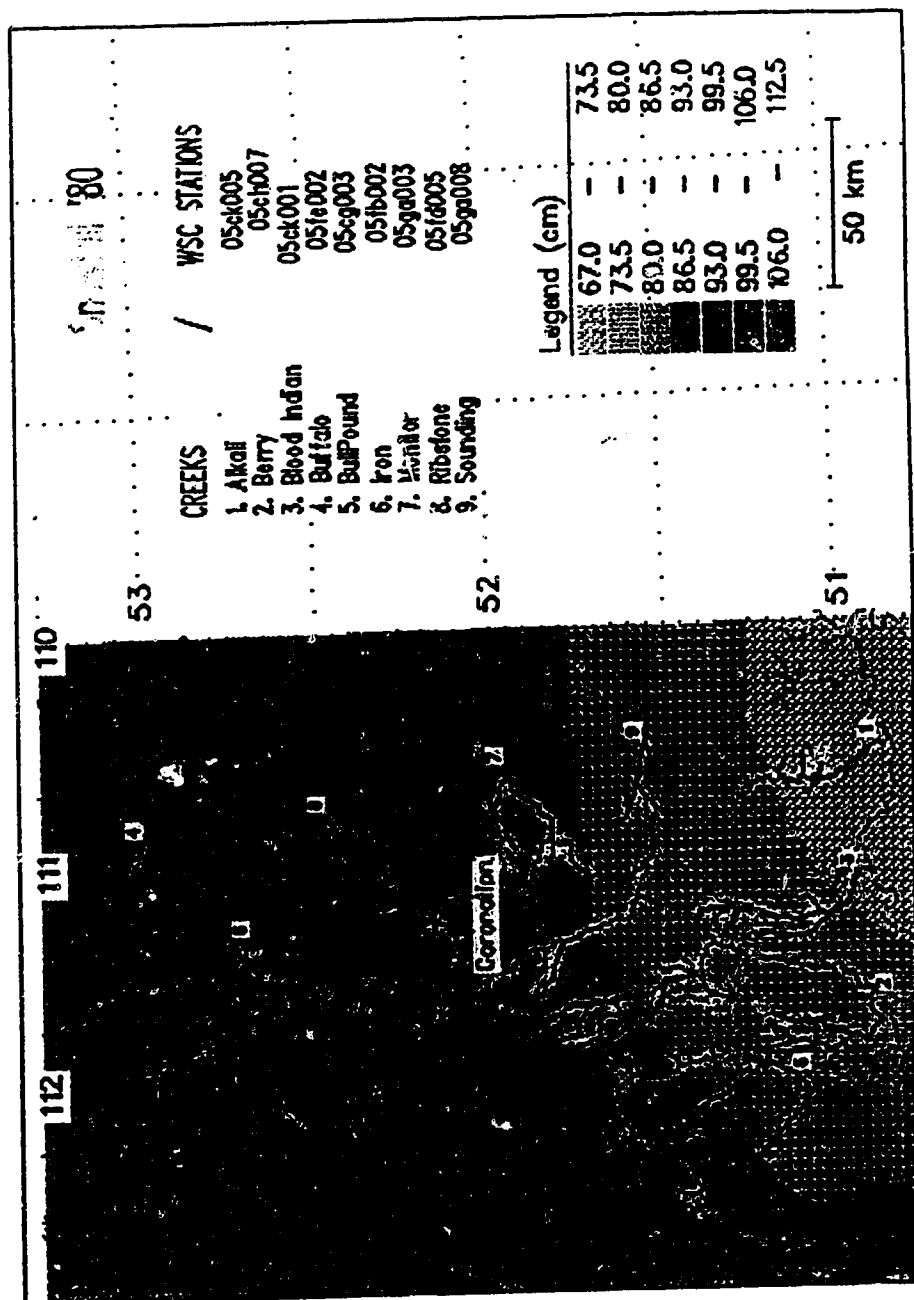


Figure B-21: 1980 - Study area winter precip., mm H₂O.

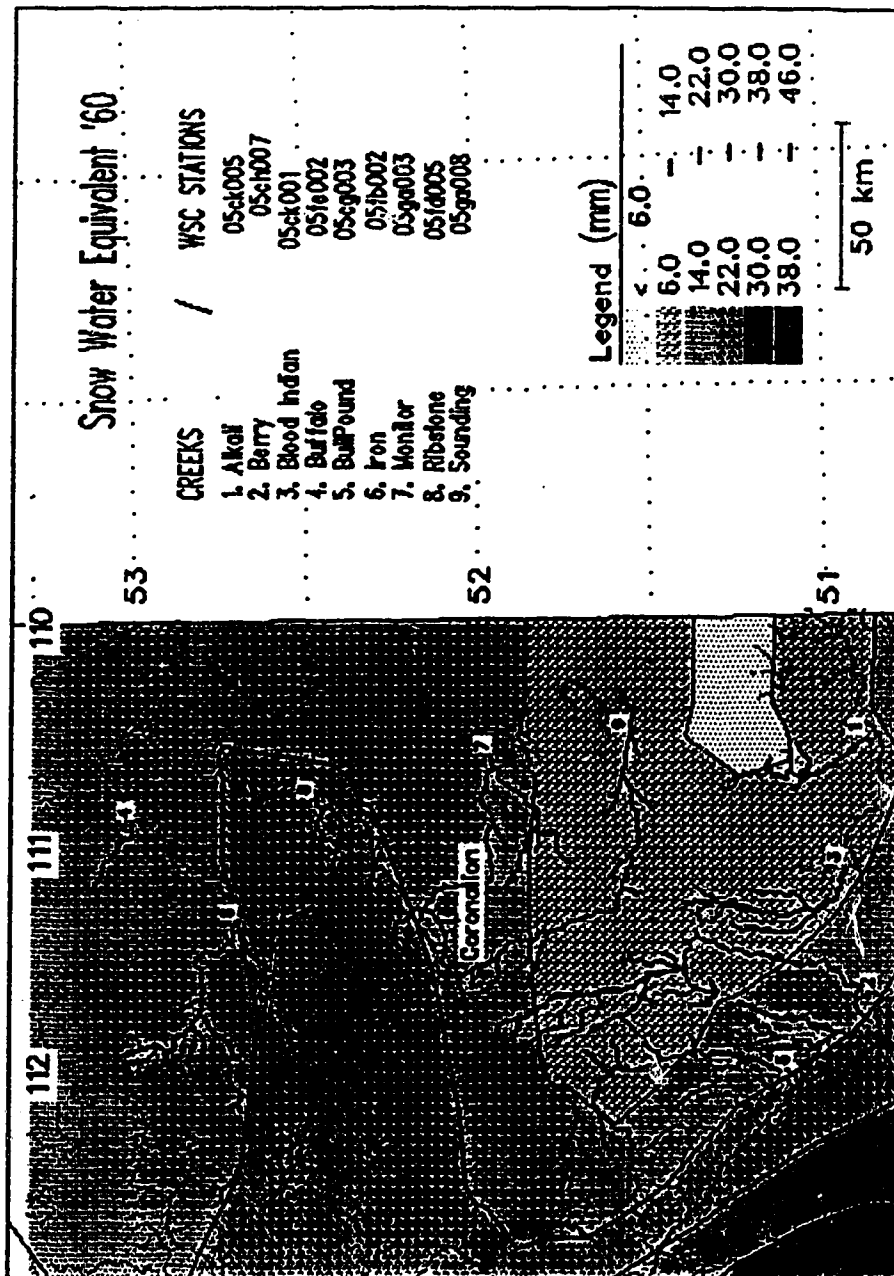


Figure B-22: 1960 - Study area SWE, mm H₂O.

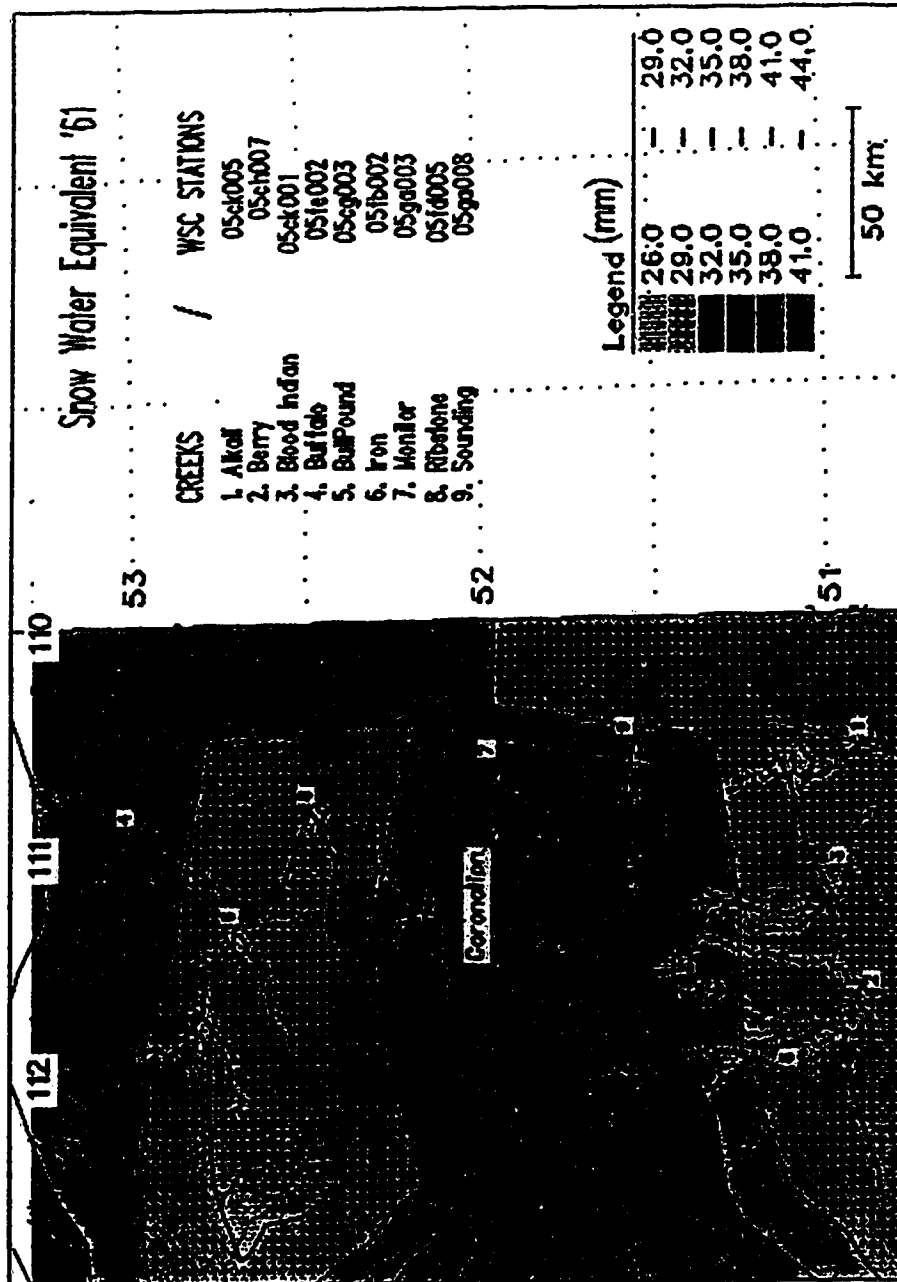


Figure B-23: 1961 - Study area SWE, mm H₂O.

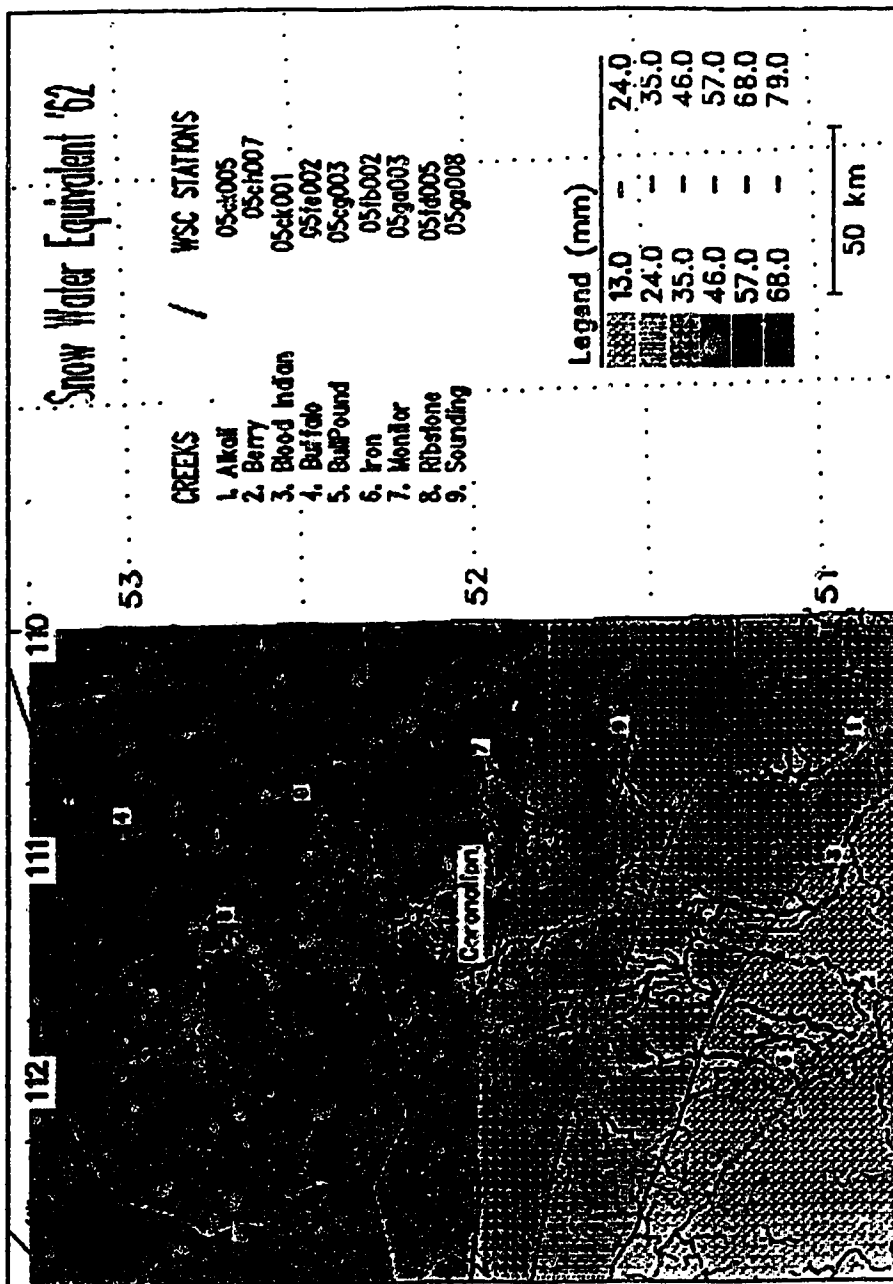


Figure B-24: 1962 - Study area SWE, mm H₂O.

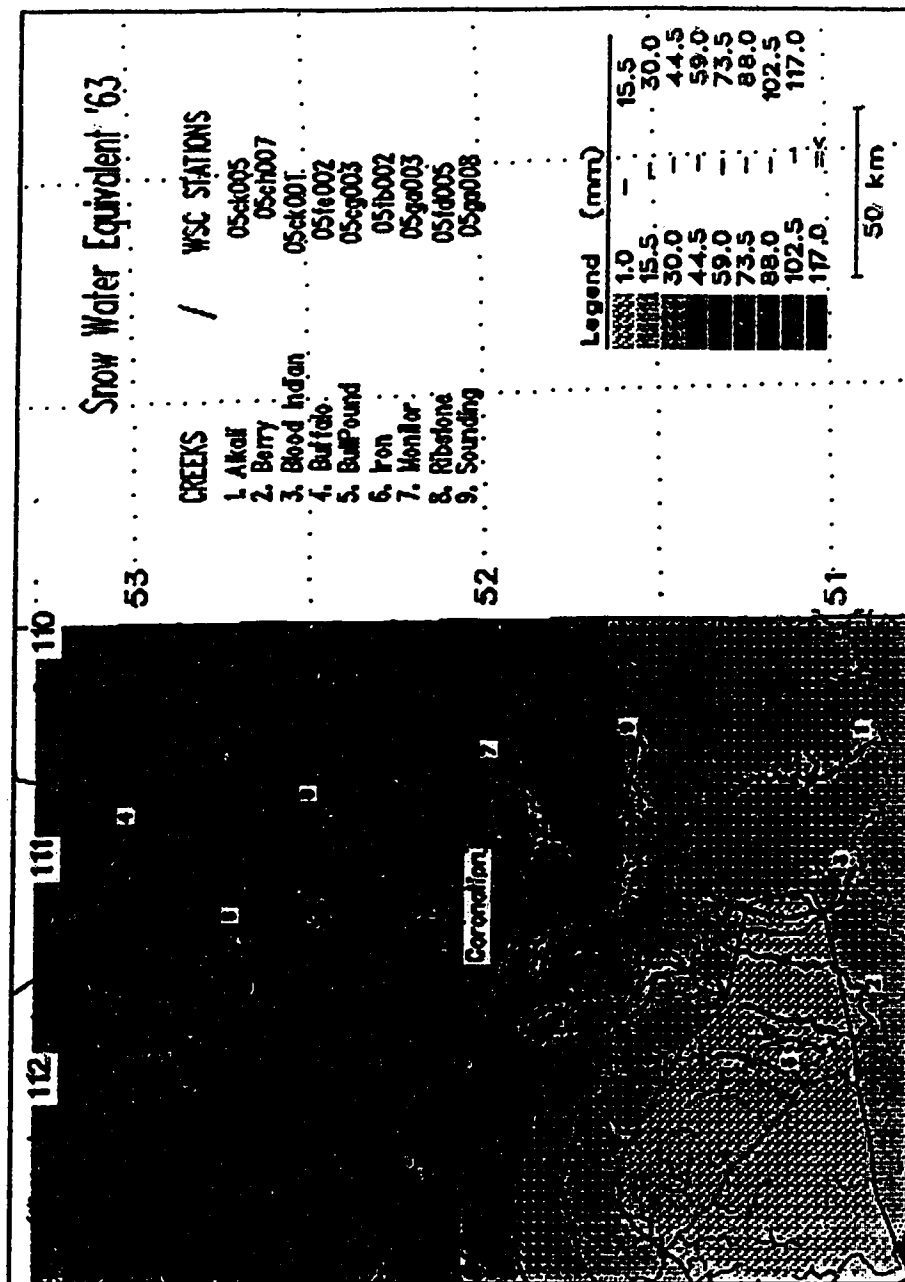


Figure B-25: 1963 - Study area SWE, mm H₂O.

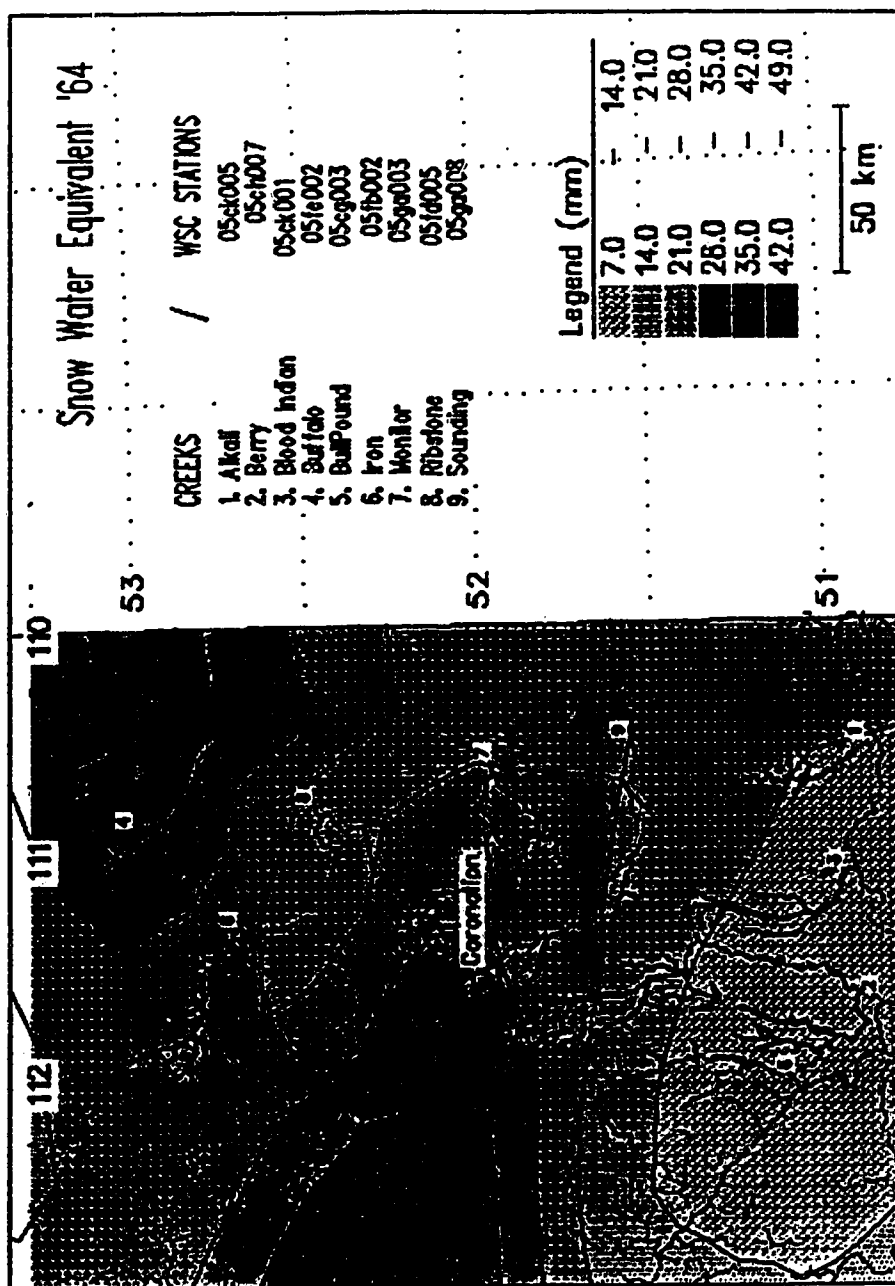


Figure B-26: 1964 - Study area SWE, mm H₂O.

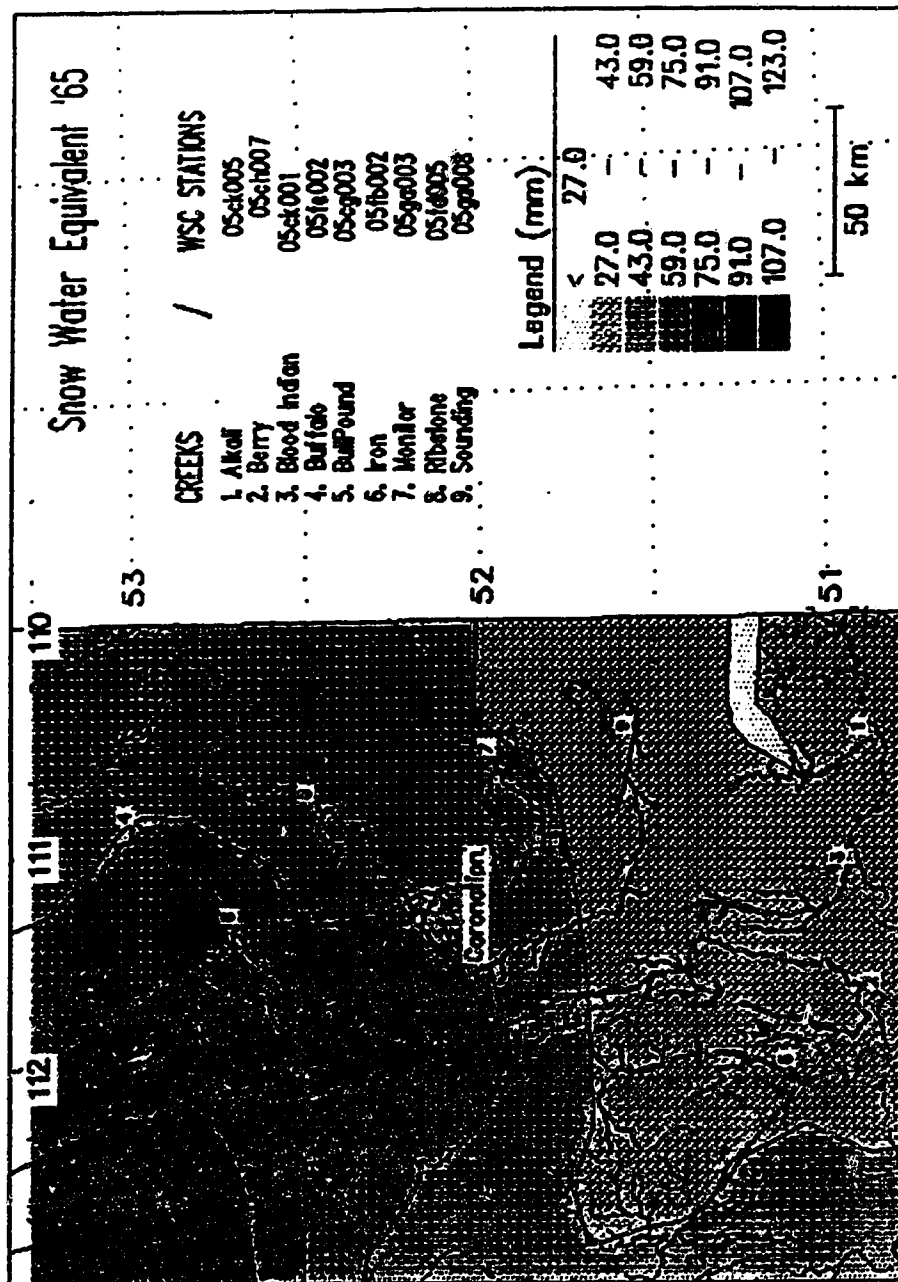


Figure B-27: 1965 - Study area SWE, mm H₂O.

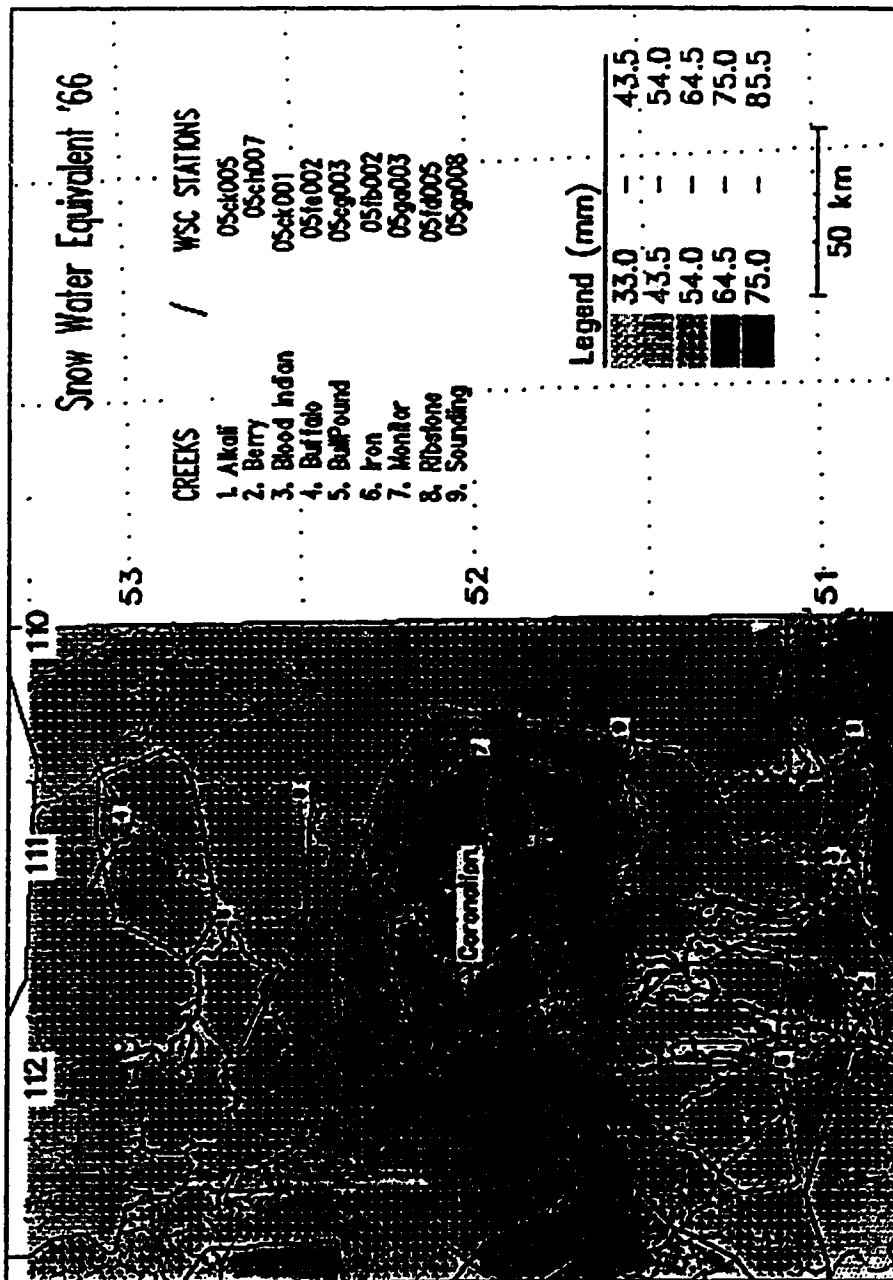


Figure B-28: 1966 - Study area SWE, mm H₂O.

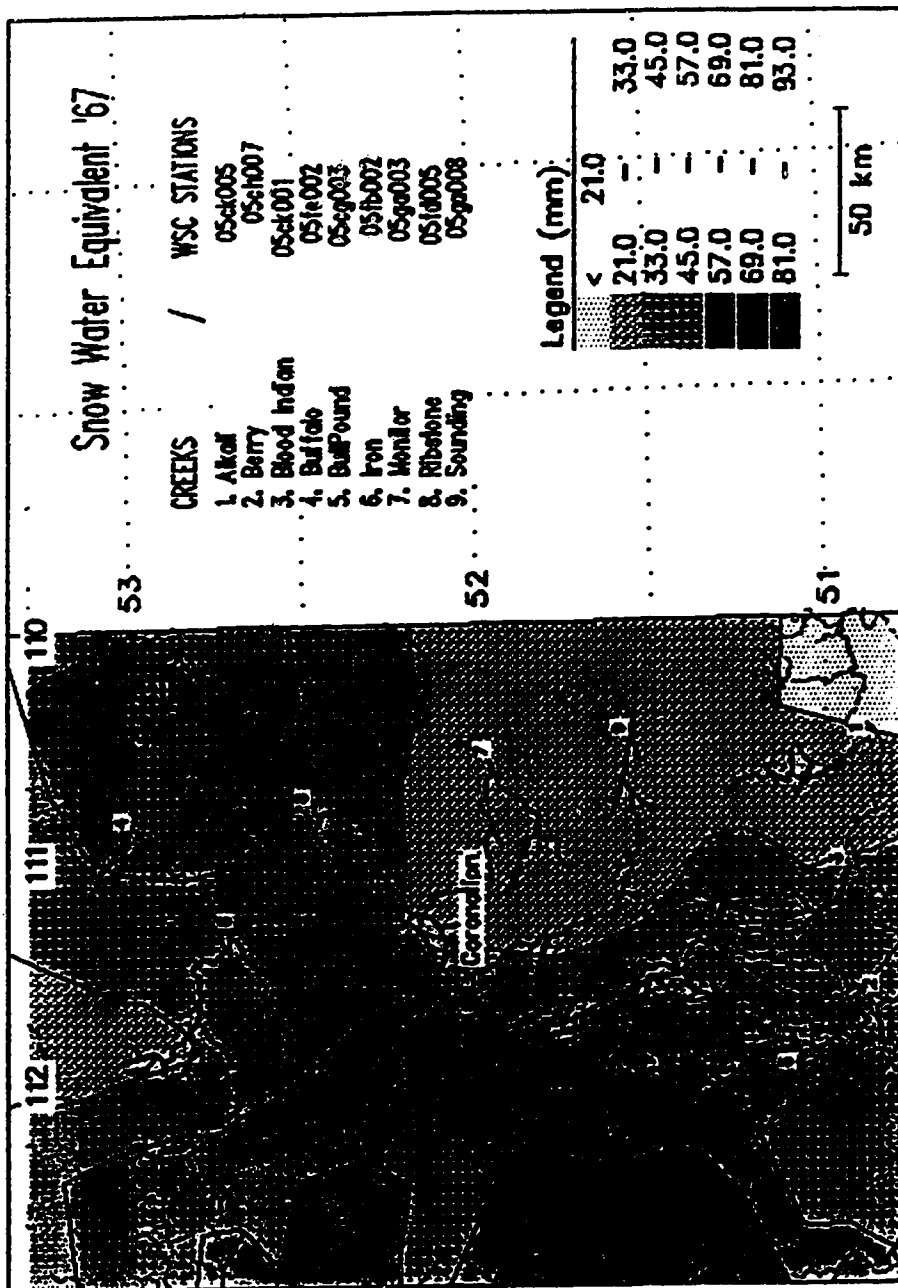


Figure B-29: 1967 - Study area SWE, mm H₂O.

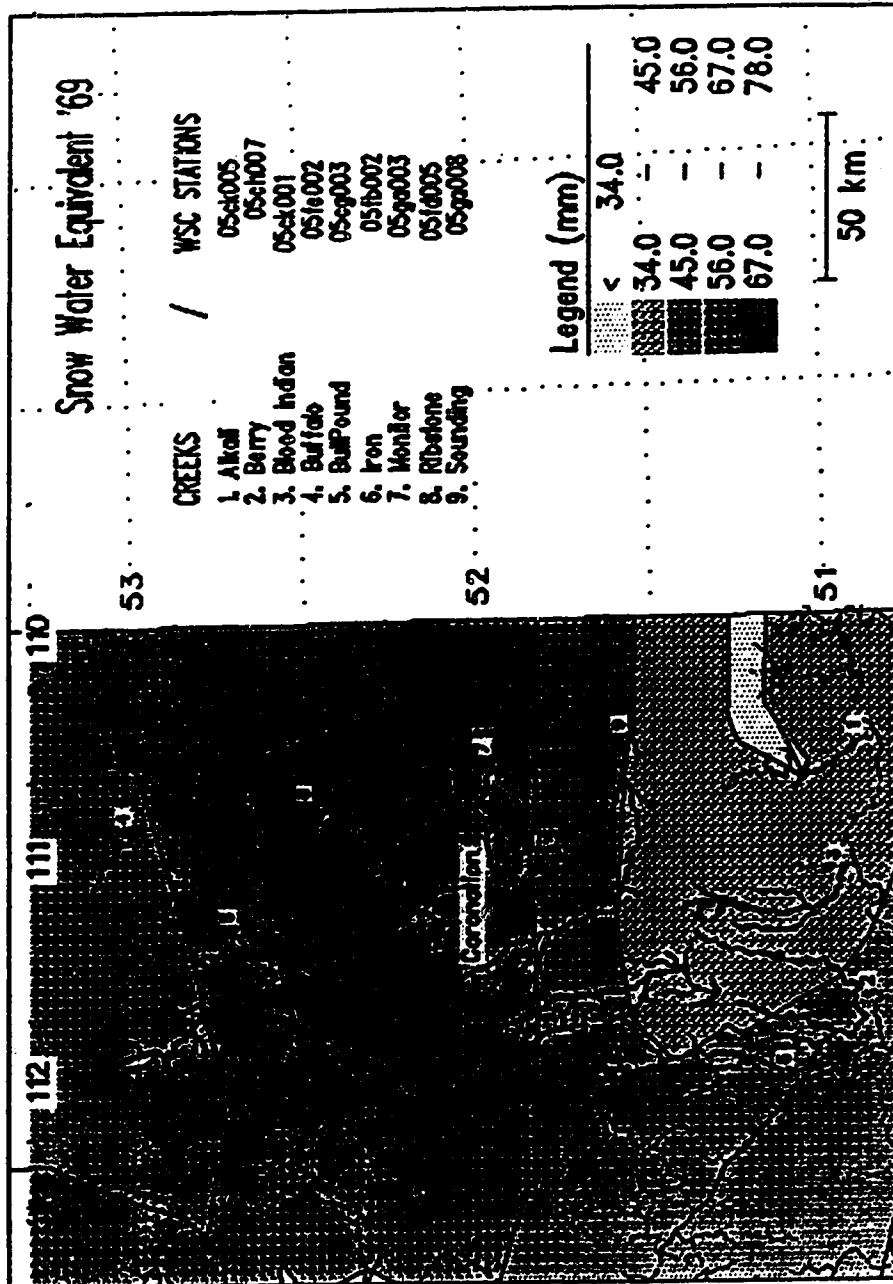


Figure B-31: 1969 - Study area SWE, mm H₂O.

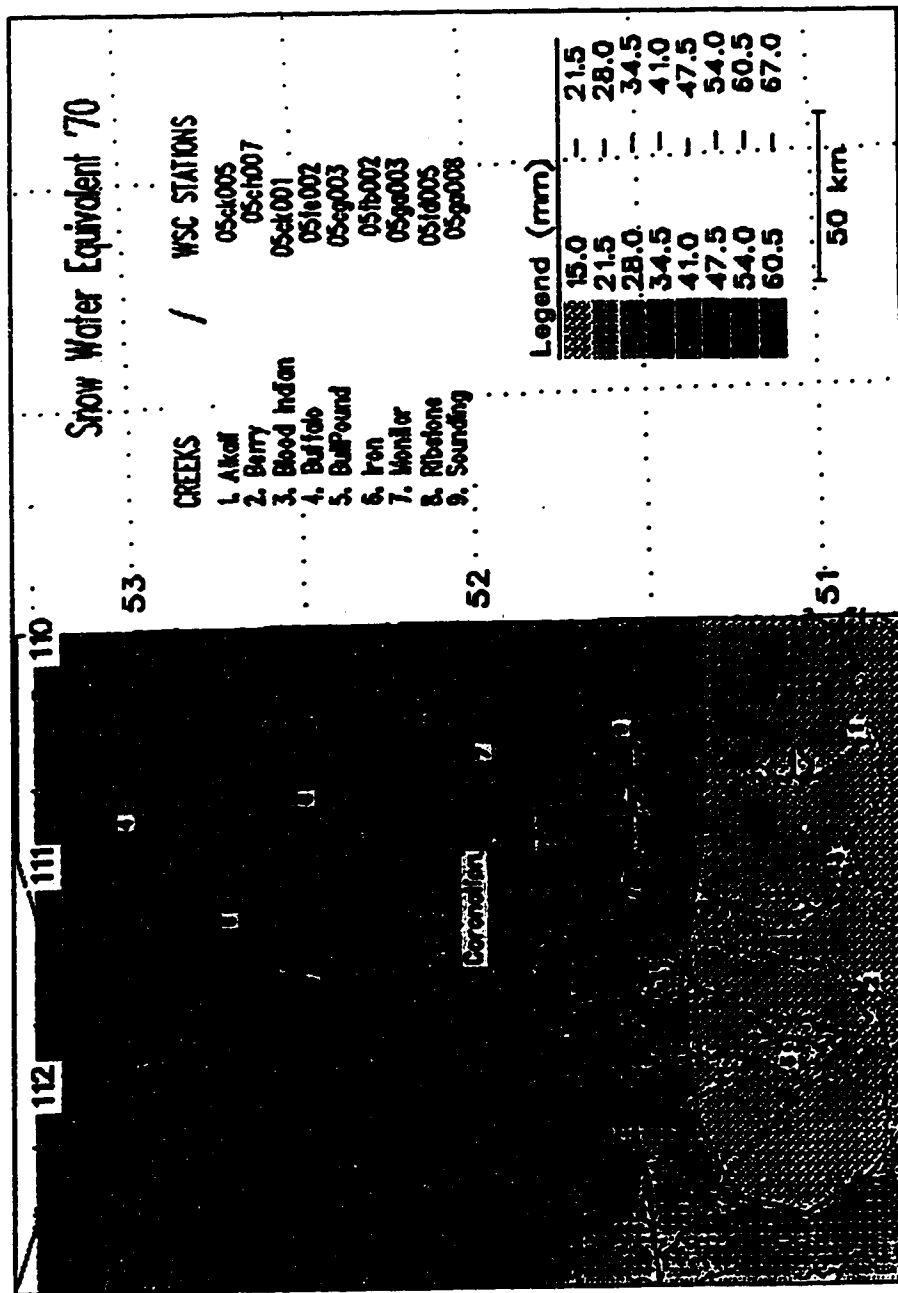


Figure B-32: 1970 - Study area SWE, mm H₂O.

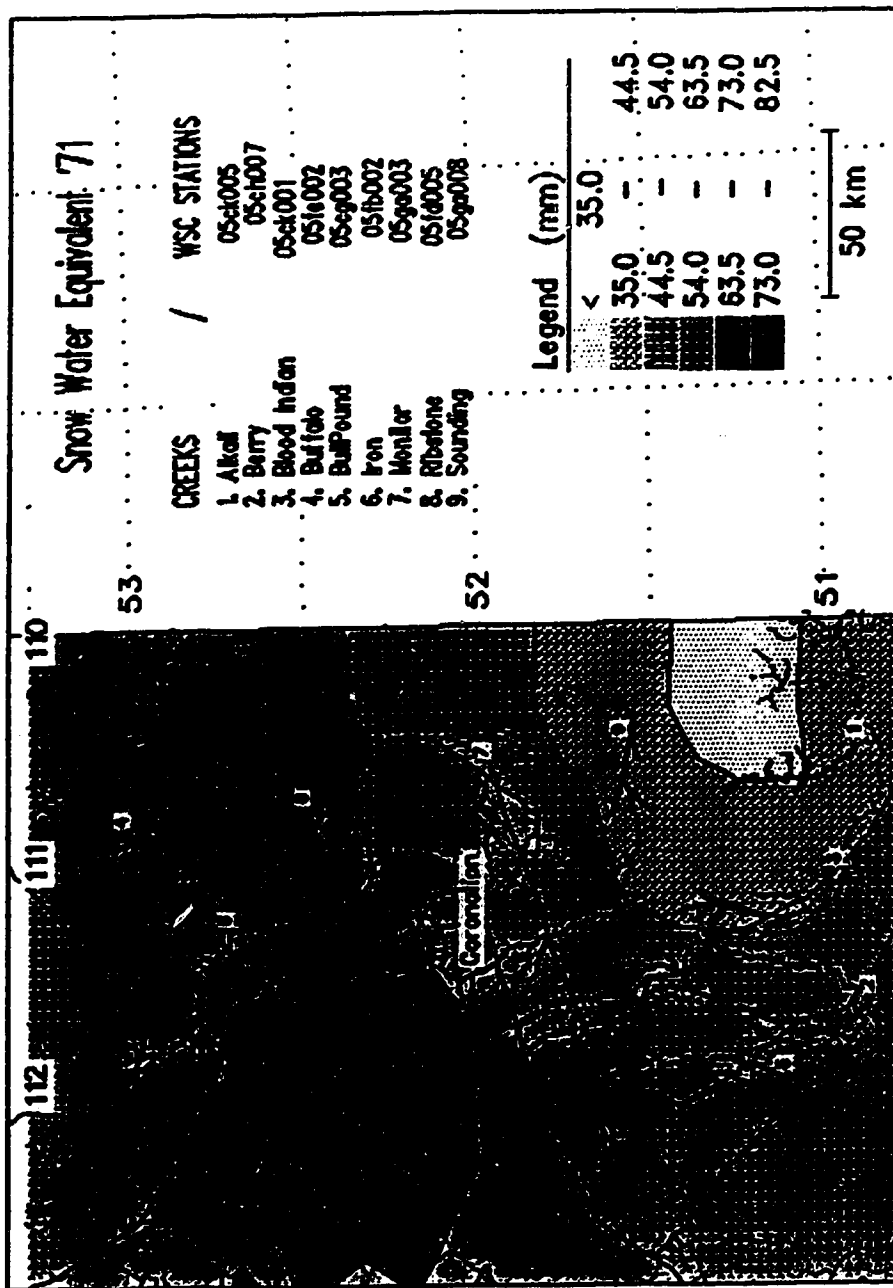


Figure B-33: 1971 - Study area SWE, mean H₂O.

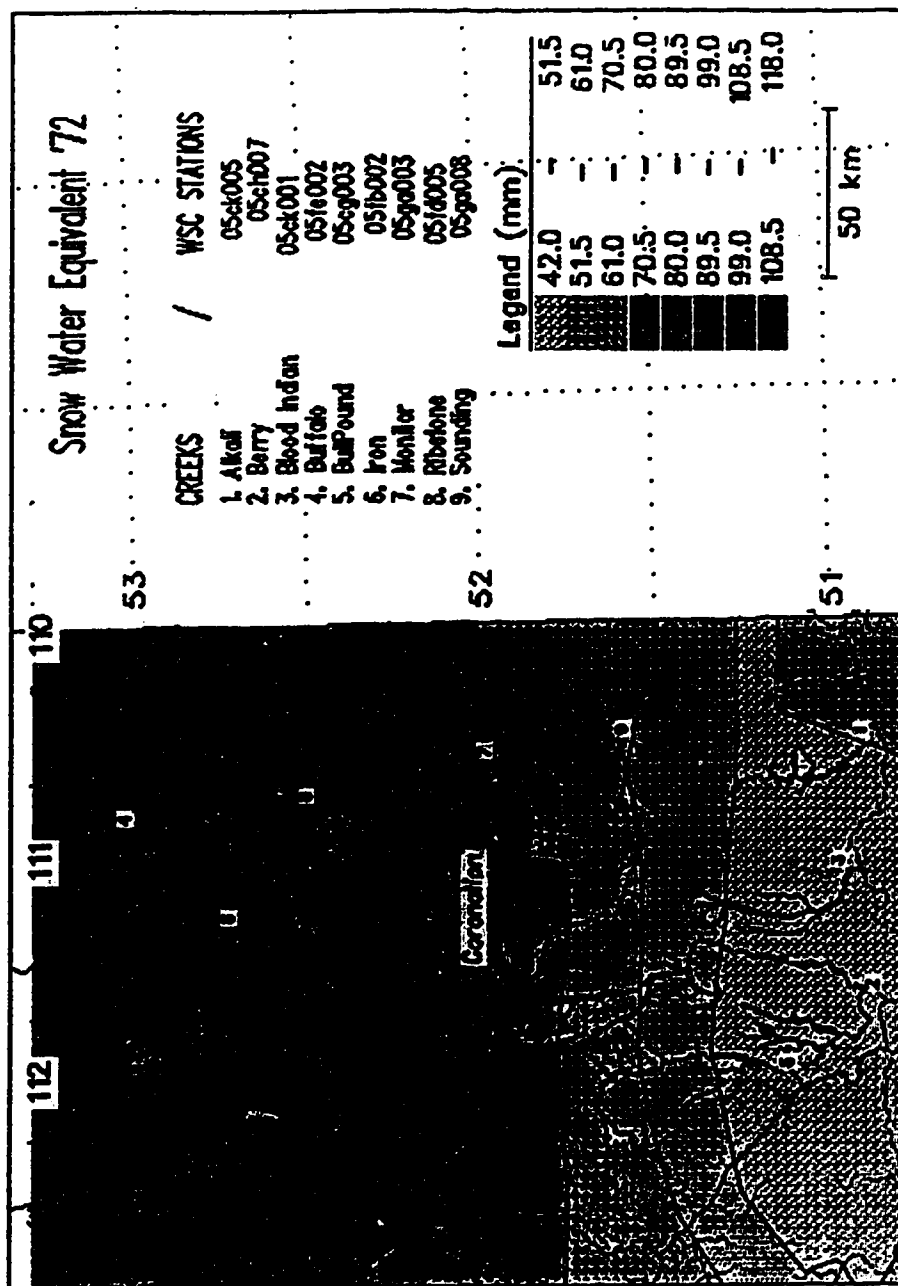


Figure B-34: 1972 - Study area SWE, mm H₂O.

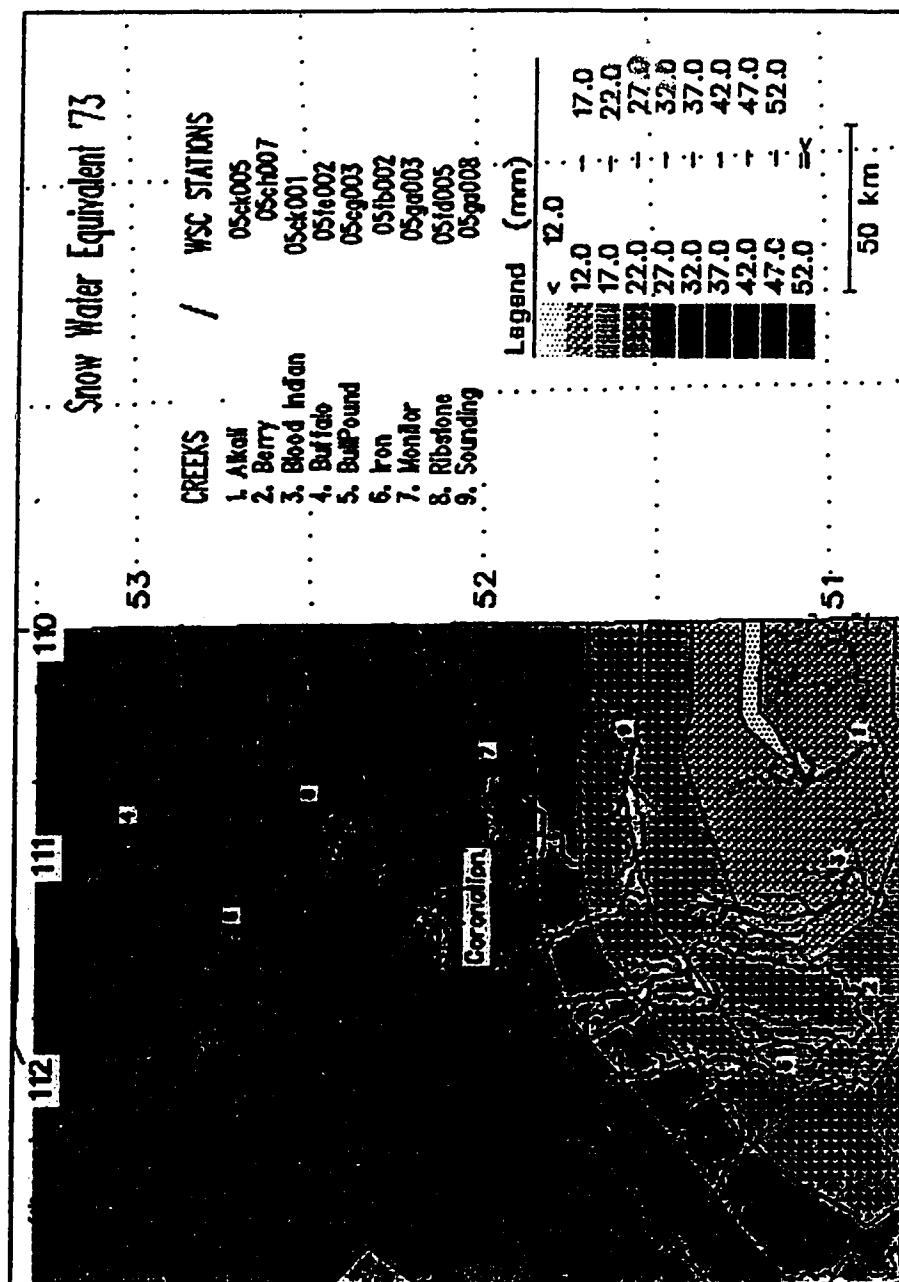


Figure B-35: 1973 - Study area SWE, mm H₂O.

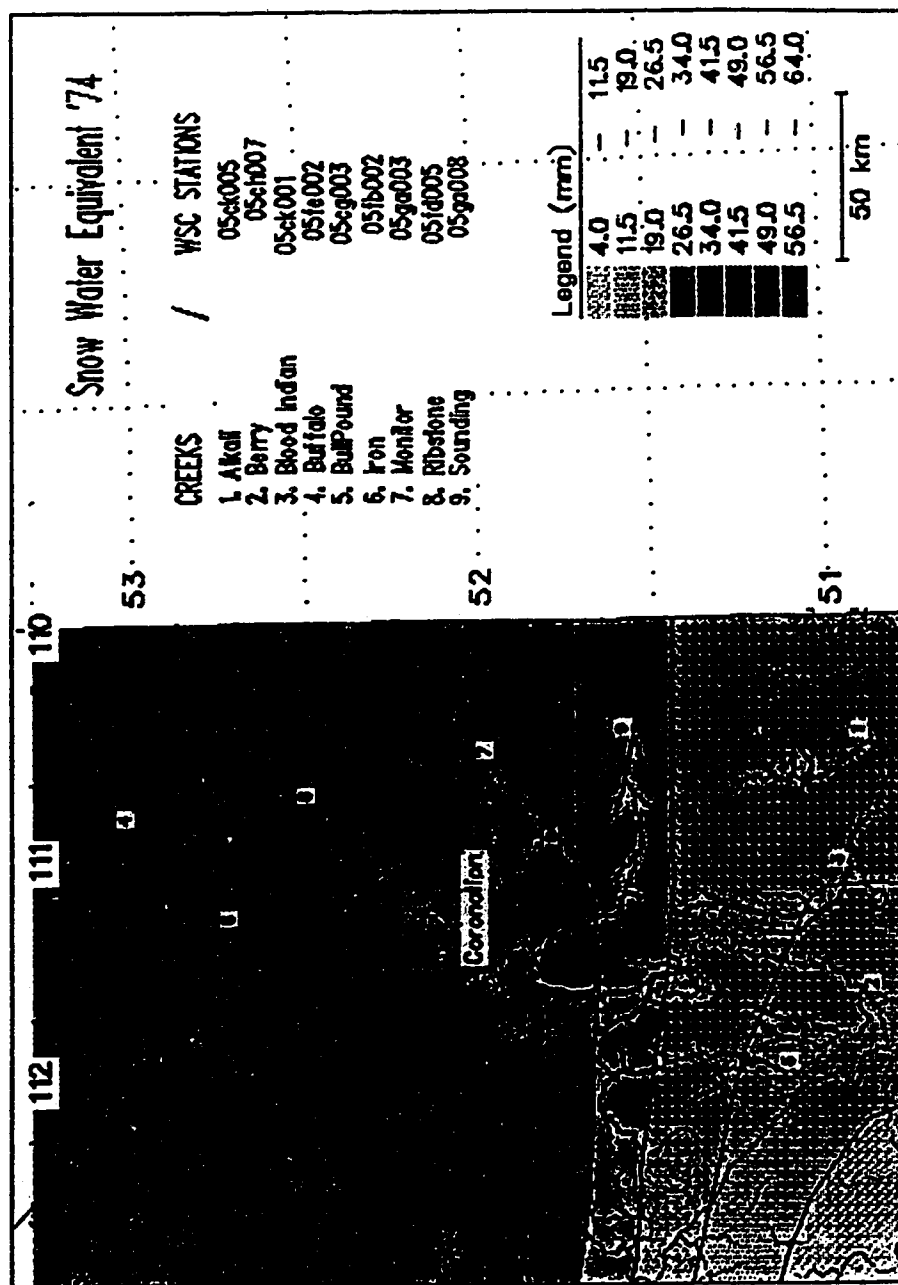


Figure B-36: 1974 - Study area SWE, mm H₂O.

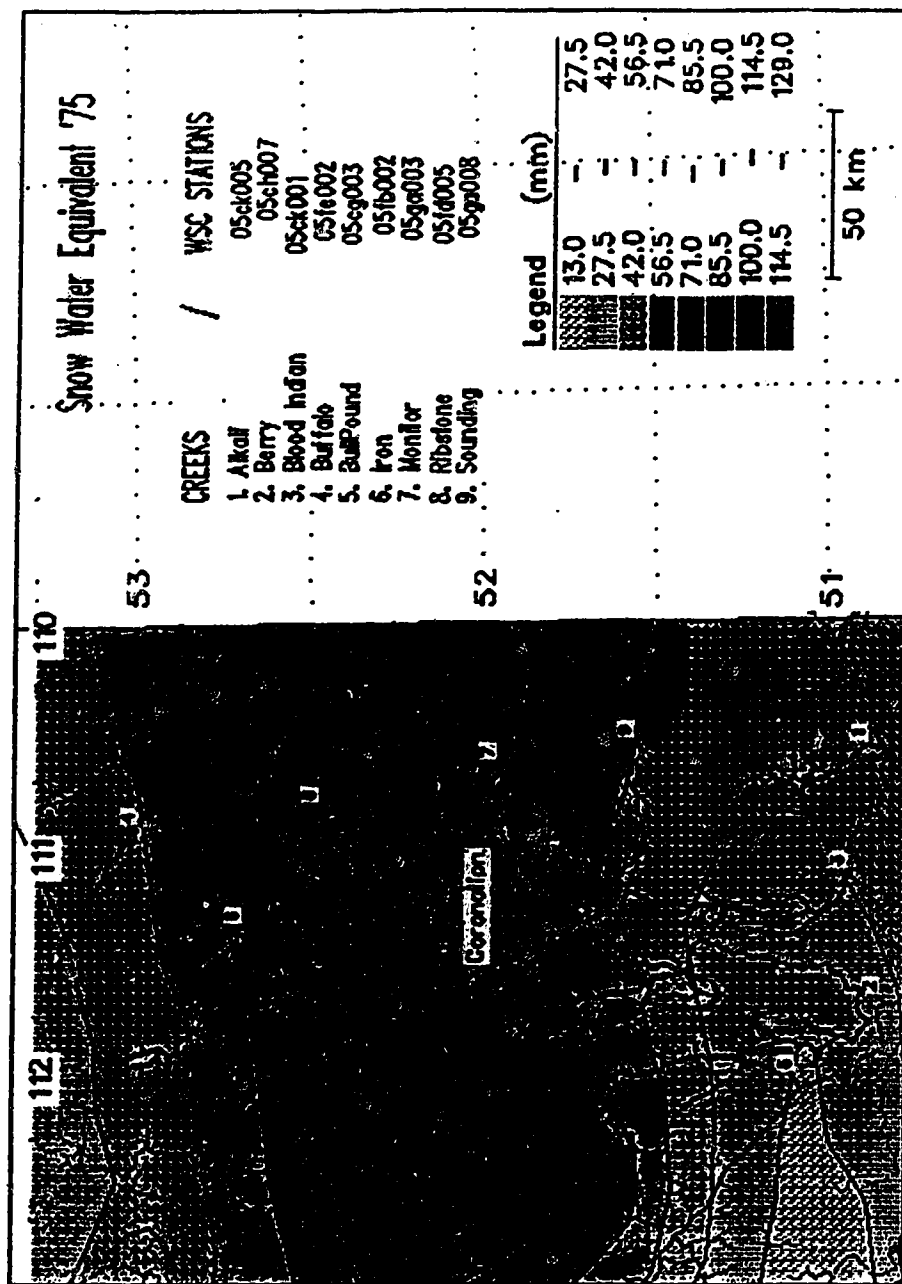


Figure B-37: 1975 - Study area SWE, mm H₂O.

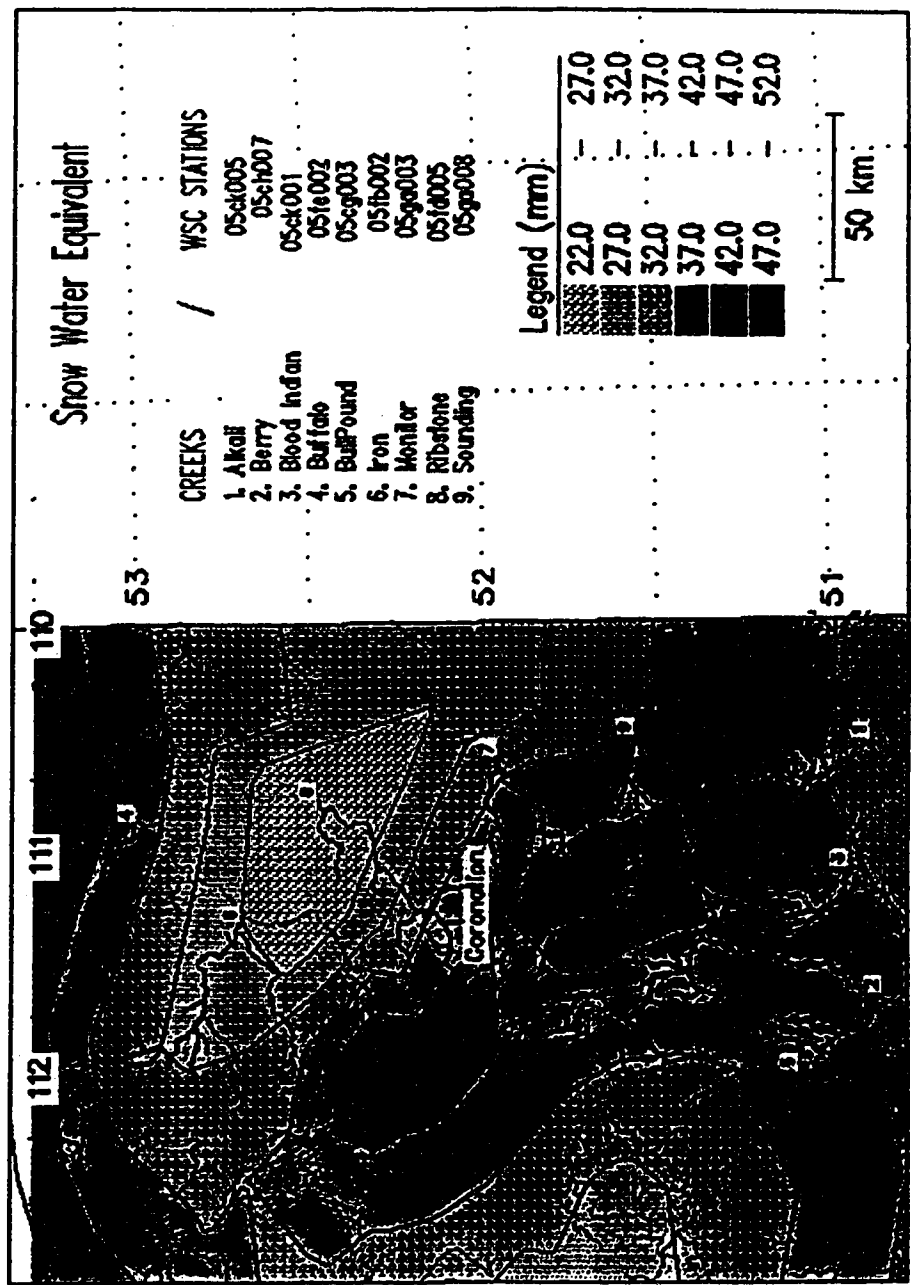


Figure B-38: 1976 - Study area SWE, mm H₂O.

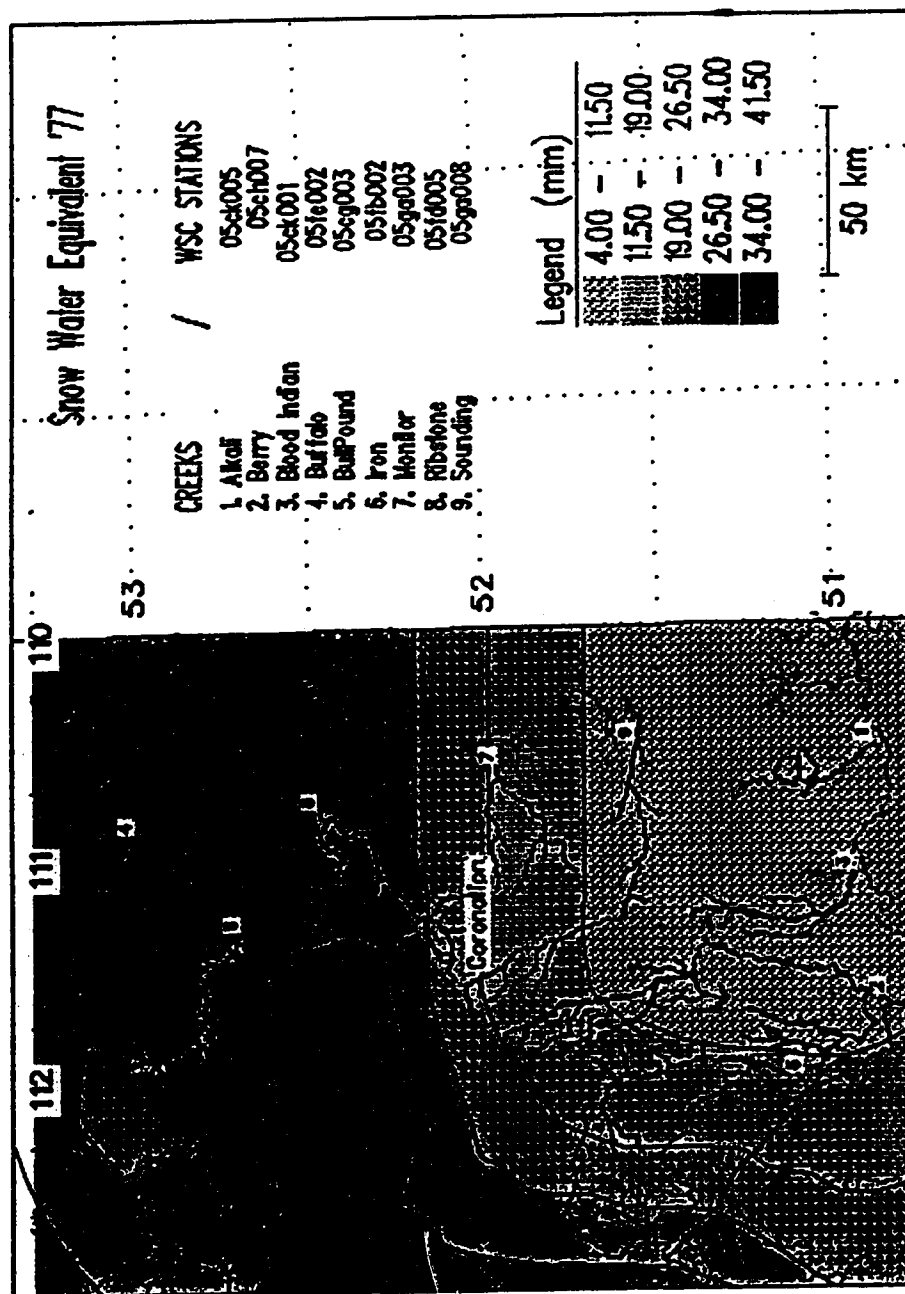


Figure B-39: 1977 - Study area SWE, mm H₂O.

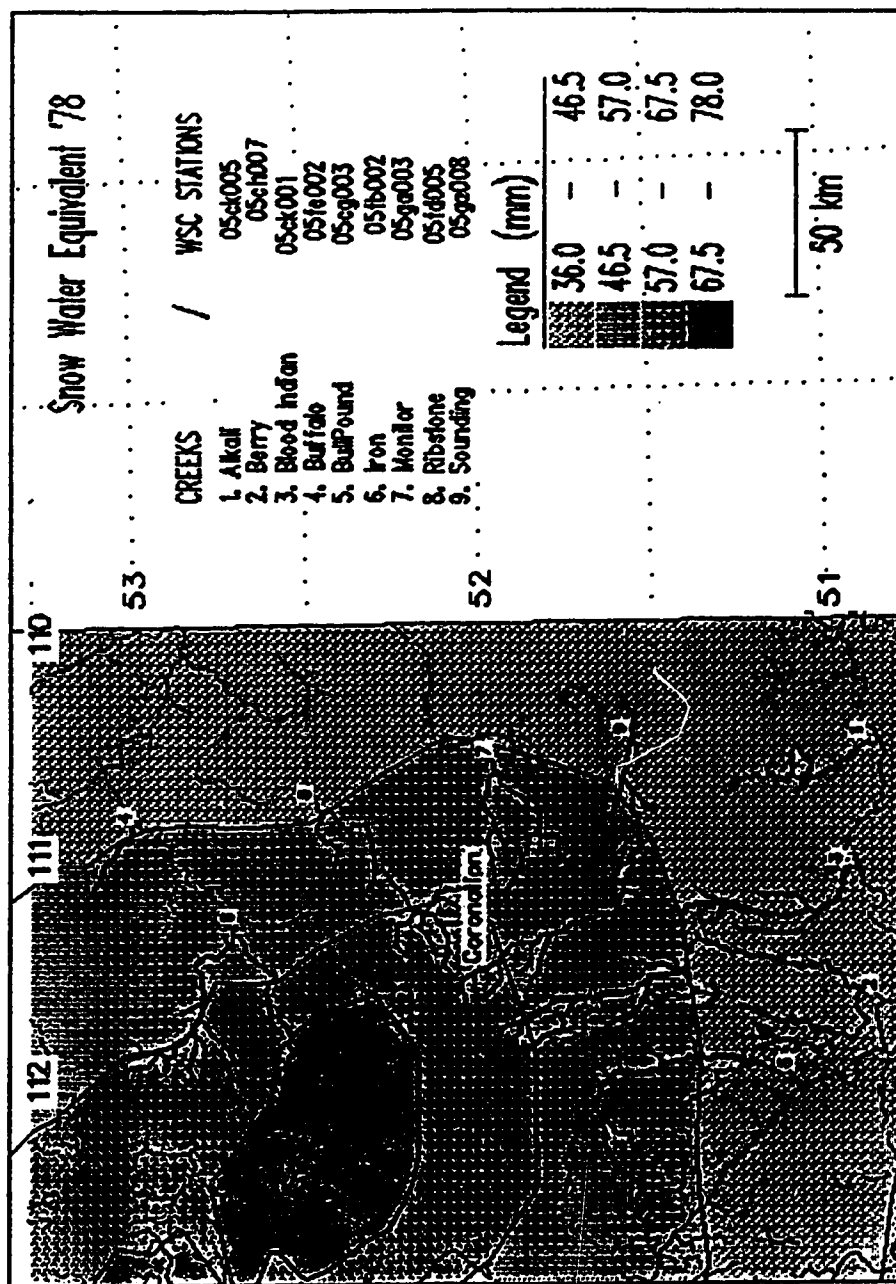


Figure B-40: 1978 - Study area SWE, mm H₂O.

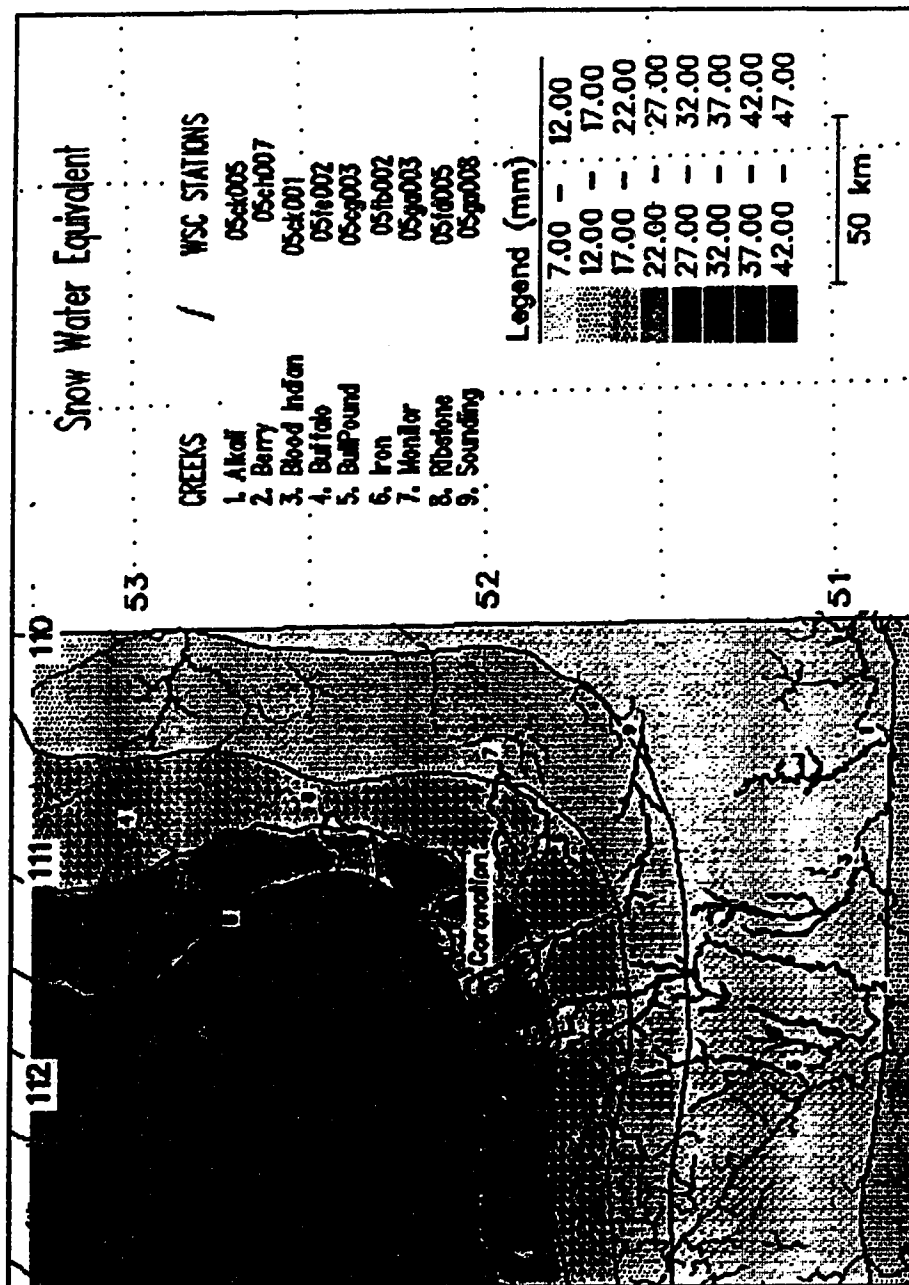


Figure B-41: 1979 - Study area SWE, mm H₂O.

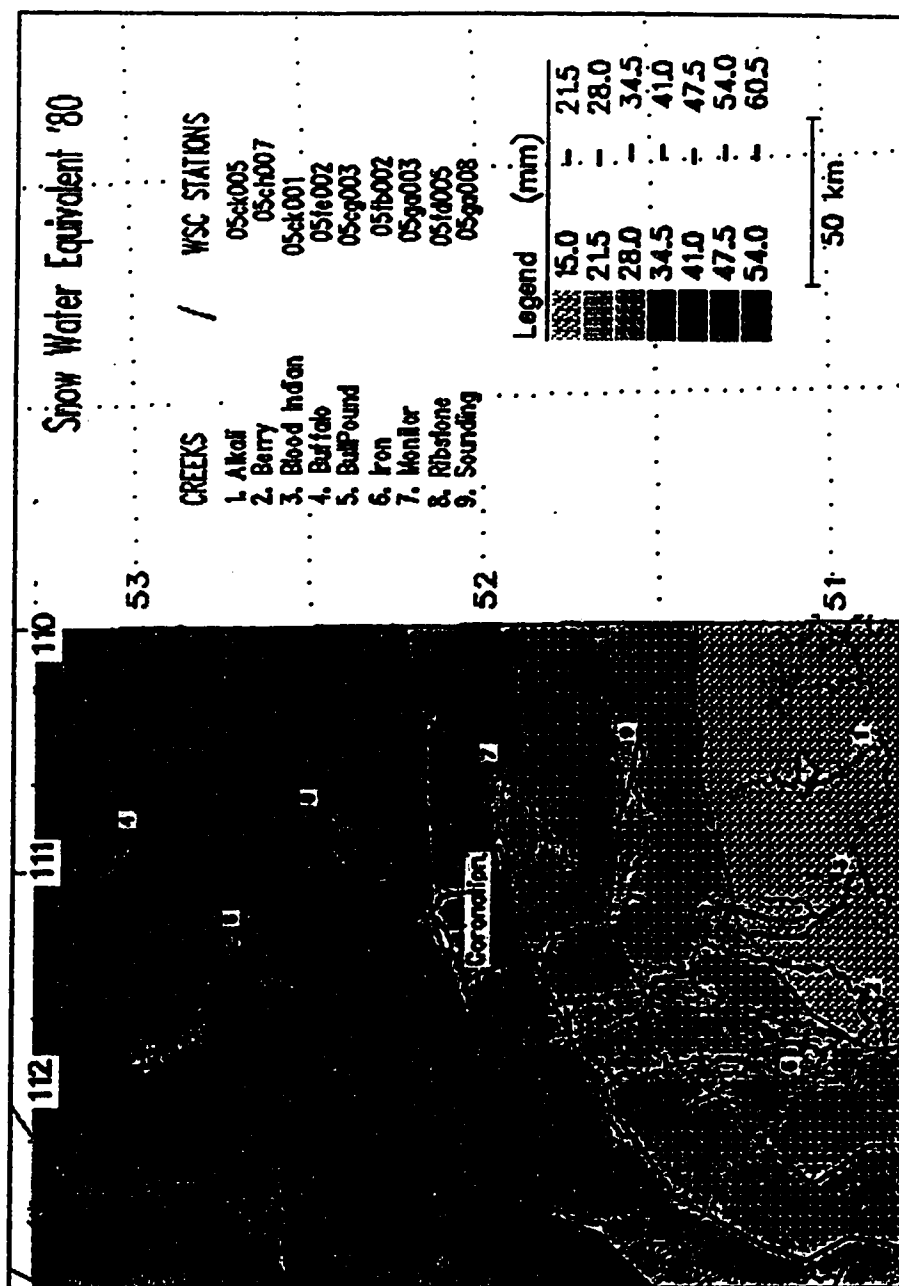


Figure B-42: 1980 - Study area SWE, mm H₂O.

Appendix C

SNOWMELT ALGORITHM

The analyses in several chapters required an estimate of the daily snowmelt as a depth of water. The method that was selected was developed for use in the UBC watershed model (Pipes and Quick, 1977). The method recognizes there are three main sources of energy which produce snowmelt: convective heat transfer from warm air; net radiant energy gain from shortwave and longwave radiation exchanges; and latent heat gain/loss from condensation or evaporation on the snow surface.

Radiation and humidity data are not readily available for remote areas. Pipes and Quick developed a simplified melt formulation using air temperature to estimate the three energy sources. The convective heat transfer is represented by the mean daily temperature above freezing. The daily temperature range is considered to represent the net radiant energy gain during the day. However, radiation melting only occurs if the minimum temperature is above freezing. The minimum temperature is utilized as an approximation of the dewpoint. If the dewpoint (minimum temperature) is below freezing, then the radiant energy is assumed to produce sublimation, rather than melting. The condensation to or evaporation from the snowpack is a function of the range of the difference between the dewpoint and the freezing point.

A snowpack that has been subjected to cold weather will have temperatures well below the melting point. The affect of antecedent temperature conditions on the snowpack are quantified with a cold storage equation containing a decaying function.

Pipes and Quick refer to this equation as a negative melt budget. The negative melt decay function limits the affect of daily temperature conditions to the previous ten days (give or take one day). The negative melt formulation is

$$TREQ_i = ANMLTF \times TREQ_{i-1} + TMEAN_i \quad (C.1)$$

where $TREQ_i$ and $TREQ_{i-1}$ are the snowpack cold storage values on days i , and $i-1$, $TMEAN_i$ is the mean temperature on day i , and $ANMLTF$ is the decay constant. $ANMLTF = 0.85$ was suggested as an appropriate value for a prairie situation (Michael Quick, Civil Engineering, UBC, pers. comm.).

When the snowpack cold storage has been exhausted, snowmelt begins. The daily snowmelt is determined with the open-area melt equation

$$MELT_i = PTM (TMAX_i + TCEADJ \times TMIN_i) \quad (C.2)$$

where i is a day counter, $MELT_i$ is the melt depth (mm), $PTM = 1 \text{ mm/}^\circ \text{C}$, (point melt factor), $TMAX_i$ is the maximum daily temperature, $TMIN_i$ is the daily minimum temperature, and $TCEADJ$ is the energy partition multiplier, defined as

$$TCEADJ = \frac{TMIN_i + T_r / 2}{XTDEWP + T_r / 2} \quad (C.3)$$

T_r is the daily range of temperature, and $XTDEWP = 18^\circ \text{C}$. $XTDEWP$ is a reference dewpoint controlling energy partitioning between melt and sublimation. The constants used were taken from the laboratory and field calibrations carried out at UBC (Michael Quick, Civil Engineering, UBC, pers. comm.).

For a day with $TMAX = 10^\circ \text{C}$, $TMIN = 2$, $TCEADJ = 0.273$, and the daily snowmelt would be 10.6 mm.

C.1. References

Pipes, Anthony and Michael C. Quick, 1977. UBC watershed model users guide.
Dept. of Civil Engineering, University of British Columbia.